



# Laboratory and Field Evaluation of Modified Asphalt Binders and Mixes for Alaskan Pavements

**Prepared by:** Missouri S&T, Department of Civil, Architectural and  
Engineering

**Date:** 2020

**Prepared for:**

Alaska Department of Transportation & Public Facilities  
Statewide Research Office  
3132 Channel Drive  
Juneau, AK 99801-7898

Center for Environmentally Sustainable Transportation in Cold Climates  
University of Alaska Fairbanks  
POB 755900  
Fairbanks, AK 99775-5900

**Sponsoring Agency Report Number:**

FHWA-AK-RD-4000-176  
INE/CESTiCC 1616

Alaska Department of Transportation & Public Facilities  
**Research & Technology Transfer**

REPORT DOCUMENTATION PAGE			Form approved OMB No.
Public reporting for this collection of information is estimated to average 1 hour per response, including the time for reviewing instructions, searching existing data sources, gathering and maintaining the data needed, and completing and reviewing the collection of information. Send comments regarding this burden estimate or any other aspect of this collection of information, including suggestion for reducing this burden to Washington Headquarters Services, Directorate for Information Operations and Reports, 1215 Jefferson Davis Highway, Suite 1204, Arlington, VA 22202-4302, and to the Office of Management and Budget, Paperwork Reduction Project (0704-1833), Washington, DC 20503			
1. AGENCY USE ONLY (LEAVE BLANK)	2. REPORT DATE 2020	3. REPORT TYPE AND DATES COVERED Final Report: 01/2017 – 08/2019	
4. TITLE AND SUBTITLE Laboratory and Field Evaluation of Modified Asphalt Binders and Mixes for Alaskan Pavements		5. FUNDING NUMBERS CESTiCC 1616	
6. AUTHOR(S) Jenny Liu and Jun Liu			
7. PERFORMING ORGANIZATION NAME(S) AND ADDRESS(ES) Department of Civil, Architectural, and Environmental Engineering Missouri University of Science and Technology 129 Butler-Carlton Hall, 1401 N. Pine Street Rolla, MO 65409-0030		8. PERFORMING ORGANIZATION REPORT NUMBER INE/CESTiCC 19.20	
9. SPONSORING/MONITORING AGENCY NAME(S) AND ADDRESS(ES) Center for Environmentally Sustainable Transportation in Cold Climates University of Alaska Fairbanks P.O. Box 755900 Fairbanks, AK 99775-5900  Alaska Department of Transportation & Public Facilities Statewide Research Office 3132 Channel Drive Juneau, AK 99801-7898		10. SPONSORING/MONITORING AGENCY REPORT NUMBER FHWA-AK-RD-4000(176) HFHWY00079	
11. SUPPLEMENTARY NOTES			
12a. DISTRIBUTION / AVAILABILITY STATEMENT No restrictions		12b. DISTRIBUTION CODE	
13. ABSTRACT (Maximum 200 words)  In order to properly characterize modified asphalt binders and mixes for Alaskan pavements, this study evaluated properties of 13 asphalt binders typically used in Alaska from three different suppliers, and 10 hot mix asphalt (HMA) mixtures which were either produced in the lab or collected from existing paving projects in Alaska. Various binder and mixture engineering properties were determined, including true high binder grades, complex modulus ( $G^*$ ), and phase angle ( $\delta$ ) at high performance temperatures, multiple stress creep recovery rate and compliance, bending beam rheometer stiffness and $m$ -value, Glover-Rowe parameter, $\Delta T$ , rheological index, and crossover frequency for binders, and rut depth, critical strain energy release rate ( $J_c$ ), Indirect tensile (IDT) creep stiffness and strength for mixtures. Binder cracking temperatures were determined using asphalt binder cracking device. Mixture cracking temperatures were determined with IDT creep compliance and strength data. It was found that rutting and cracking resistances of the mixtures with highly modified binders were better than the mixture with unmodified asphalt binder (PG 52-28). Future recommendations for highly modified asphalt binders applications and research were provided based on laboratory testing results and field survey evaluation.			
14. KEYWORDS : Modified Asphalt Binders, Rheology, Rutting, Fatigue Cracking, Low Temperature Cracking, Cracking Temperature		15. NUMBER OF PAGES 226	
		16. PRICE CODE N/A	
17. SECURITY CLASSIFICATION OF REPORT Unclassified	18. SECURITY CLASSIFICATION OF THIS PAGE Unclassified	19. SECURITY CLASSIFICATION OF ABSTRACT Unclassified	20. LIMITATION OF ABSTRACT N/A

**LABORATORY AND FIELD EVALUATION OF MODIFIED  
ASPHALT BINDERS AND MIXES FOR ALASKAN  
PAVEMENTS**

**FINAL REPORT**

**Prepared for**

**Center for Environmentally Sustainable Transportation in Cold  
Climates**

**and**

**Alaska Department of Transportation & Public Facilities**

**Authors:**

**Jenny Liu, Ph.D., P.E.**

**Jun Liu**

**Missouri University of Science and Technology**

**Report Date: 2020**

**Period Covered: 01/2017 – 08/2019**

## **DISCLAIMER**

This document is disseminated under the sponsorship of the U. S. Department of Transportation in the interest of information exchange. The U.S. Government assumes no liability for the use of the information contained in this document. The U.S. Government does not endorse products or manufacturers. Trademarks or manufacturers' names appear in this report only because they are considered essential to the objective of the document.



# METRIC (SI\*) CONVERSION FACTORS

APPROXIMATE CONVERSIONS TO SI UNITS					APPROXIMATE CONVERSIONS FROM SI UNITS				
Symbol	When You Know	Multiply By	To Find	Symbol	Symbol	When You Know	Multiply By	To Find	Symbol
<u>LENGTH</u>					<u>LENGTH</u>				
in	inches	25.4		mm	mm	millimeters	0.039	inches	in
ft	feet	0.3048		m	m	meters	3.28	feet	ft
yd	yards	0.914		m	m	meters	1.09	yards	yd
mi	Miles (statute)	1.61		km	km	kilometers	0.621	Miles (statute)	mi
<u>AREA</u>					<u>AREA</u>				
in <sup>2</sup>	square inches	645.2	millimeters squared	cm <sup>2</sup>	mm <sup>2</sup>	millimeters squared	0.0016	square inches	in <sup>2</sup>
ft <sup>2</sup>	square feet	0.0929	meters squared	m <sup>2</sup>	m <sup>2</sup>	meters squared	10.764	square feet	ft <sup>2</sup>
yd <sup>2</sup>	square yards	0.836	meters squared	m <sup>2</sup>	km <sup>2</sup>	kilometers squared	0.39	square miles	mi <sup>2</sup>
mi <sup>2</sup>	square miles	2.59	kilometers squared	km <sup>2</sup>	ha	hectares (10,000 m <sup>2</sup> )	2.471	acres	ac
ac	acres	0.4046	hectares	ha					
<u>MASS (weight)</u>					<u>MASS (weight)</u>				
oz	Ounces (avdp)	28.35	grams	g	g	grams	0.0353	Ounces (avdp)	oz
lb	Pounds (avdp)	0.454	kilograms	kg	kg	kilograms	2.205	Pounds (avdp)	lb
T	Short tons (2000 lb)	0.907	megagrams	mg	mg	megagrams (1000 kg)	1.103	short tons	T
<u>VOLUME</u>					<u>VOLUME</u>				
fl oz	fluid ounces (US)	29.57	milliliters	mL	mL	milliliters	0.034	fluid ounces (US)	fl oz
gal	Gallons (liq)	3.785	liters	liters	liters	liters	0.264	Gallons (liq)	gal
ft <sup>3</sup>	cubic feet	0.0283	meters cubed	m <sup>3</sup>	m <sup>3</sup>	meters cubed	35.315	cubic feet	ft <sup>3</sup>
yd <sup>3</sup>	cubic yards	0.765	meters cubed	m <sup>3</sup>	m <sup>3</sup>	meters cubed	1.308	cubic yards	yd <sup>3</sup>
Note: Volumes greater than 1000 L shall be shown in m <sup>3</sup>									
<u>TEMPERATURE (exact)</u>					<u>TEMPERATURE (exact)</u>				
°F	Fahrenheit temperature	5/9 (°F-32)	Celsius temperature	°C	°C	Celsius temperature	9/5 °C+32	Fahrenheit temperature	°F
<u>ILLUMINATION</u>					<u>ILLUMINATION</u>				
fc	Foot-candles	10.76	lux	lx	lx	lux	0.0929	foot-candles	fc
fl	foot-lamberts	3.426	candela/m <sup>2</sup>	cd/cm <sup>2</sup>	cd/cm <sup>2</sup>	candela/m <sup>2</sup>	0.2919	foot-lamberts	fl
<u>FORCE and PRESSURE or STRESS</u>					<u>FORCE and PRESSURE or STRESS</u>				
lbf	pound-force	4.45	newtons	N	N	newtons	0.225	pound-force	lbf
psi	pound-force per square inch	6.89	kilopascals	kPa	kPa	kilopascals	0.145	pound-force per square inch	psi
These factors conform to the requirement of FHWA Order 5190.1A *SI is the symbol for the International System of Measurements									

## **ACKNOWLEDGMENTS**

The authors wish to express their appreciation to the Alaska Department of Transportation & Public Facilities (ADOT&PF) personnel for their support throughout this study, as well as the Center for Environmentally Sustainable Transportation in Cold Climates (CESTiCC). The authors would like to thank all members of the Project Technical Advisory Committee.

Acknowledgment is also extended to Drs. Baoshan Huang and Mike Lusher for their technical support and laboratory testing, and Mr. Anyou Zhu for his contributions in material collection, laboratory testing, and data analysis related to the project.

## TABLE OF CONTENTS

<b>REPORT DOCUMENTATION PAGE</b> .....	<b>I</b>
<b>DISCLAIMER</b> .....	<b>IV</b>
<b>ACKNOWLEDGMENTS</b> .....	<b>VI</b>
<b>TABLE OF CONTENTS</b> .....	<b>VII</b>
<b>LIST OF FIGURES</b> .....	<b>X</b>
<b>LIST OF TABLES</b> .....	<b>XV</b>
<b>EXECUTIVE SUMMARY</b> .....	<b>1</b>
<b>CHAPTER 1.0 INTRODUCTION</b> .....	<b>6</b>
1.1 Problem Statement .....	6
1.2 Background.....	7
1.3 Objectives .....	12
1.4 Research Methodology .....	12
Task 1: Literature Review.....	13
Task 2: Materials Collection.....	13
Task 3: Characterization of Modified Asphalt Binders .....	14
Task 4: Laboratory Evaluation of Asphalt Mixtures .....	14
Task 5: Field Survey on Paving Projects with Highly Modified Binders.....	15
Task 6: Data Processing and Analyses .....	15
Task 7: Quarterly and Final Reports and Recommendations .....	16
<b>CHAPTER 2.0 LITERATURE REVIEW</b> .....	<b>17</b>
2.1 Background.....	17
2.2 Binder Modifiers.....	18
2.2.1 Fillers .....	18

2.2.2 Extenders.....	19
2.2.3 Polymers .....	20
2.2.4 Other Modifiers.....	22
2.3 Laboratory Testing Techniques and Specifications.....	23
2.3.1 Testing Methods and Specifications for Binders .....	23
2.3.2 Testing Methods and Specifications for Mixtures.....	29
2.4 Performance of Modified Binders and Mixtures .....	34
2.4.1 Laboratory Evaluation .....	34
2.4.2 Field Survey Results .....	39
2.5 Influencing Factors and Models .....	42
2.5.1 Empirically-Based Models.....	42
2.5.2 Mechanistic-Based Models.....	43
2.6 Modified Binders Used in Alaska.....	45
2.6.1 Climate Effect for Binder Selection.....	45
2.6.2 The History of Modified Binders Used in Alaska .....	48
2.6.3 Current Regional Status .....	50
2.6.4 Summary .....	53
<b>CHAPTER 3.0 EXPERIMENTAL DETAILS.....</b>	<b>54</b>
3.1 Materials .....	54
3.2 Binder Tests .....	56
3.2.1 Artificial aging process .....	57
3.2.2 DSR Test.....	60
3.2.3 BBR Test.....	62
3.2.4 ABCD Test.....	63
3.3 Mixture Specimen Fabrication.....	64
3.4 Laboratory Mixture Performance Tests.....	70
3.4.1 HWT Test.....	70
3.4.2 SCB Test .....	75

3.4.3 IDT creep compliance and strength tests .....	76
<b>CHAPTER 4.0 RESULTS AND ANALYSIS.....</b>	<b>79</b>
4.1 Binder Tests .....	79
4.1.1 High-Temperature Binder Grade .....	79
4.1.2 MSCR Test.....	80
4.1.3 Master Curves .....	84
4.1.4 BBR Test.....	91
4.1.5 Glover-Rowe (G-R) Parameter .....	100
4.1.6 $\Delta T$ .....	105
4.1.7 Crossover Frequency-Rheological Index Black Space .....	106
4.1.8 ABCD Test.....	108
4.2 Mixture Tests .....	109
4.2.1 HWT Test.....	109
4.2.2 SCB Test .....	115
4.2.3 IDT Test.....	116
4.2.4 Mixture Cracking Temperature.....	120
4.3 Field Evaluation.....	128
<b>CHAPTER 5.0 SUMMARIES AND CONCLUSIONS .....</b>	<b>132</b>
<b>REFERENCES.....</b>	<b>137</b>
<b>APPENDIX A JOB MIX FORMULAE.....</b>	<b>150</b>
<b>APPENDIX B AIR VOIDS OF SPECIMENS .....</b>	<b>160</b>
<b>APPENDIX C BINDER TESTING RESULTS .....</b>	<b>167</b>
<b>APPENDIX D MIXTURE TESTING RESULTS.....</b>	<b>186</b>

## LIST OF FIGURES

Figure 2.1 Alaska’s climatic zones (adapted from Miller et al. 1999) .....	45
Figure 2.2 Number of weather stations in: (a) high temperature grade; (b) low temperature grade (98% reliability and 130 weather stations in Alaska) (Zhao et al. 2016) .....	46
Figure 2.3 Environmental zones considered in the LTPP program (Perera et al. 2005) .....	47
Figure 3.1 Sieved collected aggregates.....	55
Figure 3.2 RTFO equipment.....	58
Figure 3.3 PAV equipment .....	58
Figure 3.4 DSR equipment .....	61
Figure 3.5 the BBR equipment .....	63
Figure 3.6 Asphalt binder cracking device .....	64
Figure 3.7 Superpave gyratory compactor.....	66
Figure 3.8 Masonry saw.....	67
Figure 3.9 IDT tests specimens.....	67
Figure 3.10 Gauge point fixing jig.....	68
Figure 3.11 HWT specimens after testing .....	68
Figure 3.12 SCB specimens.....	69
Figure 3.13 HWT test equipment.....	<b>Error! Bookmark not defined.</b>
Figure 3.14 Typical HWT test curve (after Yin et al. (2014)).....	72
Figure 3.15 HWT stripping number determination (Yin et al. (2014)). .....	74

Figure 3.16 SCB test equipment .....	75
Figure 3.17 IDT test equipment .....	78
Figure 4.1 <i>Jnr</i> vs % <i>R</i> for polymer modified binders at 52° C .....	<b>Error! Bookmark not defined.</b>
Figure 4.2 G* master curves of Binder#1 (PG 52-28/A) at different aging states .....	85
Figure 4.3 G* master curves of Binder#2 (PG 52-40/A) at different aging states .....	85
Figure 4.4 G* master curves of Binder#3 (PG 64-40/A) at different aging states .....	86
Figure 4.5 G* master curves of Binder#4 (PG 52-46/A) at different aging states .....	86
Figure 4.6 G* master curves of Binder#5 (PG 58-34/A) at different aging states .....	87
Figure 4.7 G* master curves of Binder#6 (PG 52-40/B) at different aging states.....	87
Figure 4.8 G* master curves of Binder#7 (PG 64-40/B) at different aging states.....	88
Figure 4.9 G* master curves of Binder#8 (PG 58-34/B) at different aging states.....	88
Figure 4.10 G* master curves of Binder#9 (PG 58-34/C) at different aging states.....	89
Figure 4.11 G* master curves of Binder#10 (PG 52-34/C) at different aging states.....	89
Figure 4.12 G* master curves of Binder#11 (PG 58-28/C) at different aging states.....	90
Figure 4.13 G* master curves of Binder#12 (PG 52-28plus/C) at different aging states.....	90
Figure 4.14 G* master curves of Binder#13 (PG 64-28/C) at different aging states.....	91
Figure 4. 15 BBR test results of Binder#1 (PG 52-28/A) at different aging states .....	92
Figure 4.16 BBR test results of Binder#2 (PG 52-40/A) at different aging states .....	93
Figure 4.17 BBR test results of Binder#3 (PG 64-40/A) at different aging states .....	93
Figure 4.18 BBR test results of Binder#4 (PG 52-46/A) at different aging states .....	94

Figure 4.19 BBR test results of Binder#5 (PG 58-34/A) at different aging states .....	94
Figure 4.20 BBR test results of Binder#6 (PG 52-40/B) at different aging states.....	95
Figure 4.21 BBR test results of Binder#7 (PG 64-40/B) at different aging states.....	95
Figure 4.22 BBR test results of Binder#8 (PG 58-34/B) at different aging states.....	96
Figure 4.23 BBR test results of Binder#9 (PG 58-34/C) at different aging states.....	96
Figure 4.24 BBR test results of Binder#10 (PG 52-34/C) at different aging states.....	97
Figure 4.25 BBR test results of Binder#11 (PG 58-28/C) at different aging states.....	97
Figure 4.26 BBR test results of Binder#12 (PG 58-28 Plus/C) at different aging states.....	98
Figure 4.27 BBR test results of Binder#13 (PG 64-28/C) at different aging states.....	98
Figure 4.28 Black Space Diagram with Glover-Rowe parameter <b>.Error! Bookmark not defined.</b>	
Figure 4.29 Glover-Rowe parameters of RTFO aged binders.....	103
Figure 4.30 Glover-Rowe parameters of 20h PAV aged binders .....	104
Figure 4.31 Glover-Rowe parameters of 40h PAV aged binders .....	104
Figure 4.32 $\Delta T$ of Alaskan asphalt binders with different aging states .....	106
Figure 4.33 Crossover frequency-rheological index black space .....	108
Figure 4.34 HWT rut depth results .....	112
Figure 4.35 HWT $\Delta \epsilon_{10,000}^{vp}$ results.....	113
Figure 4.36 Rut depth versus number of cycles for the studied Alaskan mixtures .....	115
Figure 4.37 $J_c$ values of studied Alaskan asphalt mixtures .....	116



Figure 4.38 Creep compliance values of studied Alaskan mixtures at different loading times: (a) 10 s; (b) 20 s; (c) 50 s; and (d) 100 s. ....	119
Figure 4.39 Indirect tensile strength results.....	120
Figure 4.40 Example of determination of mixture cracking temperature.....	122
Figure 4.41 Determining mixture cracking temperature for Mix #1 .....	122
Figure 4.42 Determining mixture cracking temperature for Mix #2 .....	123
Figure 4.43 Determining mixture cracking temperature for Mix #3 .....	123
Figure 4.44 Determining mixture cracking temperature for Mix #4 .....	123
Figure 4.45 Determining mixture cracking temperature for Mix #5 .....	124
Figure 4.46 Determining mixture cracking temperature for Mix #6 .....	124
Figure 4.47 Determining mixture cracking temperature for Mix #7 .....	125
Figure 4.48 Determining mixture cracking temperature for Mix #8 .....	125
Figure 4.49 Determining mixture cracking temperature for Mix #9 .....	126
Figure 4.50 Determining mixture cracking temperature for Mix #10 .....	126
Figure 4.51 Cracking temperatures of Alaskan mixtures .....	127
Figure 4.52 Richardson Hwy MP 337 Eielson AFB Intersection Improvements, PG 52-40, constructed in 2017 .....	130
Figure 4.53 Old Nenana/Ester Hill Rehabilitation, PG 52-40, constructed in 2018.....	130
Figure 4.54 Peger Rd Resurfacing / FMATS Ped Impr / NR Signal Interconnect, PG 52-40, constructed in 2017 .....	131

Figure 4.55 L & I Couplet and 5th & 6th Avenue Couplet, PG64-40, constructed in 2014/2015

..... 131

Figure 4.56 University Avenue Asphalt Surface Repairs, PG 52-28, constructed in 2010... **Error!**

**Bookmark not defined.**

## LIST OF TABLES

Table 1.1 Binder testing matrix .....	14
Table 2.1 Asphalt binder grades available in AASHTO M 320 (2016) .....	24
Table 2.2 Laboratory cracking tests summarized from NCHRP 09-57 (Zhou et al. 2016).....	31
Table 2.3 Asphalt binders being used currently in Alaska .....	46
Table 3.1 Matrix of studied binders.....	54
Table 3.2 Matrix of HMA mixtures.....	56
Table 3.3 Testing matrix (triplicates for each test).....	59
Table 3.4 Laboratory testing plan .....	70
Table 4.1 True high-temperature grades of tested Alaskan binders .....	79
Table 4.2 MSCR results.....	82
Table 4.3 Critical low temperature by limiting BBR parameters .....	99
Table 4.4 Critical temperature using different methods .....	109
Table 4.5 Examples of paving projects with highly polymerized binders... <b>Error! Bookmark not</b>	

**defined.**

## EXECUTIVE SUMMARY

Neat, unmodified PG 52-28 asphalt binder has been widely used in Alaska. However, experience indicates that hot-mix asphalt (HMA) produced with this neat binder may not be adequate for the various Alaskan climatic conditions. Recently, modified asphalts have attracted more attention. A highly-polymerized PG 64-40 HMA was recently placed in downtown Anchorage to address rutting and wear concerns in high-traffic areas and moderate low-temperature cracking concern. The low temperature grade of “-40” was selected instead of “-34” for improved workability. In addition, a “-40” low-temperature grade modified asphalt binder, PG 52-40, has been used recently in several paving projects in the Alaska Department of Transportation & Public Facilities (ADOT&PF) Northern Region (e.g. 2015 Airport Way resurfacing project in Fairbanks, Alaska). More paving projects using these highly-modified binders are expected in the upcoming construction seasons. Furthermore, the Northern Region is interested in the potential use of a colder low-temperature grade binder, such as PG 52-46, to suit its specific climatic conditions. However, data is lacking in terms of materials characterization and field performance monitoring of these modified asphalt binders and mixtures. It is essential to properly characterize the performance of the abovementioned modified asphalt binders as well as the resulting HMA in both the laboratory and the field.

The aims of this study are to conduct laboratory and field evaluation of the performance (i.e. plastic deformation and low temperature cracking performance) of various modified asphalt binders and mixes, and to quantify the performance benefits of these modified materials. The asphalt binders evaluated included one virgin binder (PG 52-28) and 12 different modified binders from three different suppliers (i.e. different base asphalts, different polymer formulations, different extender oils). Ten HMA mixtures (either Marshall or Superpave test procedures were used to produce HMA project mix designs) were either produced in the lab or collected from paving projects for laboratory performance evaluation. The performance testing specimens were fabricated in the laboratory using Superpave Gyrotory Compactor (SGC).

The binder tests included dynamic shear rheometer (DSR) tests for verification of binder grading, evaluation of viscoelastic behavior, master curves, multiple stress creep recovery (MSCR) tests associated with DSR setup, and bending beam rheometer (BBR) and asphalt binder cracking device (ABCD) tests for low-temperature performance evaluation. The Glover-Rowe parameter,  $\Delta T$ , Rheological Index, and crossover-frequency of the studied Alaskan asphalt binders at different aging states were calculated based on the complex modulus ( $G^*$ ) and phase angle ( $\delta$ ) master curves data. The mixture performance tests included Hamburg Wheel Tracking (HWT) tests for rutting resistance (plastic deformation) and moisture susceptibility, Semi-Circular Bend (SCB) tests for fatigue cracking resistance at intermediate temperatures, and indirect tensile (IDT) tests for creep compliance and low-temperature strengths. Mixture cracking temperature was determined with the IDT data.

The high-temperature performance-grade verification test results showed that the true high-temperature grades of some binders were not consistent with those provided by the suppliers. The true high temperature grades of binders #3 and #7 (PG 76-XX) were much higher than the grade indicated by the supplier, which was PG 64-XX. The true high temperature grades of binders #8 (PG 64-XX), #10 (PG 58-XX), #11 (PG 64-XX), and #12 (PG 58-XX) were one grade higher than the grade provided by the supplier. The true high temperature grade of binder #4 (PG 46-XX) was one grade lower than the grade provided by the supplier (PG 52-XX).

According to the MSCR test results, the non-recoverable compliance ( $J_{nr}$ ) of the neat binder was much higher than those of modified binders at the identical testing temperatures and stress levels, which indicated that the binder polymer modification improved the rutting (plastic deformation) resistance of the binder. The percent recovery (R) values of the modified asphalt binders were much higher than that of the neat binder. Most of the studied modified binders could be graded as “E” at 52°C without considering the percent difference of non-recoverable creep compliance ( $J_{nr-diff}$ ). The  $J_{nr-diff}$  values of the most of the modified binders at the testing temperatures exceeded the maximum criteria of 75%.

According to BBR results, the stiffness and m-value criteria showed similar critical low temperatures for each binder, when the binders were under unaged or Rolling Thin-Film Oven (RTFO) aged states. However, for 40h Pressure Aging Vessel (PAV) aged binders, the critical temperatures limiting by m-value were much higher than those limiting by stiffness. The test results verified the low temperature PG of the most studied binders. However, the tested low

temperature PGs of binder #4 (PG52-40), binder #7 (PG64-40), and binder #9 (PG 58-34) were one grade lower than those indicated by the suppliers. Glover-Rowe (G-R) parameter showed the potential to evaluate the low-temperature cracking resistance of the Alaskan binders. The location of G-R parameter for each binder in Black Space Diagram approached the Glover-Rowe damage zone (i.e.,  $180 \text{ kPa} \leq \text{G-R parameter} \leq 450 \text{ kPa}$ ) as the asphalt binder aged. The results showed that only the binders from supplier C with 40h PAV aging state (i.e., binders #10, #11, #12, #13) reached the threshold values, while other aged binders were not at risk for cracking, according to their locations of G-R parameters in Black Space Diagram.  $\Delta T$  increased as the asphalt aged, indicating that  $\Delta T$  has potential to evaluate and quantify the cracking susceptibility (durability loss) of the binder as well. The ABCD critical cracking temperature results showed that the measured cracking temperatures by ABCD were lower (colder) than the calculated cracking temperatures by BBR for all binders tested. The disparity could be attributed to the difference in the mechanism of the two different tests/procedures. The binder #4 (PG 52-46/A) did not crack at  $-60^\circ\text{C}$  during ABCD test.

According to the HWT test highly modified mixtures showed better rutting resistance than the control (unmodified) mixture. The Alaskan mixtures studied were not susceptible to moisture damage at the tested temperatures, as predicted by the HWT test. From the SCB test results, it appeared that the Mix #5 was the most fatigue cracking resistant mixture while the Mix #3 was the most susceptible to fatigue cracking at  $25^\circ\text{C}$ , and the unmodified mixture (Mix #8) showed better fatigue cracking resistance than some of the modified mixtures. Other fatigue tests

such as Illinois Flexibility Index test (I-FIT) and Fatigue Beam test are recommended to be conducted to consolidate the conclusion. The IDT creep compliance results indicated that the Mix #10 showed the least creep stiffness among the studied Alaskan mixtures. The mixture with the unmodified binder (Mix #8) showed the lowest  $D_t$  value at the testing temperatures, which implied that the mixtures with modified binders were softer than the mixture with the unmodified binder (Mix #8) at low temperatures. The unmodified mixture showed the highest IDT strength among all the studied Alaskan mixtures at the temperatures of  $-20^{\circ}\text{C}$  and  $-10^{\circ}\text{C}$ . The unmodified mixture showed higher cracking temperature than most of modified mixtures, with the exception of Mix #7. No statistical difference between Mix #7 and Mix #8 was found. The mixtures with binders with low-temperature PG of -40 showed lower cracking temperatures than the mixture with binder with low-temperature PG of -34.

According to the field surveys in recent years and interview with ADOT&PF engineers, the pavements with highly polymerized asphalt binders generally outperformed the pavements with unmodified asphalt binder.



## CHAPTER 1.0 INTRODUCTION

### 1.1 Problem Statement

Neat, unmodified PG 52-28 asphalt binder has been widely used in Alaska. However, experience indicates that hot-mix asphalt (HMA) produced with this neat binder may not be adequate for the various Alaskan climatic conditions. Recently, modified asphalts have attracted more attention. A highly-polymerized PG 64-40 HMA was recently placed in downtown Anchorage to address rutting and wear concerns in high-traffic areas and moderate low-temperature cracking concern. The low temperature grade of “-40” was selected instead of “-34” for improved workability. In addition, a “-40” low-temperature grade modified asphalt binder, PG 52-40, has been recently used in several paving projects in the Alaska Department of Transportation & Public Facilities (ADOT&PF) Northern Region (e.g. 2015 Airport Way resurfacing project in Fairbanks). More paving projects using these highly-modified binders are expected in the upcoming construction seasons. Furthermore, the Northern Region is interested in the potential use of a colder low-temperature grade binder, such as PG 52-46, to suit its specific climatic conditions. However, data is lacking in terms of materials characterization and field performance monitoring of these modified asphalt binders and mixtures. It is essential to properly characterize the performance of the abovementioned modified asphalt binders as well as the resulting HMA in both the laboratory and the field.

## 1.2 Background

Modification on some neat (non-modified) asphalt cements is required in order to meet specifications, producing modified asphalt binder. The use of modified binder has increased significantly in recent years mainly due to the increased demand on HMA pavements, development of Superpave asphalt binder specifications, environmental and economic pressure, and public agencies' willingness to pay higher-cost for longer pavement service life (Brown et al. 2009). Typically, modified asphalt is used to achieve the following improvements: lower stiffness at high construction temperatures to facilitate pumping of binder, mixing and compaction of HMA, higher stiffness at high service temperatures to reduce rutting and shoving, lower stiffness and faster relaxation properties at low service temperatures to reduce thermal cracking, and increased adhesion between asphalt binder and aggregate to reduce stripping (Terrel and Epps 1988; Brown et al. 2009).

The list of asphalt modifiers is rapidly changing with innovative additives being constantly developed. Fillers are among the earliest materials used to modify asphalt binder properties. Typically, increasing filler content lowers the optimum asphalt content, increases the density, and increases the stability of HMA (Brown et al. 1989). Extenders such as sulfur (Kandhal et al. 1983) and lignin (Terrel & Rimsritong 1979) were prominently investigated after the 1973 oil embargo. The most commonly used asphalt modifiers are polymers. Polymers are

very large molecules that are made of long chains or clusters of smaller molecules (monomers) (Brown et al. 2009). The physical properties of a polymer are determined by the sequence and chemical structure of the monomers, therefore the polymer can be engineered to obtain a broad range of properties when varying its composition monomers. Polymers are generally divided into two categories: elastomers and plastomers. Elastomers include natural rubber, styrene-butadiene rubber (SBR) latexes or SBR, styrene-butadiene-styrene (SBS) block copolymers, styrene-isoprene-styrene (SIS) block copolymers, polychloroprene latexes, and crumb rubber modifiers (Brown et al. 2009). These polymers add very little strength to the asphalt until they are stretched, but resist deformation from applied stress by stretching and recovering their shape quickly when stress is removed (Hines 1993). Among the elastomers, SBS and SBR are most often used in HMA to bump the PG high temperature grade of the modified binder for higher rutting resistance. Plastomers exhibit quick early strength on loading due to a tough, rigid, three dimensional network which is also resistant to deformation, but may fracture under strain (Hines 1993). These polymers include polyethylene, polypropylene, ethyl vinyl acetate (EVA), polyvinyl chloride (PVC), ethylene propylene (EPDM), and polyolefins (Brown et al. 2009). Another commonly used modifier is Polyphosphoric Acid (PPA) developed for improving both high and low temperature performance, which can be used as a modifier in combination with polymers (Daranga et al. 2009). Typical modifiers used to improve low temperature properties of asphalt binder include various kinds of oil depending on certain applications, especially high

flash point oils (Shi et al. 2001; Rubab et al. 2011; Golalipour 2013). Other binder modifiers are generally used for specific purposes: fibers are used due to their potential of reinforcing and improving the tensile strength and cohesion of HMA mixtures (NAPA 1994); recycling agents are used to restore aged asphalt cement to requirements of asphalt cement specifications (Little et al. 1981); antistripping agents are used to minimize or eliminate stripping of asphalt cement from aggregate in HMA mixtures (Tunnicliff & Root 1982).

Characterization methods and tests for modified binders have evolved along with their increased use. Since the Superpave performance grading (PG) was developed as part of Superpave system (Anderson & Kennedy 1993), modification efforts have focused on increasing the PG grades of asphalt binder at various situations. The Superpave binder tests, therefore, were generally adopted to characterize both neat and modified binders. Some additional tests were adopted by asphalt practitioners to characterize modified asphalt only, such as separation test for assessment of polymer-asphalt compatibility (ASTM 2014), solubility test (ASTM 2009), recovery and stress-strain tests for measurement of the binder's ability to stretch when loaded and unloaded including elastic recovery, force ductility, and toughness and tenacity tests (ASTM 2012), etc. In the meantime, extensive efforts were also conducted for better characterization of modified asphalt binders. The most comprehensive national study was the National Cooperative Highway Research Program (NCHRP) project 9-10, which was completed in 2001 and resulted in NCHRP Report 459, *Characterization of Modified Asphalt Binders in Superpave Mix Design*

(Bahia et al. 2001). The study indicated that AASHTO MP1 specification, *Standard Specifications for Performance Graded Asphalt Binder* did not adequately characterize the performance of modified asphalt binders. The low temperature cracking performance of modified binders was specifically included in a National Pooled Fund Study, *Investigation of Low Temperature Cracking in Asphalt Pavements* (Marasteanu et al. 2007; Marasteanu et al. 2012). One of the key findings for modified binders is that low temperature cracking performance cannot rely entirely on PG of the binder and a critical need exists for an asphalt mixture specification. It was also found that Disc-Shaped Compact Tension (DCT) and Semi-Circular Bend (SCB) fracture tests could discriminate between different modified HMA mixes. The abovementioned research efforts along with many others not mentioned have motivated the update of current specifications for characterizing modified binder. One of the most significant improvements is the development of AASHTO M-332 (2014), *Performance-Graded Asphalt Binder Using Multiple Stress Creep Recovery (MSCR) Test*, which was based on research findings showing that the non-recoverable creep compliance ( $J_{nr}$ ) from MSCR test (AASHTO T-350) could identify the rutting performance of modified binder significantly better than the PG high temperature parameter,  $G^*/\sin\delta$  (FHWA 2011). Another significant move applicable to both modified and non-modified binders is to specify a critical low cracking temperature which reflects both the rheological and failure characteristics of a binder by combining Superpave bending beam rheometer (BBR) and direct tension tester (DTT) results (Bouldin et al. 2000). The

critical low cracking temperature determination (AASHTO R49) has been included in the current AASHTO specification M320 (2016) as verification of low temperature grade determined by both BBR and DTT tests.

In recent years, modified asphalt binders have been used in a number of studies to address specific pavement distresses or issues in Alaska. A study on Rutting Analysis for Anchorage Pavements assessed rutting performance of one polymer modified PG 64-28 binder in the Central Region (Ahmed 2007). In Alaska's first trial warm mix asphalt project established in ADOT&PF's Southcoast Region, modified binder PG 58-28 was used as base asphalt to produce WMA binder mixed with various dosages of Sasobit (Liu and Li 2011). Nine projects using PG 64-34 binder were evaluated in another study to establish a catalog of dynamic modulus for pavement analysis and develop correlations between simple performance test results and HMA performance (Li and Liu 2014). The PG 64-34 binder was also used in a project to assess the engineering properties and performance of paving interlayer-reinforced asphalt pavement (Li et al. 2016). The low-temperature performance of modified binders such as PG 58-34 and PG 64-34 was investigated in a recent study (Zhao et al. 2016). Another recently completed study conducted to characterize Alaskan HMA containing reclaimed asphalt pavement also included modified binders such as PG 58-34 and PG 52-40 (Liu et al. 2016). Past research efforts have promoted the use of modified asphalt in Alaska. However, Alaskan modified binders, especially highly modified binders (such as PG 52-40 and PG 64-40) used in recent paving projects, have

not been systematically characterized in these past studies. Currently PG 58-28 and PG 64-28 have had acceptable performance in ADOT&PF Southcoast Region. However, for areas with extreme conditions like interior and central Alaska, local characterization is extremely important. In addition, no other study has been found, which addresses Alaska's situation with respect to locally available materials (from local producers) and climatic conditions.

### **1.3 Objectives**

The main objectives of this study are to conduct laboratory and field evaluation of the performance (i.e. rutting and low temperature cracking performance) of various modified asphalt binders and mixes, to quantify the performance benefits of these modified materials, and to assist Alaska DOT/PF develop a Statewide "PG+" specification for asphalt binders based on all of the testing performed.

### **1.4 Research Methodology**

The following major tasks were accomplished to achieve the objectives of this study:

- Task 1: Literature Review
- Task 2: Materials Collection
- Task 3: Characterization of Modified Asphalt Binders
- Task 4: Laboratory Evaluation of Asphalt Mixtures
- Task 5: Field Survey on Paving Projects with Highly Modified Binders
- Task 6: Data Processing and Analyses

- Task 7: Quarterly and Final Reports and Recommendations

### ***Task 1: Literature Review***

The literature review covered the up-to-date practices and research findings of using modified binder, particularly in cold climates. Specific focuses were laboratory-testing techniques, field survey results, effects of influencing factors, corrective measures to address the concerns, and empirical and mechanistic models for assessment of the potential distresses such as rutting and low temperature cracking, and recommended PG+ specification with acceptance. Alaskan air and pavement temperature studies were reviewed to assess the adequacy of the high and low Performance Grade (PG) temperatures used for Alaskan binders (as determined from the LTTPBind software). The review included Kraton's HiMA mixes placed nationwide in paving projects and tested at accelerated testing facilities. This mix uses the same SBS polymer type and dosage as Anchorage's PG 64-40 mixes. The review included the state-of-practice in terms of MSCR,  $\Delta T$ , black space diagram, master curve rheological indices and parameters, as they relate to rutting, cracking and binder viscoelastic behavior. This task is presented in Chapter 2.

### ***Task 2: Materials Collection***

Asphalt binders were collected from selected suppliers in Alaska. Binder grades covered PG 52-28 (as control neat binder), PG 64-40, PG 52-40, PG 58-34, PG 52-34, PG 64-28, and PG 52-46. Asphalt mixtures were either collected from identified field projects or produced in the



Asphalt Lab at Missouri University of Science and Technology (MST). Details of materials information and job mix formula were provided. This task is presented in Chapter 3.

***Task 3: Characterization of Modified Asphalt Binders***

Binder characterization focused on evaluating high and low temperature behavior of the various modified binders at various aged stages. Table 1.1 summarizes the binder testing matrix.

This task is presented in Chapter 3.

Table 1.1 Binder testing matrix

<b>Test</b>	<b>Property</b>	<b>Binder status</b>	<b>Standard</b>
Dynamic shear rheometer (DSR)	Viscoelastic behavior + rutting	RTFO RTFO+20h PAV, RTFO+40h PAV	AASHTO T315
MSCR	Rutting	RTFO	AASHTO T350
BBR	Low temperature cracking	RTFO RTFO+20h PAV, RTFO+40h PAV	AASHTO T313
Asphalt binder cracking device (ABCD)	Low temperature cracking	RTFO+20h PAV	AASHTO TP92

***Task 4: Laboratory Evaluation of Asphalt Mixtures***

The SCB test (ASTM D8044) and the Hamburg wheel tracking (HWT, AASHTO T324) were used to evaluate cracking and rutting resistance of asphalt mixtures produced with the above binders. HWT test temperatures (50°C for mixtures with PG 64-40; 40°C for the other mixtures) were decided after consulting with the technical advisory committee, and mix parameters obtained from the HWT were determined according to information found in Yin et

al.'s study (2014). The indirect tensile (IDT, AASHTO 322-07) tests, including tensile strength and tensile creep compliance properties, were conducted for evaluation of low temperature cracking performance. The description of the mixture performance tests listed in this task is presented in Chapter 3.

#### ***Task 5: Field Survey on Paving Projects with Highly Modified Binders***

Pavement surveys were conducted on selected field sites paved with modified asphalt mixtures, which included recently constructed sections such as Old Nenana/Ester Hill Rehabilitation project using PG 52-40 binder and downtown Anchorage section using PG 64-40 binder, as well as previously established and future sites using modified binders in interior and central Alaska.

#### ***Task 6: Data Processing and Analyses***

Data obtained from previous tasks was processed and analyzed. The binder and mixture performance data along with the field survey data were synthesized to provide a catalog of Alaskan asphalt materials with modified binders. Further data processing and analyses included:

- Correlating results of binder DSR rutting index and MSCR test with mixture rutting performance data from HWT tests, and explored modified binder's contribution to potential improvement on mixture's rutting resistance;
- Using DT creep and strength data collected in Task 4 to calculate cracking temperature of mixtures; and comparing and correlating cracking temperature of asphalt binder with that

of mixture to investigate how modified binder contributes to the mixture's low temperature performance; and using rheological master curve for complex modulus ( $G^*$ ) and phase angle ( $\delta$ ), Black Space Diagram ( $G^*$  versus  $\delta$ ), and corresponding rheological indices and parameters; and

- Quantifying relative loss of relaxation due to long-term aging using BBR  $\Delta T$  results.

***Task 7: Quarterly and Final Reports and Recommendations***

Quarterly and progress reports were submitted during the above tasks. Upon completion of the aforementioned tasks, a final report was completed. The report included literature review, description of the research methods and approach for this project, laboratory and field evaluation results as well as discussion of the results. A summary of conclusions and recommendations to ADOT&PF was provided.

## CHAPTER 2.0 LITERATURE REVIEW

### 2.1 Background

Asphalt is one of man's oldest engineering materials due to its early-known adhesive and waterproofing properties (Barth 1962). Commercial asphalt broadly includes two categories: natural asphalts and petroleum refined asphalts. Although the first asphalt pavement was placed using Trinidad Lake natural asphalt in 1876, the good quality of the refined asphalts has forced the natural asphalts into a position of relative unimportance (Traxler 1961; Brown et al. 2009). Asphalt cement is the most commonly used refined asphalt type in flexible pavement construction. At ambient temperatures, it is a black, sticky, semisolid, and a highly viscous material with adhesive and waterproofing characteristics (Brown et al. 2009). When heated at high enough temperature, asphalt cement can be readily liquefied for mixing with mineral aggregates to produce HMA. During mixing, the sticky asphalt cement adheres to the aggregate particles and binds them together. HMA is very strong paving material after compaction and cooling to ambient temperature, which can sustain heavy traffic loads on highways and heavy duty airfields.

The performance of asphalt binder is highly temperature dependent. An ideal asphalt binder should be produced to satisfy the following features (Terrel and Epps 1988): lower viscosity at construction temperatures to facilitate pumping of the liquid asphalt, and further

mixing and compaction of HMA; higher stiffness at high service temperatures to reduce rutting and shoving during the summer time; lower stiffness and faster relaxation properties at low temperatures to reduce thermal cracking during winter time; increased adhesion between asphalt binder and aggregate in the presence of moisture to reduce stripping. The need for these binder features and the development of the performance grading system have motivated the industry of binder modification.

## **2.2 Binder Modifiers**

There exist numerous binder modifiers in the current asphalt industry. Several key questions must be considered before any modifier is widely used (McGennis 1995): What improvement is needed? What modifier will work best? How should the modifier be incorporated into the binder and/or mixtures? Should compatibility be considered? How should the binder be stored to maintain its properties over a length of time? How should the binder be specified? Does the modifier affect routine test results? Can the modifier mixture be recycled? What is the effect on life cycle cost? The following is a discussion of several typical modifiers.

### **2.2.1 Fillers**

Fillers are among the earliest materials used to modify asphalt binder properties. They can be from various sources such as crushing and screening of aggregates, fly ash, and Portland cement. Typically, mineral fillers are used to fill the voids between the aggregate particles in HMA. The increase of filler content lowers the optimum asphalt content, increases the density,

and increases the stability (Brown et al. 1989). However, asphalt binder properties have been reported to be affected by addition of fillers. For example, a stiffening or reinforcing effect has been observed on HMA when baghouse fines were added (Kandhal 1981). However, the stiffening degree was highly dependent upon Rigden void content, which represented voids between the fine particles in the dry compacted state (Brown et al. 2009).

### ***2.2.2 Extenders***

The Federal Highway Administration (FHWA) promoted asphalt extenders such as sulfur (Kandhal et al. 1983) and lignin (Terrel and Rimsritong 1979) for investigation after the 1973 oil embargo. Sulfur is a non-metallic chemical element. It is a crystalline solid at room temperature, but melts into liquid with lower viscosity than asphalt cement when heated to HMA production and construction temperatures ranging from 250 °F to 290 °F (121 °C to 143 °C). Generally, the performance of pavements constructed with sulfur extended asphalt binder has been found equal to conventional HMA pavements (Fromm 1981; Kandhal 1982). However, only a portion of sulfur was believed to function as binder modifier with the remaining portion acting like a filler.

Wood lignin is a cementitious material that binds wood fibers together and is a high volume waste from pulp and paper production. Terrel and Rimsritong (1979) evaluated the use of lignins in three possible ways: as a substitute for asphalt, as an extender for asphalt cement in HMA, and as an extender of emulsified asphalt in conjunction with rubber in cold mixtures. Their findings were positive at the time that using wood lignin as a partial replacement of asphalt

is technically and economically feasible. However, using lignin alone was found to be impossible as a substitute for asphalt.

### ***2.2.3 Polymers***

The most commonly used asphalt modifiers are polymers. A polymer is a very large molecule that is made of long chains or clusters of smaller molecules (monomers). The physical properties of the polymer are determined by the sequence and chemical structure of the monomers (Brown et al. 2009). Therefore, a broad range of properties can be engineered when varying a polymer's composition monomers. For asphalt modification, polymers can be divided into two categories: elastomers or rubbers, and plastomers or plastics.

#### ***2.2.3.1 Elastomers (Rubbers)***

Elastomer polymers generally stretch and recover their shape quickly when stress is applied and released, therefore resisting deformation. Very little strength is added to asphalt cement from these polymers when they are stretched, but their tensile strength increases with elongation (Hines 1993). Typical elastomers include natural rubber, styrene-butadiene rubber (SBR) latexes or SBR, styrene-butadiene-styrene (SBS) block copolymers, styrene-isoprene-styrene (SIS) block copolymers, polychloroprene latexes, and crumb rubber modifiers (Brown et al. 2009). SBS and SBR are most often used elastomers in HMA. The asphalt industry uses SBS and SBR as common additives to bump the PG high temperature to make asphalt mixture more resistant to rutting. Crumb rubber from recycled tires is another elastomer that has been widely

promoted and used in the asphalt paving industry. It is primarily used in HMA by two processes: the wet process blends the crumb rubber with the asphalt cement prior to HMA mixing, typically in the field; the dry process mixes the crumb rubber with aggregate before asphalt cement is incorporated (Brown et al. 2009). Terminal blended (TR) rubberized asphalt is going mainstream in recent years. Differing from the “wet process”, the TR rubberized asphalt is manufactured at the refinery or terminal, not in the field.

#### *2.2.3.2 Plastomers (Plastics)*

Plastomers generally resist deformation because of their tough, rigid, three-dimensional network. These polymers include polyethylene, polypropylene, ethyl vinyl acetate (EVA), polyvinyl chloride (PVC), ethylene propylene (EPDM), and polyolefins (Brown et al. 2009). They exhibit quick early strength applied stress but may fracture under strain (Hines 1993). Low density polyethylene (LDPE) is an important plastomer used in HMA, which can also be collected by recycling. The high viscosity of polyethylene modified asphalt increases the mixing and laydown temperature of HMA by about 35 °F compared to unmodified HMA. EVA is another important plastomer that is available in the form of free-flowing pellets in bags or bulk. It must be compatible with the neat asphalt to obtain the desired properties.

#### *2.2.3.3 Combinations*

As discussed above, modifying asphalt cements with elastomers usually result in more flexible and resilient HMA pavements. On the other hand, the stiffness of HMA pavements is



generally increased when plastomers are added. However, many other factors may determine the modification results, including chemical composition and concentration of the modifier, crude source of the asphalt, refining process, and grade of the neat asphalt, etc. (Brown et al. 2009)

Further, elastomers and plastomers can be combined to provide special properties to the modified asphalt to satisfy a desired situation. For example, the addition of a plastomer may increase the rutting resistance of HMA in summer but makes no contribution to its low-temperature cracking performance in winter. The combination of this plastomer and an elastomer such as rubber may improve HMA's low-temperature properties as well. However, adverse side effects and cost should be thoroughly balanced when any polymer combination is used for a paving project.

#### ***2.2.4 Other Modifiers***

Other modifiers are generally used for specific purposes, including fibers, softening agents, stiffening agents, antistripping agents, etc. Fibers are used to reinforce and improve the tensile strength of HMA (NAPA 1994, McDaniel 2015). They also have the potential of improving the cohesion of HMA and permitting higher asphalt contents than conventional HMA without draindown problem (Brown et al. 2009), which is especially important for open-graded friction courses. Softening or recycling agents are used to restore the physical and/or chemical properties of the aged asphalt cement to requirements of a new asphalt cement (Little et al. 1981). Stiffening agents like gilsonite and Trinidad lake asphalt are sometimes used to modified neat asphalt for certain applications such as use in high stress areas. Antistripping agents are used

to minimize or eliminate binder stripping in HMA. They can be liquid additives that are surface active to increase adhesion of asphalt to aggregate, or lime additives that are added to the aggregate prior to mixing with asphalt cement (Brown et al. 2009).

## **2.3 Laboratory Testing Techniques and Specifications**

### ***2.3.1 Testing Methods and Specifications for Binders***

The method that is mostly adopted by state highway departments nowadays to classify asphalt cements is the PG system. Developed in the Strategic Highway Research Program (SHRP), the PG was meant to be performance-based, which is to address three primary performance distresses of HMA pavements: permanent deformation (rutting), fatigue cracking, and low temperature (thermal) cracking (Brown et al. 2009). The binder modification has been focused on changing PGs of asphalt binder since the development of the Superpave PG grading system (Anderson and Kennedy 1993). This classification considers asphalt performance at high, intermedium, and low temperatures, and involves testing the asphalt unaged, aged in the thin film oven test, and aged in the pressure aging vessel. The latest PG specification is detailed in AASHTO M 320 (2016). Table 2.1 shows the binder grades available in AASHTO M 320 (2016). A simple interpretation is that a PG 58-28 should provide an asphalt cement that is stiff enough to resist rutting at high service temperatures up to 58 °C and flexible enough to resist thermal cracking at low service temperatures down to -28 °C.

Table 2.1 Asphalt binder grades available in AASHTO M 320 (2016)

<b>High Temperature Grades (°C)</b>	<b>Low Temperature Grades (°C)</b>
PG 46	-34, -40, -46
PG 52	-10, -16, -22, -28, -34, -40, -46
PG 58	-16, -22, -28, -34, -40
PG 64	-10, -16, -22, -28, -34, -40
PG 70	-10, -16, -22, -28, -34, -40
PG 76	-10, -16, -22, -28, -34
PG 82	-10, -16, -22, -28, -34, -40

In this system, the rolling thin film oven (RTFO) test specified in AASHTO T 240 (2013) and pressure aging vessel (PAV) test following AASHTO R 28 (2016), are adopted to simulate the short-term and long-term asphalt aging, respectively. To ensure that asphalt binder is sufficiently fluid for pumping and mixing, the rotational viscometer is used for determining the viscosity of asphalt at high construction temperatures (AASHTO T 316 2013). The rheological properties of asphalt binder can be determined using a DSR according to AASHTO T 315 (2016). A rutting factor of the asphalt,  $G^*/\sin\delta$ , at high service temperature, and a fatigue factor,  $G^*\cdot\sin\delta$ , at intermediate temperature can be determined from the DSR test to build Superpave binder specification (AASHTO M 320 2016). The Superpave system uses BBR and direct tension tester (DTT) to specify asphalt's low temperature performance according to AASHTO T 313 (2016) and AASHTO T 314 (2016), respectively.

Researchers have never stopped seeking more accurate or effective methods of characterizing modified asphalt binders, namely “PG Plus” tests. The National Cooperative

Highway Research Program (NCHRP) project, Characterization of Modified Asphalt Binders in Superpave Mix Design (Bahia et al. 2001), is one of the most comprehensive studies of its kind. The NCHRP Report 459 derived from this project concluded that the commonly-used AASHTO MP1 specification, Standard Specifications for Performance Graded Asphalt Binder, at the time did not adequately characterize the performance of modified asphalt binders. To establish a better rating of binders in terms of mixture rutting, the viscous component of the creep stiffness,  $G_v$ , was recommended to replace the Superpave parameter  $G^*/\sin\delta$ . For better correlation between binder rating and mixture fatigue, the number of cycles to crack propagation,  $N_p$ , was recommended to replace the existing parameter  $G^*\cdot\sin\delta$ . Both the two proposed parameters could be obtained from newly developed testing procedures with the DSR. For thermal cracking, it was recommended that binder specification include a direct measure of the glass transition temperature of the binder, and a consideration of a region-specific design-cooling rate.

One of the most important improvements for characterization of modified binder is the development of AASHTO M 332 (2014), *Performance-Graded Asphalt Binder Using Multiple Stress Creep Recovery (MSCR) Test*. The MSCR test (AASHTO T 350 2014) uses the well-established creep and recovery test concept to evaluate a binder's potential for rutting performance (FHWA 2011). Its use to determine binder's high temperature grade was motivated by the poor correlation observed between the existing parameter  $G^*/\sin\delta$  and the rutting performance of modified asphalt mixture. The major difference between the MSCR and the old

Superpave high temperature specifications is how grade bumping is done. Under the old system, the need of binder grade bumps requires testing at higher temperatures, sometimes providing very misleading information. For the MSCR system, the test can be done at one specific temperature. The FHWA (2011) used Accelerated Loading Facility (ALF) to evaluate full scale test sections constructed with multiple neat and modified binders to evaluate the relationship of the MSCR specification parameter  $Jnr$  and existing PG parameter  $G^*/\sin\delta$  to actual rutting. Test sections were built with neat, air-blown, SBS-modified, crumb rubber-modified and Elvaloy-modified binders. It was found that the  $Jnr$  from MSCR test could identify the rutting performance of modified binder significantly better than the PG high temperature parameter,  $G^*/\sin\delta$  (FHWA 2011).

The low temperature cracking performance of modified binders was thoroughly investigated in a National Pooled Fund Study, Investigation of Low Temperature Cracking in Asphalt Pavements (Marasteanu et al. 2007; Marasteanu et al. 2012). It was found that PG system seemed to be “blind” to improved fracture properties at low temperature due to polymer modification. One of the key findings was that the failure strain at the minimum pavement temperature obtained from the direct tension test correlated best with field occurrence of thermal cracking. Physical hardening had a significant effect on binder properties and seemed to be an important variable for BBR and fracture testing. It was strongly recommended that the selection of fracture resistant binders be based on simple-to-perform true fracture tests.

The AASHTO BBR specification controls the thermal cracking of binder by limiting the asphalt binder stiffness based on an assumption that binders with higher stiffness will crack at a warmer temperature than softer binders (Devol 2010). The ABCD was developed to directly measure the cracking temperatures of asphalt binders and in conjunction with other test methods to accurately grade asphalt binders for low-temperature performance (Kim 2005; Kim 2010). The ABCD utilizes a metal ring with a very low coefficient of thermal expansion, surrounded by a ring layer of asphalt to be tested. When the temperature drops at a rate of 20 °C per hour, the thermal stresses develop within the asphalt until the outer asphalt ring cracks then the test is ended. The temperature point at which the asphalt cracks is measured as the cracking temperature that can be compared with the low temperature PG of the asphalt binder.

The cracking temperature of both modified and non-modified binders can also be determined with the Superpave BBR and DTT tests by combining their rheological and failure characteristics (Bouldin et al. 2000). The thermal stress curve of a binder can be derived from BBR data and the strength curve can be developed with DTT data obtained at different temperatures. The binder cracking temperature is determined at the intersection of thermal stress and strength curves (AASHTO R 49 2013). AASHTO M 320 (2016) includes this cracking temperature as verification of low temperature grade determined by BBR and DTT tests.

In order to conveniently monitor the loss of durability of asphalt pavement, two potential parameters were identified for this purpose (Anderson et al. 2011). The first was a DSR

parameter, calculated as  $G''/(\eta'/G')$ . The second one was  $\Delta T$ , the difference in continuous grade temperature for stiffness and relaxation properties determined by BBR test. Anderson et al. (2011) tested binders in their unaged condition, as well as binders that had undergone long-term aging in the PAV at 100 °C and 2.1 MPa pressure for 20, 40, and 80 hours. The parameters  $G''/(\eta'/G')$  and  $\Delta T$  appeared to quantify the loss of relaxation properties as an asphalt binder aged. Field test sections that were built on airfield asphalt pavements confirmed the laboratory findings. A threshold value of  $G''/(\eta'/G')$  and  $\Delta T$  was determined based on the study results to provide an indication of a loss of durability that could result in a greater risk of non-load associated cracking.

The simple rheological plots of  $G^*$  versus  $\delta$ , commonly referred to as Black Space Diagrams, have also been considered to predict asphalt's low-temperature or age-induced cracking (King et al. 2012). The Black Space Diagrams can be directly measured by DSR, so the mathematical shifts of data obtained at various temperatures due to time-temperature superposition (TTS) of asphalt binder can be avoided. The TTS data shifting may miss the phase changes in the binder, such as wax crystallization known to cause low temperature physical hardening. The same low temperature portion of Black Space master curve is reported to be most relevant to age-related damage mechanisms, because crack growth accelerates as pavements cool.

In addition to the abovementioned tests, other tests have been adopted by asphalt practitioners to characterize special situations for modified asphalts, such as separation test for

assessment of polymer-asphalt compatibility (ASTM D7173 2014), solubility test (ASTM D5546 2009), recovery and stress-strain tests for measurement of the binder's ability to stretch when loaded and unloaded including elastic recovery, force ductility, and toughness and tenacity tests (ASTM D5801 2012).

### ***2.3.2 Testing Methods and Specifications for Mixtures***

The most commonly used rutting evaluation method for HMA is perhaps the AASHTO T 340 (2015), Standard Method of Test for Determining Rutting Susceptibility of HMA Using the Asphalt Pavement Analyzer (APA). During the test, samples with the target air voids of  $7 \pm 0.5\%$  are loaded under a pneumatic hose by a 445 N (100 lbf) steel wheel and tested at temperature between 4 and 72 °C (40 and 160 °F). Rut depth at 8000 cycles are typically recorded for comparison of rutting performance.


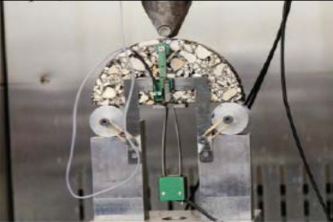
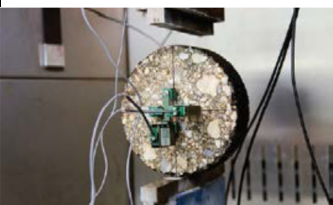

In spite of their wide use, the HWT parameters, SIP and the rut depth at a certain number of load cycles, have been questioned regarding their accuracy and variability. Three new parameters,  $LC_{SN}$ ,  $LC_{ST}$ , and  $\Delta\varepsilon_{10,000}^{vp}$ , were recently proposed by Yin et al. (2014) to introduce a novel method to analyze the HWT results.  $LC_{SN}$  represents the maximum number of load cycles that the asphalt mixture can resist in the HWT before the adhesive fracture occurs between asphalt and aggregate.  $LC_{ST}$  is stripping life of mixture that represents the number of additional load cycles after  $LC_{SN}$  needed for the rut depth accumulated by the predicted stripping strain to reach the common HWT failure depth of 0.5 in. (12.5 mm).  $\Delta\varepsilon_{10,000}^{vp}$  is viscoplastic strain








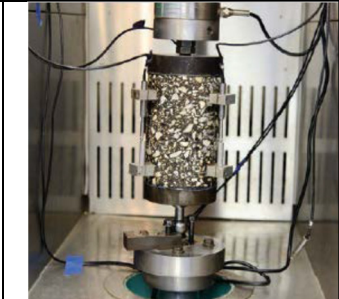
increment calculated as the slope of the projected viscoplastic strain by the Tseng-Lytton model at 10,000 load cycles (Yin et al. 2014).  $LC_{SN}$  and  $LC_{ST}$  were proposed to evaluate mixture susceptibility to moisture before and after stripping happens, respectively.  $\Delta\varepsilon_{10,000}^{vp}$  was used to quantify mixture rutting resistance while  $LC_{SN}$  was meant to complementarily the rutting resistance in the presence of water.

A comprehensive review of existing cracking tests suitable for routine asphalt mixture designs was conducted in by the NCHRP 9-57 (Zhou et al. 2016), *Experimental Design for Field Validation of Laboratory Tests to Assess Cracking Resistance of Asphalt Mixtures*. A total of 10 cracking tests were identified with some considered practical while others showing promise. Table 2.2 summarizes detailed descriptions of 10 tests, including test configuration, cracking type evaluated and parameter, test standard or specification, time, variability, correlation to field performance, test sensitivity to mix design parameters, and adoption by states.

Table 2.2 Laboratory cracking tests summarized from NCHRP 09-57 (Zhou et al. 2016)

Name	Configuration	Cracking	Test	Correlation to field performance	Test sensitivity to mix design parameters	Adoption by states
Disk-shaped compact tension (DCT)		<ul style="list-style-type: none"> <li>Type: low temperature cracking and reflection cracking</li> <li>Parameter: fracture energy</li> </ul>	<ul style="list-style-type: none"> <li>Standard: ASTM D7313 (Monotonic test)</li> <li>Time: 1-6 min</li> <li>Variability: low (COV=10–15%)</li> </ul>	Good correlation with low-temperature cracking validated at MnRoad	Asphalt binder, aggregate, RAP/RAS, and aging; insensitive to AV and Pb	Adopted by Minnesota and Wisconsin; being considered by Colorado, South Dakota, and Montana
SCB at low temperature		<ul style="list-style-type: none"> <li>Type: low temperature cracking</li> <li>Parameter: fracture energy</li> </ul>	<ul style="list-style-type: none"> <li>Standard: AASHTO TP105 (Monotonic test)</li> <li>Time: 30 min</li> <li>Variability: medium (COV=20%)</li> </ul>	Good correlation with low-temperature cracking validated at MnRoad	Asphalt binder, aggregate, RAP/RAS, AV, and Pb	Being considered by Utah, South Dakota, Pennsylvania, and Montana
IDT for low temperature cracking		<ul style="list-style-type: none"> <li>Type: low temperature cracking</li> <li>Parameter: creep compliance and tensile strength</li> </ul>	<ul style="list-style-type: none"> <li>Standard: AASHTO T322</li> <li>Time: 4-6 hours</li> <li>Variability: low (COV&lt;11%)</li> </ul>	Creep compliance and tensile strength inputs to TCMODEL; calibrated and validated through original SHRP and MEPDG	Asphalt binder, aggregate, RAP/RAS, aging	AASHTO T322 is required by AASHTOWare
Uniaxial thermal stress and strain test (TSRST)		<ul style="list-style-type: none"> <li>Type: low temperature cracking</li> <li>Parameter: fracture temperature (coefficient of thermal contraction from UTSST)</li> </ul>	<ul style="list-style-type: none"> <li>Standard: AASHTO TP10/University of Nevada at Reno (Monotonic test)</li> <li>Time: 3-5 hours</li> <li>Variability: low (COV= around 10%)</li> </ul>	Validated with test sections during SHRP program; MnRoad test results showed moderate correlation with field performance	Asphalt binder, aggregate, AV, Pb, and aging	Being considered by Nevada

Texas overlay test (OT)		<ul style="list-style-type: none"> <li>• Type: reflection cracking and bottom-up fatigue cracking</li> <li>• Parameter: No. of cycles (or fracture parameters: A and n)</li> </ul>	<ul style="list-style-type: none"> <li>• Standard: Tex-248-F (cyclic tests)</li> <li>• Time: 30 min-3 hours</li> <li>• Variability: relatively high (COV=30-50%)</li> </ul>	Good correlation with reflection cracking; promising correlation with fatigue cracking validated with FHWA-ALF and NCAT test track	Binder, aggregate, Pb, RAP/RAS, aging, etc.	Adopted by Texas and New Jersey; being considered by Montana, Nevada, Florida, and Ohio
Bending beam fatigue (BBF) test		<ul style="list-style-type: none"> <li>• Type: bottom-up fatigue cracking</li> <li>• Parameter: No. of cycles (or fatigue equation)</li> </ul>	<ul style="list-style-type: none"> <li>• Standard: AASHTO T321 (cyclic tests)</li> <li>• Time: 1 hour to days</li> <li>• Variability: very high (COV&gt;50%)</li> </ul>	Correlation with bottom-up fatigue cracking historically validated	Asphalt binder, aggregate, RAP/RAS, aging, etc.	California- special pavement design; being considered by Nevada and Georgia
SCB at intermediate temperature		<ul style="list-style-type: none"> <li>• Type: top-down fatigue cracking and reflection cracking</li> <li>• Parameter: critical energy release rate</li> </ul>	<ul style="list-style-type: none"> <li>• Standard: LTRC (Monotonic test)</li> <li>• Time: 30 min</li> <li>• Variability: medium (COV=20%)</li> </ul>	Good correlation to field cracking reported by LTRC	Asphalt binder, aggregate, RAP/RAS	Adopted by Louisiana and Wisconsin; being considered by Oklahoma and New Mexico
IDT- University of Florida (UF) for top-down fatigue cracking		<ul style="list-style-type: none"> <li>• Type: top-down cracking</li> <li>• Parameter: energy ratio</li> </ul>	<ul style="list-style-type: none"> <li>• Standard: University of Florida: M<sub>r</sub> test (optional), D<sub>t</sub> test, and tensile strength test</li> <li>• Time: 1-2 hours</li> <li>• Variability: possibly low, similar to AASHTO T322</li> </ul>	Validated with field cores in Florida and confirmed at NCAT test track	Insensitive to change in binder viscosity	Being considered for adoption by Florida

<p>Simplified viscoelastic continuum damage (S-VECD) fatigue test</p>		<ul style="list-style-type: none"> <li>• Type: bottom-up and top-down fatigue cracking</li> <li>• Parameter: damage parameters (or predicted no. of cycles)</li> </ul>	<ul style="list-style-type: none"> <li>• Standard: AASHTO TP107 (cyclic tests)</li> <li>• Time: 1 hour to 1 day (2–3 more days if E* test is considered)</li> <li>• Variability: low in general, but need further evaluation</li> </ul>	<p>S-VECD used with more advanced models (LVECD and VECD-FEP++) to simulate pavement performance; validated with FHWAALF test lanes and verified in North Carolina</p>	<p>Sensitive to binder content, RAP, aging, etc. as reported by Richard Kim’s study</p>	<p>Being considered by Oklahoma, Georgia, Pennsylvania, and North Carolina</p>
<p>Repeated direct tension (RDT) test</p>		<ul style="list-style-type: none"> <li>• Type: bottom-up and top-down fatigue cracking</li> <li>• Parameter: Paris’ law parameters, endurance limit, healing properties, average crack size</li> </ul>	<ul style="list-style-type: none"> <li>• Standard: Texas A&amp;M University (cyclic tests)</li> <li>• Time: 1-2 hours</li> <li>• Variability: low in general, but need further evaluation</li> </ul>	<p>Correlations with bottom-up and top down fatigue cracking being developed under several research projects; methods being validated with LTPP data</p>	<p>Model coefficients functions of AV, P<sub>b</sub>, gradation; modulus, aging, etc.</p>	<p>Unknown</p>

## **2.4 Performance of Modified Binders and Mixtures**

Researchers around the world have worked on evaluating the benefits of polymer modification on pavement performance since its introduction (Yildirim 2007). A 1997 survey of state departments of transportation (DOT) in the U.S. indicated that 47 out of the 50 states showed their interest in using modified binders and 35 of them reporting that they would use greater amounts (Bahia et al. 1997).

### ***2.4.1 Laboratory Evaluation***

The intent of Superpave PG system was to eliminate the need for selecting and specifying specific types of modifiers and modification methods. State agencies, however, wanted to know if unmodified and modified binders with the same PGs gave the same performance.

Blankenship et al. (1998) conducted laboratory evaluation of five different PG 70-22 binders in Kentucky, including two SBS-modified, one SBR modified, one chemically modified, and one neat binders. The lab tests focused on parameters related to rutting, fatigue, low temperature cracking and moisture damage. It was found that these PG 70-22 binders differed as far as rutting, moisture damage and modulus testing, although the rutting difference was no more than 10 mm between the binders.

In 2001, Sargand and Kim (2001) evaluated the rutting and fatigue resistance of Superpave mixes in Ohio, covering three different gradations and three PG 70-22 binders (unmodified, SBS and SBR modified). The laboratory evaluation used a triaxial repeated load test, a static creep test, the APA test, and the flexural beam fatigue test. It was found that the polymer modified mixes were markedly more rut and fatigue resistance than the neat binder, even though all three had the same PG grade.

The FHWA conducted a study in 2002 to evaluate the effects of polymer-modified asphalt binders with identical Superpave PGs on the low-temperature cracking resistances of asphalt mixtures (Stuart and Youtcheff 2002). The polymer modified binders involved contained varied modification chemistries. This would indicate what types of modification provided properties that were, or were not, correctly captured by the Superpave asphalt binder specification. The low-temperature property of binder was represented by critical cracking temperature ( $T_{cr}$ ) determined by Superpave BBR and DTT tests, and the TSRST was used for mixture. Eleven asphalt binders were evaluated: two unmodified asphalt binders, an air-blown asphalt binder, and eight polymer-modified asphalt binders. The correlations between the TSRST fracture temperatures and asphalt  $T_{cr}$  results, BBR creep stiffness ( $S$ ), BBR  $m$ -value, and the BBR limiting temperature, were poor to weak. However, the correlation using  $T_{cr}$  was good after removing the data for ethylene styrene interpolymer (ESI), with the  $r$ -square value increased from 0.54 to 0.85.

A similar analysis was conducted on the same group of binders (Stuart 2002) to determine if the Superpave high-temperature rheological properties of polymer-modified asphalt binders correlate to asphalt mixture rutting resistance (Stuart 2002). Binder high temperature properties were measured by a DSR. Mixture rutting resistance was measured by repeated shear at constant height (RSCH), and the French Pavement Rutting Tester (French PRT). Overall, good correlations were found between the high-temperature properties of the asphalt binders and mixture rutting resistance, but the two laboratory mixture tests did not provide the same conclusions concerning which asphalt binders did not behave as expected. It was recommended that full-scale pavement tests were needed to verify this finding.

In 2003, Mohammad et al. (2003) evaluated the possibility of recycling SBS modified asphalt for resurfacing pavement. The impact of the extraction and recovery process on the binder was found to be minimal. The SBS modified binder that experienced eight-year's services in Route US61 in Louisiana was recovered and found to have experienced intensive oxidative age hardening. The recycled binder seemed quite brittle, and blends of this recycled binder and virgin binder were stiffer than anticipated at both low and high temperatures. When the percentage of the recycled binder increased, the rutting resistance of the binder blends were found to increase while fatigue resistance decreased.

Yildirim et al. (2004) investigated waste toner that contains styrene acrylic copolymers as an asphalt binder modifier. The research focused on developing proper binder designs that included blending time, performance grading, storage stability, and mixing and compaction temperature calculations. It was found that the stiffness of the blend increased as the percentage of the toner content increased.

In the past decade or so, polyethylene has been evaluated as an important source of modifier for the asphalt industry. Two types of polyethylene, LDPE and high density polyethylene (HDPE), were added in two states (grinded and not grinded) to modify bitumen in HMA in 2007 by Awwad and Shbeeb (2007). Marshall Mix design was used in this research and the optimum asphalt content was determined at 5.4%. The two types of polymers were added in seven proportions by weight of the total binder: 6, 8, 10, 12, 14, 16 and 18%. It was found that ground HDPE polyethylene modifier provides better engineering properties such as better resistance against fatigue and deformation and better adhesion between the aggregate and asphalt than the unmodified ones. The recommended proportion of the modifier was 12% by the weight of bitumen content.

Casey et al. (2008) explored a pen-grade binder containing recycled HDPE through fundamental bitumen tests. A mixing methodology was developed in the research. The optimum mixing process was selected according to the type of modifier, mixing time and mixing temperature. The testing results showed that the binder containing 4% HDPE produced the most promising results. Results of the modified binder and mix were compared with the performance of materials using the traditional binders. Wheel track and fatigue tests showed that the modified binder did out-perform traditional binders used in stone mastic asphalt, although the binder did not deliver equivalent performance levels to a proprietary polymer modified binder.

Polypropylene fibers were also reported for use as polymer modifiers for asphalt. Tapkın et al. (2010) conducted flow and Marshall Stability tests on samples modified with different types of waste polypropylene and polypropylene fiber. The results showed that the addition of polypropylene fibers resulted in the improved Marshall Stabilities and Marshall Quotient values that represented a kind of pseudo stiffness. The research also proposed a model in which the physical properties of standard Marshall specimens were used to predict the Marshall stability, flow and Marshall Quotient values obtained from the mechanical tests. The physical properties included polypropylene type, polypropylene percentage, bitumen percentage, specimen height, unit weight, voids in mineral aggregate, voids filled with asphalt, and air voids.

Moghaddam et al. (2014) evaluated the use of polyethylene terephthalate (PET) flakes as modifier in asphalt mixture as an alternative solution to overcome the potential risks arising from producing large amount of waste PET. The PET is a non-biodegradable semi-crystalline thermoplastic polymer, which is considered one of the major types of plastics that can be found in Municipal Solid Waste (MSW). The research was focused on deformation characteristics of unmodified and PET modified asphalt mixtures. Different percentages of PET were attempted



for this investigation, including 0%, 0.2%, 0.4%, 0.6%, 0.8% and 1% by weight of aggregate particles. Dynamic creep test was performed at different temperatures and different stress levels. It was found that permanent deformation characteristics of asphalt mixture were considerably improved by addition of PET, when the permanent strain was markedly decreased in PET modified mixture compared to the conventional mixture at all stress levels and temperatures.

In recent years, new modifiers have been constantly developed to seek improving binder performance. A new SBS polymer technology, highly modified asphalt, or HiMA, was recently developed by Kraton Corporation for asphalt paving (Kluttz 2015). The HiMA has twice loading than that of ordinary modified asphalt, making the asphalt more like an asphalt-modified rubber than a rubber-modified asphalt. The mixes made with HiMA are readily workable and easy to lay in the field, and are reported to have many times the fatigue and deformation resistance of ordinary modified asphalt. The HiMA technology was evaluated using a test track at the National Center for Asphalt Technology (NCAT) at Auburn University. The test crack was 1.7 mile and was 18% thinner than a control group that was constructed as well. After 2+ years and 10,000,000 axle loads, the HiMA section showed only 1/3 as much rutting. NCAT estimated that the HiMA section would show better fatigue performance as well.

Another one of the most mentioned modifiers the polyphosphoric acid (PPA) (Fee et al. 2010; Xiao et al. 2014). Fee et al. (2010) conducted a series of laboratory tests to demonstrate the performance PPA with each formulation of asphalt and aggregate, together with polymer, antistripping agents, and other additives. The tests included dynamic shear rheometer, Hamburg, Lottman, and multiple stress creep and recovery tests, which were conducted on a matrix of a common asphalt with aggregate, three antistripping agents, two types of polymers, and PPA. The performance of PPA-modified asphalt were observed to be improved with the addition of

antistripping agents such as hydrated lime and a phosphate ester, a particular polyamine compound. Similar observations were found on asphalt binders modified by other polymers such as SBS and Elvaloy.

#### ***2.4.2 Field Survey Results***

Field evaluation of asphalt pavement containing modified binders was not documented well until 1980s. The California Department of Transportation (Caltrans) conducted a two-year study (Reese and Predoehl 1989) to: 1) evaluate the aging rate and improvements of modified asphalt binders in temperature susceptibility; 2) screen the modified binders using the California Tilt-Oven Durability (CATOD) Test; 3) determine whether the modified binders were durable in hot and cold climates; and 4) recalibrate the CATOD procedure for modified binders if necessary. Four polymer modified binders were used on two test sections in hot climate and one test section in cold climate. It was found that the addition of polymer could increase the resistance of asphalt mixture to aging and cracking.

To consolidate work done in Florida with polymer modified binders, mainly ground tire rubber (GTR) and SBS, field sections were evaluated (Roque et al. 2005). Field data was mostly anecdotal, not involving controlled scientific studies. In most cases observations indicated good performance relative to prior history in existing location. SBS-modified asphalt was highly recommended for intersections (high volume, slow moving traffic) and open-graded friction course (OGFC); however, environmental benefit of use of rubber in pavements cannot be overlooked (investigating hybrid binder).

Polymer-modified binders have been used in Illinois since 1992 (Illinois DOT 2005). Three types of elastomeric copolymer were approved for use: styrene-butadiene diblock (SB), SBS, and SBR. Plastomer-modified asphalt cements were not allowed in Illinois. Polymer-

modified binders have been commonly prescribed for conventional dense-graded HMA as well as special HMA mixes, such as OGFC and stone-matrix asphalt (SMA) mixes. The benefits observed at various sections include improved performance under extreme hot-cold temperature variations, improved binder viscosity and adhesion, and improved adhesive bonding to aggregate particles. These benefits have helped pavement resist rutting under extremely heavy loads, and improve its fatigue resistance from repeated cycles of heavy truck loading due to increased elasticity. The long-term pavement performance of using polymer-modified HMA is under investigation.

The Missouri DOT built two test sections at the NCAT Pavement Test Track in 2009 to validate GTR as a substitute for polymer modification in asphalt binders (Willis et al. 2012). Field sections were evaluated during a six-year period for rutting, smoothness, texture, and cracking. In addition, laboratory characterization was conducted in accordance with standard procedures on field collected samples including stiffness, rutting, cracking, and moisture susceptibility. The data showed that polymer-modified mixtures can be substituted by GTR mixtures without sacrificing asphalt mixture performance. No cracking or rutting was observed on the sections containing GTR mixture which was placed in 2009 and had completed 20 million equivalent single axle loads.

Early-life pavement distress surveys were conducted in Wisconsin between 2004 and 2012 to evaluate the suitability of Wisconsin's asphalt binder modification guidelines (Bahia et al. 2013). The ability of the binder selection criteria to quantify the effect of modified binder use on field performance was assessed. A set of modified binders corresponding to constructed field sections across Wisconsin were tested using recently developed characterization procedures under consideration or standardized by AASHTO as provisional standards. No rutting was

observed in any section in Wisconsin. The studied Wisconsin binders exceeded the most extreme binder rutting grade requirements according to AASHTO MP 19 (MSCR) at the local high performance temperatures. The results confirm previous notions that rutting is not a significant concern in Wisconsin, and development of advanced binder criteria and classification systems for rutting resistance of binders may not be as essential as that of thermal and fatigue cracking.

NCAT helped with several field projects using GTR modified asphalt mixture in recent years (NCAT 2016). One project was developed by NCAT and Alabama DOT to conduct laboratory and field evaluation in order to compare the performance of GTR modified asphalt mixture to that of a polymer modified asphalt mixture. The asphalt contents and gradations differed slightly between the two mixtures due to the differences in binders. The target thickness for each mixture was 1.5 inches and the target density was 93% of  $G_{mm}$ . An inertial profiler was used to measure the rut depths, texture, and smoothness of each test section, while the cracking performance was evaluated by monitoring three 100-ft test strips of each section. Both sections were observed free of cracking after five years of trafficking, and rutting was less than 4 mm. No deterioration in pavement smoothness or change in texture was noticed on both test sections. Missouri DOT sponsored a similar experiment that began in 2009 at the NCAT Test Track, in which two sections were built to compare a GTR modified mixture to a polymer modified mixture. No difference was observed in the performance of these two test sections after 10 million equivalent single axle loads (ESALs). The polymer modified test section underwent 10 million ESALs then was removed in the summer of 2012. The GTR section was subjected to a total of 20 million ESALs of traffic. In both sections, there was minimal rutting and no cracking found.

## **2.5 Influencing Factors and Models**

The distress models of asphalt mixture can be categorized as empirical and mechanistic models. The empirical models are developed through regression analyses of field data, which are useful in identifying influencing factors that affect the specific distress. However, the predictive capability of empirical models, as reported by the  $R^2$  value, is strictly limited to the data set on which the model was developed. In addition, empirical models do not fully explain the distress phenomenon at a fundamental level. Conversely, the mechanistic models depend on principles of mechanics of materials, which are computationally more complex. Based upon principles of mechanics, the mechanistic models usually require the solution of a system of linear or non-linear equations.

### ***2.5.1 Empirically-Based Models***

When it comes to rutting prediction, little formal work had been done prior to 1960 (Sousa et al. 1991). The empirical measures of the shear resistance of pavement components provided by the California Bearing Ratio (CBR) pavement design method were used at the time to insure an adequate thickness that presumably limited the rutting in the pavement to a tolerable amount. A simple empirical model was developed by Uzan and Lytton (1982) concerning wheel-load and tire-pressure effects within the pavement layers.

For cracking, Fromm and Phang (1972) developed a number of regression equations in the early 1970s to predict the cracking index using a testing program carried out on 33 pavement sections in Ontario. The cracking index is calculated based on the cracking occurrences of multiple cracking, full cracking, and half-half cracking per 150 m of two-lane pavement. A similar empirical study was conducted by Haas et al. (1987) with data gathered from 26 airport

pavements in Canada. An empirical model was proposed based on laboratory tests, field surveys and statistical analyses. The transverse crack spacing was used to represent the cracking performance of asphalt pavement, and the selected variables included thickness of asphalt concrete, minimum temperature recorded on site, penetration number and coefficient of thermal contraction of the material.

### ***2.5.2 Mechanistic-Based Models***

One early rutting prediction model based on mechanistic properties of asphalt pavements was presented in 1972 as the layer-strain methodology (Romain 1972). The early Shell subgrade strain was modified and used to model for rutting acceptance by Claessen et al. (1977). Kenis (1977) Stepwise regression techniques were used by Finn et al. (1983) to build mechanistic-empirical models to relate rutting in both conventional and full-depth pavements to stress, surface deflection, and number of load repetitions. Abdulshafi (1983) introduced the use of viscoelastic-plastic considerations of predicting rutting of asphalt pavements. The dynamic creep testing was combined with layer-strain analysis to predict rutting in full-scale pavements by Echmann (1987). Generally, early models associated permanent deformation to excessive vertical strains on top of the subgrade, and the cumulative ruts occurring in all layers of the pavement system were used to represent the total permanent deformation with time and enhanced knowledge. In the Mechanistic-Empirical Pavement Design Guide (MEPDG) proposed in 2004, a predictive rutting system was developed to evaluate the permanent deformation within all rut susceptible layers, with rut depth of each layer modeled as a function of time and traffic repetition (ARA, Inc. 2004). The asphalt mixture rutting prediction model in the MEPDG software was recalibrated by NCHRP Project 09-36 with details presented in its report 709 (Von Quintus et al. 2012). This recalibration was done with measured material properties and

performance data from Long-Term Pavement Performance Program Special Pavement Studies (LTPP SPS) and other full-scale pavement sections, including sections built with modified asphalt binders.

Most mechanistic thermal cracking models focus on the asphalt concrete surface. The National Pooled Fund Study conducted by Marasteanu et al. (2007) summarized the development of the cracking models of asphalt mixture in history. Hills and Brien (1966) developed an early method to predict the temperature at which asphalt concrete will fracture. Based on data collected from two test roads in Canada, Christison et al. (1972) performed different stress analyses and compared the fracture temperature predictions. The Hills and Brien method was further implemented by Finn et al. (1977) in the computer program COLD. The program assumed either a pseudo-elastic slab or beam and solved equations numerically to calculate the thermal gradient within the pavement that was used to determine the thermal stresses. The thermal cracking (TC) model was incorporated in the MEPDG design guide, which is composed of calculation of three parts: thermal stress, crack propagation, and crack amount (ARA, Inc. 2004). Other important models included the fictitious crack model (FCM) (Hillerborg et al. 1976) and frictional constraint model (Zubeck and Vinson 1996; Tim and Voller 2003). The FCM is also called the cohesive zone model that takes consideration of the interface friction between the asphalt surface layer and the layer below. The frictional constraint model predicts crack spacing on the basis of the balance between the friction on the top of the aggregate base and the accumulated thermal stress.

## 2.6 Modified Binders Used in Alaska

### 2.6.1 Climate Effect for Binder Selection

Alaska is the largest state in the United States by area. Alaska's climatic conditions vary from low temperatures and light precipitation in the Arctic zone to moderate temperatures and heavy precipitation in the Maritime zone (Figure 2.1) (Miller et al. 1999). The significant climatic variation requires a wide range of PGs for asphalt binder used in Alaska.

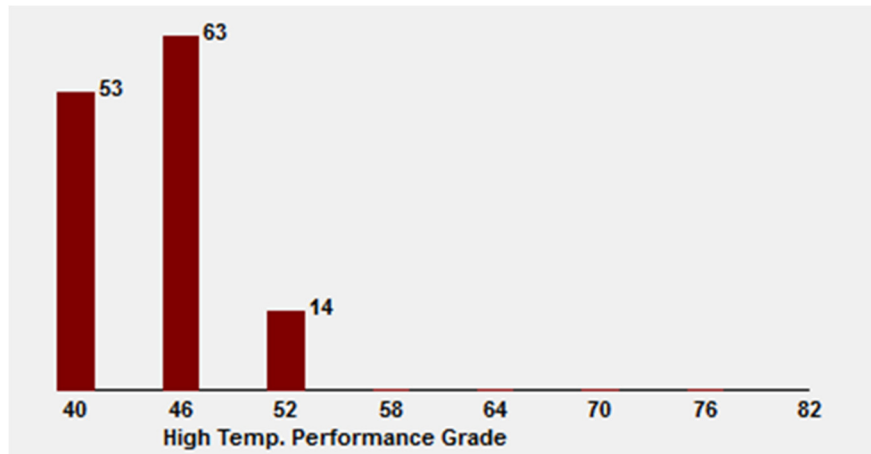


Figure 2.1 Alaska's climatic zones (adapted from Miller et al. 1999)

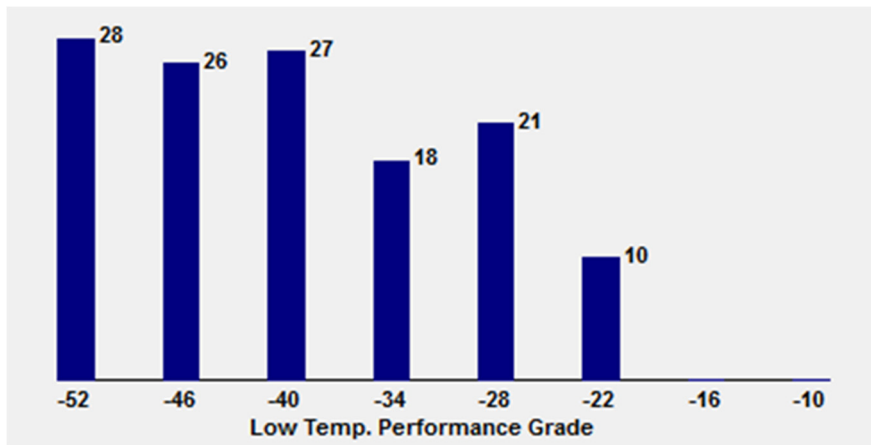
The LTPPBind software developed based on the long-term pavement performance (LTPP) database could provide users with the ability to apply regional temperature and traffic conditions to select asphalt binders (FHWA 2017). Zhao et al. (2016) used the latest version of LTPPBind (Pavement Systems LLC 2005) at the time to calculate the recommended PGs at 98% reliability on both ends. This binder PG distribution was determined based on 130 weather



stations in Alaska as shown in Figure 2.2. It is noted that all the crude oil sources produce a base asphalt of PG 52-28 in Alaska (Zhao et al. 2016). It is not hard to observe that this base binder PG 52-28 cannot satisfy the PG requirement in many locations according to Figure 2.2. For comparison, Table 2.3 lists what is being used currently in Alaska.



(a)



(b)

Figure 2.2 Number of weather stations in: (a) high temperature grade; (b) low temperature grade (98% reliability and 130 weather stations in Alaska) (Zhao et al. 2016)

Table 2.3 Asphalt binders being used currently in Alaska

$T_H$ (°C) \ $T_L$ (°C)	64	58	52
-40	X	-	X
-34	X	X	X
-28	X	X	X

The moisture distribution may also affect the selection for binder grade. The LTPP program divided the U.S. into four different environmental zones: dry freeze, dry no-freeze, wet freeze, and wet no-freeze (Perera et al. 2005). Figure 2.3 shows the geographical regions corresponding to these environmental zones. The threshold between the wet and the dry zone generally corresponds to an annual precipitation of 508 mm (20 in), while the boundary between the freezing and nonfreezing zones generally corresponds to an annual freezing index of 89 Celsius degree-days (192.2 Fahrenheit degree-days). Although Alaska is not included in the geographical drawing shown in Figure 2.3, the environmental conditions of the locations of projects evaluated in this study can be determined based on the recommended boundary values.

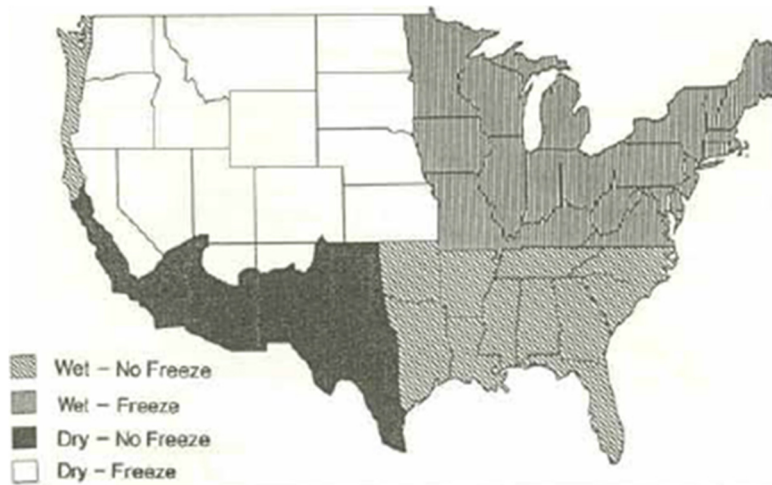


Figure 2.3 Environmental zones considered in the LTPP program (Perera et al. 2005)

### ***2.6.2 The History of Modified Binders Used in Alaska***

Modified asphalt binder have been used in Alaska's road systems since the early 1980s (Raad et al. 1997). The modifiers included SBR polymers, SBS polymers, ULTRAPAVE and crumb rubber-modified (CRM) (both the dry process, Plus Ride, and wet process).

Rubberized asphalt pavements were built in Alaska as part of the early binder modification efforts and a number of studies investigated the performance of rubberized asphalt mixes in Alaska in the 1990s (Raad and Saboundjian 1998). A comprehensive study was published in 1997 (Saboundjian and Raad 1997) that compared the fatigue, thermal cracking, and permanent deformation resistance of several Alaskan CRM asphalt mixtures with that of conventional mixes. Both laboratory and field evaluation was conducted. The results showed that the CRM mixes enhanced fatigue resistance in the lab and thermal cracking resistance in both the lab and the field, compared to conventional mixes. Similar fatigue performance was observed on field sections built with both mix types. However, conventional mixes outperformed CRM mixes in resisting permanent deformation, in both the lab and the field. A follow-up study was conducted to develop design equations for rubberized pavements in Alaska with the focus on the fatigue behavior (Raad and Saboundjian 1998). The study also used the fatigue equations to compare the fatigue life of conventional and rubberized pavements for different surface layer temperatures and foundation support conditions.

Raad et al. (1997) conducted a study to characterize asphalt and polymer modified asphalt mixes from a number of selected sites using SHRP Superpave PG grading system, TSRST, and Superpave IDT test on field specimens. Results of the study indicated that in general significant improvement in the low temperature cracking resistance when polymer modifiers were used. The corresponding reduction in crack sealing costs are estimated to be

between 30% and 40%. Minimum air and pavement temperature correlations were developed using field data covering Alaska's climatic zones. Contour maps for Alaskan roads corresponding 50% and 98% reliability minimum pavement temperature were developed in the study.

In 1999, ADOT&PF conducted a study about the constructability of polymer-modified asphalt concretes together with the University of Alaska Anchorage and Fairbanks (Zubeck et al. 1999). Fluorescent microscopic images and elasticity tests were used in the study to evaluate the compatibility of the polymer and the asphalt cement. An indication of storage stability was provided separation tests. The conventional tests included penetration, softening point and viscosity at several temperatures. The results showed that only a few of the 36 polymer-modified binders mixed in the laboratory met the criteria set for the compatibility, storage stability, improved temperature susceptibility and mixing temperature. The most discriminating factors were found to be storage stability and maximum allowable mixing temperatures, both of which caused constructability problems in polymer-modified asphalt mixtures. The study further analyzed seven polymer-modified binders and three traditional binders using Superpave binder tests, and their corresponding mixtures using the TSRST and Georgia Wheel Rutting Test. According to the test results, polymer- modification improved the performance of all base asphalts.

In recent years, modified asphalt binders have been widely used in a number of actual projects to address specific pavement distresses or issues in Alaska. The rutting performance of one polymer modified PG 64-28 binder used in ADOT&PF's Central Region was evaluated in a study based on rutting analysis of Anchorage pavements (Ahmed 2008). A modified binder PG 58-28 was used as base binder to produce warm mix asphalt (WMA) in DOT's Southcoast Region (Liu and Li 2011). The project was Alaska's first trial WMA project in which various

dosages of Sasobit were used to produce WMA. In another study that established a catalog of dynamic modulus of Alaskan asphalt mixtures, nine mixtures using PG 64-34 binder were included (Li and Liu 2014). The dynamic modulus data of these mixtures were documented for pavement analysis and used to develop correlations between simple performance test results and HMA performance. The PG 64-34 binder was also included in a project that assessed the engineering properties and performance of paving interlayer-reinforced asphalt pavement (Li et al. 2016). Zhao et al. (2016) comprehensively summarized the current status of asphalt binder adaptation efforts in Alaska and the low-temperature performance of modified binders such as PG 58-34 and PG 64-34 was investigated. In another recently completed study, Alaskan HMA containing recycled asphalt pavement was characterized (Liu et al. 2016). Mixtures using PG 58-34 and PG 52-40 binders were included in the study to produce RAP mixtures.

### ***2.6.3 Current Regional Status***

ADOT&PF divides the state of Alaska into three Regions: Northern Region, Central Region, and Southcoast Region. Due to the variation in their climates, material sources and traffic levels, the status of using modified binders in the three DOT Regions varies significantly. To obtain the up-to-date status, materials engineers from all the three Regions were contacted with the information summarized below.

The use status of modified binders in ADOT&PF's Northern Region was summarized according to personal communication with Mrs. Heidi Schaefer (Schaefer 2017). The binder used in Northern Region is typically produced from North Slope crude from refineries in the Fairbanks area. For the past two years, however; the crude source was from Cook Inlet in the Anchorage area as Flint Hills refinery in Fairbanks stopped refining. Now the Petro Star refinery in Fairbanks is producing asphalt binder from North Slope Crude for use in the Northern Region.

Typically, a General Contractor when bidding a project selects the asphalt supplier. Emulsion Products provides most of the binder used in the Northern Region. Denali Materials and US Oil provided binders for the Northern Region in the past as well. Currently PG 52-28 binder is used in most cases for surface courses. PG 52-28 binder is used for ATB courses in the Northern Region as well. Modified binders such as PG 58-34 (Alaska Highway Tanana River Bridge), PG 64-28 (Dayville Road Reconstruction), and PG 64- 34 (Fairbanks Airport Runway, Richardson Highway North Pole Interchange, etc.) were used in the Northern Region in the past. However, clear reduction of thermal cracks was not observed, then ADOT&PF engineers started to explore the use of higher modification in the low temperature end, thus PG 52-40 has been used a bit more often in recent years. It is specified for use in several bridge projects even if its long-term performance has not been verified, as the binder cost is only a small portion of the entire cost of a bridge project. The Northern Region has used PG 52-40 in projects close to town for the convenience of monitoring, such as Peger Road and Airport Way resurfacing jobs in Fairbanks. PG 52-40 has been used in airfield pavements as well, such as Gulkana Airport Apron & Taxiway Paving, Shishmaref Airport Resurfacing, and Kotzebue Airport & Safety Improvements projects. A few short sections on Richardson Highway and Parks Highway have been paved with PG 52-40. According to ADOT&PF engineers in the Northern Region, pavements constructed with PG 52-40 binder perform very well after years, including those that experience extremely cold temperatures up to Cold Foot (Dalton Highway MP 197- 209). The increased cost is the main concern. In addition, higher temperature is required to heat up the binder as the modified binder is more viscous when polymer is added. However, the use of warm mix asphalt technologies may compensate the need for higher temperature.

Mr. Paul Dougherty provided information about ADOT&PF's Central Region (Dougherty 2017), in which PG 52-28 base binder is mostly used in pathways and low volume roads. It is used in ATB as well in some projects such as Sterling Highway MP 114-135 Pavement Preservation. Modified asphalt has been widely used in highway and other pavements construction. PG 52-34 has been used to the North of Anchorage with improved low-temperature cracking resistance. In recent years, the trend in that area has been using higher grade at low temperature-grade such as PG 52-40 (e.g. Schrock Road Pavement Preservation). A representative project was constructed with PG 52-40 binder in the surface course on Parks Highway in 2014. In Anchorage and its surrounding areas, PG 58-34 has been used mostly to enhance the high grade to resist plastic deformation due to increased traffic level in projects such as Abbott Road Rehabilitation. To the south of Anchorage, PG 52-34 is used (e.g. Alaska Peninsula Highway: King Salmon Naknek Preservation). The high grade is "52" because the pavement is strong enough to resist permanent deformation under relatively low traffic volume in the area. "-34" is selected as the low grade to provide enough low-temperature cracking resistance. Representative projects include many sections in Sterling Highway. For consistency, the same binder grade is used in ATB as in the surface course in most jobs in the Central Region. From 2015, a highly modified binder PG 64-40 has been used in areas with very high traffic volume such as Downtown Anchorage and Glenn Highway (Hiland to Eklutna). This binder is used to provide additional resistance to plastic deformation and tire wear in these high-traffic areas. PG 64-40 has been used on multiple projects since 2015.

According to Mr. Robert Trousil (Trousil 2017), two binders have been predominantly used in ADOT&PF's Southcoast Region, PG 58-28 and PG 64-28, both of which are modified binders. The high grade of "64" is selected in some warmer areas in the Region such as south of

Juneau. Typical PG 64-28 projects include Sunny Point Intersection Improvements, Glacier Highway Brotherhood Bridge Replacement, Juneau Egan Drive Pavement Rehabilitation, etc. Representative PG 58-28 projects cover Glacier Highway Pavement Rehabilitation (Lena to Tee Harbor), and Haugen Drive & Bike Path in Petersburg, etc. Some projects use PG 58-28 Plus binder such as KTN Water Street Rehabilitation and Yakutat Areawide Paving. The low grade of “-28” is generally good enough for the entire Region due to its low latitude. However, because of the expansion of this Region, some colder areas in the north have been included in this Region. This has motivated a trend to use PG 58-34 binder in these colder areas. In addition, many thermal cracks have been observed on runways at Gustavus airfield in the past few years. PG 58-34 has been planned for use in this airfield as well.

#### ***2.6.4 Summary***

The past research efforts have promoted the use of modified asphalt in Alaska. However, Alaskan modified binders, especially highly modified binders (such as PG 52-40 and PG 64-40) used in recent paving projects, have not been systematically characterized in these past studies. Currently PG 58-28 and PG 64-28 have had acceptable performance in ADOT&PF’s Southcoast Region. However, for areas with extreme conditions like interior and central Alaska, local characterization is extremely important. In addition, no other study has been found, which addresses Alaska’s situation with respect to locally available materials (from local producers) and climatic conditions.



## CHAPTER 3.0 EXPERIMENTAL DETAILS

### 3.1 Materials

13 asphalt binders used in ADOT&PF paving projects were collected, including one unmodified binder (PG 52-28) and 12 polymer modified binders, from three different suppliers.

Table 3.1 summarizes binder information.

Table 3.1 Matrix of studied binders

<b>Binder #</b>	<b>Binder PG</b>	<b>Source</b>	<b>PG+ Requirements for ADOT&amp;PF*</b>
1	PG 52-28	A	-
2	PG 52-40	A	-
3	PG 64-40	A	-
4	PG 52-46	A	-
5	PG 58-34	A	-
6	PG 52-40	B	AASHTO M332
7	PG 64-40	B	AASHTO M332
8	PG 58-34	B	AASHTO M332
9	PG 58-34	C	-
10	PG 52-34	C	-
11	PG 58-28	C	-
12	PG 58-28 plus	C	Toughness and Tenacity; Elastic Recovery
13	PG 64-28	C	-

\* Detailed specification is included in the Appendix A

ADOT&PF divides the state into three regions: Southcoast, Central, and Northern. For this project, loose asphalt mixtures from the Central and Northern regions were selected for characterization. Southcoast region materials were excluded based on availability and logistical difficulties as well as on the recommendation of ADOT&PF professionals. Eight mixes were proposed for the Central region and two mixes were proposed for the Northern region. Due to

the lack of highway construction projects with PG 52-46, Mix #10 was produced in the laboratory by following the JMF provided by ADOT&PF professionals. The mixtures studied in this experiment are summarized in Table 3.2. Descriptions of all JMFs used in this study can be found in Appendix A.

The contractors involved selected the materials used for plant-produced mixes. The loose mixtures (plant-produced mixes) for this project were collected by ADOT&PF professionals and shipped to Missouri S&T. The aggregates (Figure 3.1) used for the laboratory produced mixture (Mix #10) were collected from Alaska based on the JMF. The sieving analysis tests were performed to verify the aggregate gradations. The binder, PG 52-46, used for Mix #10 was collected from supplier A.



**Figure 3.1 Sieved collected aggregates**

Table 3.2 Matrix of HMA mixtures

Mix #	Region	Mix Type	Binder PG/Supplier	Aggregate Source	Project Name/No./Contractor/Year
1	Central	Type VH	PG 64-40/A (binder #3)	MP 261 Parks/Cange-Pittman MP 44 Parks	Parks Hwy MP 35-40 Pav. Presev/56703/QAP/2016
2		Type VH	PG 58-34/A (binder #5)	MP 78 Parks Pit	Abbott Rd. Rehab-Phase 1/59190/QAP/2016
3		Type VH	PG 64-40/B (binder #7)	MP 216.5 Parks Hwy/ Birchwood Pit	Glenn Highway, Hiland to Eklutna/59028/Granite/2016
4		Type IIA	PG 52-40/B (binder #6)	MP 39 Glenn Hwy/AS&G/Granite	Alyeska Highway resurfacing/58526/Granite/2016
5		Type VS	PG 58-34/B (binder #8)	MP 39 Glenn Hwy/AS&G	AIA Taxiway R Improvements/57590/Granite/2016
6		Type VH	PG 64-40/B (binder #7)	MP 39 Glenn Hwy/AS&G & Dupont, WA	5th&6th Ave, L&I couplet Preserv /57835/Granite /2015
7		Type V	PG 58-34/B (binder #8)	MP 39 Glenn Hwy / AS&G	W. Dowling Ph.II Recon. / 51030 / Granite / 2015
8	Northern	Type IIB	PG 52-28/A (binder #1)	Metro Pit Fairbanks	FMATS Pedestrian, Peger Rd Resurfacing/63035/GWI/2016
9		Type IIB	PG 52-40/A (binder #2)	Metro Pit Fairbanks	Peger Rd Resurfacing /GWI/2016
10		Type IIB	PG 52-46/A (binder #4)	Metro Pit Fairbanks/ Tanana River Valley	Lab Produced

### 3.2 Binder Tests

Binder tests were conducted for neat binder, commonly used modified binders, and highly modified binders according to Superpave specifications and previous studies. Table 3.3 lists the binder-testing matrix. The DSR was employed to assess the viscoelastic behavior, to obtain the master curves and black space diagram, and to evaluate the rutting resistance, of

binders. The BBR and ABCD tests were used to evaluate the low temperature cracking resistance of binders.

### ***3.2.1 Artificial aging process***

The rolling thin film oven (RTFO) test was conducted to simulate the effect of short-term aging during mixing and construction, according to AASHTO T 240 *Standard Method of Test for Effect of Heat and Air on a Moving Film of Asphalt Binder (Rolling Thin-Film Oven Test)*. The basic RTFO procedure takes unaged asphalt binder samples in cylindrical glass bottles and places these bottles in a rotating carriage within an oven. The carriage rotates within the oven while the 325°F (163°C) temperature ages the samples for 85 minutes, and the airflow blown into the bottles at 4000 ml/minute. Figure 3.2 shows major RTFO equipment.

The pressure-aging vessel (PAV) test was conducted to simulate the effect of long-term aging. The PAV aging tests were conducted on RTFO residues. The RTFO residue was subjected to elevated temperature (100°C) and pressure (2070 kPa) for 20 hours to simulate in-service aging over a 5 to 10 year period according to AASHTO R28 *Standard Practice for Accelerated Aging of Asphalt Binder Using a Pressurized Aging Vessel (PAV)*. In order to simulate even longer aging times in the field, the PAV tests (the procedures were based on AASHTO R28, except the testing time) were also conducted at 40 hours. Figure 3.3 shows the major PAV equipment.



Figure 3.2 RTFO equipment



Figure 3.3 PAV equipment

Table 3.3 Testing matrix (triplicates for each test)

Test	Properties	Parameters or Outputs	Binder status	Test temperatures (°C)	Standard	Equipment
Frequency Sweep	Viscoelastic behavior	Master curve ( $G^*$ and $\delta$ ); Black space diagram; Glover-Rowe Parameter; R-value	RTFO; RTFO+20h PAV; RTFO+40h PAV	5, 15, 25, and 35°C	AASHTO T315	DSR
Binder grading	Rutting	Rutting parameter ( $G^*/\delta$ )	Original RTFO	Two for each (-6°C and high PG) <sup>a</sup>	AASHTO T315	DSR
MSCR	Rutting	$Jnr$ ; Percent recovery ( $R$ )	RTFO	Two for each (-6°C and high PG) <sup>a</sup>	AASHTO T350	DSR
BBR	Thermal cracking	$S$ ; m-value <sup>b</sup>	RTFO; RTFO+20h PAV; RTFO+40h PAV	Three for each ( $\pm 6^\circ\text{C}$ and Low PG +10°C) <sup>c</sup>	AASHTO T313	BBR
ABCD	Thermal cracking	Critical cracking temperature	RTFO+20h PAV	-	AASHTO TP92	ABCD

<sup>a</sup> For example, PG 64-22 should be tested at 58°C and 64°C;

<sup>b</sup> m-value is defined as the rate of change of stiffness with time;

<sup>c</sup> For example, PG 52-28 should be tested at -12°C, -18°C, and -24°C.

### 3.2.2 DSR Test

The frequency sweep tests were conducted using a DSR (Anton Paar MCR 302, Figure 3.4) to evaluate the viscoelastic behavior at in-service and high temperatures, according to AASHTO T 315 *Standard Method of Test for Determining the Rheological Properties of Asphalt Binder Using a Dynamic Shear Rheometer (DSR)*. The tests were conducted on the asphalt samples with different aging states (i.e. RTFO, 20h PAV, 40h PAV). The stress control model was applied, and a target stress value of 10% was applied to RTFO residues and that of 1% was applied to PAV residues. The  $G^*$  and  $\delta$  were obtained at different combinations of temperature and loading frequency. Frequency sweep tests were conducted at 5°C, 15 °C, 25°C, and 35°C. The parallel plate geometry (8 mm) with a 2-mm gap were used. The loading frequency varied from 0.1 rad/s to 100 rad/s.  $G^*$  and  $\delta$  master curves (at reference temperature of 15°C) were generated using rheology analysis (RHEA) software. Black space diagrams, Glover-Rowe Parameter, and R-value were obtained using the data from master curves.

The DSR tests ( $G^*/\sin\delta$  grading tests) were also conducted on original (unaged) and RTFO residues at specific temperatures and load frequency (10 rad/s). The strain control model with a 12% and 10% of strain was applied for unaged and RTFO residues, respectively. The testing temperatures were selected based on the PG of to be tested asphalt binder. Generally speaking, the binders were tested at binder's high-grade temperature and one grade below. The  $G^*/\sin\delta$  of binder was obtained at each testing temperature, and was compared with the Superpave specification of 1.0 kPa and 2.20 kPa for unaged and RTFO residues, respectively. Two replicates were tested for each sample.



Figure 3.4 the DSR equipment

MSCR tests were conducted on RTFO residues by using the same DSR according to AASHTO T 350 *Standard Method of Test for Multiple Stress Creep Recovery (MSCR) Test of Asphalt Binder Using a Dynamic Shear Rheometer (DSR)*. MSCR test is the latest improvement to the Superpave PG asphalt binder specification. It uses the well-established creep and recovery test concept to evaluate the binder's potential for permanent deformation, a 1-second creep load is applied to the asphalt binder sample. After the 1-second load is removed, the sample is allowed to recover for 9 seconds. The test starts with the application of a low stress (0.1 kPa) for 20 creep/recovery cycles (use the first ten cycles for conditioning the specimen) then the stress increased to 3.2 kPa and repeated for an additional 10 cycles. Two replicates were tested for each sample.



### 3.2.3 BBR Test

The BBR tests were conducted on and RTFO and PAV (both 20h and 40h) residues at various low temperatures to obtain the continuous low temperature grade (critical temperature ( $T_c$ )) for both stiffness (S) and m-value, which is defined as the rate of change of stiffness with time, according to AASHTO T 313 *Standard Method of Test for Determining the Flexural Creep Stiffness of Asphalt Binder Using the Bending Beam Rheometer (BBR)*. Figure 3.5 shows the major BBR equipment. Superpave specified that the measured S value at 60 seconds must be less than 300 MPa and the m-value at this time of loading must be at least 0.30. For the test, a sample of asphalt binder was molded into a beam measuring 6.25 x 12.5 x 127 mm (Figure 3.7). This sample was then simply supported at two points 102 mm apart in a controlled temperature fluid bath. The beam was then loaded at the midpoint by a 100 g load that, under normal gravity conditions, produces 0.98 N of force. By using the Simple Beam theory, the stiffness and m-value were determined. Two replicates were tested for each sample. The  $\Delta T$  which is defined as the difference between critical temperatures for stiffness and m-value, was calculated to quantify the relative loss of relaxation due to the effect of aging (AI 2019).



Figure 3.5 the BBR equipment

#### **3.2.4 ABCD Test**

The ABCD is a device to directly measure the cracking temperatures for thermal cracking of asphalt binders, and can be used by itself or in conjunction with other test methods to accurately grade asphalt binders for low temperature performance. In this study, the testing procedures in this study followed AASHTO TP92. The 20 h PAV residues were tested. The ABCD consists of a metal ring, a strain gauge glued to the inner side of the ring, an environmental chamber (Figure 3.6), and a data acquisition system. The ABCD utilizes the dissimilar coefficients of thermal expansion/contraction of asphalt binders and metals. Before the test, hot asphalt is poured into the mold to form the asphalt ring after it cools down. During the testing, as temperature drops at a rate of 20°C/h, the metal ring provides contraction restraint to the asphalt binder ring. A thermal stress is developed during this process and leads to the final crack of the binder sample. At the crack temperature, the microstrain developed in the tested

asphalt binder is measured and this indicates the thermal cracking resistance property of the asphalt binder. Four replicates were used for each test.

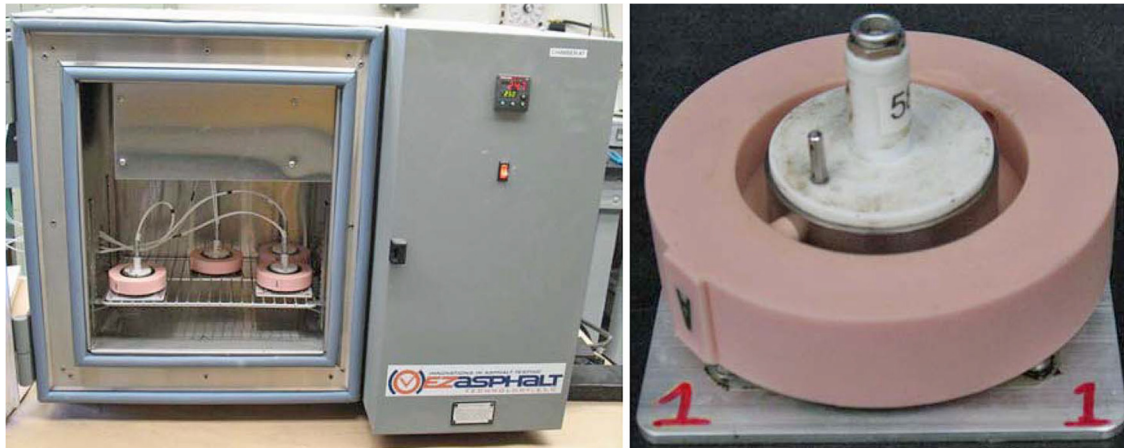


Figure 3.6 Asphalt binder cracking device

### 3.3 Mixture Specimen Fabrication

The laboratory-produced mixture (Mix #10) was fabricated following the JMF. Each aggregate gradation was weighed and placed in an oven at 165°C for 2 hours. Asphalt binder (PG 52-46) was heated at 165°C for about 1 hour to gain enough workability based on the recommendation of the supplier. The aggregates and the asphalt binder were then mixed using a mixer. The Rice tests were conducted based on AASHTO T209 *Theoretical Maximum Specific Gravity and Density of Bituminous Paving Mixtures* for both plant and Lab produced mixes to measure the theoretical maximum specific gravity (Gmm). The laboratory produced loose asphalt mix was placed in the oven at 165°C for an additional 2 hours to simulate short-term aging. The HMA test specimens (both laboratory and plant produced) were fabricated using the Superpave gyratory compactor (SGC) (Figure 3.7) according to AASHTO PP 60 *Preparation of Cylindrical Performance Test Specimens Using the Superpave Gyratory Compactor (SGC)*. The

target air voids of testing specimens was  $7.0 \pm 0.5\%$ . An estimate of the HMA required was determined using the  $G_{mm}$ , target height, and target air void content using Equation 3.1.

$$Mass = \left[ \frac{100 - (Va_t + F)}{100} \right] * G_{mm} * 176.7147 * H \quad (3.1)$$

where

Mass = estimated mass of mixture to prepare a test specimen to target air voids

$Va_t$  = target air void content for the test specimen, percent by volume

$G_{mm}$  = maximum specific gravity of the mixture

H = height of the gyratory specimen, cm

F = air void adjustment factor: 1.0 for fine-graded; 1.5 for coarse-graded

Using the estimated mass from Equation 3.1, a trial specimen was prepared. The bulk specific gravity was measured, and the air void content was determined. The mass was then adjusted using the following equation:

$$Mass_{adj} = \left[ \frac{100 - Va_t}{100 - Va_m} \right] * Mass \quad (3.2)$$

where

$Mass_{adj}$  = adjusted gyratory specimen mass, g

$Va_t$  = target air void content for the test specimen, percent by volume

$Va_m$  = measured trial test specimen air void content, percent by volume

Mass = mass used to prepare the gyratory specimen for the trial test specimen

Using the adjusted mass from Equation 3.2, a second trial gyratory specimen was fabricated. The bulk specific gravity was measured and the air void content was determined. If

the air void tolerance was not satisfied, the mass was again adjusted. The process was repeated until the air void content was within the acceptable range.



Figure 3.7 Superpave gyratory compactor

In order to produce the specimens for IDT tests, samples were compacted into gyratory cylinder with a diameter of 150 mm and a height of 70 mm, and then they were cut into 50 mm thick pieces using a masonry saw (Figure 3.8). Both ends were cut to ensure a more consistent air void distribution along the height of the test specimens. Figure 3.9 shows the representative specimens for IDT tests. Studs for mounting linear variable differential transformers (LVDTs) were then attached to the IDT specimens using a gauge point fixing jig (Figure 3.10). Owing to the IDT creep compliance test is a non-destructive test, the specimens were firstly used for the creep compliance test, and then used for IDT tensile strength test which is a destructive test. Three replicates were tested for each sample.



Figure 3.8 Masonry saw



Figure 3.9 IDT tests specimens



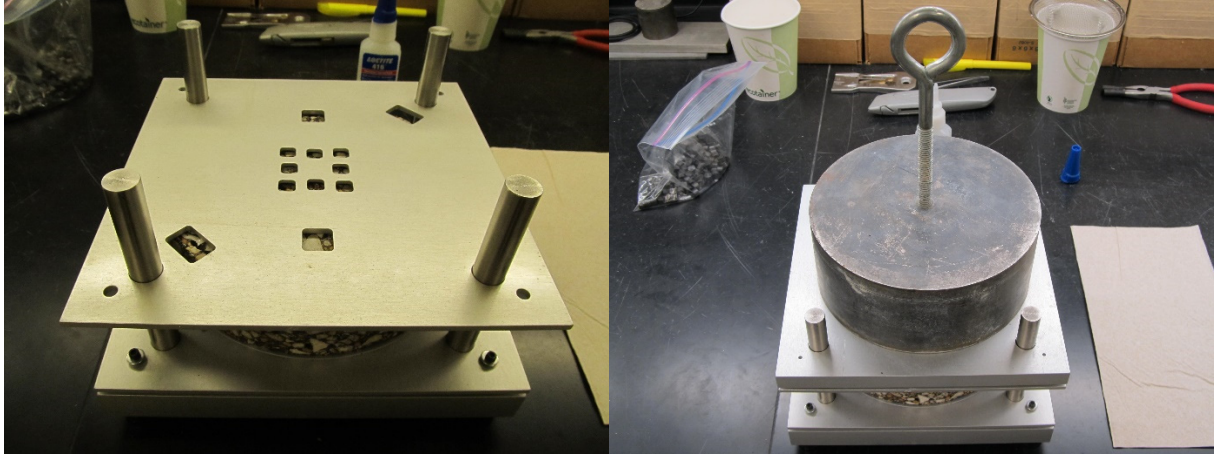


Figure 3.10 Gauge point fixing jig

For specimens tested in the HWT tests, samples were compacted into gyratory cylinder of 150 mm in diameter by 124 mm in height. The compacted sample was cut along its horizontal axis to produce two test specimens having a diameter of 150 mm and a height of 62 mm. Then the 150-mm diameters specimens were sawed along a secant line to achieve the gap width between two specimens no greater than 7.5 mm. Three replicates were tested for each sample. Figures 3.11 shows the HWT specimens.



Figure 3.11 HWT specimens after testing

The semi-circular shaped specimens for SCB tests were prepared by cutting the gyratory cylinder of 150 mm in diameter by 127 mm in height into three equal circular test samples 38 mm thick with three saws (cut five times, all specimens with two cut faces). Then the cylinder specimens were cut along its central axis into two semi-circular specimens whose height and radius were within 1 mm of each other. After this, each semi-circular specimen was straight notched at the center along the symmetric axis of the specimen. Three notch depths (i.e. 25mm, 32mm, and 38mm) were used. Three replicates were tested for each sample. Figure 3.12 shows semi-circular specimens.

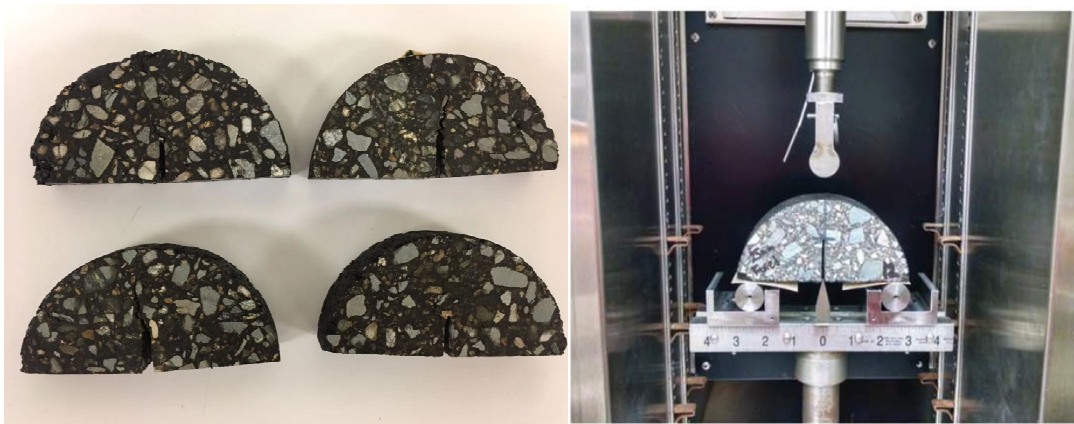


Figure 3.12 SCB specimens

The air voids of all test specimens were confirmed following AASHTO T 269, *Percent Air Voids in Compacted Dense and Open Asphalt Mixtures*. The air voids of test specimens were determined using Equation 3.3. The air voids of all the test specimens are presented in Appendix B.

$$\text{Percent Air Voids} = 100 \left( 1 - \frac{G_{mb}}{G_{mm}} \right) \quad (3.3)$$



### 3.4 Laboratory Mixture Performance Tests

Table 3.4 shows a detailed laboratory testing plan of modified asphalt mixture.

Laboratory tests included HWT test for rutting evaluation, SCB test for fatigue cracking resistance assessment, and creep compliance and tensile strength from IDT for low-temperature cracking evaluation.

Table 3.4 Laboratory testing plan

Test	Property	Standard	Test temperature
HWT test	Rutting; Moisture-susceptibility	AASHTO T324; Yin et al., (2014)	50 °C for mixtures with PG 64-40; 40 °C for the other mixtures
SCB test	Fatigue cracking	ASTM D8044-16	25°C
IDT Creep Compliance and Strength	Low temperature cracking	AASHTO T322-07	-20, -10, and 0 °C for mixture with PG 52-28; -30, -20, and -10 °C for the other mixtures

#### 3.4.1 HWT Test

The HWT test was conducted to evaluate the rutting resistance of the different mixtures in this project according to AASHTO T324 *Standard Method of Test for Hamburg Wheel-Track Testing of Compacted Asphalt Mixtures*. The water temperature was set as 50°C for the mixtures with PG 64-40. For other mixtures, the water temperature was set as 40°C. The water temperatures used in this project were selected per the request of engineers of ADOT&PF.

Figure 3.13 shows the Asphalt Pavement Analyzer (APA) configured for HWT testing in our project. The APA device for HWT testing tracks a loaded steel wheel back and forth directly on a mixture specimen. The 47 mm wide and 203.2 mm diameter wheel is tracked across a submerged (underwater) sample for 20,000 cycles using a 158 lb (705 N) load.

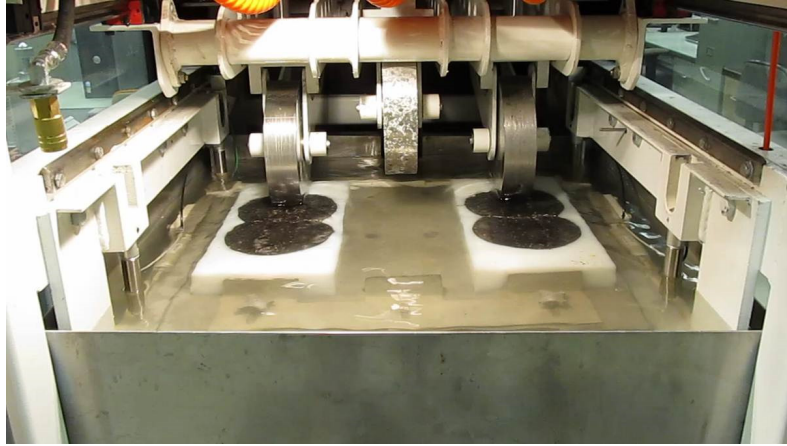


Figure 3.13 HWT test equipment

During testing, rut depths were measured continuously with a series of LVDTs on the sample. Figure 3.14 presents the typical HWT test curve (i.e., rut depth at the center of the specimen versus load cycle). According to Yin et al. (2014), the curve can be determined from three main phases:

- (1) The post-compaction phase, which is usually regarded as the specimens' consolidation phase owing to the densification of wheel load. This phase usually occurs within the first 1,000 load cycles.
- (2) The creep phase, which is the deformation phase of the asphalt mixture due to the viscous flow. During this phase, the rut depth of the mixture usually increasing at an almost constant rate with the increase of load cycle.
- (3) The stripping phase, which is the phase that the deformation cause of the asphalt mixture is the combination of viscous flow and stripping or raveling. This phase starts once the bond between the asphalt binder and the aggregate starts degrading.

Currently, the stripping inflection point (SIP) and rut depth at a specific number of load cycles are the most two widely used parameters to assess the moisture susceptibility and rutting potential of mixtures, respectively. The SIP is graphically represented at the intersection of the fitted lines that characterize the creep phase and the stripping phase.

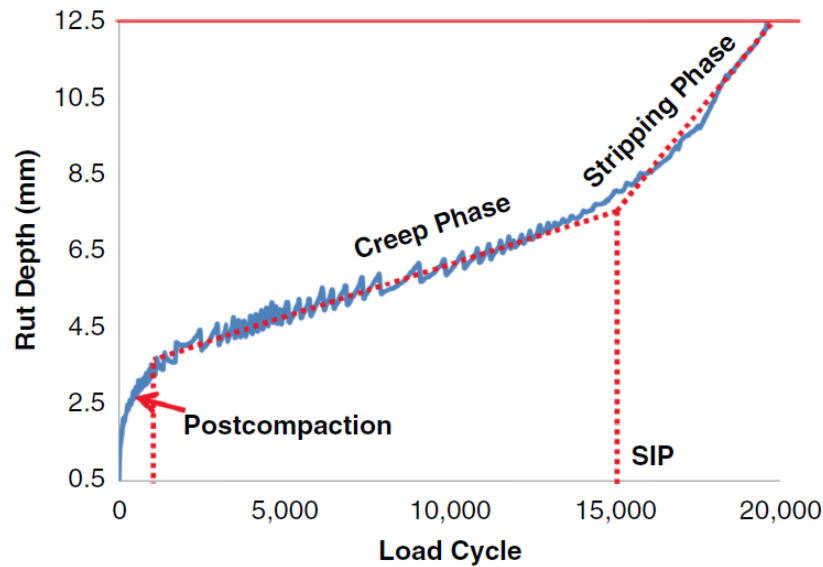


Figure 3.14 Typical HWT test curve (after Yin et al. (2014))

In addition to these two traditional parameters of HWT test, three novel parameters ( $LC_{SN}$ ,  $LC_{ST}$ , and  $\Delta\epsilon_{10,000}^{vp}$ ) developed by Yin et al. (2014) were also used in this study to discriminate asphalt mixtures with different moisture susceptibility and rutting potential.  $LC_{SN}$  and  $LC_{ST}$  were proposed to evaluate mixture susceptibility to moisture before and after the stripping number (SN), respectively.  $LC_{SN}$  is meant to complement  $\Delta\epsilon_{10,000}^{vp}$  to evaluate mixture resistance to rutting in the presence of water. Mixtures with higher  $LC_{SN}$  and  $LC_{ST}$  values are expected to be less moisture susceptible as compared with those with lower  $LC_{SN}$  and  $LC_{ST}$  values. Mixtures with lower  $\Delta\epsilon_{10,000}^{vp}$  values are expected to have better resistance to rutting as

compared with those with higher  $\Delta\varepsilon_{10,000}^{vp}$  values. The following paragraphs present the general background of these three parameters.

Yin et al. (2014) applied the following function (Equation 3.4) to fit the HWT curves.

$$RD_{LC} = \rho * \left[ \ln \left( \frac{LC_{ult}}{LC} \right) \right]^{-1/\beta} \quad (3.4)$$

where, LC = number of load cycles;  $RD_{LC}$  = rut depth at a certain number of load cycles (mm); and  $LC_{ult}$ ,  $\rho$ , and  $\beta$  = model coefficients, and three coefficients were determined from a nonlinear regression analysis.

$LC_{SN}$  (Figure 3.15) is the abscissa value (load cycles) of critical point (at this point, the curvature of HWT test curve changes from negative to positive) of the HWT test curves, which represents the maximum number of load cycles that the asphalt mixture can resist in the HWT test before the stripping occurs. It can be obtained by setting the second derivative of the Equation 3.4 to zero, as shown in Equation 3.5.

$$LC_{SN} = LC_{ult} \exp \left( -\frac{\beta+1}{\beta} \right) \quad (3.5)$$

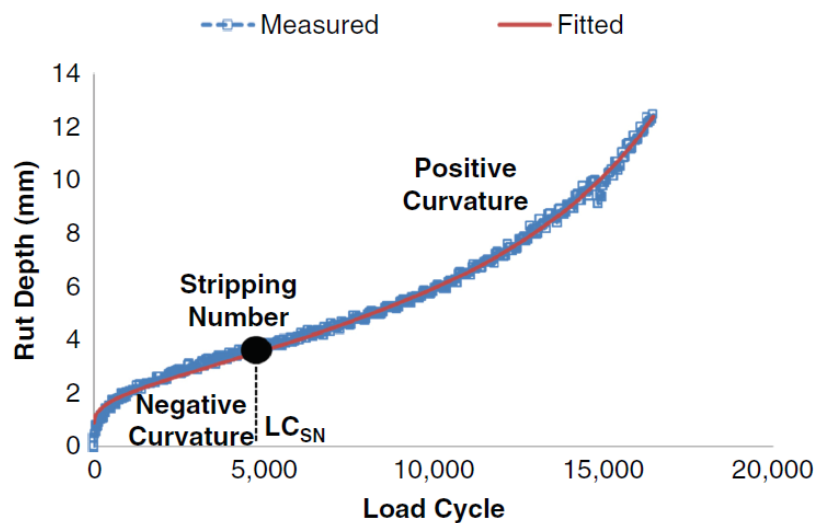


Figure 3.15 HWT stripping number determination (Yin et al. (2014)).

$LC_{ST}$  is the stripping life of the mixture that represents the number of additional load cycles after  $LC_{SN}$  needed for the rut depth accumulated by the predicted stripping strain to reach the common HWT test failure depth of 0.5 in. (12.5 mm).  $LC_{ST}$  can be determined by taking the stripping strain ( $\epsilon^{st}$ ) which is the difference between the total permanent strain ( $\epsilon^p$ ) and the projected viscoplastic strain ( $\epsilon^{vp}$ ) to the ratio of the 0.5 in. (12.5 mm) to the specimen thickness.  $\epsilon^p$  can be calculated from Equation 3.6.  $\epsilon^{vp}$  is the primary cause for the rut depth accumulated before the stripping number (SN) and can be calculated from Equation 3.7. Therefore,  $\epsilon^{st}$  can be depicted as Equation 3.8.

$$\epsilon^p = \frac{RD_{LC}}{T} \quad (3.6)$$

$$\epsilon^{vp} = \epsilon_{\infty}^{vp} \exp \left[ - \left( \frac{\alpha}{LC} \right)^{\lambda} \right] \quad (3.7)$$

$$\epsilon^{st} = \frac{RD_{LC}}{T} - \epsilon_{\infty}^{vp} \exp \left[ - \left( \frac{\alpha}{LC} \right)^{\lambda} \right] \quad (3.8)$$

where,  $\epsilon^{vp}$  = viscoplastic strain;  $\epsilon_{\infty}^{vp}$  = saturated viscoplastic strain in the HWT test specimen; and  $\alpha$  and  $\lambda$  = model coefficients.  $\epsilon_{\infty}^{vp}$ ,  $\alpha$ , and  $\lambda$  can be determined from a nonlinear regression analysis. Once  $\epsilon_{\infty}^{vp}$ ,  $\alpha$ , and  $\lambda$  are determined, the  $\epsilon^{st}$  versus load cycle HWT test curve can be fitted by a step function (Equation 3.9), then take the function to the ratio of the 0.5 in. (12.5 mm) to the specimen thickness, the  $LC_{ST}$  can be determined (Equation 3.10).

$$\epsilon^{st} = \begin{cases} \epsilon_0^{st} \{ \exp[\theta(LC - LC_{SN})] - 1 \} & \text{if } LC - LC_{SN} \geq 0 \\ 0 & \text{if } LC - LC_{SN} \leq 0 \end{cases} \quad (3.9)$$

$$LC_{ST} = \frac{1}{\theta} \ln \left( \frac{12.5}{T * \epsilon_0^{st}} + 1 \right) \quad (3.10)$$

$\Delta\varepsilon_{10,000}^{vp}$  is calculated as the slope of the projected viscoplastic strain by the Equation 3.7 at a certain number of load cycles (i.e., 10,000 load cycles), as described in Equation 3.11.

$$\Delta\varepsilon_{10,000}^{vp} = \alpha^\gamma \gamma \varepsilon_\infty^{vp} \exp \left[ - \left( \frac{\alpha}{10,000} \right)^\gamma \right] (10,000)^{-(\gamma+1)} \quad (3.11)$$

### 3.4.2 SCB Test

The SCB test was conducted on each mixture to evaluate fatigue-cracking performance at an intermediate temperature of 25 °C. The SCB tests were performed based on the Louisiana SCB test Method (ASTM D8044-16 *Standard Test Method for Evaluation of Asphalt Mixture Cracking Resistance using the Semi-Circular Bend Test (SCB) at Intermediate Temperatures*).

An Instron® Auto SCB (Figure 3.16) was used to conduct all SCB tests.



Figure 3.16 SCB test equipment

The SCB test was conducted by loading the sample monotonically to failure at a constant crosshead deformation rate of 0.5 mm/min rate. The Fracture Energy needed to cause failure was determined for each sample by computing the area under the load versus displacement curve up

to the peak load. The critical strain energy release rate ( $J_c$ ) was calculated by fitting the average strain energy per thickness of the sample with each notch depth (Equation 3.12). In general, the higher the  $J_c$ , the better the fatigue cracking resistance.

$$J_c = \frac{-1}{b} \left( \frac{dU}{da} \right) \quad (3.12)$$

where,  $b$  = the sample thickness (m);  $a$  = sample notch depth (m);  $U$  = strain energy up to peak load of failure (kJ);  $\frac{dU}{da}$  = change of strain energy with notch depth (kJ/m).

The strain energy ( $U$ ) can be calculated using the quadrangle rule provided in Equation 3.13.

$$U = \sum_{i=1}^n \left\{ (u_{i+1} - u_i) \times P_i + \frac{1}{2} \times (u_{i+1} - u_i) \times (P_{i+1} - P_i) \right\} \quad (3.13)$$

where,  $P_i$  = applied load (kN) at the  $i$  load step application;  $P_{i+1}$  = applied load (kN) at the  $i+1$  load step application;  $u_i$  = crosshead displacement (m) at the  $i$  step;  $u_{i+1}$  = crosshead displacement (m) at the  $i+1$  step.

### **3.4.3 IDT creep compliance and strength tests**

The IDT creep compliance and strength tests were conducted to assess the low temperature cracking resistance of different modified mixtures according to AASHTO T 322 *Standard Method of Test for Determining the Creep Compliance and Strength of Hot Mix Asphalt (HMA) Using the Indirect Tensile Test Device*. Figure 3.17 shows the main equipment for IDT tests. The temperature chamber is MTS model 651.34. The temperature is controllable from -30 to +100°C,  $\pm 0.2^\circ\text{C}$ . A programmed data acquisition system was used to record the load and deformation of the specimens during testing.

The definition of creep compliance in AASHTO T 322 is “the time-dependent strain divided by the applied stress”. The test is conducted by imposing a static compressive load along

a diametral axis of the cylindrical specimen at the target test temperature for about 100 seconds. Creep compliance testing is non-destructive, so each specimen can be tested at several temperatures. In this study, tests were conducted at three different temperatures at 10°C intervals according to the binder's low temperature grade. For mixtures with PG 52-28, the test temperatures were -20, -10, and 0°C. Otherwise, the test temperatures were -30, -20, and -10°C. During the loading period, vertical and horizontal deformations were measured on the two parallel faces of the specimen using two LVDTs per specimen face. Three replicates were applied. The creep compliance of each mixture was calculated according to the function (Equation 3.14) from AASHTO T 322.

$$D_t = \frac{\Delta X \times D_{avg} \times b_{avg}}{P_{avg} \times GL} \times C_{cmpl} \quad (3.14)$$

where,  $D_t$  = creep compliance (1/kPa);  $\Delta X$  = trimmed mean of the horizontal deformations (m),  $D_{avg}$  = average specimen diameters (m);  $b_{avg}$  = average specimen thickness (m);  $P_{avg}$  = average force during the test (kN);  $GL$  = gage length (38mm); and  $C_{cmpl}$  = creep compliance parameter at any given time, computed as:

$$C_{cmpl} = 0.6354 \times \left(\frac{X}{Y}\right)^{-1} - 0.332 \quad (3.15)$$

where,  $\frac{X}{Y}$  = the ratio of the horizontal to vertical deformations.

Tensile strength is another important parameter for evaluating the low temperature cracking resistance of mixtures. Higher tensile strength at low temperatures indicates higher resistance to low temperature cracking. Unlike creep compliance test, the tensile strength test is destructive, i.e. the specimen is loaded until tensile failure occurs and cannot be used again. The tests were conducted by applying a load to the specimens at a rate of 12.5 mm of vertical ram



movement per minute, and were conducted at the temperatures used for the creep test. The indirect tensile strength  $S$  was calculated using Equation 3.16.

$$S = \frac{2 \times P_{f,n}}{\pi \times b \times D} \quad (3.16)$$

where,  $P_{f,n}$  = failure (peak) load;  $b$  = specimen thickness; and  $D$  = specimen diameter.



Figure 3.17 IDT test equipment

## CHAPTER 4.0 RESULTS AND ANALYSIS

This chapter summarizes data results and analysis for both binder and mixture tests. The high-temperature and low-temperature properties of 13 Alaskan asphalt binders were evaluated. Engineering properties of asphalt mixtures including, rutting susceptibility, moisture sensitivity, fatigue resistance, and low-temperature performances are presented as well.

### 4.1 Binder Tests

#### 4.1.1 High-Temperature Binder Grade

According to  $G^*/\sin\delta$  values obtained on virgin (original) and RTFO-aged binders, the true high temperature grades of the tested binders were obtained. The grades are presented in Table 4.1. As shown, the true high temperature grades of binders #3 and #7 (PG 76-XX) were much higher than the grade indicated by the supplier, which was PG 64-XX. The true high temperature grades of binders #8 (PG 64-XX), #10 (PG 58-XX), #11 (PG 64-XX), and #12 (PG 58-XX) were one grade higher than the grade provided by the supplier. The true high temperature grade of binder #4 (PG 46-XX) was one grade lower than the grade provided by the supplier (PG 52-XX). Detailed data information can be found in Appendix C.

Table 4.1 True high-temperature grades of tested Alaskan binders

Binders	Aging state	Fail temperature* (°C)	True high temperature Grade
#1 (PG 52-28/A*)	Original	55.2	52
	RTFO	56.5	
#2 (PG 52-40/A)	Original	60.3	52
	RTFO	57.5	
#3 (PG 64-40/A)	Original	84.5	76
	RTFO	76.9	

Binders	Aging state	Fail temperature* (°C)	True high temperature Grade
#4 (PG 52-46/A)	Original	55.8	46
	RTFO	51.7	
#5 (PG 58-34/A)	Original	65.8	58
	RTFO	62.1	
#6 (PG 52-40/B)	Original	53	52
	RTFO	68.6	
#7 (PG 64-40/B)	Original	81.9	76
	RTFO	80.6	
#8 (PG 58-34/B)	Original	81.7	64
	RTFO	68	
#9 (PG 58-34/C)	Original	58.8	58
	RTFO	60.3	
#10 (PG 52-34/C)	Original	62.5	58
	RTFO	62	
#11 (PG 58-28/C)	Original	66.6	64
	RTFO	64.5	
#12 (PG 52-28plus/C)	Original	62.6	58
	RTFO	60.7	
#13 (PG 64-28/C)	Original	66.9	64
	RTFO	67.7	

Note: \* Fail temperature criteria:  $\text{Min } G^*/\sin\delta = 1.0 \text{ kPa}$  for original binder;  $\text{Min } G^*/\sin\delta = 2.2 \text{ kPa}$  for RTFO binder

#### 4.1.2 MSCR Test

MSCR tests were performed on RTFO aged asphalt binders in accordance with AASHTO T350. The MSCR test is the latest improvement to the Superpave PG asphalt binder specification. The tests results are listed in Table 4.2, typically interpreted by non-recoverable  $J_{nr}$  and recovery percentage ( $R$ ) under two different stress levels (i.e., 0.1 kPa and 3.2 kPa). As shown, the  $J_{nr}$  of neat binder was much higher than those of modified binders at identical testing temperatures and stress levels, which indicated that the binder polymer modification improved

the rutting resistance of the binder. According to AASHTO M332 *Performance-Graded Asphalt Binder Using Multiple Stress Creep Recovery (MSCR) Test*, the asphalt binder can be graded based on the  $Jnr$  value at 3.2 kPa. There are four grades at a given testing temperature based on the traffic level: standard traffic (S, fewer than 10 million ESALs), heavy traffic (H, 10 to 30 million ESALs), very high traffic (V, greater than 30 million ESALs), and extremely high traffic (E, greater than 30 million ESALs with standing traffic). If  $Jnr(3.2)$  is lower than or equal to  $0.5 \text{ kPa}^{-1}$ , the binder is graded as “E” at the desired temperature, if  $Jnr(3.2)$  is higher than  $0.5 \text{ kPa}^{-1}$  but lower than or equal to  $1 \text{ kPa}^{-1}$ , the binder is graded as “V”, if  $Jnr(3.2)$  is higher than  $1 \text{ kPa}^{-1}$  but lower than or equal to  $2 \text{ kPa}^{-1}$ , the binder is graded as “H”, if  $Jnr(3.2)$  is higher than  $2 \text{ kPa}^{-1}$  but lower than or equal to  $4.5 \text{ kPa}^{-1}$ , the binder is graded as “S”. As shown in Table 4.2, most of studied modified binders can be graded as “E” at  $52^\circ\text{C}$  without considering the percent difference of non-recoverable creep compliance ( $Jnr\text{-diff}$ ) which is used to evaluate the stress susceptibility of asphalt binder. The AASHTO M 332 specifies the maximum  $Jnr\text{-diff}$  value of 75% for each high-performance temperature. However, as can be seen in Table 4.2, the  $Jnr\text{-diff}$  values of modified binders at most of the testing temperatures beyond the maximum criterial of 75%. In addition, for modified binders (especially for the modified binders from suppliers A and B), the  $Jnr$  values were extremely low, with some of them even lower than 0.001. The  $R$  values for those modified binders were extremely high, with some of them almost 100%.

Figure 4.1 shows the “ $Jnr$  vs %R” relationship for all the studied modified binders at  $52^\circ\text{C}$ , according to AASHTO R 92 *Standard Practice for Evaluating the Elastic Behavior of Asphalt Binders Using the Multiple Stress Creep Recovery (MSCR) Test*. As shown, the data points for most of the studied modified binders were plotted on or above the elasticity limiting

curve. The data points represent for binder #12 (PG 52-28plus/C) and binder #13 (PG 64-28/C) were plotted under the curve, which implied that these binders had plastic properties.

Table 4.2 MSCR results

<b>Binder #/Binder PG/ Supplier</b>	<b>Temperature (°C)</b>	<b>R<sub>0.1</sub> (%)</b>	<b>R<sub>3.2</sub> (%)</b>	<b>Jnr(0.1) (1/kPa)</b>	<b>Jnr(3.2) (1/kPa)</b>	<b>Jnr-diff (%)</b>	<b>Grade</b>
#1/PG 52-28/A	46	5.07	1.34	1.018	1.0999	8.04	-
	52	6.27	0.86	2.2993	2.8223	22.75	S
	58	0.56	0.36	6.7546	7.1594	5.99	-
#2/PG 52-40/A	46	98.23	95.4	0.0159	0.0423	166.68	-
	52	99.16	95.39	0.0123	0.0664	437.57	E
	58	100.75	89.34	-0.0184	0.2349	-1374.32	-
#3/PG64-40/A	52	99.87	98.55	0.0007	0.0079	1037.72	E
	58	99.6	98.59	0.0029	0.0102	250.28	-
	64	98.63	97.79	0.0133	0.0204	53.34	-
#4/PG52-40/A	46	96.32	71.11	0.0570	0.5184	809.56	-
	52	95.12	51.20	0.1296	1.5336	1083.42	V
	58	87.98	25.38	0.5467	4.5574	733.58	-
#5/PG 58-34/A	52	98.77	93.79	0.013	0.067	416.52	E
	58	91.12	95.69	1.803	0.0728	-96.95	-
	64	98.55	94.41	0.0397	0.1317	231.87	-
#6/PG 52-40/B	52	90.09	78.51	0.5479	0.1681	-69.32	E
	58	101.57	75.68	-0.0181	0.3296	-1936.16	-
	64	97.66	74.23	0.0379	0.5308	1300.71	-
#7/PG 64-40/B	52	99.54	98.86	0.0027	0.0071	162.19	E
	58	99.27	98.46	0.0054	0.0114	111.17	-
	64	98.38	97	0.0155	0.0268	72.93	-
#8/PG 58-34/B	52	99.45	84.97	0.0038	0.1082	2778.36	E
	58	99.04	90.92	0.0115	0.1143	893.04	-
	64	98.79	79.77	0.0242	0.4382	1713.05	-
#9/PG 58-34/C	52	82.6	38.1	0.2439	1.1238	360.81	H
	58	98.76	28.26	0.0172	2.4229	14017.61	-
	64	73.08	5.72	1.2605	7.8864	479.68	-
#10/PG 52-34/C	52	57.33	29.74	0.5114	1.0135	98.16	H
	58	56.13	18.52	1.032	2.5378	145.92	-
	64	90.55	10.41	0.2829	5.5684	1868.52	-
#11 (PG 58-28/C)	52	59.86	45.45	0.3200	0.4685	46.38	E
	58	52.52	33.35	0.7833	1.2257	56.48	-
	64	42.55	18.07	1.9261	3.1985	66.06	-

Binder #/Binder PG/ Supplier	Temperature (°C)	R <sub>0.1</sub> (%)	R <sub>3.2</sub> (%)	Jnr(0.1) (1/kPa)	Jnr(3.2) (1/kPa)	Jnr-diff (%)	Grade
#12 (PG 52-28plus/C)	52	10.33	2.20	1.1355	1.3107	15.43	V
	58	4.71	0.01	2.9076	3.3550	15.39	-
	64	0.7	0	6.7907	7.6852	13.17	-
#13 (PG 64-28/C)	52	46.56	31.95	0.2626	0.3590	36.73	E
	58	36.54	18.03	0.6897	1.0303	49.38	-
	64	24.27	7.64	1.8031	2.7037	49.95	-

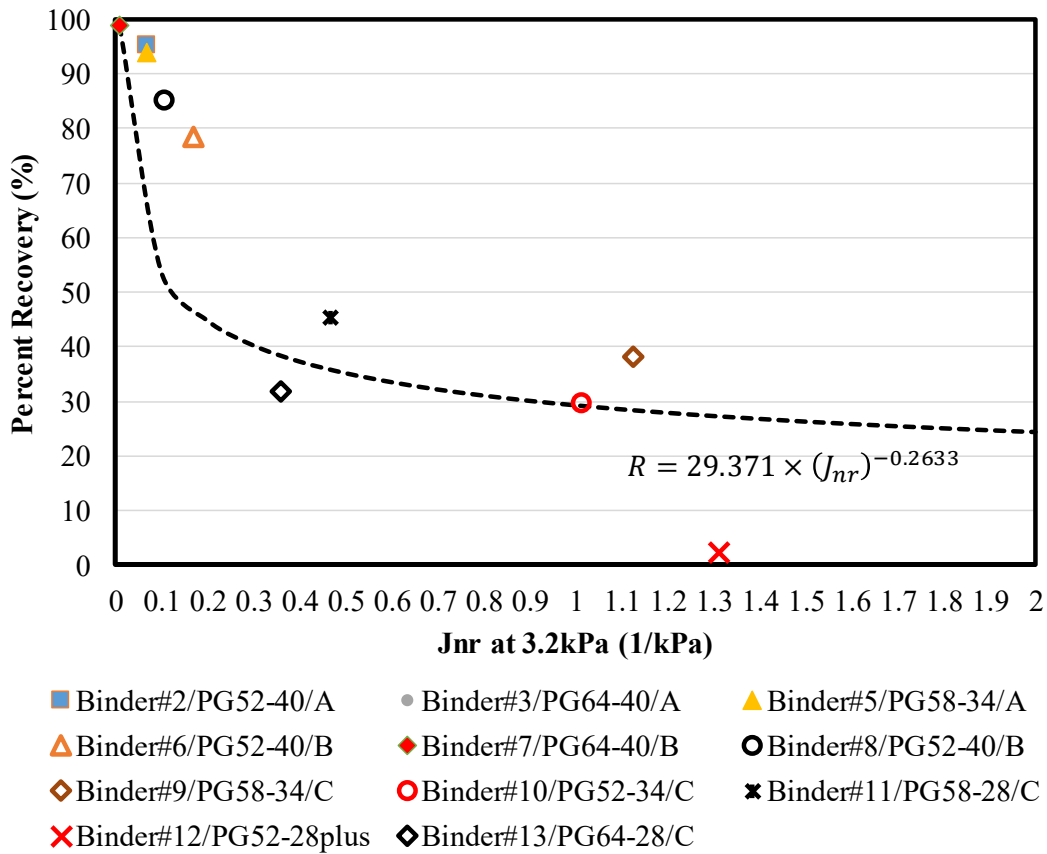


Figure 4.1 *Jnr* vs %*R* for polymer modified binders at 52° C

### 4.1.3 Master Curves

Figures 4.2 through 4.14 present  $G^*$  master curves of binders at different aging states (i.e., RTFO, 20h PAV, and 40h PAV) with a reference temperature of 15°C. The master curves were constructed by using RHEA software. RHEA software is a general tool for performing rheological analysis of materials that behave according to linear visco-elastic theory. The CA model (Equation 4.1) is applied to build master curve in this program. The software can automatically build the rheological master curve for asphalt materials with the data from DSR frequency sweep testing by applying the time-temperature superposition principle. In this study, the temperature-frequency sweep testing data at 5, 15, 25, and 35°C were collected to build the master curves.

$$G^*(\omega) = G_g \left[ 1 + \left( \frac{\omega_c}{\omega} \right)^{\frac{\log 2}{R}} \right]^{\frac{-R}{\log 2}} \quad (4.1)$$

where  $G^*(\omega)$  = complex shear modulus;  $G_g$  = glass modulus assumed equal to 1 Gpa;  $\omega_c$  = crossover frequency at the defining temperature (rad/s);  $\omega$  = frequency (rad/s); and  $R$  = rheological index.

These master curves can be used as a reference for comparison purposes and to predict curves at extreme frequency zones that are technically interesting but experimentally out of reach. As can be seen in Figures 4.2 to 4.14, as expected, the  $G^*$  increased with the increase of frequency, indicating that the asphalt binders could be stiffer at high frequency or low temperature (by applying time-temperature superposition principle).

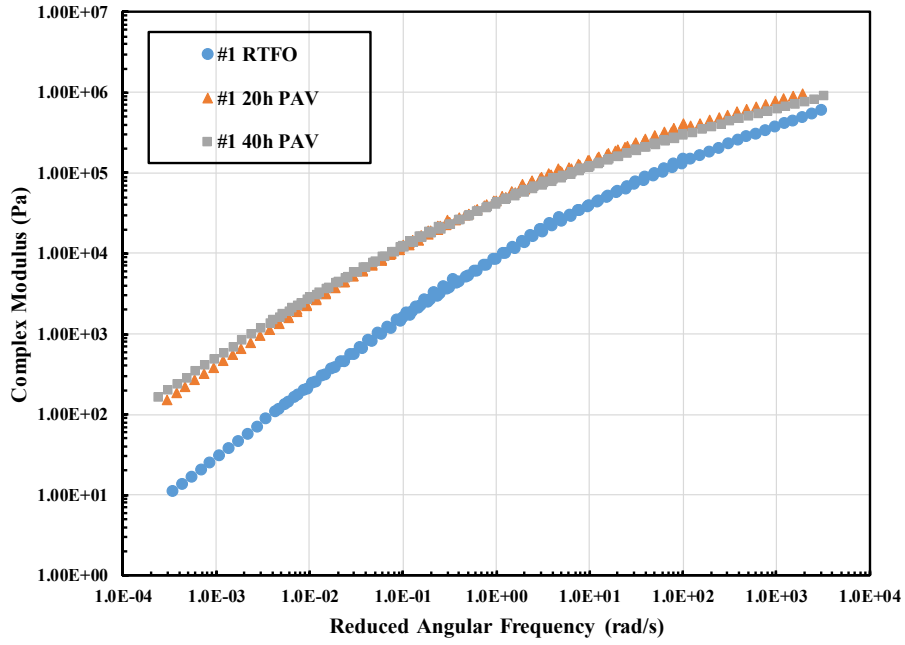


Figure 4.2  $G^*$  master curves of Binder#1 (PG 52-28/A) at different aging states

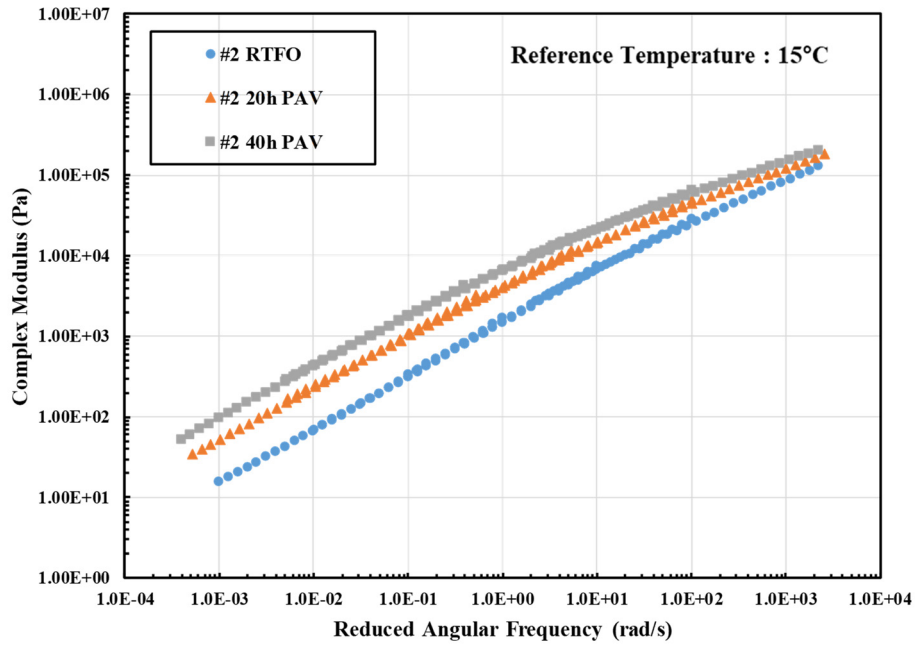


Figure 4.3  $G^*$  master curves of Binder#2 (PG 52-40/A) at different aging states



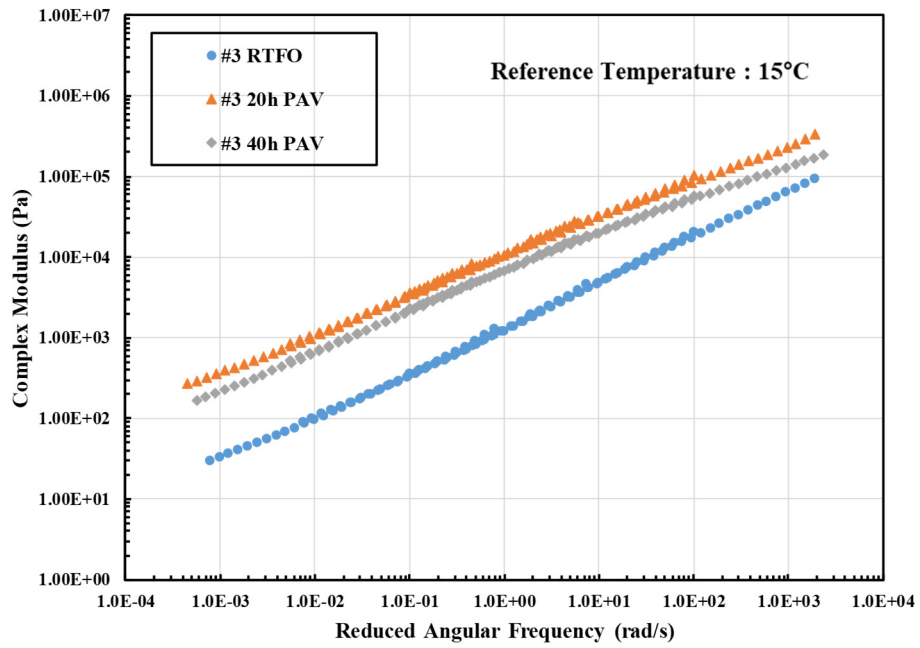


Figure 4.4  $G^*$  master curves of Binder#3 (PG 64-40/A) at different aging states

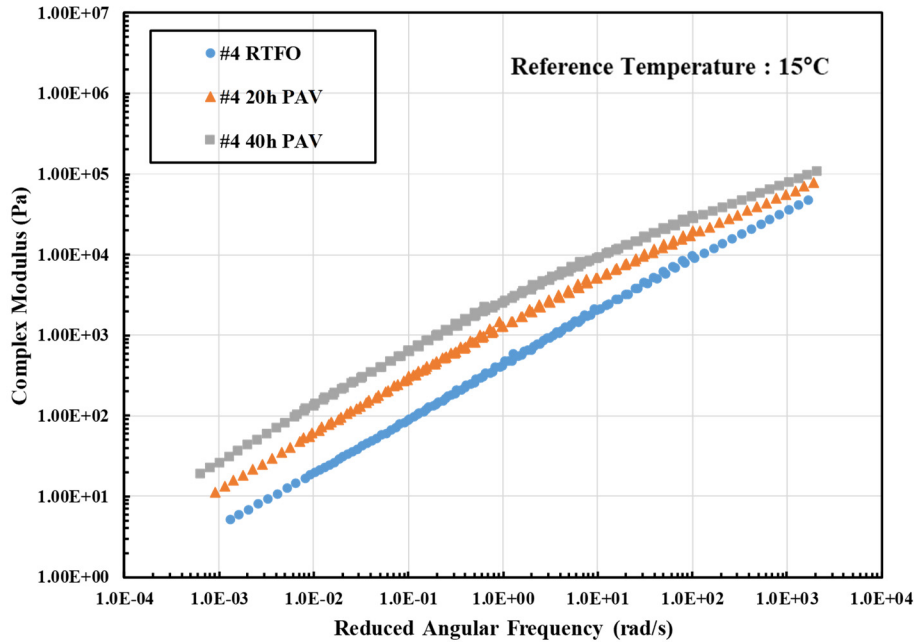


Figure 4.5  $G^*$  master curves of Binder#4 (PG 52-46/A) at different aging states

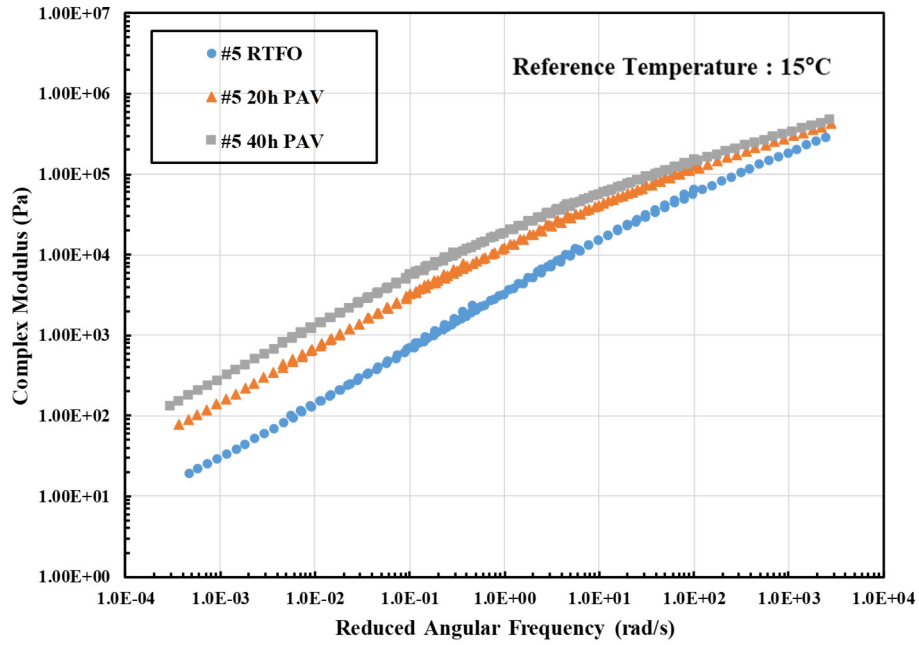


Figure 4.6  $G^*$  master curves of Binder#5 (PG 58-34/A) at different aging states

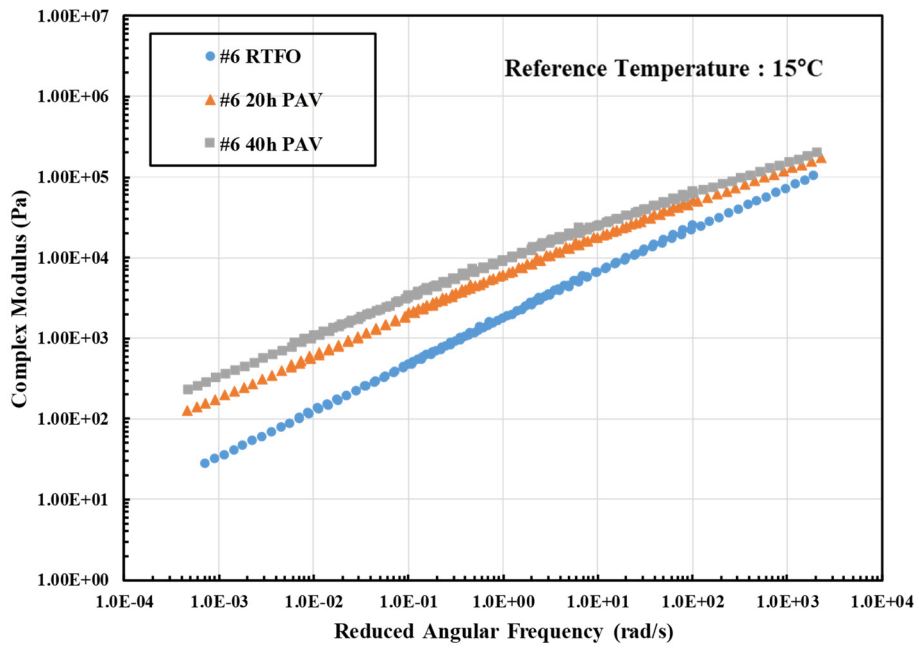


Figure 4.7  $G^*$  master curves of Binder#6 (PG 52-40/B) at different aging states

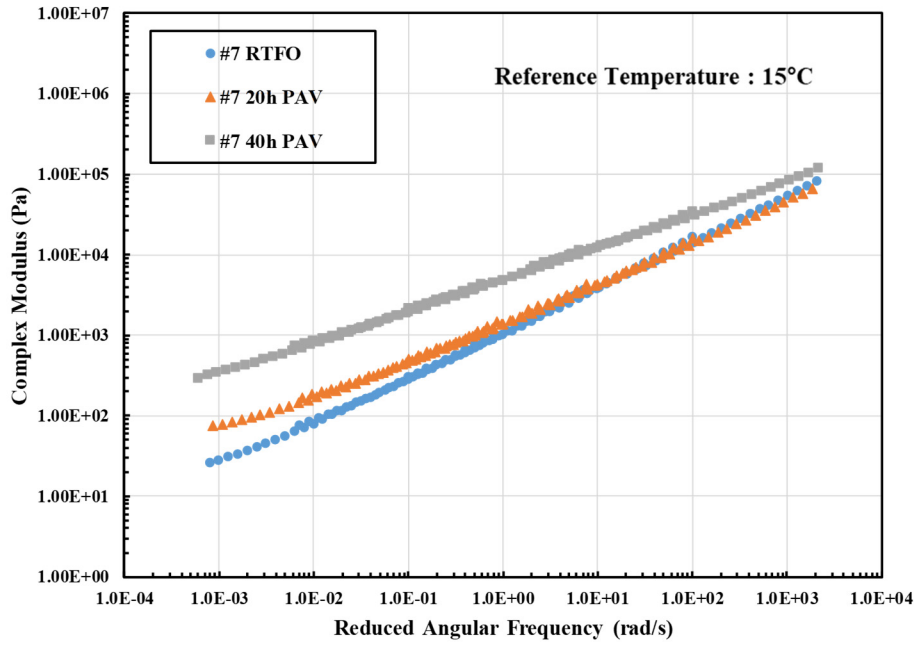


Figure 4.8  $G^*$  master curves of Binder#7 (PG 64-40/B) at different aging states

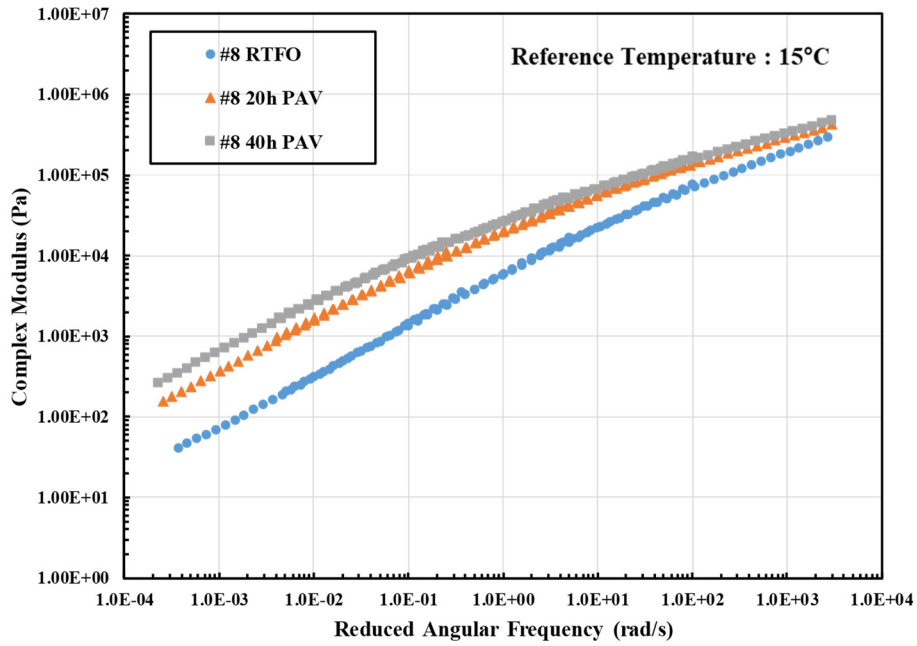


Figure 4.9  $G^*$  master curves of Binder#8 (PG 58-34/B) at different aging states

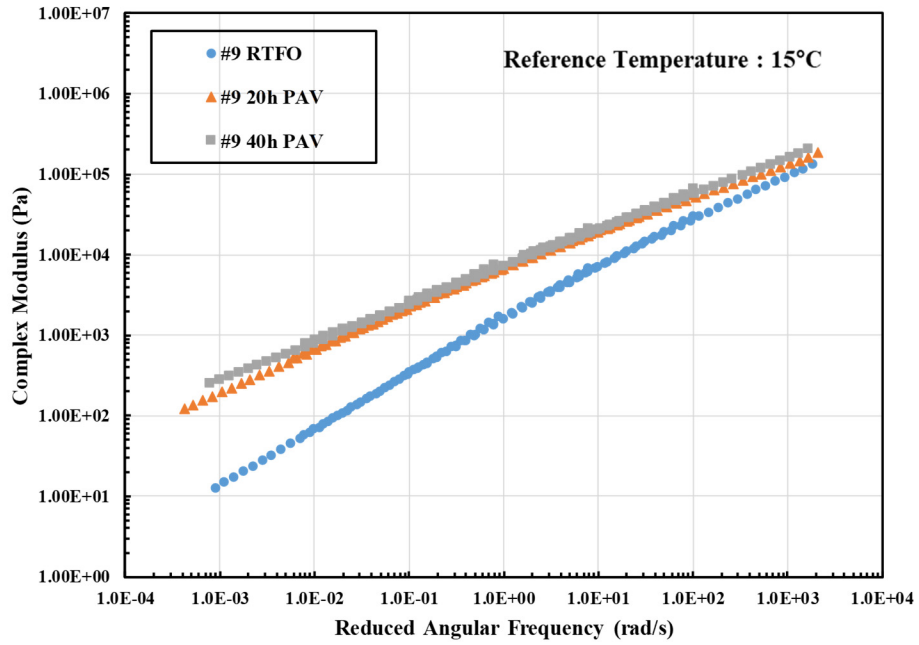


Figure 4.10  $G^*$  master curves of Binder#9 (PG 58-34/C) at different aging states

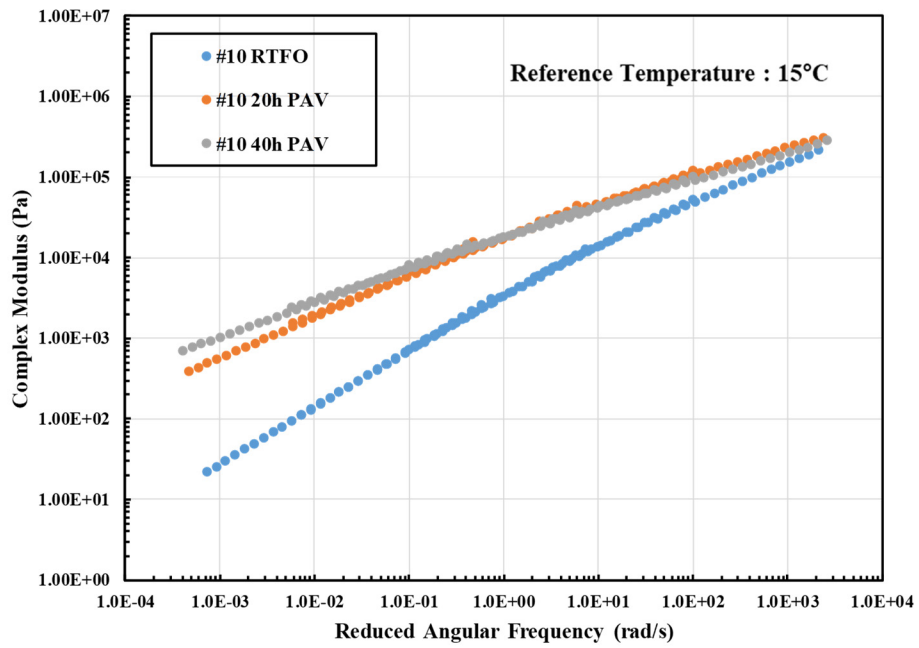


Figure 4.11  $G^*$  master curves of Binder#10 (PG 52-34/C) at different aging states

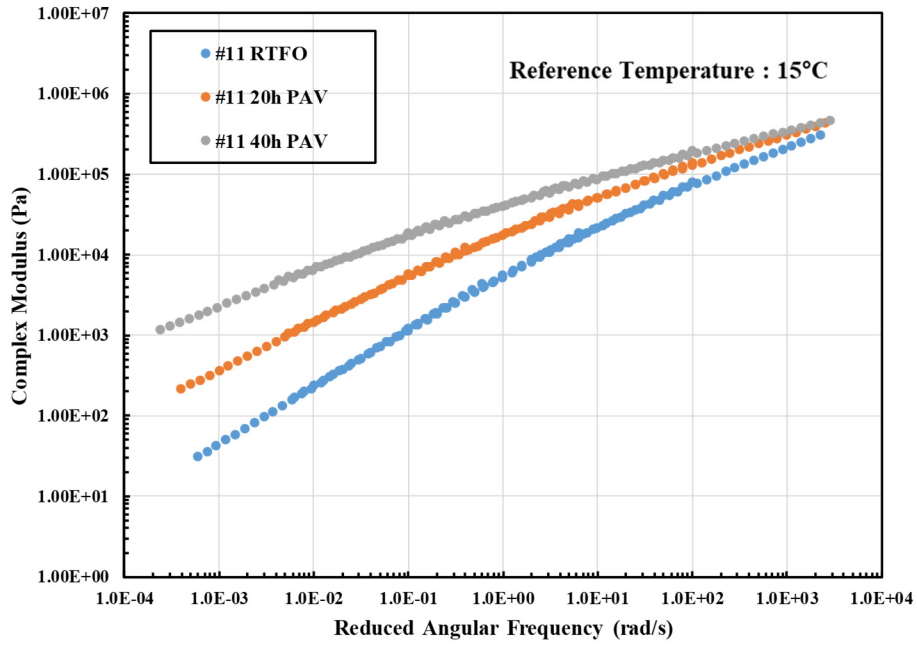


Figure 4.12  $G^*$  master curves of Binder#11 (PG 58-28/C) at different aging states

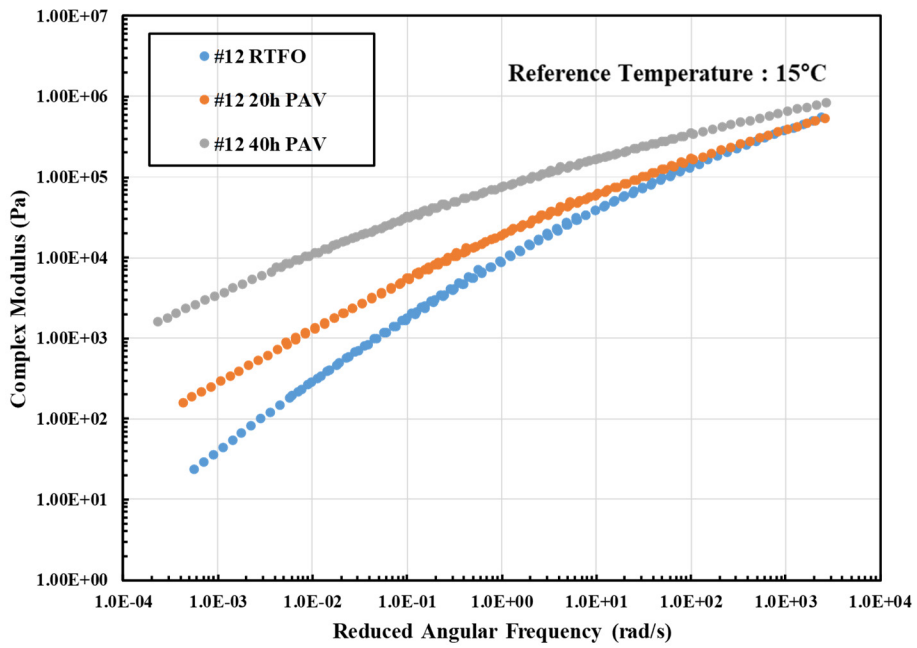


Figure 4.13  $G^*$  master curves of Binder#12 (PG 52-28plus/C) at different aging states

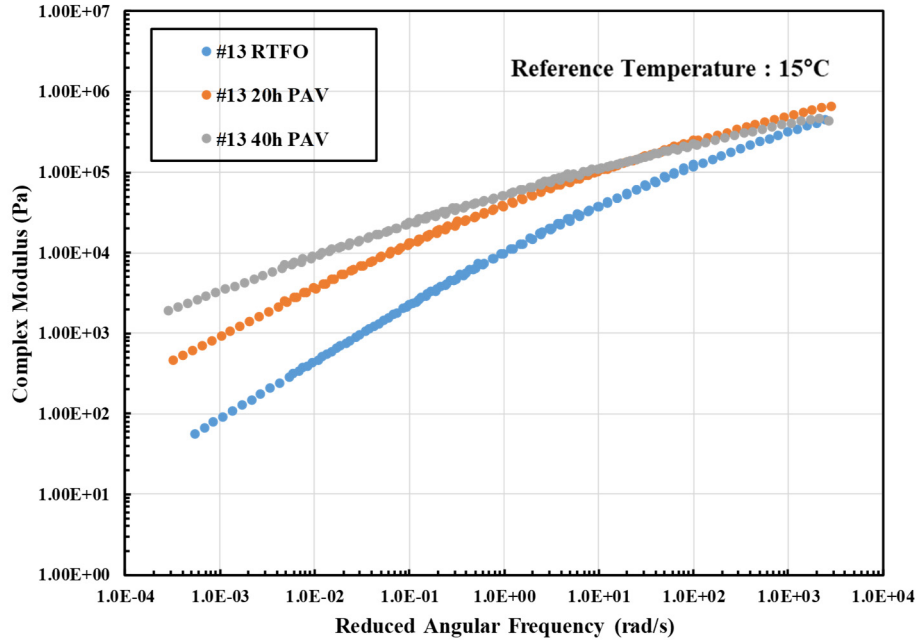


Figure 4.14 G\* master curves of Binder#13 (PG 64-28/C) at different aging states

#### 4.1.4 BBR Test

The BBR tests were conducted on asphalt binders with three different aging states at different temperatures. Figures 4.15 through 4.27 present the BBR test results for different binders. As shown in these figures, the temperatures at the intersections of the parallel dashed threshold line of each parameter (stiffness (300 MPa) and m-value (0.3) at 60 seconds) and the dotted lines generated by connecting tested values at different temperatures were used to determine the critical temperatures. It should be noted that the stiffness decreased while the m-value increased with the increase of temperature. For data lines without intersection, the following equations were applied to calculate the critical temperatures:

$$T_{c,s} = T_1 + \left[ \frac{\text{Log}(300) - \text{Log}(S_1)}{\text{Log}(S_1) - \text{Log}(S_2)} \times (T_1 - T_2) \right] - 10 \quad (4.2)$$

$$T_{c,m} = T_1 + \left[ \frac{0.3 - m_1}{m_1 - m_2} \times (T_1 - T_2) \right] - 10 \quad (4.3)$$

where,  $T_1$  and  $T_2$  are temperatures 1 and 2, respectively, °C;  $S_1$  and  $S_2$  are stiffness at  $T_1$  and  $T_2$ , respectively, MPa;  $m_1$  and  $m_2$  are m-value at  $T_1$  and  $T_2$ , respectively.

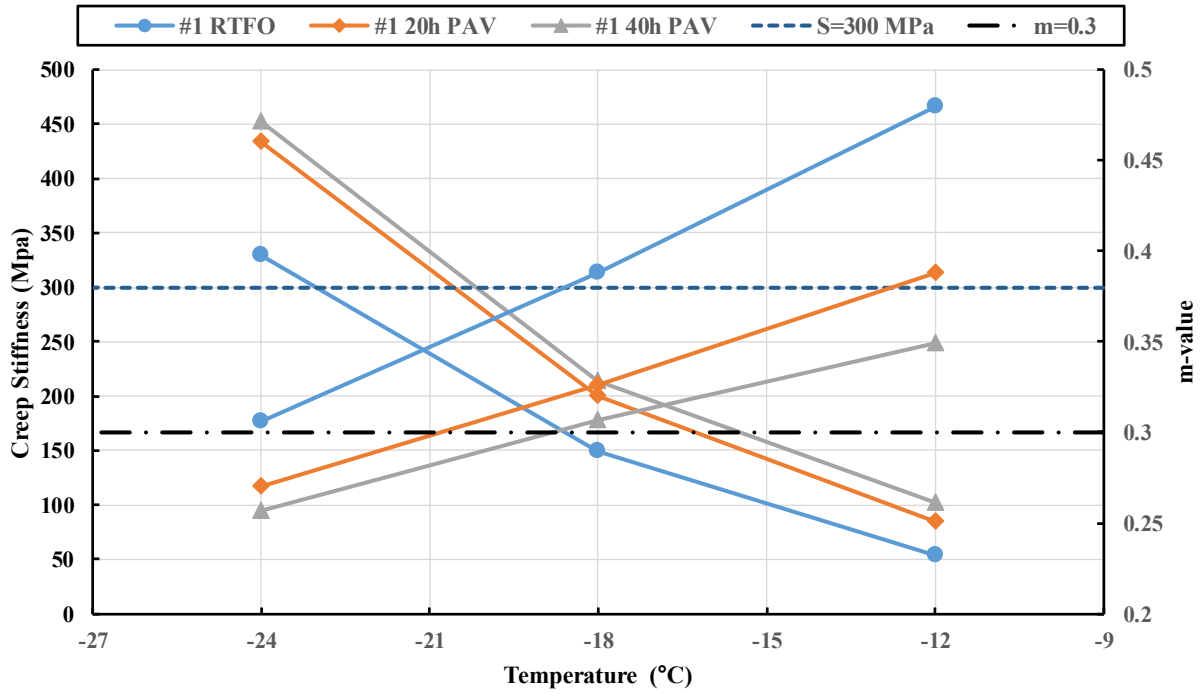


Figure 4.15 BBR test results of Binder#1 (PG 52-28/A) at different aging states

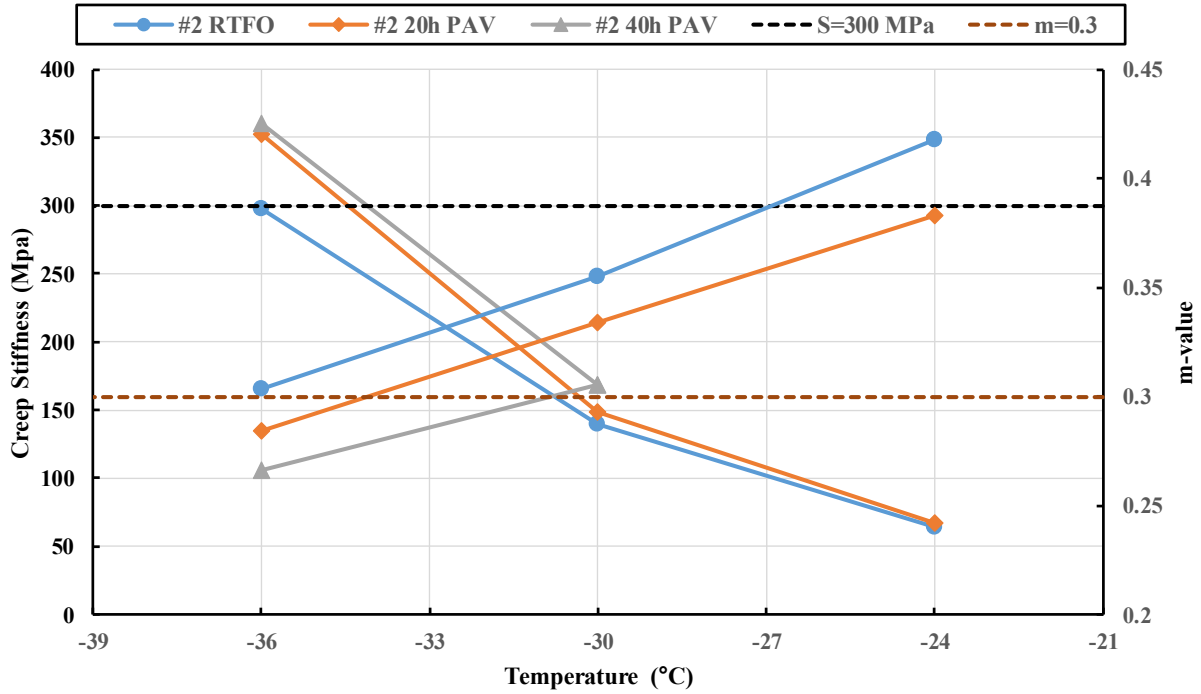


Figure 4.16 BBR test results of Binder#2 (PG 52-40/A) at different aging states

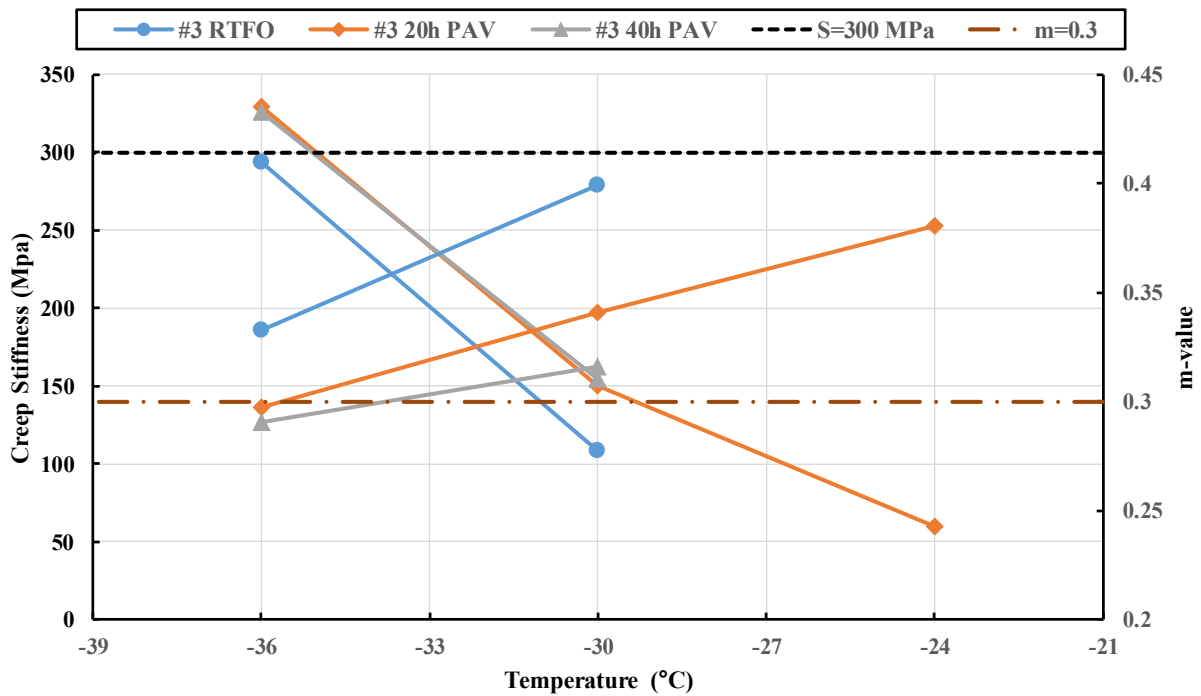


Figure 4.17 BBR test results of Binder#3 (PG 64-40/A) at different aging states



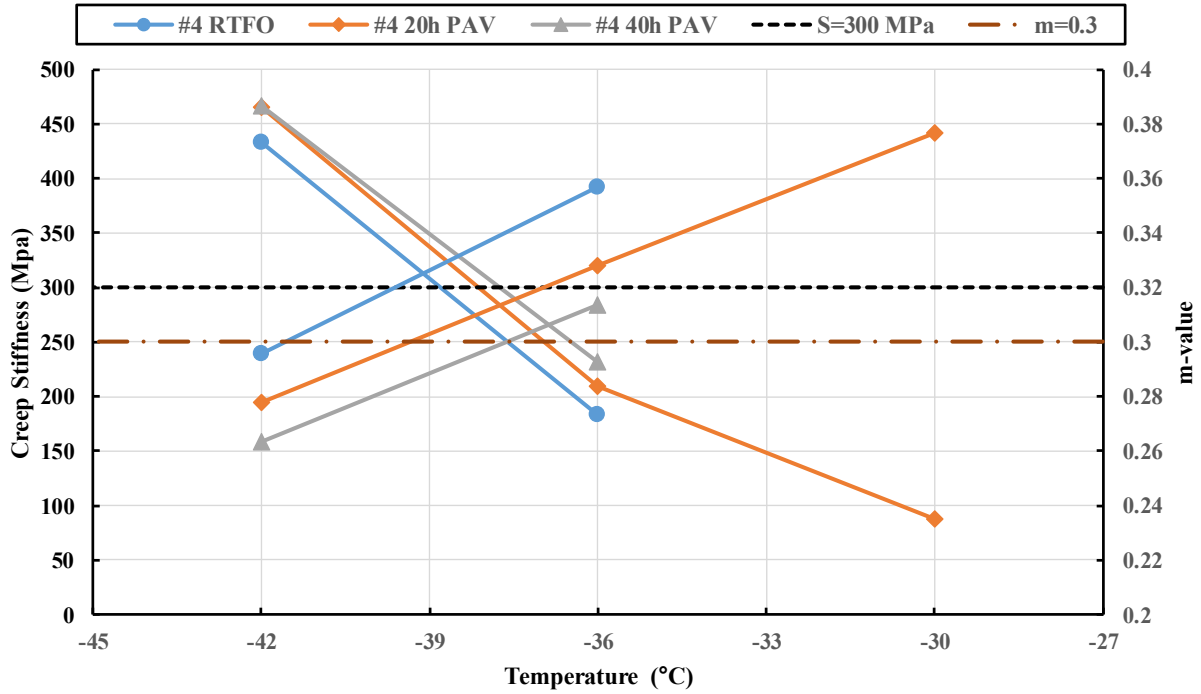


Figure 4.18 BBR test results of Binder#4 (PG 52-46/A) at different aging states

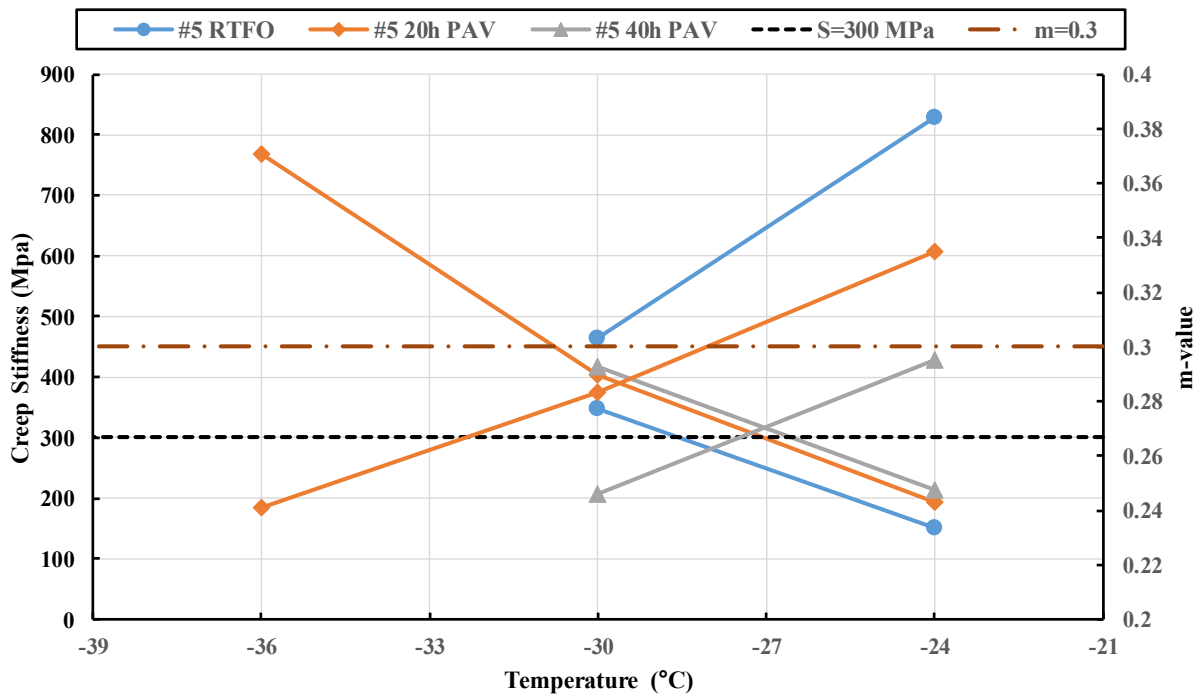


Figure 4.19 BBR test results of Binder#5 (PG 58-34/A) at different aging states

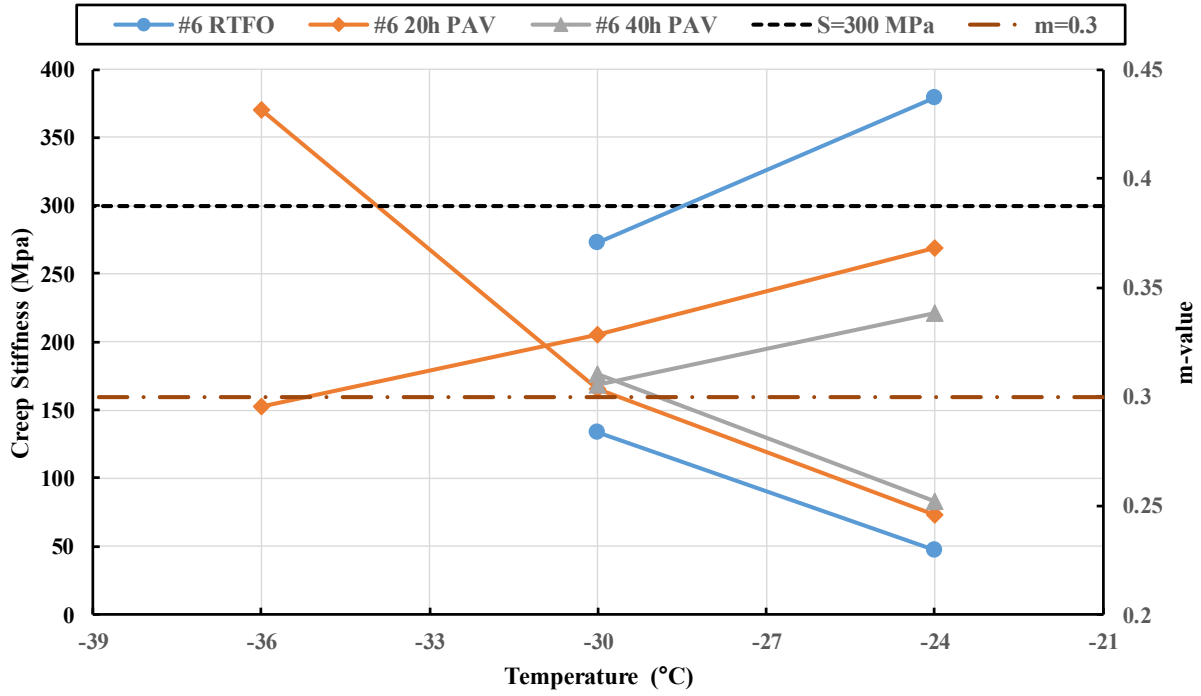


Figure 4.20 BBR test results of Binder#6 (PG 52-40/B) at different aging states

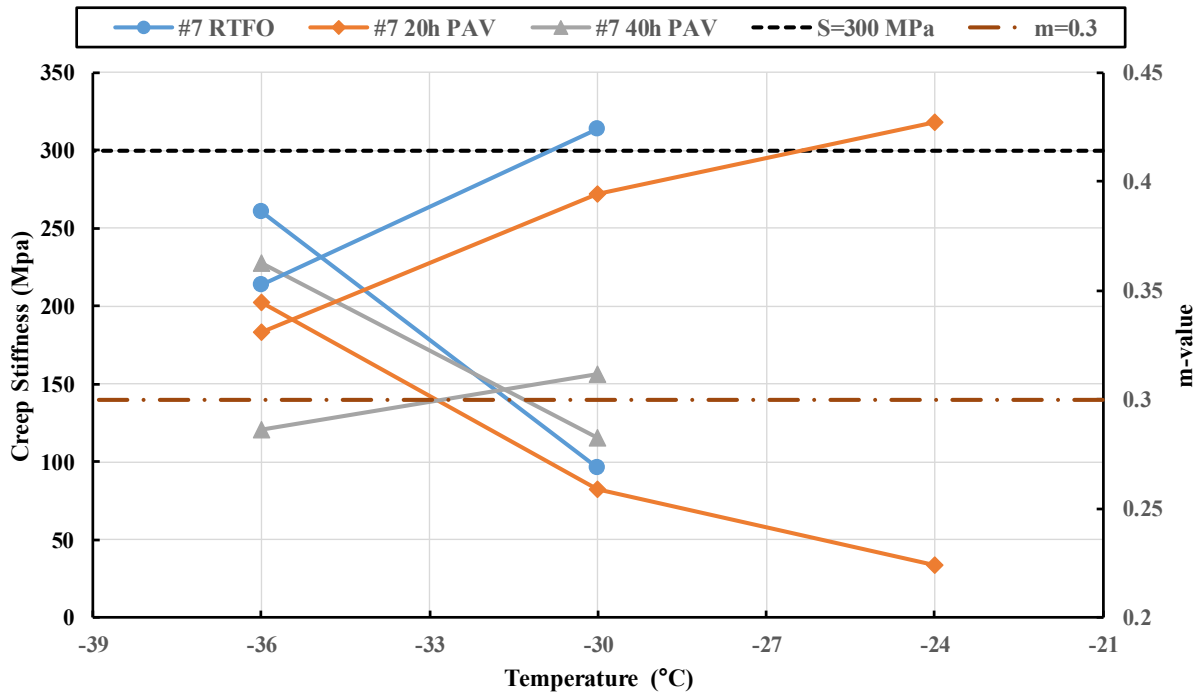


Figure 4.21 BBR test results of Binder#7 (PG 64-40/B) at different aging states

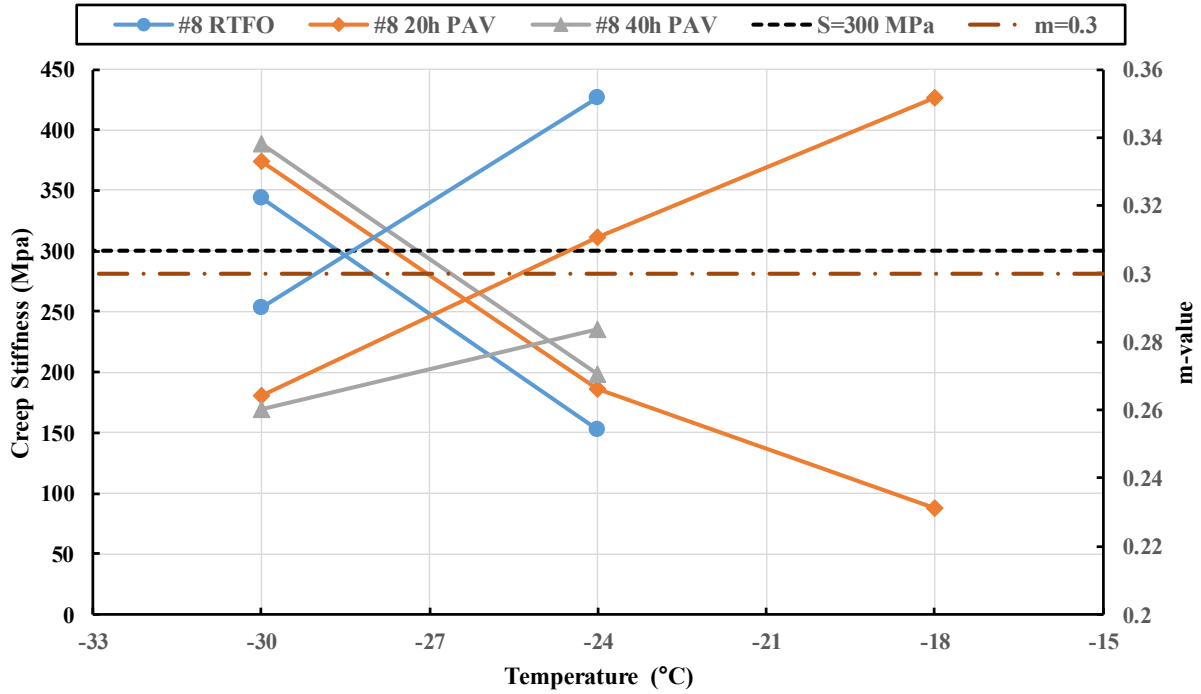


Figure 4.22 BBR test results of Binder#8 (PG 58-34/B) at different aging states

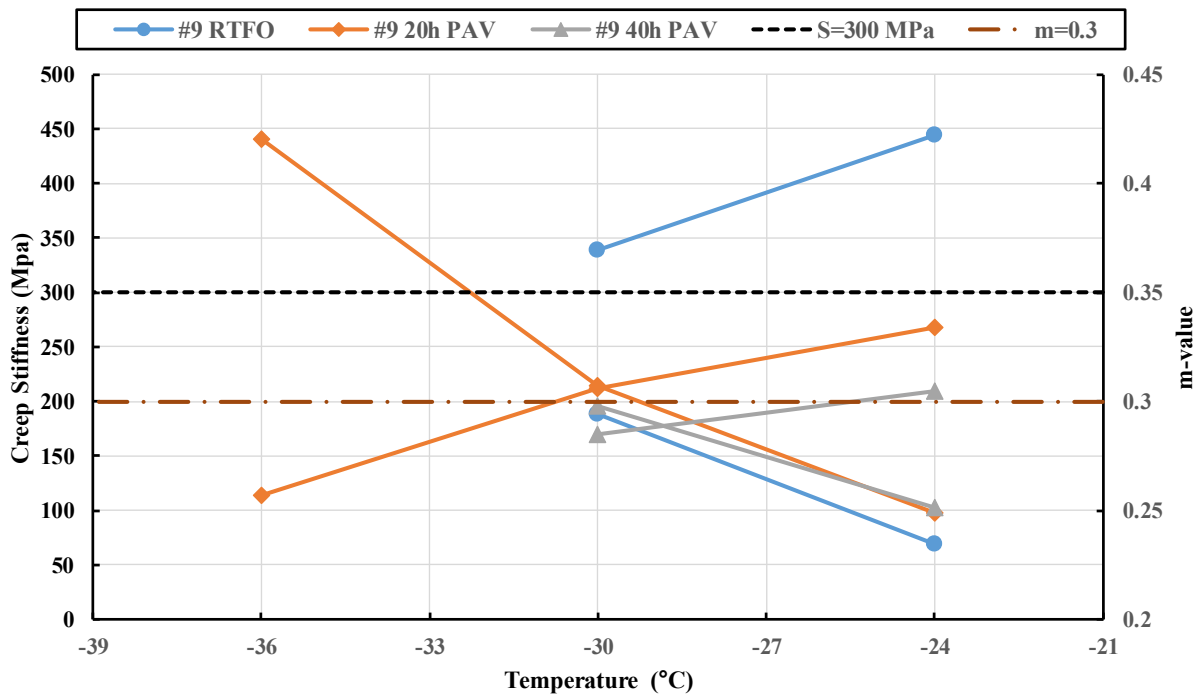


Figure 4.23 BBR test results of Binder#9 (PG 58-34/C) at different aging states

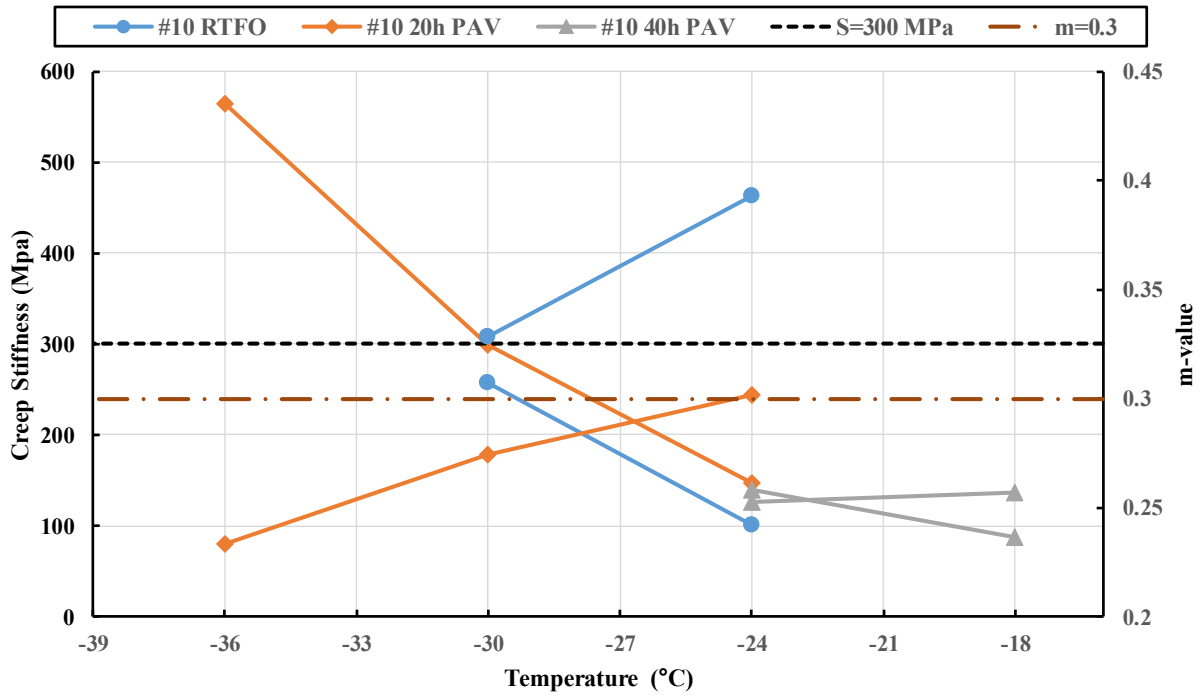


Figure 4.24 BBR test results of Binder#10 (PG 52-34/C) at different aging states

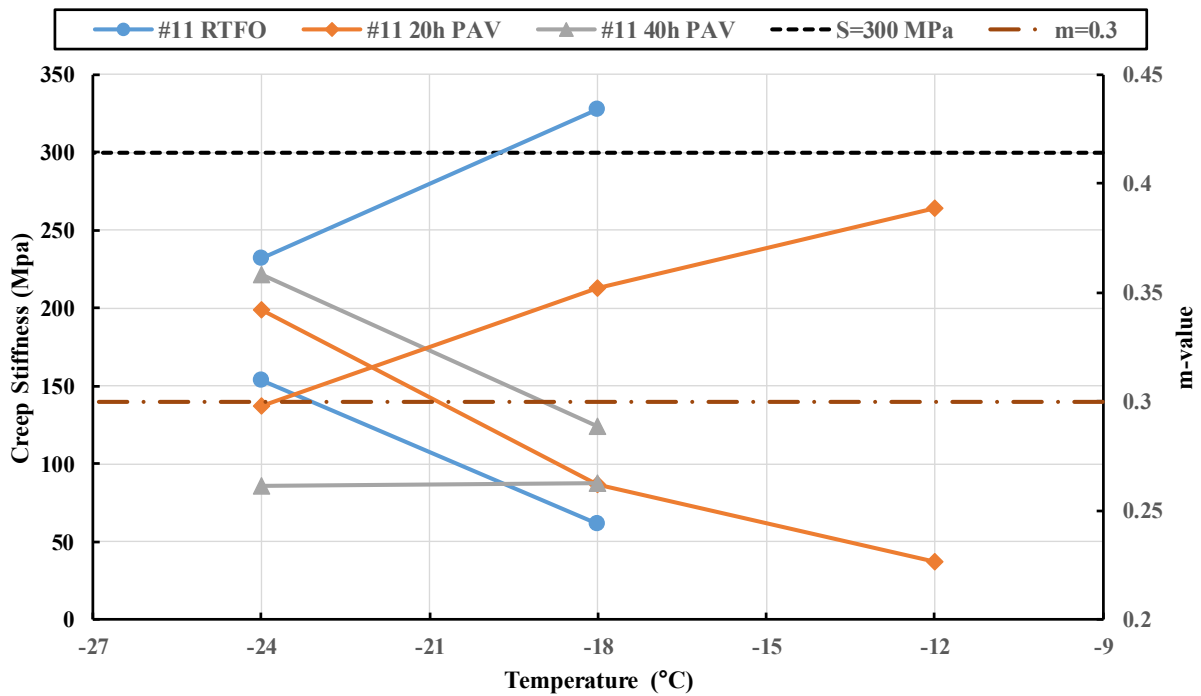


Figure 4.25 BBR test results of Binder#11 (PG 58-28/C) at different aging states

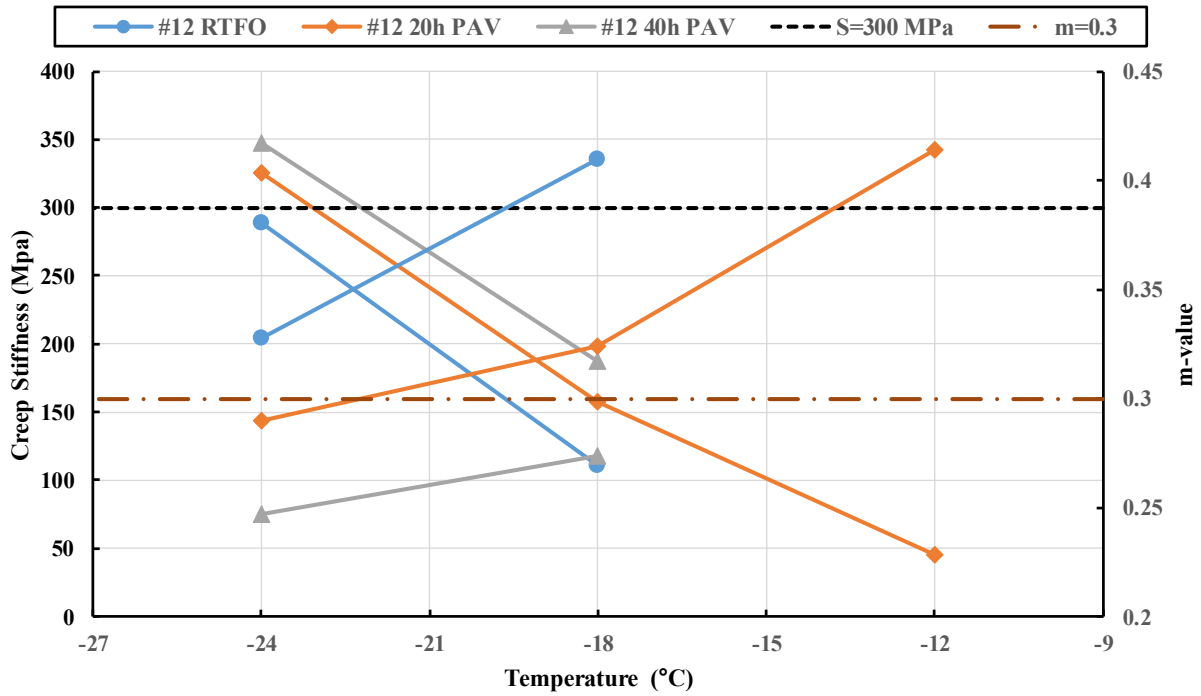


Figure 4.26 BBR test results of Binder#12 (PG 58-28 Plus/C) at different aging states

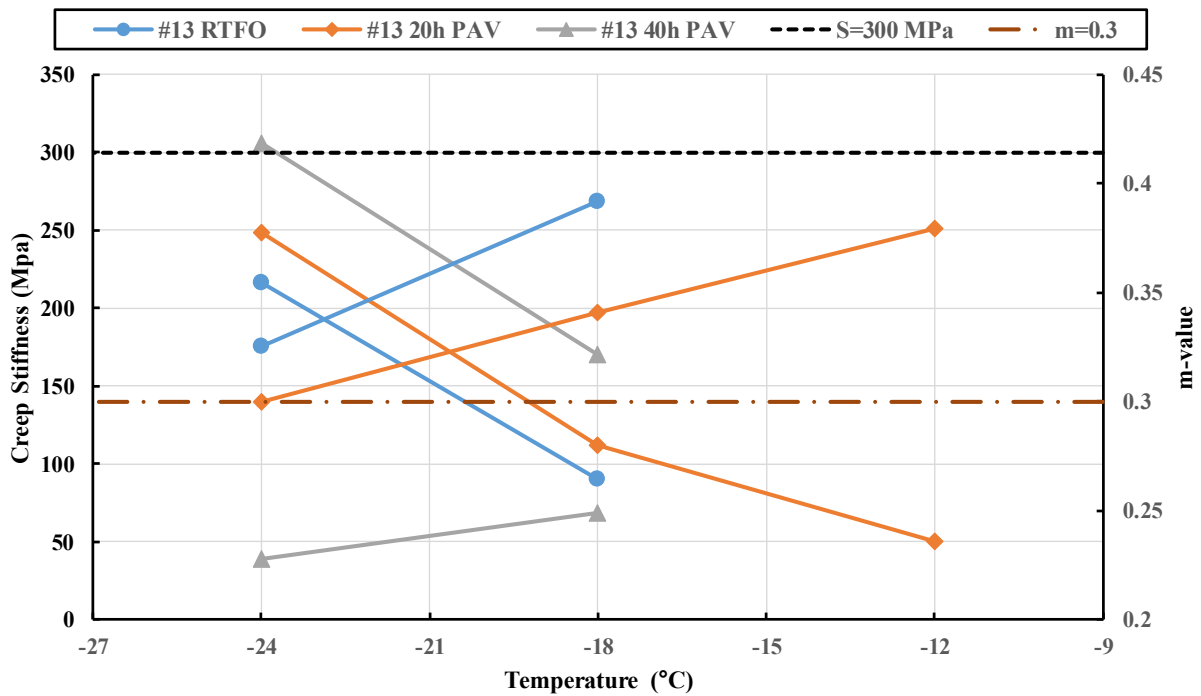


Figure 4.27 BBR test results of Binder#13 (PG 64-28 /C) at different aging states

Table 4.3 presents the critical temperature of each binder by limiting binder stiffness (300 kPa) at 60 seconds and m-value (0.3). It can be seen that the short-term aged binder showed higher critical temperature than the long-term aged binder, which is expected. The two criteria give similar results for RTFO aged and 20h PAV aged binders. However, for 40h PAV aged binder, the critical temperature limiting by m-value is much higher than the one limiting by stiffness. The test results verified the low temperature PG of most of studied binders. However, the tested low temperature PGs of binder #4 (PG52-40/A), binder #7 (PG64-40/B), and binder #9 (PG 58-34/C) are one grade lower than those indicated by the suppliers.

Table 4.3 Critical low temperature by limiting BBR parameters

<b>Binder</b>	<b>Aging Condition</b>	<b>Critical Temperature Limiting Stiffness at 300 kPa, °C</b>	<b>Critical Temperature Limiting m-value at 0.3, °C</b>	<b>PG Low Temperature, °C</b>	<b><math>\Delta T</math>, °C</b>
#1/PG 52-28/A	RTFO	-33.3	-34.4	-28	1.17
	20h PAV	-31.1	-30.8		-0.34
	40h PAV	-30.7	-28.8		-1.93
#2/PG 52-40/A	RTFO	-46.1	-46.4	-40	0.30
	20h PAV	-44.9	-44.1		-0.80
	40h PAV	-44.6	-40.8		-3.74
#3/PG64-40/A	RTFO	-46.1	-48.9	-40	2.83
	20h PAV	-45.3	-45.6		0.29
	40h PAV	-45.3	-43.8		-1.57
#4/PG52-46/A	RTFO	-49.4	-51.6	-46	2.16
	20h PAV	-48.7	-49.4		0.66
	40h PAV	-48.2	-47.6		-0.59

Table 4.3 Critical low temperature by limiting BBR parameters (Continue)

Binder	Aging Condition	Critical Temperature Limiting Stiffness at 300 kPa, °C	Critical Temperature Limiting m-value at 0.3, °C	PG Low Temperature, °C	ΔT, °C
#5/PG 58-34/A	RTFO	-38.9	-40.2	-34	1.31
	20h PAV	-37.6	-38.1		0.49
	40h PAV	-37	-33		-3.66
#6/PG 52-40/B	RTFO	-44.7	-46.3	-40	1.63
	20h PAV	-44.4	-44.4		-0.08
	40h PAV	-44.2	-41		-3.19
#7/PG 64-40/B	RTFO	-46.8	-50.4	-46	3.52
	20h PAV	-48.6	-48.9		0.32
	40h PAV	-48.5	-42.7		-5.74
#8/PG 58-34/B	RTFO	-39	-39	-34	0.03
	20h PAV	-38	-35.4		-2.73
	40h PAV	-37.7	-29.8		-7.85
#9/PG 58-34/C	RTFO	-43	-47.3	-40	4.31
	20h PAV	-42.8	-40.7		-2.10
	40h PAV	-43.9	-35.4		-8.50
#10/PG 52-34/C	RTFO	-41	-42.6	-34	1.62
	20h PAV	-40	-34.3		-5.73
	40h PAV	-43.9	-27		-10.00
#11 (PG 58-28/C)	RTFO	-38.4	-39.8	-28	1.37
	20h PAV	-37	-33.8		-3.24
	40h PAV	-37.1	N/A		-9.50
#12 (PG 52- 28plus/C)	RTFO	-34.2	-36	-28	1.80
	20h PAV	-33.3	-32.2		-1.09
	40h PAV	-32.5	-22		-10.57
#13 (PG 64-28/C)	RTFO	-36.3	-36.2	-28	-0.02
	20h PAV	-35.4	-33.9		-1.45
	40h PAV	-33.8	-13.8		-20.04

#### 4.1.5 Glover-Rowe (G-R) Parameter

The G-R parameter is defined as  $G^*(\cos\delta)^2/\sin\delta$  at 15°C and 0.005 rad/s. It was originally developed by Glover (2005) in the form of  $G'/(\eta'/G')$  (hereafter referred to as Glover parameter). The Glover parameter has been shown to closely relate to the asphalt pavement

cracking (Anderson et al. 2011). Glover et al. (2005) suggested that a Glover parameter of 0.0009 MPa and of 0.003 MPa are the borderlines of initial cracking and severe cracking, respectively. Rowe (2011) simplified the Glover parameter to a new one (Glover-Rowe parameter,  $G^*(\cos\delta)^2/\sin\delta$ ) with  $G^*$  and  $\delta$  at 15°C and 0.005 rad/s. Rowe (2011) also suggested the two failure curves in Black Space Diagram indicate the onset of cracking and severe damage, respectively. Equations 4.4 and 4.5 present the formulas for these two curves, respectively. The Glover-Rowe parameter correlates well with the thermal cracking of asphalt pavement (King et al. 2012; Mensching et al. 2015; Mensching et al. 2016; Jacques et al. 2016; Shamborovsky 2016; Mogawer et al. 2017).

$$G^*(\cos\delta)^2/\sin\delta = 180 \text{ Kpa} \quad (4.4)$$

$$G^*(\cos\delta)^2/\sin\delta = 450 \text{ Kpa} \quad (4.5)$$

Figure 4.28 presents the Glover-Rowe parameters of studied binders in Black Space Diagram. As shown, the G-R parameters of the studied asphalt binders approached the damage zone in the Black Space Diagram as the asphalt binder aged, which was consistent with the findings of Anderson et al. (2011) and Rowe (2011). The results showed that only the binders from supplier C (i.e., binders #10, #11, #12, #13) with 40h PAV aging state reached the threshold values, while other aged binders were not at risk for cracking according to their locations of G-R parameters in Black Space Diagram. As can be seen from Figure 4.28, the  $\delta$  of modified binders from suppliers A and B was insensitive to aging at the temperature-frequency combination of 15°C and 0.005 rad/s. The  $\delta$  is an important parameter to characterize the relaxation behavior of asphalt. The insensitivity of  $\delta$  with aging inferred that the relaxation properties did not change a lot as the asphalt ages. However, it should be noted that asphalt binder is a viscoelastic material which exhibits temperature and frequency dependent behavior.



According to the Glover et al. (2005), the temperature-frequency combination of 15°C and 0.005 rad/s is approximately equivalent to the temperature-frequency combination of 47.5°C and 10 rad/s based on the time-temperature superposition principle. Therefore, although the G-R parameter correlates well with low temperature cracking of asphalt, the individual  $\delta$  at temperature-frequency combination of 15°C and 0.005 rad/s cannot serve as a low temperature cracking susceptibility indicator. Thus, the insensitivity of  $\delta$  in this case does not mean the low-temperature relaxation properties of Alaskan modified binders did not change as the asphalt aged.

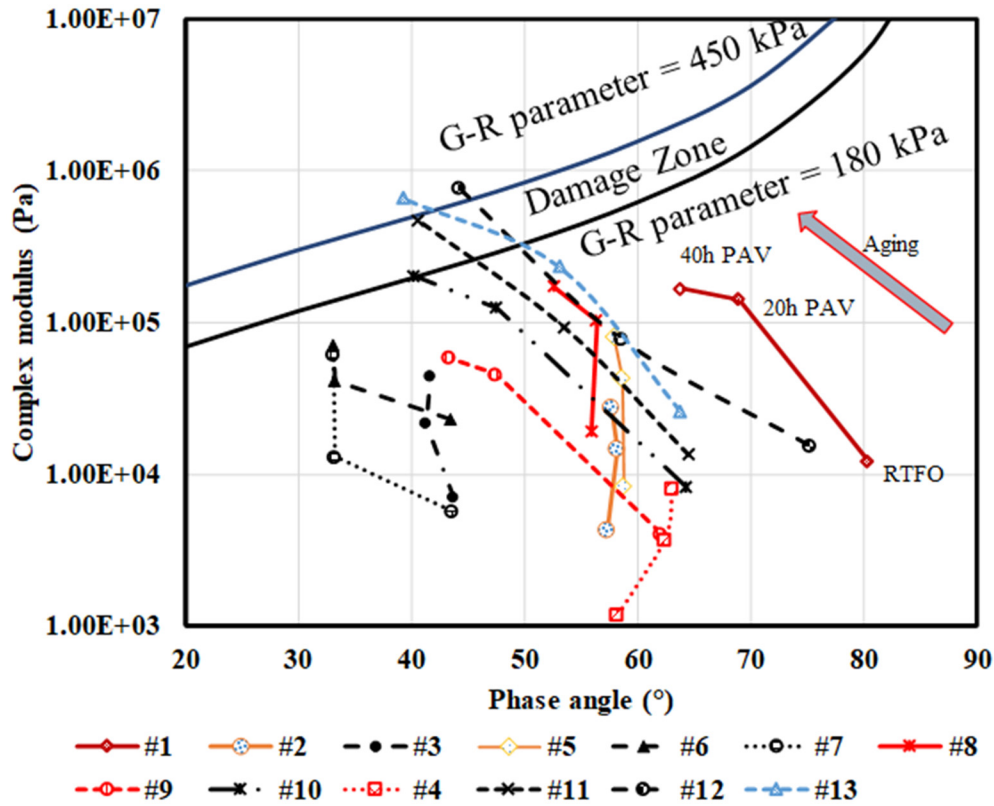


Figure 4.28 Black Space Diagram with Glover-Rowe parameter

Figures 4.29 to 4.31 present the Glover-Rowe parameters of the Alaskan asphalt binders with different aging states. The figures are presented on a semi-log scale to help to illustrate and to compare. As shown in this figure, binder #4 (PG52-46/A) showed the lowest G-R parameter value, regardless of aging states.

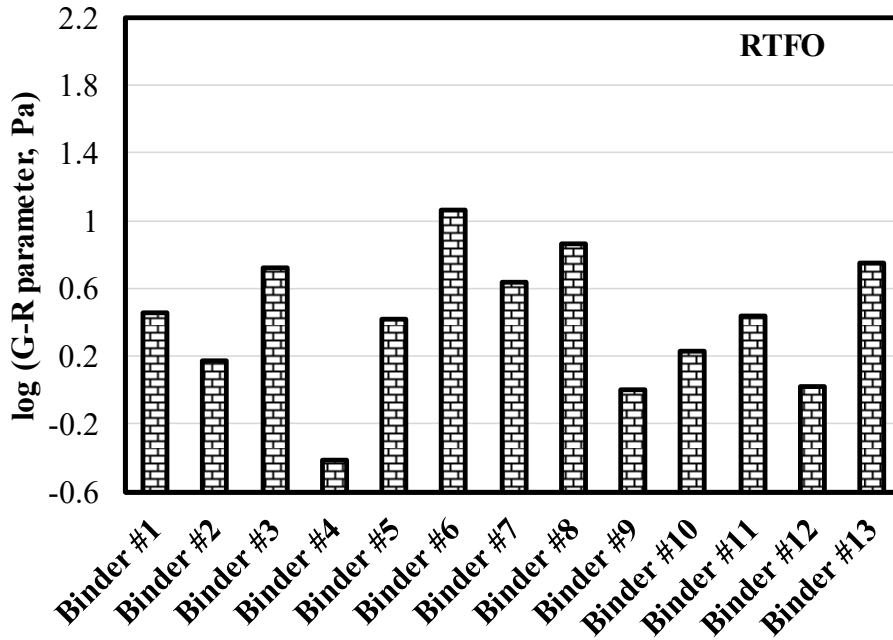


Figure 4.29 Glover-Rowe parameters of RTFO aged binders

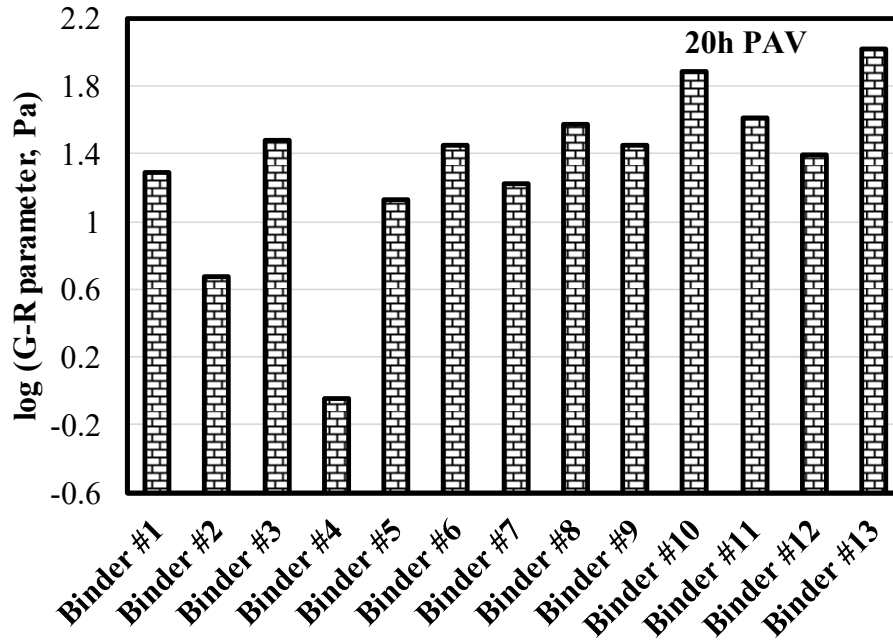


Figure 4.30 Glover-Rowe parameters of 20h PAV aged binders

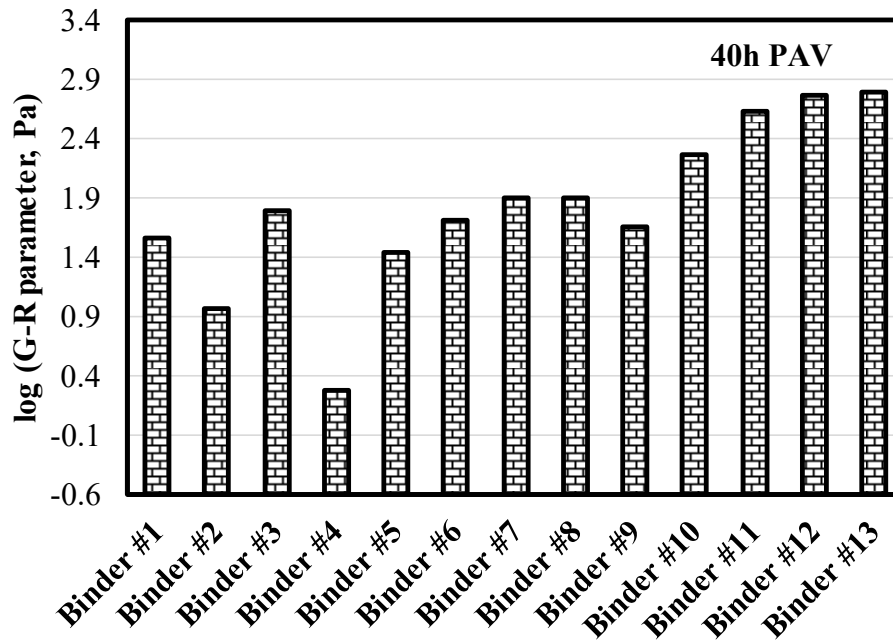


Figure 4.31 Glover-Rowe parameters of 40h PAV aged binders

#### 4.1.6 $\Delta T$

$\Delta T$  was developed by Anderson et al. (2011), which is defined as the difference between the critical low temperatures of the asphalt binders, determined using the BBR, where the stiffness at 60s of loading time is exactly equal to 300 MPa ( $T_{c,s}$ ) and the m-value at 60s of loading time is exactly equal to 0.3 ( $T_{c,m}$ ). Equation 4.6 presents the definition, and  $T_{c,m}$  and  $T_{c,s}$  can be calculated according to Equations 4.2 and 4.3. As indicated by Anderson et al. (2011), the asphalt binder that is more susceptible to cracking could be more m-controlled, thus has lower  $\Delta T$  value.

$$\Delta T = T_{c,s} - T_{c,m} \quad (4.6)$$

Figure 4.32 presents the  $\Delta T$  results of studied binders. As can be seen in Figure 4.32, for each binder,  $\Delta T$  increased as the asphalt aged, indicating that  $\Delta T$  has potential to evaluate and quantify the cracking susceptibility (durability loss) of the binder. Anderson et al. (2011) indicated that  $\Delta T$ s of -3 and -5 could be the indications of onset cracking and severe damage, respectively. As shown in Figure 4.32,  $\Delta T$  of all modified binders (except binders #3 and #4) with 40h PAV aging state reached the threshold value of -3. The modified binders from suppliers B and C even showed lower than -5, the indication of severe damages, at 40h PAV aging state. However, recalling the Glover-Rowe parameter results, only the binders from supplier C with 40h PAV aging state reached the damage zone.

Binder #4 (PG 52-46/A) showed the highest  $\Delta T$  value at both 20h PAV and 40h PAV aging states, while binder #9 (PG 58-34/C) showed the highest  $\Delta T$  value at RTFO aging state.  $\Delta T$  of modified binders were more sensitive to aging than that of neat binder. Especially for binder #8 (PG 58-34/B), the  $\Delta T$  of RTFO aged binder was 4.3 while that of 40h PAV aged

binder went up to -8.5. Long-term aged binder #13 showed most prone to cracking since it showed lowest  $\Delta T$  value, which was consistent with the results of Glover-Rowe parameter. Among all 20h PAV aged binders, binder #10 showed lowest  $\Delta T$  value, and it reached the severe cracking threshold value of -5 °C. Binders from different supplier had entirely different  $\Delta T$  values even though they had the same PG.

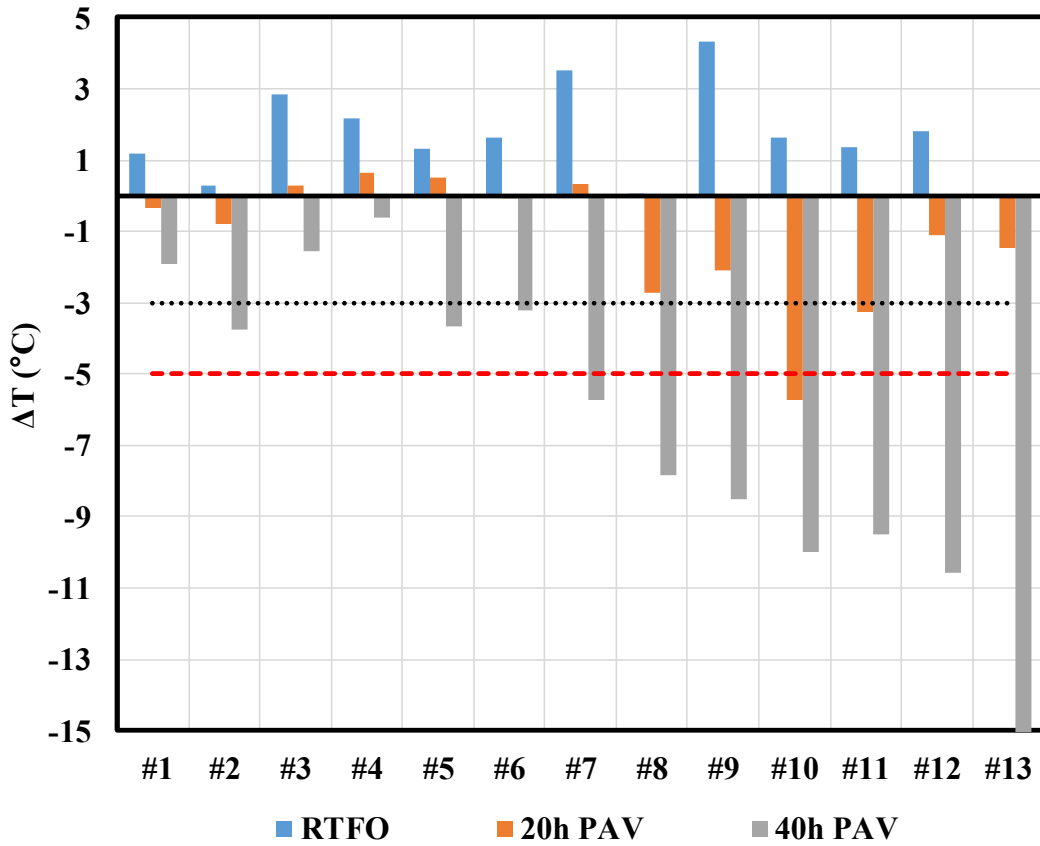


Figure 4.32  $\Delta T$  of Alaskan asphalt binders with different aging states

#### 4.1.7 Crossover Frequency-Rheological Index Black Space

The crossover frequency,  $\omega_c$ , is defined as the frequency when storage modulus ( $G'$ ) equal to loss modulus ( $G''$ ) at the desired temperature. In general, as the crossover frequency at the reference temperature decreases, the hardness of asphalt binder increases. The rheological

index,  $R$ , is defined as the difference between the log of the glassy modulus and the log of the dynamic modulus at the crossover frequency. As can be seen from Equation 4.1,  $R$  could be the shape parameter of  $G^*$  master curve. As  $R$  increased, the  $G^*$  master curve could become more flat, which indicated the asphalt binder could have a more gradual transition from elastic behavior to viscous behavior. The crossover frequency-rheological index black space is frequently applied to evaluate the cracking resistance of the asphalt binder. As indicated by Mensching et al. (2016) and Romero and Jones (2013), for general binders, with the increase of aging time, the crossover frequency of binder could decrease while rheological index could increase. Mensching et al. (2016) indicated that data for asphalt binders which are more prone to cracking should locate in the bottom-right corner of the crossover frequency-rheological index black space. Figure 4.33 shows the crossover frequency-rheological index black space for the studied Alaskan asphalt binders. For most binders, with the increase of aging time, the crossover frequency decreased, and the rheological index increased. However, for binder #7 which was PG 64-40/B, it showed the opposite trend. Similar to the G-R parameter and  $\Delta T$  results, the binders from supplier C with 40h PAV aging state were easily distinguished from other binders. Their corresponding data points plotted in the bottom-right corner. Although the results presented in Figure 4.33 indicated that the crossover frequency-rheological index black space has the potential to evaluate the cracking resistance of most of Alaskan asphalt binders except for binders with the grade of PG 64-40, the authors would not recommend to apply the black space if the data for other evaluation indices such as G-R parameter and  $\Delta T$  are available. For some of the Alaskan modified binders, the crossover frequency and R-value could not be obtained precisely due to the low  $\delta$  values (sometimes lower than  $45^\circ$  along the whole frequency range) and insensitivity of  $\delta$  to frequency.

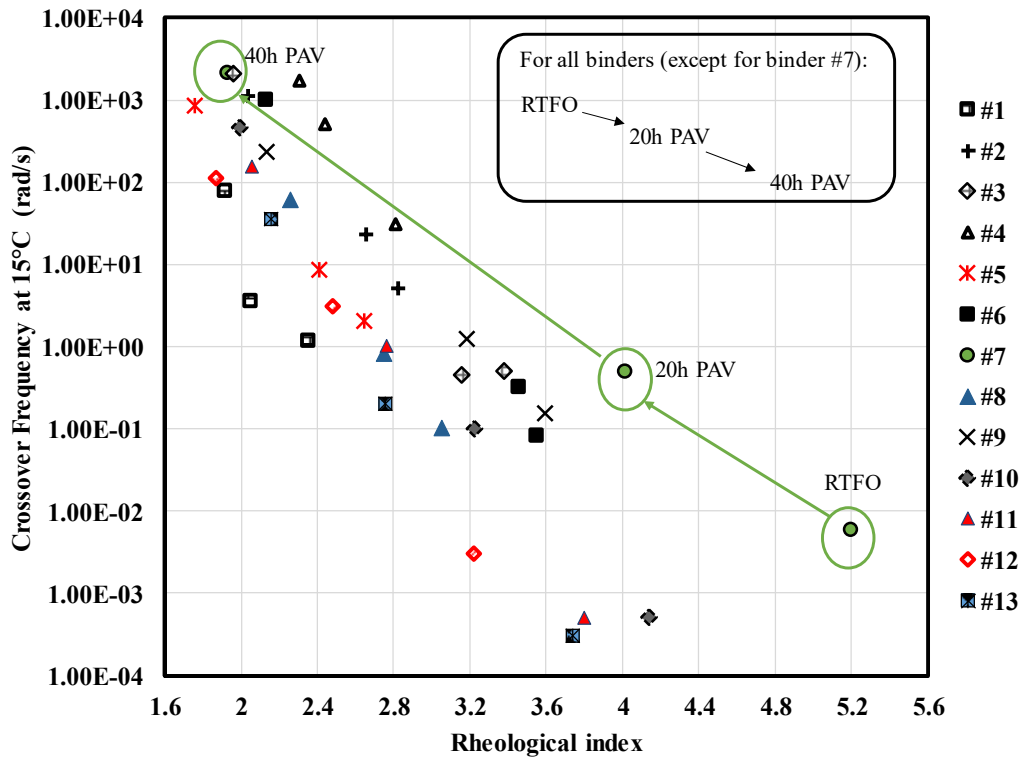


Figure 4.33 Crossover frequency-rheological index black space

#### 4.1.8 ABCD Test

The ABCD critical cracking temperatures and the critical temperatures determined based on BBR data for 20h PAV aged binders are organized in Table 4.4. Generally, the measured cracking temperatures by ABCD were lower (colder) than the calculated cracking temperatures by BBR for all binders tested. The disparity can be attributed to the difference in the mechanism of the two different tests/procedures. It should be noted that the binder #4 (PG 52-46/A) did not crack at -60°C, which was the lowest limit of test temperature range. Detailed data information can be found in Appendix C.

Table 4.4 Critical temperature using different methods

<b>Binder</b>	<b>Critical Temperature Limiting Stiffness at 300 kPa, °C</b>	<b>Critical Temperature Limiting m-value at 0.3, °C</b>	<b>ABCD Critical Temperature, °C</b>
#1 (PG52-28)/A	-31.1	-30.8	-34.2
#2 (PG52-40)/A	-44.9	-44.1	-50.3
#3 (PG64-40)/A	-45.3	-45.6	-51.9
#4 (PG52-46)/A	-48.7	-49.4	<-60
#5 (PG58-34)/A	-37.6	-38.1	-44.3
#6 (PG52-40)/B	-44.4	-44.4	-50.7
#7 (PG64-40)/B	-48.6	-48.9	-56.7
#8 (PG58-34)/B	-38	-35.4	-47.4
#9 (PG58-34)/C	-42.8	-40.7	-49.6
#10 (PG52-28)/C	-40	-34.3	-47.7
#11 (PG58-28)/C	-37	-33.8	-45.4
#12 (PG52-28Plus)/C	-33.3	-32.2	-35.2
#13 (PG64-28)/C	-35.4	-33.9	-43.3

## 4.2 Mixture Tests

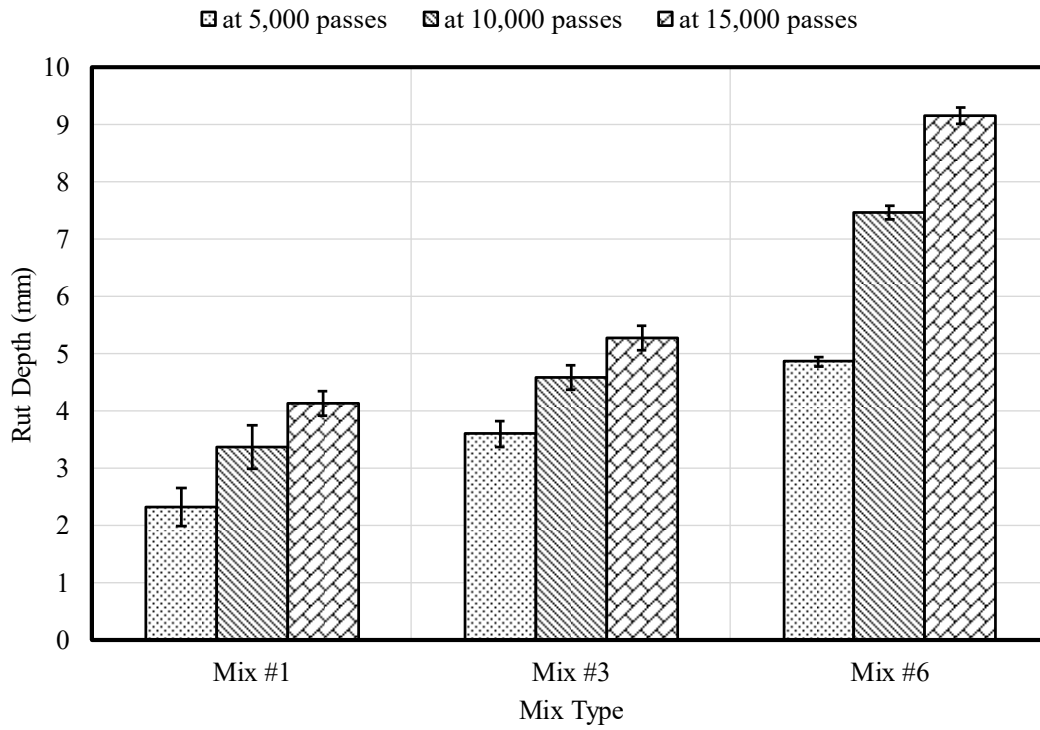
### 4.2.1 HWT Test

Figure 4.34 presents the average rut depths after 5,000, 10,000, and 15,000 cycles from the HWT test for the studied mixtures. It should be noted that, as indicated before, the testing temperature for Mixes #1 (Type VH, PG 64-40/A), #3 (Type VH, PG 64-40/B), and #6 (Type VH, PG 64-40/B) was 50°C. For other mixtures, the testing temperature was 40°C. However, for Mix #10 (Lab mixed, PG 52-46/A), which was the lab-produced mixture with PG 52-46, the mixture samples disintegrated before completing the test at 40°C. The rut depths for Mix #10 presented in Figure 2(a) were the representatives at room temperature (at about 25°C). By comparing the rut depths of Mixes #1, #3, and #6 (Figure 4.34), it can be found that Mix #1 was

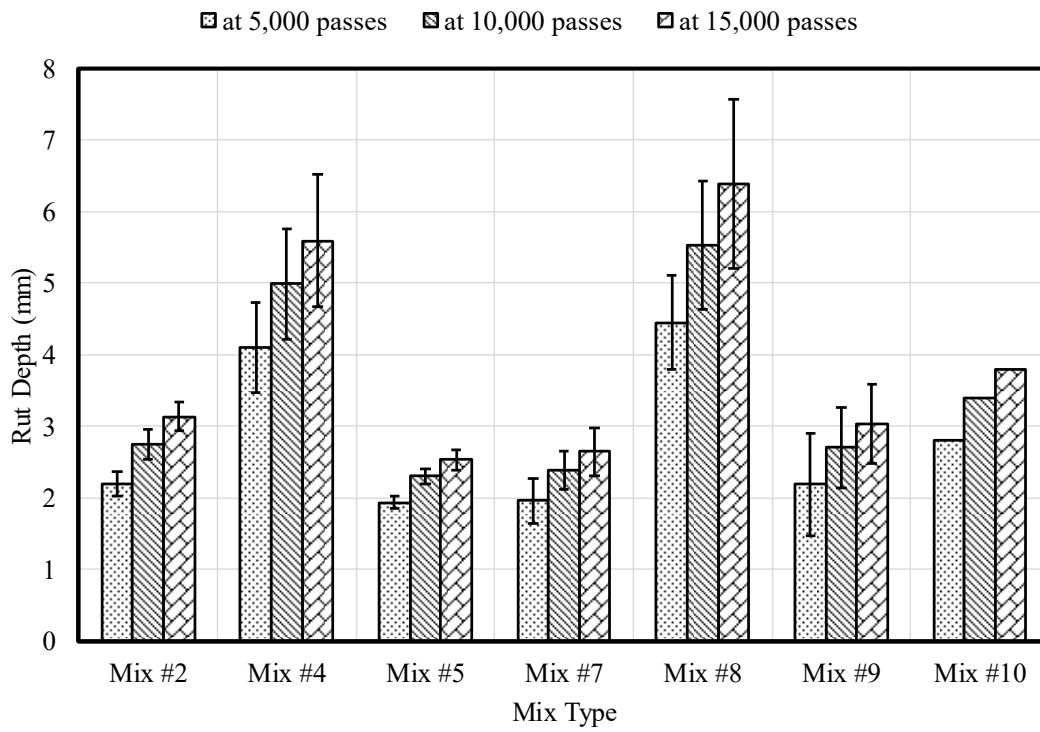


the most rutting resistant. It is observed that, at the testing temperature of 40°C, the mixture with neat asphalt binder (Mix #8 with PG 52-28) showed greater rut depth than the mixtures with modified asphalt binders, which may indicate that the asphalt modification improved the rutting resistance of the asphalt mixture. However, it should be noted that the mixtures that were tested do not have exactly the same aggregate gradation and properties, this may also affect the testing results.

According to Yin et al. (2014), asphalt mixtures with higher  $\Delta\varepsilon_{10,000}^{vp}$  values are expected to be more susceptible to rutting than those with lower  $\Delta\varepsilon_{10,000}^{vp}$  values. As shown in Figure 4.35, the  $\Delta\varepsilon_{10,000}^{vp}$  results were not consistent with the rut depth results, in terms of rutting resistances of Mixes #1, #3, and #6. The  $\Delta\varepsilon_{10,000}^{vp}$  results showed that Mix #3 was the most rutting resistant. However, both the  $\Delta\varepsilon_{10,000}^{vp}$  and rut depth results identified the improvement in rutting resistance by asphalt modification.

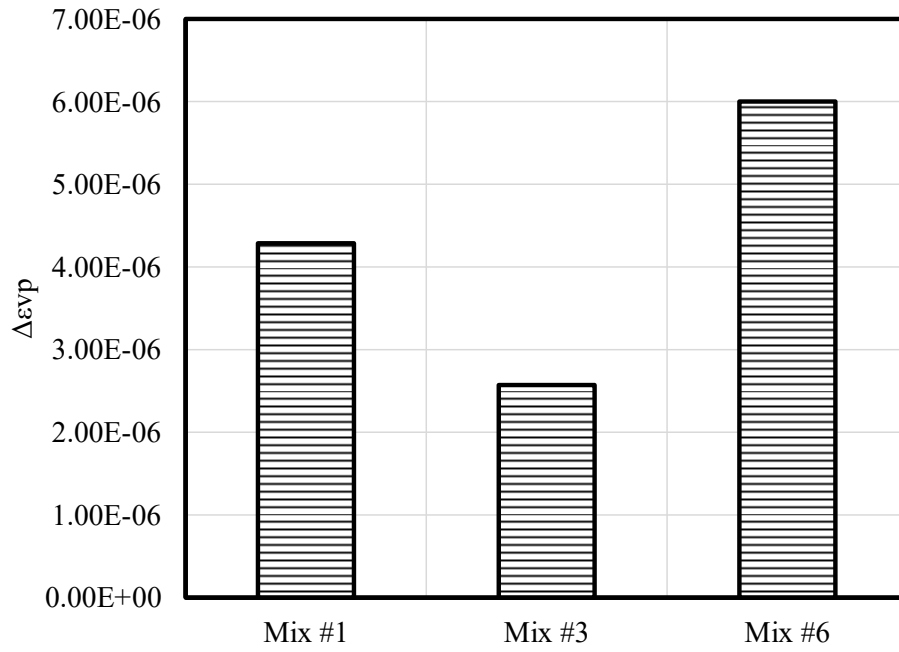


(a)

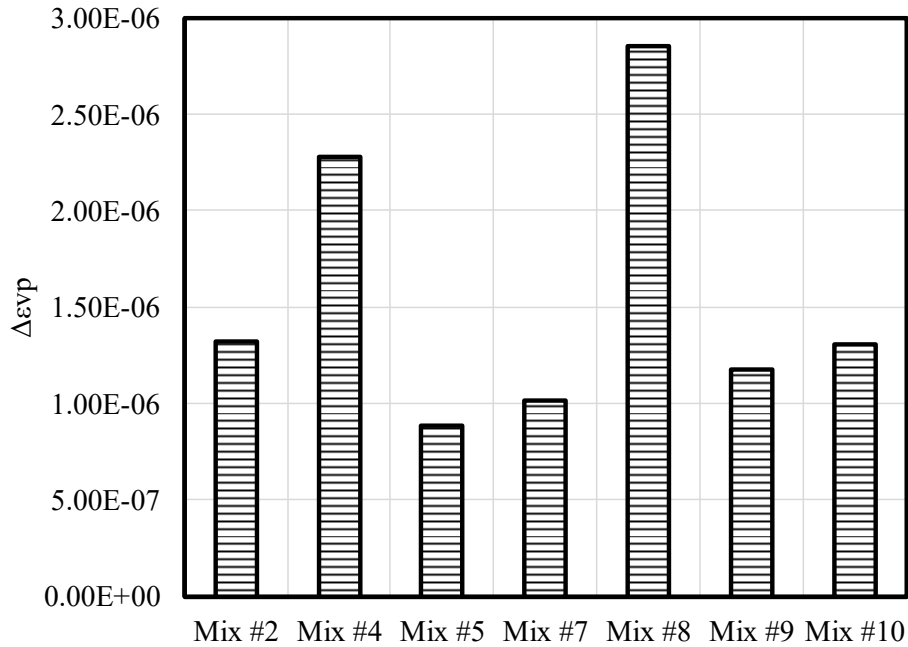


(b)

Figure 4.34 HWT rut depth results: (a) at 50°C and (b) at 40°C



(a)



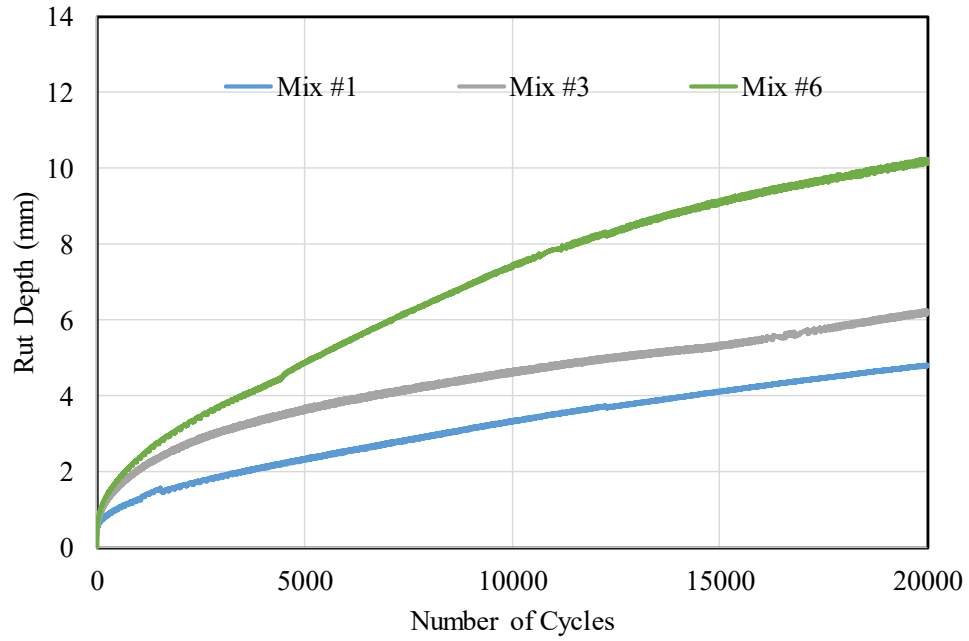
(b)

Figure 4.35 HWT  $\Delta \epsilon_{10,000}^{vp}$  results: (a) at 50°C and (b) at 40°C

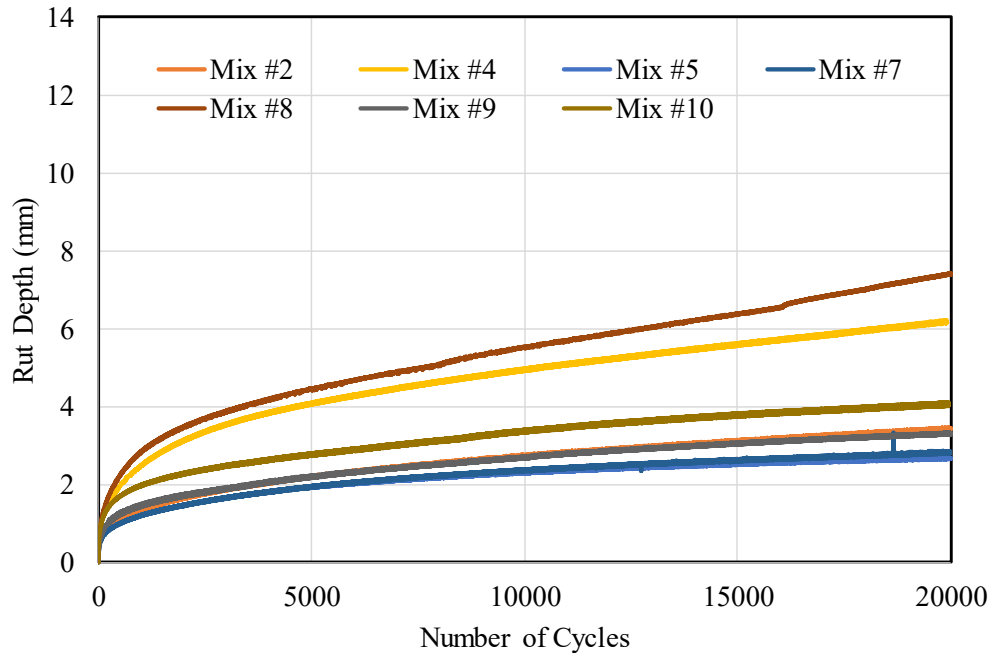
As previously mentioned, the stripping inflection point (SIP) is a generally accepted parameter to evaluate the moisture susceptibility of asphalt mixtures. As shown in Figure 3.18, SIP is graphically represented at the intersection of the fitted lines that characterize the creep phase and the stripping phase. In addition, the parameters,  $LC_{SN}$  and  $LC_{ST}$  proposed by Yin et al. (2014) could also be used to evaluate the moisture susceptibility of asphalt mixtures. However, in this study, these two parameters could not be calculated based on the data obtained, which indicated that the studied Alaskan mixtures were not susceptible to moisture damage.

Figure 4.36 presents the rut depth versus the number of cycles for the studied mixtures. As shown, there were no tertiary regions be found for the curves of studied mixtures. Therefore,

no SIPs could be determined, which may indicate that the Alaskan mixtures studied were not susceptible to moisture damage at the tested temperatures, as measured by the HWT test.



(a)



(b)

Figure 4.36 HWT rut depth versus number of cycles for the studied Alaskan mixtures: (a) at 50°C and (b) at 40°C

#### 4.2.2 SCB Test

The fracture mechanics concept has been successfully used to characterize the fracture resistance of the asphalt mixtures. Figure 4.37 presents the  $J_c$  values of the studied Alaskan asphalt mixtures at 25°C, detailed information such as the change of the dissipated strain energy with the notch depth for each mixture can be found in Appendix D. It should be noted that the mixture samples for Mix #10 (Lab mixed, PG52-40/A) were very soft at 25°C, and disintegrated before testing during the conditioning period. The  $J_c$  value for Mix #10 presented in Figure 3.37 was collected at 7°C. In general, asphalt mixtures with higher  $J_c$  are more resistant to fatigue cracking. As shown in Figure 4.37, Mix #5 (Type VS, PG 58-34/B) showed the highest  $J_c$  value among the studied mixtures. Mix #3 (Type VH, PG 64-40/B) showed the lowest  $J_c$  value. The

mixture with unmodified asphalt binder (Mix #8, Type IIB, PG 52-28/A) showed higher  $J_c$  value than most of mixtures with modified asphalt binders. From the test results, it appeared that the unmodified mixture (Mix #8) showed better fatigue cracking resistance than some of the modified mixtures. Other fatigue tests such as Illinois Flexibility Index test (I-FIT) and Fatigue Beam test were recommended to be conducted to verify the results.

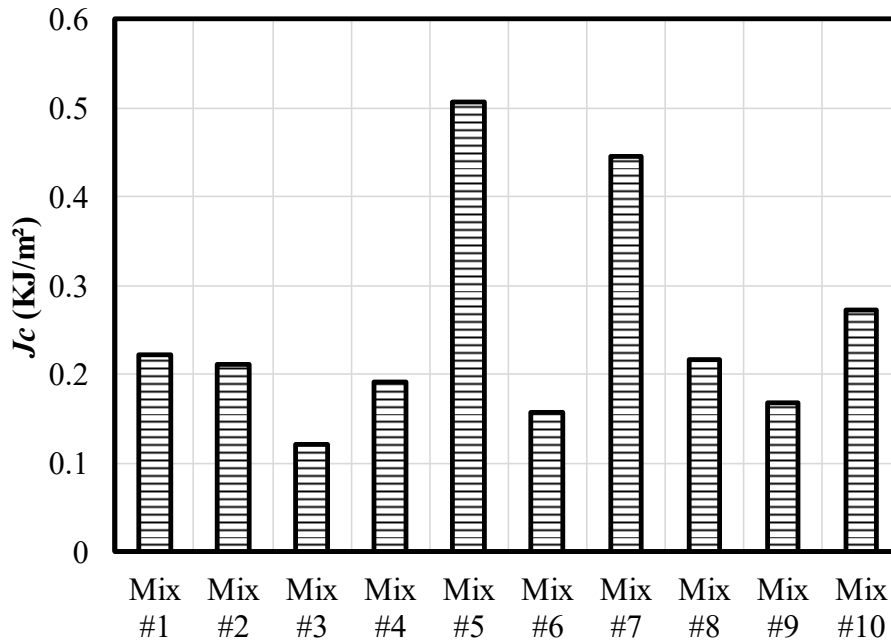
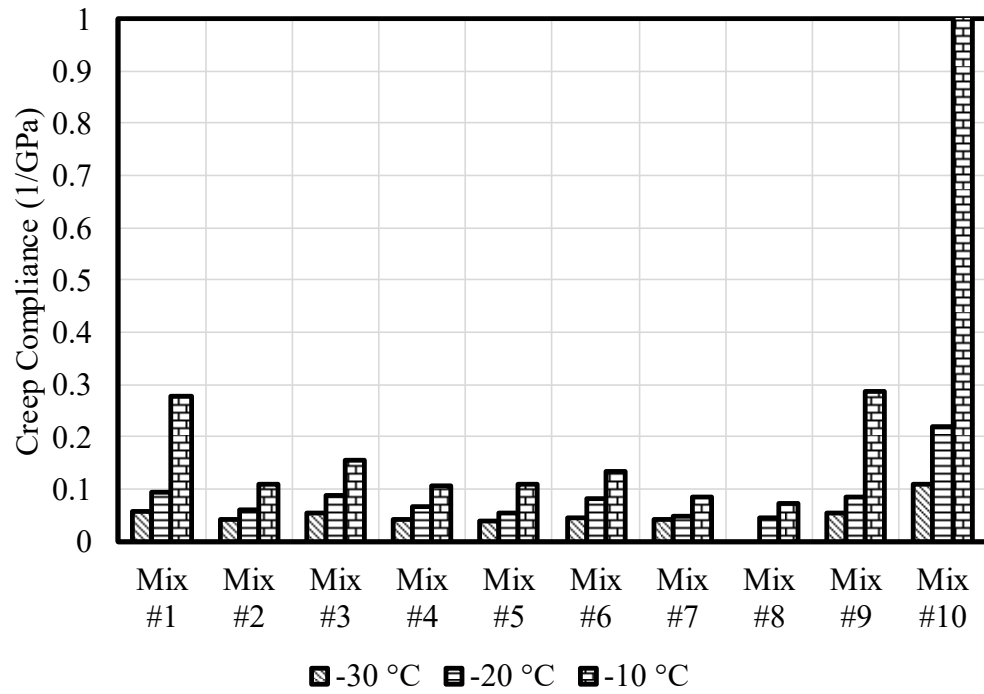


Figure 4.37 SCB  $J_c$  values of studied Alaskan asphalt mixtures at 25 °C

#### 4.2.3 IDT Test

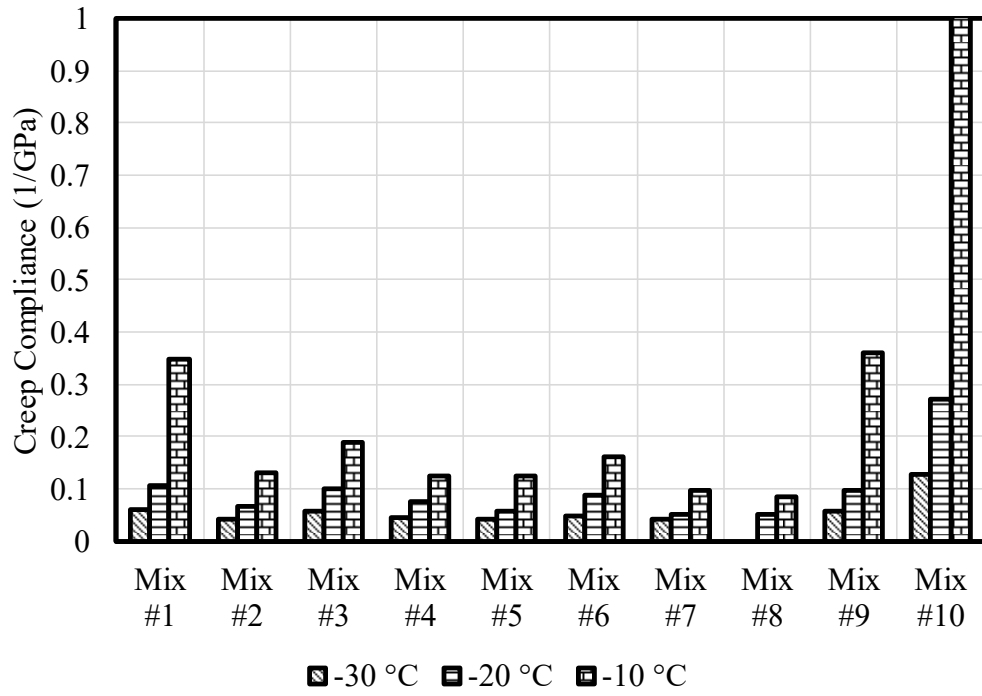
Figure 4.38 compares the IDT creep compliance ( $D_t$ ) of all of the studied Alaskan mixtures at loading times of 10 s, 20 s, 50 s, and 100 s at three temperatures, i.e., -10, -20, and -30°C. In general, creep compliance increased with an increase of temperature, which was correlated to the trend of stiffness over temperature. Higher  $D_t$  values are desirable for low-temperature cracking-resistant mixtures. The  $D_t$  results indicated that Mix #10 showed the least creep stiffness among the studied Alaskan mixtures. The mixture with unmodified binder (Mix

#8, Type IIB, PG 52-28/A) showed the lowest  $D_t$  value under each temperature, which indicated that the mixtures with modified binders were softer than the mixture with unmodified binder (Mix #8) at low temperatures.

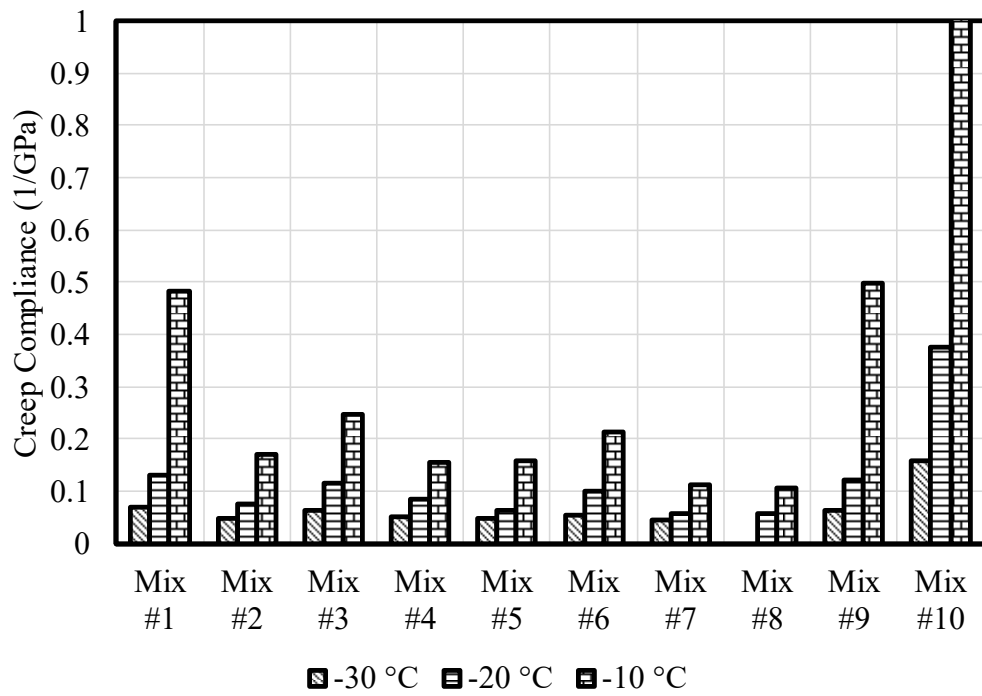


(a) 10 s

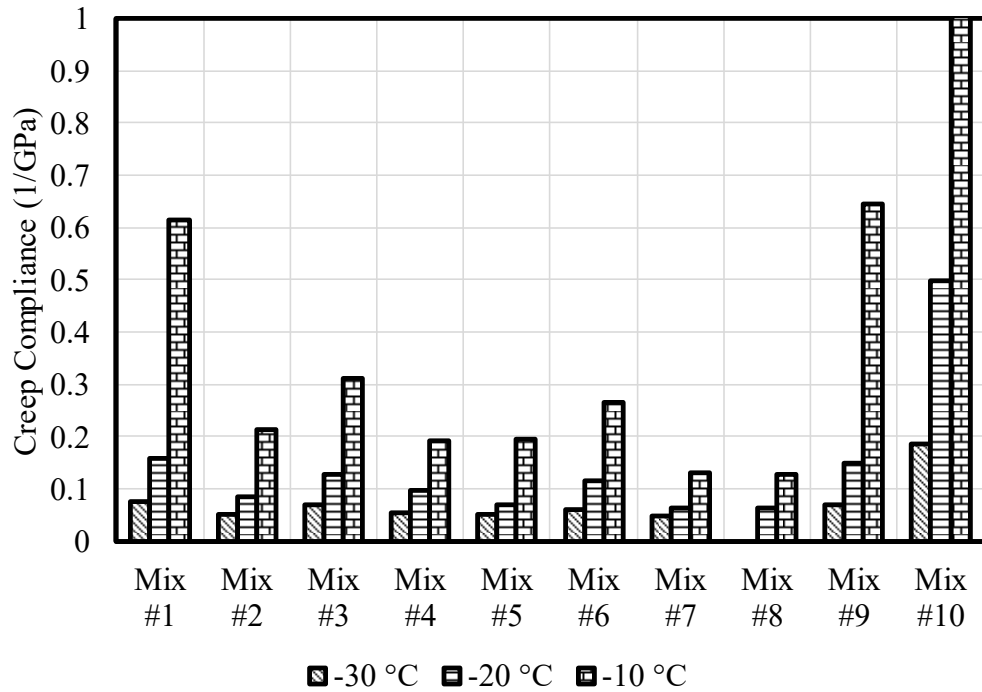




(b) 20 s



(c) 50 s



(d) 100 s

Figure 4.38 Creep compliance values of studied Alaskan mixtures at different loading times: (a) 10 s; (b) 20 s; (c) 50 s; and (d) 100 s.

Tensile strength is a widely used evaluation parameter for asphalt mixtures for their low-temperature cracking resistance. Higher tensile strength at low temperatures is more desirable for low-temperature cracking resistance. Figure 4.39 presents the tensile strength values of Alaskan mixtures. As shown, tensile strength of all mixtures decreased with an increase in temperature because of their corresponding higher elastic property under lower temperature. The mixture with unmodified binder (Mix #8, Type IIB, PG 52-28/A) showed the highest tensile strength values while Mix #10 (Lab mixed, PG52-46/A) showed the lowest tensile strength value, regardless of temperatures. However, it should be noted that this does not mean that Mix #8 had better thermal cracking resistance than the modified asphalt mixtures, since the thermal cracking

resistance of asphalt mixture is also closely related to its thermal stress relaxation capability, as indicated previously. In addition, as shown in Figure 4.39, the tensile strength values of some of mixtures with modified binders (e.g. Mixes #4 (Type IIA, PG 52-40/B), #5 (Type VS, PG 58-34/B), #6 (Type VH, PG 64-40/B), and #7 (Type V, PG 58-34/B)) were insensitive to temperature when the temperature changed from -20°C to -30°C.

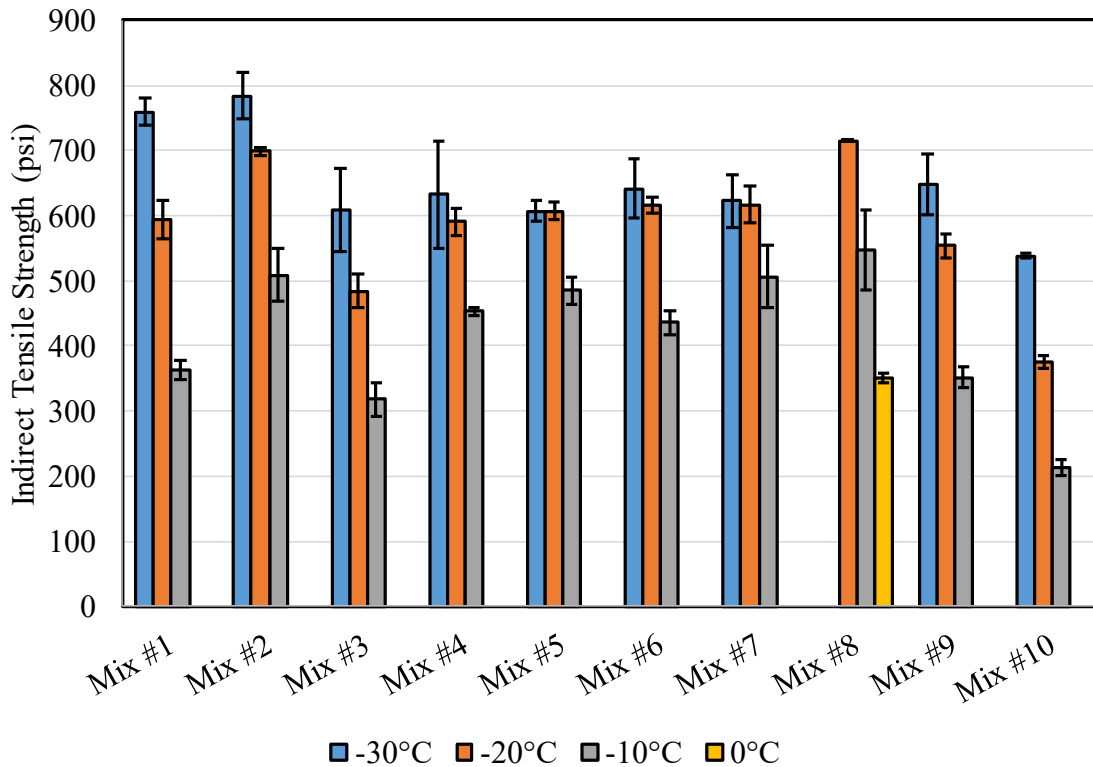


Figure 4.39 Indirect tensile strength results

#### 4.2.4 Mixture Cracking Temperature

According to Hills and Brien (1966), low-temperature cracks initiate when the thermally induced tensile stress in the pavement exceeds the strength of the asphalt mixture at that temperature as the temperature drops, and cracking temperature can be predicted at the intersection of the tensile strength-temperature curve and the thermal stress-temperature curve

(Figure 4.40). In this study, the  $D_t$  data was used to generate the thermal stress curve of each mixture according to the procedure described in Christensen (1998) and coded in the LTStress software (2012 version). The indirect tensile strength data in Figure 4.39 was used to develop the strength curves. Figures 4.41 to 4.50 present the process of mixture cracking temperature determination for each mix.

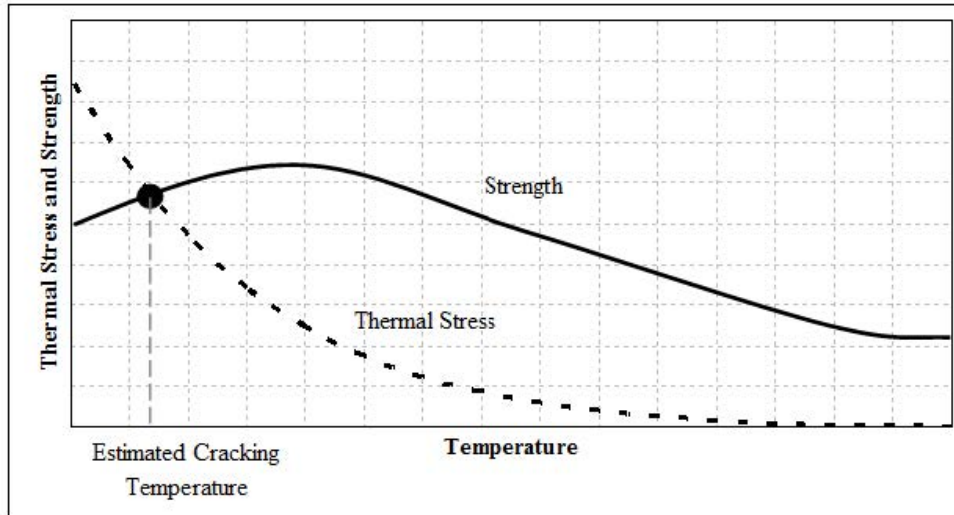


Figure 4.40 Example of determination of mixture cracking temperature

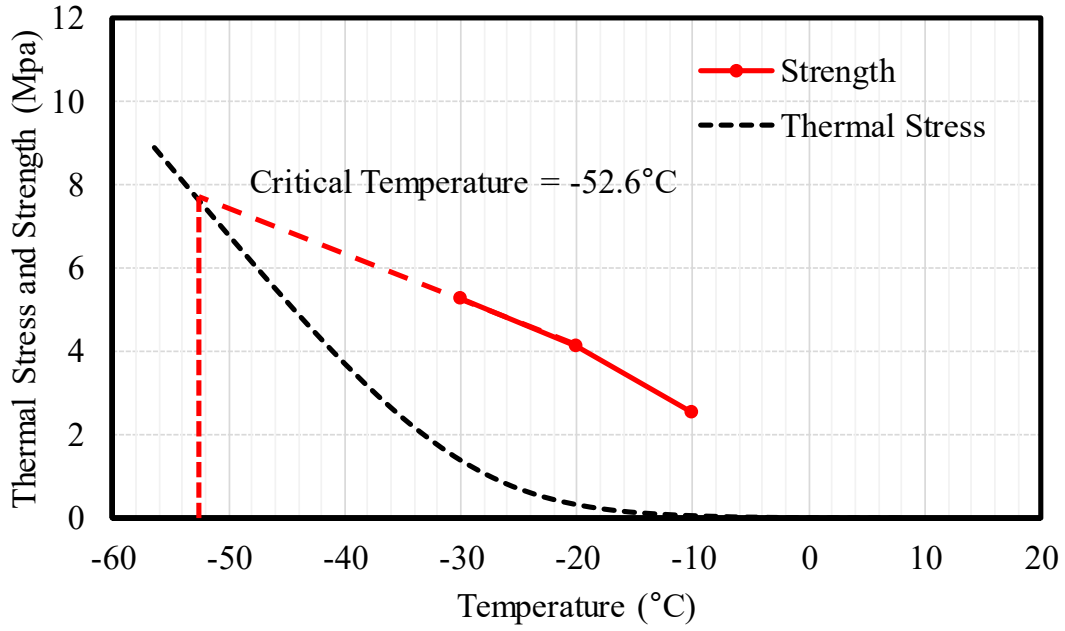


Figure 4.41 Determining mixture cracking temperature for Mix #1

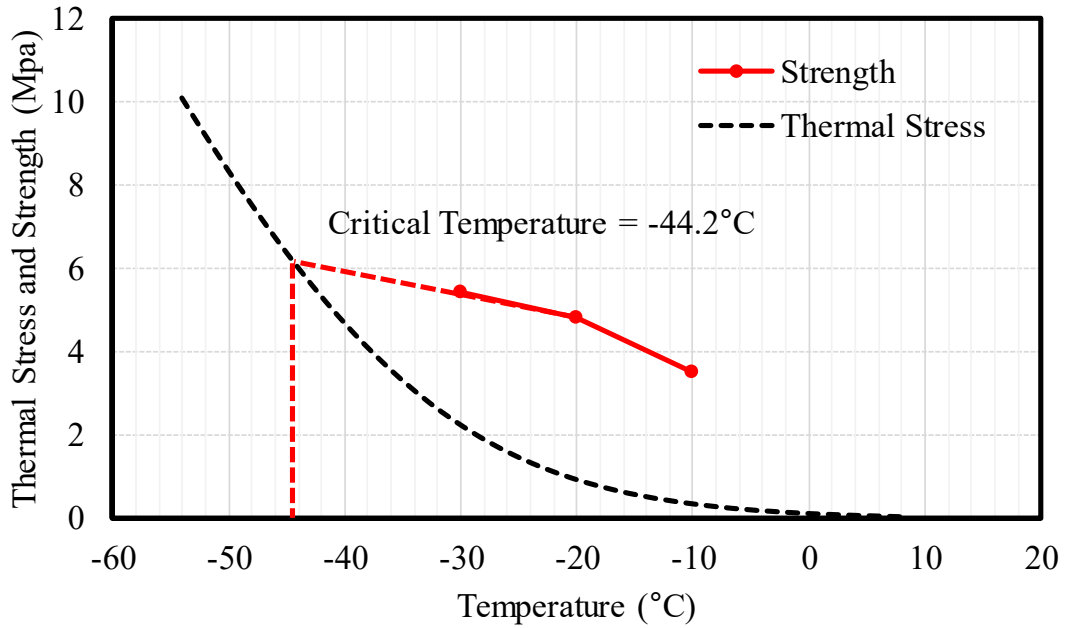


Figure 4.42 Determining mixture cracking temperature for Mix #2

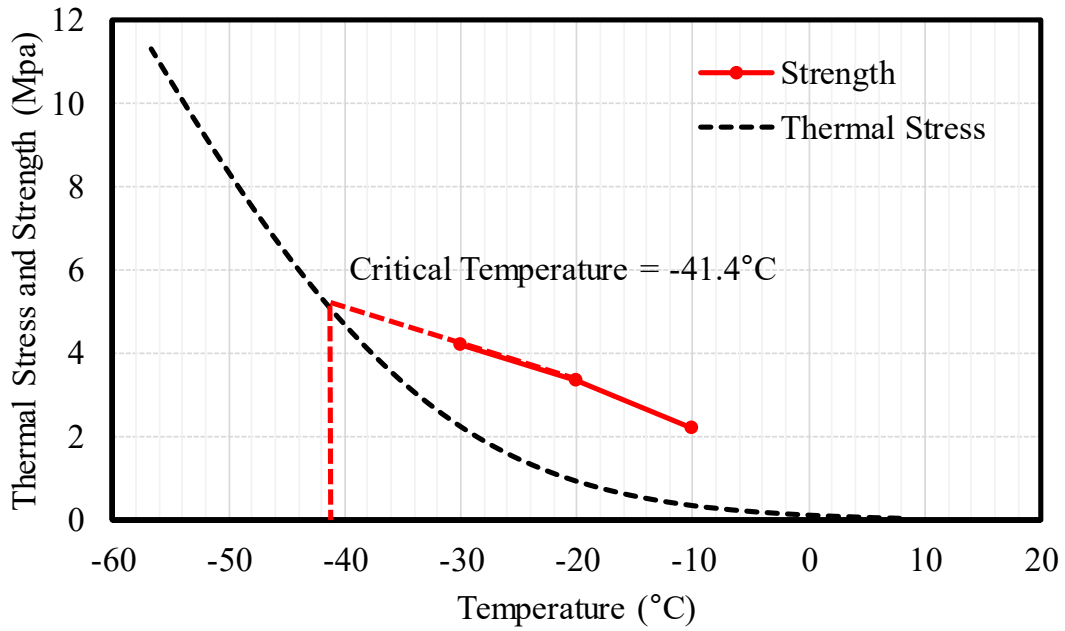


Figure 4.43 Determining mixture cracking temperature for Mix #3

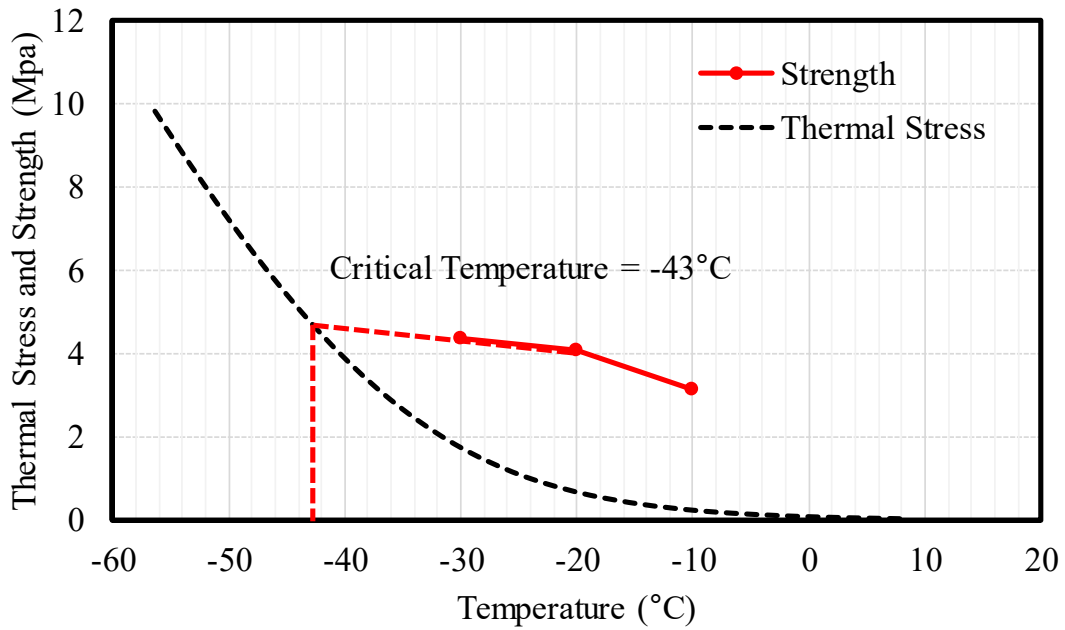


Figure 4.44 Determining mixture cracking temperature for Mix #4

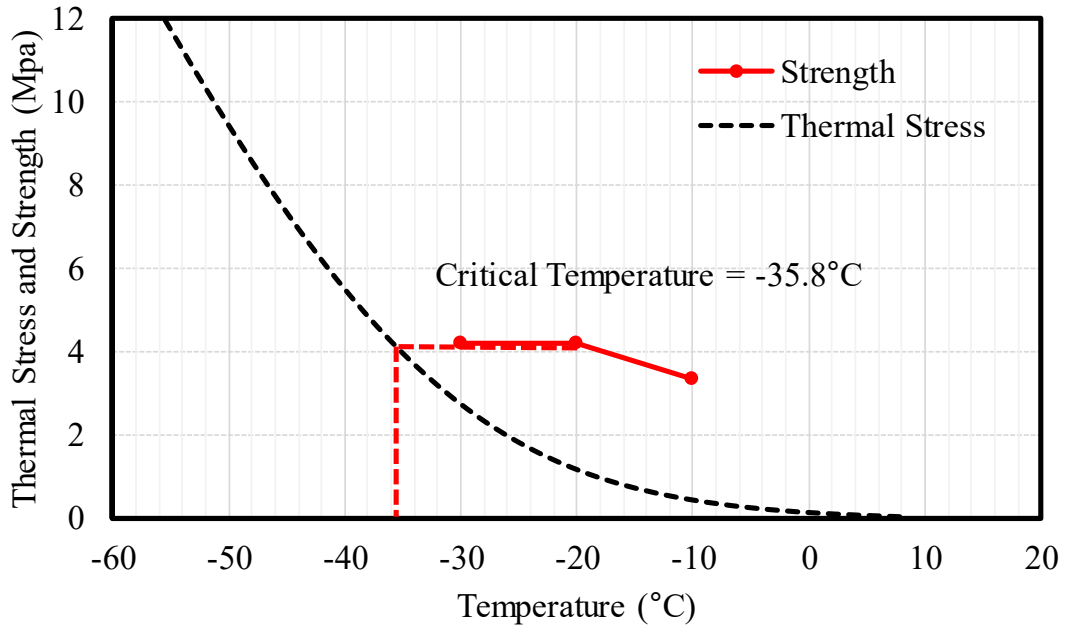


Figure 4.45 Determining mixture cracking temperature for Mix #5

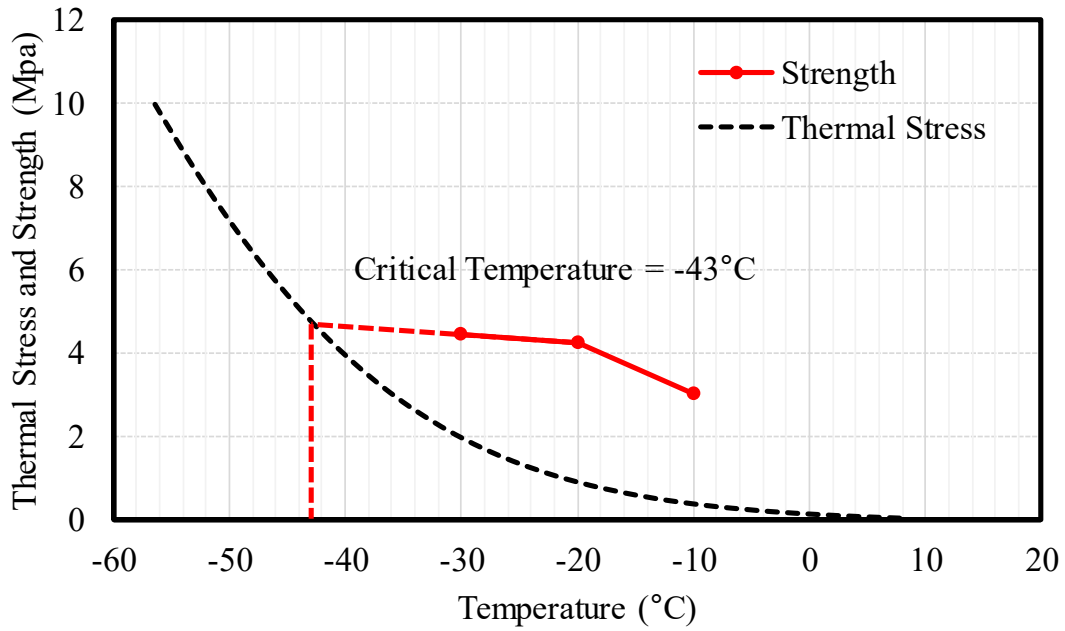


Figure 4.46 Determining mixture cracking temperature for Mix #6

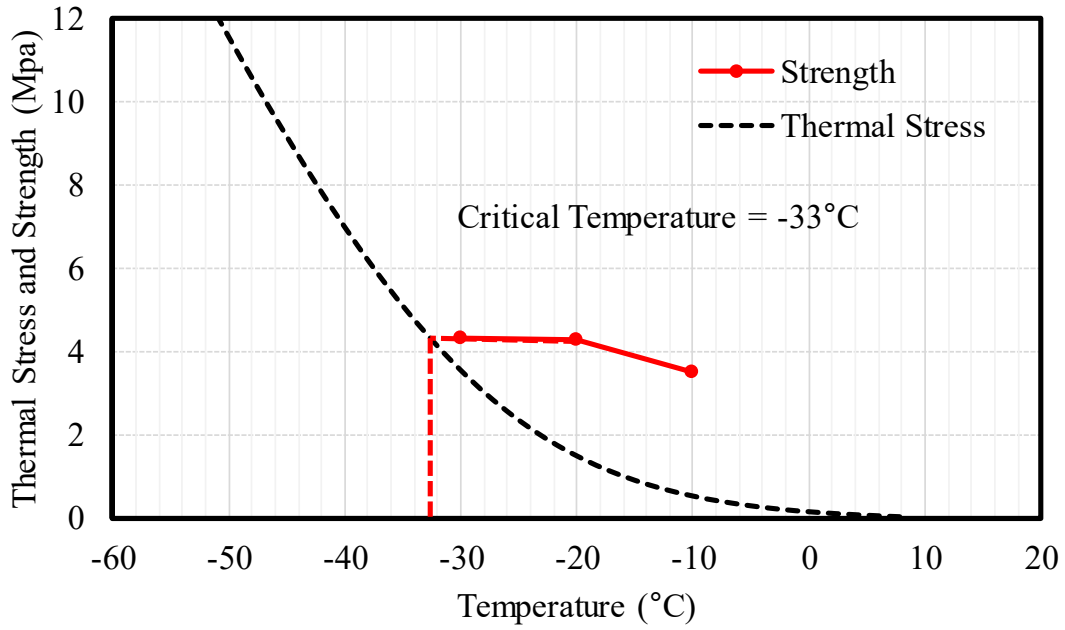


Figure 4.47 Determining mixture cracking temperature for Mix #7

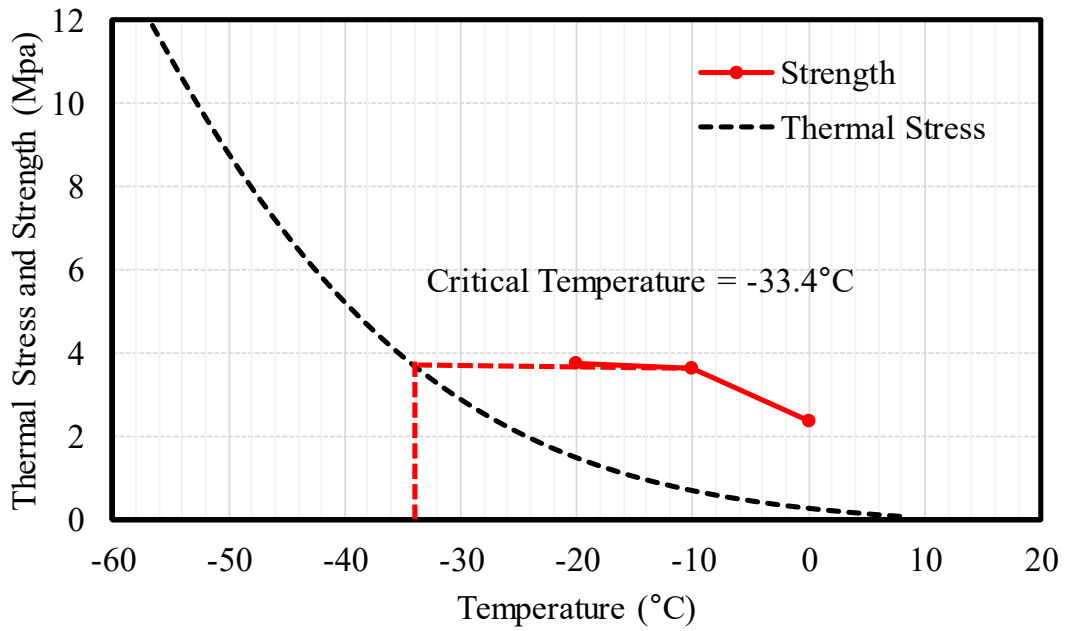


Figure 4.48 Determining mixture cracking temperature for Mix #8



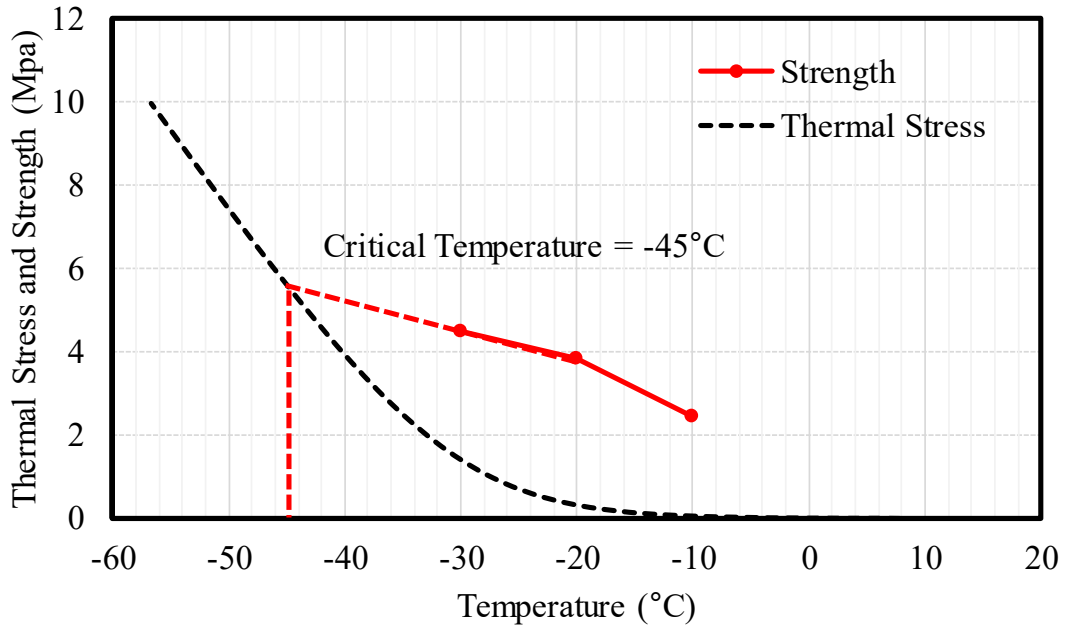


Figure 4.49 Determining mixture cracking temperature for Mix #9

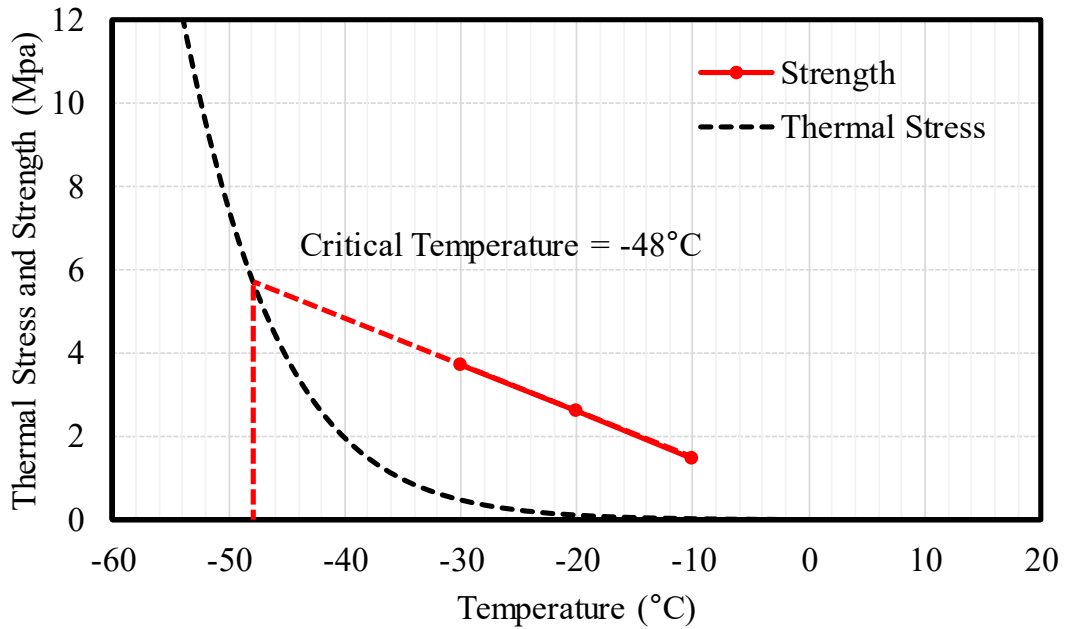


Figure 4.50 Determining mixture cracking temperature for Mix #10

Figure 4.51 presents the predicted cracking temperatures for the studied Alaskan mixtures. As shown, Mix #1 showed the lowest cracking temperature, which indicated that Mix #1 was predicted to perform the best in terms of low-temperature cracking. The mixture with unmodified binder (Mix #8) showed higher cracking temperature than most of modified mixtures, with the exception of Mix #7. No statistical difference between Mixes #7 and #8 was found. It can also be observed that the mixtures with PG 58-34 (e.g. Mix #2) could have lower cracking temperatures than the mixtures with PG 64-40 (e.g. Mix #3), which implied the mixture with PG 58-34 (although higher low-temperature PG) can show better low-temperature cracking resistance than that with PG 64-40.

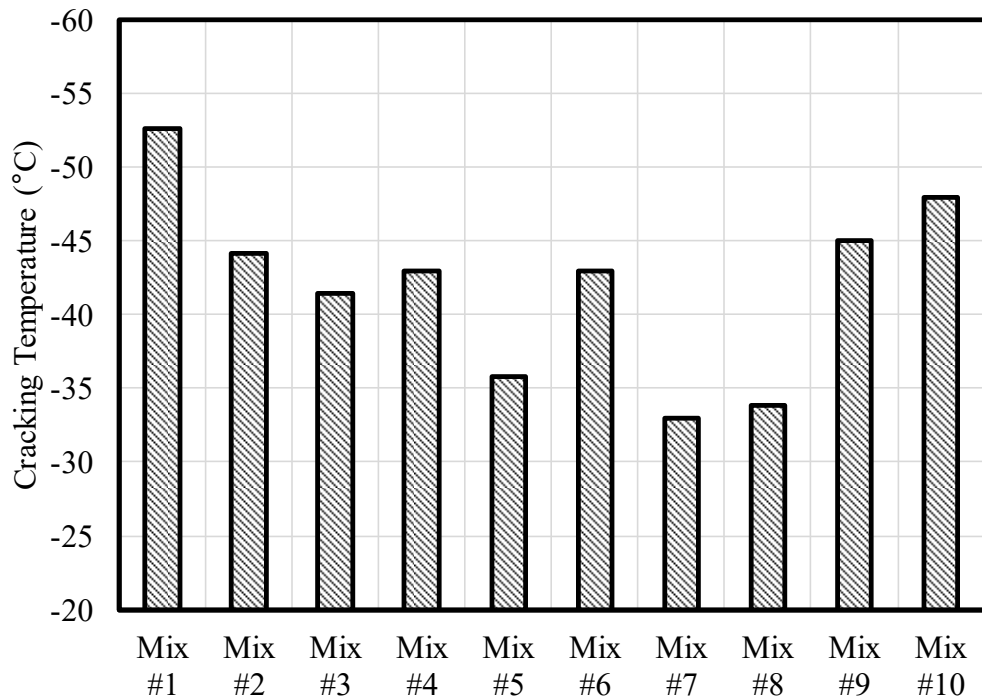


Figure 4.51 Cracking temperatures of Alaskan mixtures

### 4.3 Field Evaluation

A number of paving projects using highly polymerized asphalt binders have been completed in Alaska. Table 4.5 lists some (but not limited to) completed paving projects. According to the field survey on July 27<sup>th</sup>, 2019 (Figures 4.52 to 4.54) and the interview with the ADOT&PF engineers, varied performance was observed in terms of thermal cracking resistance of the asphalt pavements. Overall, the pavements with highly polymerized asphalt binders obviously outperformed the pavements with unmodified asphalt binder (PG 52-28). For example, for Richardson Hwy MP 337 Eielson AFB Intersection Improvements project (Figure 4.52), which was both constructed in 2017, no crack was observed during the field survey on July 27<sup>th</sup>, 2019. Minor cracks were observed in Old Nenana/Ester Hill Rehabilitation project (Figure 4.53) and Peger Rd Resurfacing / FMATS Ped Impr / NR Signal Interconnect project (Figure 4.54), which were constructed in 2018 and 2017, respectively. For projects with PG 64-40 binder in Anchorage (for example, L & I Couplet and 5th & 6th Avenue Couplet, constructed in 2014/2015), the pavement surface was comparative smooth with minor rutting and no crack was observed according to the survey by the pavement management team of ADOT&PF in 2016 (Figure 4.55). In addition, the field survey results revealed that the pavement sections at busy traffic areas (e.g. Fairbanks Downtown) showed more severe cracking than those at low-volume traffic areas. As most paving projects with highly polymerized asphalt binders were constructed in recent years, long term performance monitoring is needed to facilitate the application of highly modified binders in asphalt pavements.

Table 4.5 Examples of paving projects with highly modified asphalt binders

<b>Construction ID</b>	<b>Projects Descriptions</b>	<b>Binder/Supplier</b>	<b>Construction Year</b>
0610(007)	Airport Way PM - Stage II, NR Signal Intercon, & NR Pedestrian Imprvements	PG 52-40/A	2015
0002247	Birch Hill Bicycle & Pedestrian Facility	PG 52-40/A	2017
IM-DP-065-4(8)	Dalton Highway MP 197-209 Rehabilitation	PG 52-40/A	2011
000S413	Fairbanks Noble Street Upgrade	PG 52-40/A	2016
0002344/0644018	Farmers Loop Resurfacing & Farmers Loop Signal Interconnect	PG 52-40/A	2017/2018
0002344/0644018	Farmers Loop Resurfacing & Farmers Loop Signal Interconnect	PG 52-40/A	2017/2018
0002402	Fairbanks Metropolitan Area Transportation System Area Surface Upgrades FFY2017	PG 52-40/A	2017
AIP302011000520	Gulkana Airport Apron & Taxiway Repaving	PG 52-40/C	2015
0002257	Old Nenana/Ester Hill Rehabilitation	PG 52-40/A	2018
0A44(019)	Parks Hwy MP 237 Riley Creek Bridge Replacement (CMGC)	PG 52-40/A	2015
0002(304)	Peger Rd Resurfacing / FMATS Ped Impr / NR Signal Interconnect	PG 52-40/A	2016
BR-071-4(18)	Richardson Highway MP 228 One Mile Creek Bridge Replacement	PG 52-40/A	2011
BR-0714(22)	Richardson Hwy MP 201 Phelan Creek Bridge #0579	PG 52-40/A	2013
0714023	Richardson Hwy MP 235 Ruby Creek Bridge #0594	PG 52-40/A	2017
0A23022	Richardson Hwy MP 337 Eielson AFB Intersection Improvements	PG 52-40/A	2017
63626	Deadhorse Airport Rehabilitation	PG 52-40/A	2010
61427	Shishmaref Airport Resurfacing	PG 52-40/A	2016
56705	L & I Couplet and 5th & 6th Avenue Couplet	PG 64-40/B	2014/2015



Figure 4.52 Richardson Hwy MP 337 Eielson AFB Intersection Improvements, PG 52-40,  
constructed in 2017



Figure 4.53 Old Nenana/Ester Hill Rehabilitation, PG 52-40, constructed in 2018





Figure 4.54 Peger Rd Resurfacing / FMATS Ped Impr / NR Signal Interconnect, PG 52-40,  
constructed in 2017



Figure 4.55 L & I Couplet and 5th & 6th Avenue Couplet, PG64-40, constructed in 2014/2015

## CHAPTER 5.0 SUMMARIES AND CONCLUSIONS

The aim of this study was to conduct laboratory and field evaluation of the performance (i.e. rutting and low temperature cracking performance) of various modified asphalt binders and mixes, and to quantify the performance benefits of these modified materials. The asphalt binders included one virgin binder (PG 52-28) and 12 modified binders from three different suppliers. 10 HMA mixtures were either produced in the lab or collected from paving projects for laboratory performance evaluation. The binder tests included DSR tests for verification of binder grading, evaluation of viscoelastic behavior, master curves, MSCR tests associated with DSR setup, and BBR and ABCD tests for low-temperature performance evaluation. The Glover-Rowe parameter,  $\Delta T$ , Rheological Index, and crossover-frequency of the studied Alaskan asphalt binders at different aging states were calculated based on the  $G^*$  and  $\delta$  master curves data. The mixture performance tests included HWT tests for rutting resistance and moisture susceptibility, SCB tests for fatigue cracking resistance at intermediate temperatures, and IDT tests for creep compliance and low-temperature strengths. Mixture Cracking temperatures of mixtures were determined using the IDT data. Based on the testing results and analyses, the following conclusions were made:

- The verification tests of high-temperature grades of the studied Alaskan binders were conducted. The results showed that the true high-temperature grades of some binders were not consistent with those provided by the suppliers. The true high temperature grades of binders #3 and #7 (PG 76-XX) were much higher than the grade indicated by the supplier, which is PG 64-XX. The true high temperature grades of binders #8 (PG 64-XX), #10 (PG

58-XX), #11 (PG 64-XX), and #12 (PG 58-XX) were one grade higher than the grade provided by the supplier. The true high temperature grade of binder #4 (PG 46-XX) was one grade lower than the grade provided by the supplier (PG 52-XX).

- According to the MSCR test results, the  $J_{nr}$  of neat binder was much higher than those of modified binders at the identical testing temperatures and stress levels, which indicated that the binder polymer modification improved the rutting resistance of the binder. Most of studied modified binders can be graded as “E” at 52°C without considering the  $J_{nr-diff}$ . The  $J_{nr-diff}$  values of the most of studied modified binders at the testing temperatures beyond the maximum criterial of 75%.
- The viscoelastic behavior of the studied Alaskan asphalt binders was characterized in terms of  $G^*$  and  $\delta$  data as well as their master curves. These data can be used to develop the Alaskan material library and further used in various software or models for binder or mixture characterization.
- According to BBR results, the stiffness and m-value criteria showed similar critical low temperatures for each binder, when the binders were under unaged or RTFO aged aging states. However, for 40h PAV aged binders, the critical temperatures limiting by m-value is much higher than those limiting by stiffness. The test results verified the low temperature PG of most of studied binders. However, the tested low temperature PGs of binder #4 (PG52-40), binder #7 (PG64-40), and binder #9 (PG 58-34) were one grade lower than those indicated by the suppliers.
- Glover-Rowe (G-R) parameter showed potential to evaluate the low-temperature cracking resistance of the Alaskan binders. The location of G-R parameter for each binder in Black



Space Diagram was approaching the Glover-Rowe damage zone (i.e.,  $180 \text{ kPa} \leq \text{G-R parameter} \leq 450 \text{ kPa}$ ) as the asphalt binder ages. The results showed that only the binders from supplier C with 40h PAV aging state (i.e., binders #10, #11, #12, #13) reached the threshold values, while other aged binders were not at risk for cracking according to their locations of G-R parameters in Black Space Diagram.

- $\Delta T$  increased as the asphalt ages, indicating that  $\Delta T$  has potential to evaluate and quantify the cracking susceptibility (durability loss) of the binder.
- The crossover frequency-rheological index black space showed the potential to evaluate the cracking resistance of most of Alaskan asphalt binders except for binders with the grade of PG 64-40. However, the crossover frequency and R-value of some binders could not be obtained precisely.
- The ABCD critical cracking temperature results showed that the measured cracking temperature by ABCD was lower (colder) than the calculated cracking temperature by BBR for all binders tested. The disparity can be attributed to the difference in the mechanism of the two different tests/procedures. The binder #4 (PG 52-46/A) did not crack at  $-60^\circ\text{C}$ .
- The rut depth results and  $\Delta\varepsilon_{10,000}^{vp}$  results were not consistent in terms of the rutting resistance of Mixes #1, #3, and #6. But they all identified the improvement in rutting resistance by asphalt modification.
- The studied Alaskan mixtures were not susceptible to moisture damage at the tested temperatures, as predicted by the HWT test.
- From the SCB test results, it appeared that the unmodified mixture (Mix #8) showed better fatigue cracking resistance than some of the modified mixtures. Other fatigue tests such as

Illinois Flexibility Index test (I-FIT) and Fatigue Beam test were recommended to be conducted to verify the results.

- The  $D_t$  results indicated that Mix #10 showed the least creep stiffness among the studied Alaskan mixtures. The mixture with unmodified binder (Mix #8) showed the lowest  $D_t$  value under each temperature, indicated that the mixtures with modified binders were softer than the mixture with unmodified binder (Mix #8) at low temperatures. The unmodified mixture showed the highest IDT strength among all the studied Alaskan mixtures at the temperatures of -20°C and -10°C.
- The unmodified mixture showed higher cracking temperature than most of modified mixtures, with the exception of Mix #7. No statistical difference between Mix #7 and Mix #8 was found. The mixtures with binders with low-temperature PG of -40 showed lower cracking temperatures than the mixture with binder with low-temperature PG of -34.
- According to the field surveys in recent years and interview with ADOT&PF engineers, the pavements with highly polymerized asphalt binders generally outperformed the pavements with unmodified asphalt binder.

The following recommendations are made based on the findings of this study:

- The rutting and low-temperature cracking resistance of highly modified binders such as PG 52-40 and PG 64-40 were apparently better than that of unmodified binder (PG 52-28). It is recommended that the highly modified binder be further used for better rutting and cracking resistance.
- The binder test results obtained were generally used to develop the material library in Alaska for highly modified binders. It is recommended that the mixtures with different highly

modified binders be prepared in the Lab by using control variable method (the only variable is asphalt binder type). By doing this, the properties of mixtures with different highly modified binders could be compared.

- The G-R parameter and  $\Delta T$  had potential to evaluate the low-temperature cracking of the highly modified binders. Further use of these methods for binder evaluation in Alaska is recommended.
- Periodically monitoring field sections with highly modified binders and control (unmodified) binder are recommended to correlate the laboratory testing results and actual field performance of highly modified mixtures.

## REFERENCES

- AASHTO M 320. (2016). “Standard Specification for Performance-Graded Asphalt Binder.” American Association of State Highway and Transportation Officials, Washington, D.C.
- AASHTO M 332. (2014). “Standard Specification for Performance-Graded Asphalt Binder Using Multiple Stress Creep Recovery (MSCR) Test.” American Association of State Highway and Transportation Officials, Washington, D.C.
- AASHTO R 28. (2016). “Standard Practice for Accelerated Aging of Asphalt Binder Using a Pressurized Aging Vessel (PAV).” American Association of State Highway and Transportation Officials, Washington, D.C.
- AASHTO R 49. (2013). “Standard Practice for Determination of Low- Temperature Performance Grade (PG) of Asphalt Binders.” American Association of State Highway and Transportation Officials, Washington, D.C.
- AASHTO T 240. (2013). “Standard Method of Test for Effect of Heat and Air on a Moving Film of Asphalt Binder (Rolling Thin-Film Oven Test).” American Association of State Highway and Transportation Officials, Washington, D.C.
- AASHTO T 313. (2016). “Standard Method of Test for Determining the Flexural Creep Stiffness of Asphalt Binder Using the Bending Beam Rheometer (BBR).” American Association of State Highway and Transportation Officials, Washington, D.C.
- AASHTO T 314. (2016). “Standard Method of Test for Determining the Fracture Properties of Asphalt Binder in Direct Tension (DT).” American Association of State Highway and Transportation Officials, Washington, D.C.

- AASHTO T 315. (2013). “Standard Method of Test for Determining the Rheological Properties of Asphalt Binder Using a Dynamic Shear Rheometer (DSR).” American Association of State Highway and Transportation Officials, Washington, D.C.
- AASHTO T 316. (2013). “Standard Method of Test for Viscosity Determination of Asphalt Binder Using Rotational Viscometer.” American Association of State Highway and Transportation Officials, Washington, D.C.
- AASHTO T 324. (2016). “Standard Method of Test for Hamburg Wheel-Track Testing of Compacted Hot Mix Asphalt (HMA).” American Association of State Highway and Transportation Officials, Washington, D.C.
- AASHTO T 340. (2015). “Standard Method of Test for Determining Rutting Susceptibility of Hot Mix Asphalt (HMA) Using the Asphalt Pavement Analyzer (APA).” American Association of State Highway and Transportation Officials, Washington, D.C.
- AASHTO T 350. (2014). “Standard Method of Test for Multiple Stress Creep Recovery (MSCR) Test of Asphalt Binder Using a Dynamic Shear Rheometer (DSR).” American Association of State Highway and Transportation Officials, Washington, D.C.
- Asphalt Institute (AI) (2019). “Use of the delta Tc Parameter to Characterize Asphalt Binder Behavior” IS-240. ASPHALT INSTITUTE TECHNICAL ADVISORY COMMITTEE
- Abdulshafi, A. A. (1983). “Viscoelastic/Plastic Characterization, Rutting and Fatigue of Flexible Pavements.” Doctoral Dissertation, Ohio State University, Columbus, OH.
- Anderson, D. A., and Kennedy, T. W. (1993). “Development of SHRP Binder Specification (with Discussion).” Journal of the Association of Asphalt Paving Technologists, 62.
- Ahmed, M. J. (2008). “Analysis of Rutting for Anchorage Pavements.” M.Sc. Thesis, University of Alaska Fairbanks, Fairbanks, AK.

- Anderson, R. M., King, G. N., Hanson, D. I., and Blankenship, P. B. (2011). "Evaluation of the Relationship Between Asphalt Binder Properties and Non-Load Related Cracking." *Journal of the Association of Asphalt Paving Technologists*, 80, 615-664.
- ARA, Inc. (2004). *Guide for Mechanistic-Empirical Design of New and Rehabilitated Pavement Structures*. ERES Division, Champaign, IL.
- ASTM D5546. (2009). "Standard Test Method for Solubility of Asphalt Binders in Toluene by Centrifuge." ASTM International, West Conshohocken, PA.
- ASTM D5801. (2012). "Standard Test Method for Toughness and Tenacity of Bituminous Materials." ASTM International, West Conshohocken, PA.
- ASTM D7173. (2014). "Standard Practice for Determining the Separation Tendency of Polymer from Polymer Modified Asphalt." ASTM International, West Conshohocken, PA.
- Awwad, M. T., and Shbeeb, L. (2007). "The Use of Polyethylene in Hot Asphalt Mixtures." *American Journal of Applied Sciences*, 4(6), 390-396.
- Bahia, H. U., Hanson, D. I., Zeng, M., Zhai, H., Khatri, M. A., and Anderson, R. M. (2001). "Characterization of Modified Asphalt Binders in Superpave Mix Design." National Cooperative Highway Research Program, Report 459.
- Bahia, H., Perdomo, D., and Turner, P. (1997). "Applicability of Superpave Binder Testing Protocols to Modified Binders." *Transportation Research Record: Journal of the Transportation Research Board*, 1586, 16-23.
- Bahia, H. U., Tabatabaee, H. A., Mandal, T., and Faheem, A. (2013). "Field Evaluation of Modified Asphalt Binder Guidelines – Phase II." Wisconsin Highway Research Program Report No. 0092-13-02, Modified Asphalt Research Center, University of Wisconsin Madison, Madison, WI.

Barth, E. J. (1962). "Asphalt Science and Technology." Gordon and Breach Science Publishers, New York, NY.

Blankenship, P. B., Myers, A. H., Clifford, A. S., Thomas, T. W., King, H. W., and King, G. N. (1998). "Are all PG 70-22s the same? Lab tests on KY I-64 field samples." *Journal of the Association of Asphalt Paving Technologists*, 67, 493-552.

Bouldin, M. G., Dongre, R., Row, G. M., Sharrock, M. J., and Anderson, D. A. (2000). "Predicting Thermal Cracking of Pavements from Binder Properties: Theoretical Basis and Field Validation." In *Proceedings of the Association of Asphalt Paving Technologists*, 69, 455-496.

Brown, E. R., Kandhal, P. S., Roberts, F. L., Kim, Y. R., Lee, D. Y., and Kennedy, T. W. (2009). "Hot Mix Asphalt Materials, Mixture Design, and Construction, Third Edition." NAPA Research and Education Foundation, Lanham, Maryland.

Brown, E. R., McRae, J. L., and Crawley, A. B. (1989). "Effect of Aggregates on Performance of Bituminous Concrete." In *Implication of aggregates in the design, construction, and performance of flexible pavements*. ASTM Special Technical Publication 1016.

Casey, D., McNally, C., Gibney, A., and Gilchrist, M. D. (2008). "Development of a Recycled Polymer Modified Binder for Use in Stone Mastic Asphalt." *Resources, Conservation and Recycling*, 52(10), 1167-1174.

Christison, J. T., Murray, D. W. and Anderson, K. O. (1972). "Stress Prediction and Low Temperature Fracture Susceptibility of Asphaltic Concrete Pavements." *Proceedings of the Association of Asphalt Paving Technologists*, 41, 494-523.

Claessen, A. I. M., Edwards, J. M., Sommer, P., and Uge, P. (1977). "Asphalt Pavement Design - The Shell Method." In *Volume I of proceedings of 4th International Conference on*

- Structural Design of Asphalt Pavements, Ann Arbor, Michigan, August 22-26, 1977 (No. Proceeding).
- Devol J. R. (2010). "Asphalt Binder Cracking Device (ABCD): Inter-Laboratory Study – 2009." Technotes April 2010, Washington State Department of Transportation, Olympia, WA.
- Dougherty, P. (2017). Personal Communication. Alaska Department of Transportation & Public Facilities, Central Region, Anchorage, AK.
- Echmann, B. (1987). "Rut Depth Prediction: A Practical Verification." In Sixth International Conference, Structural Design of Asphalt Pavements, 1, 209-219.
- Fee, D., Maldonado, R., Reinke, G., and Romagosa, H. (2010). "Polyphosphoric Acid Modification of Asphalt." Transportation Research Record: Journal of the Transportation Research Board, 2179, 49-57.
- FHWA (Federal Highway Administration). (2011). "The Multiple Stress Creep Recovery (MSCR) Procedure." Federal Highway Administration TechBrief, FHWA-HIF-11-038.
- FHWA (Federal Highway Administration). (2017). "LTPP\_products." (<http://www.fhwa.dot.gov/research/tfhrc/programs/infrastructure/pavements/ltpp/product.cfm>) (April 25, 2017).
- Finn, F. N., Monismith, C. L., and Markevich, N. J. (1983). "Pavement Performance and Asphalt Concrete Mix Design." In Proceedings of the Association of Asphalt Paving Technologists, 52, 121-150.
- Finn, F., Saraf, C.L., Kulkarni, R., Nair, K., Smith, W., and Abdullah, A. (1977). "User's Manual for the Computer Program Cold." NCHRP Report 1-10B, Transportation Research Board, Washington, D.C.



- Fromm, H. J., Bean, D. C., and Miller, L. (1981). "Sulphur-Asphalt Pavements Performance and Recycling (with Discussion)." In Association of Asphalt Paving Technologists Proceedings, 50, 98-115.
- Fromm, H. J., and Phang, W. A. (1972) "A Study of Transverse Cracking of Bituminous Pavements." In Proceedings of the Association of Asphalt Paving Technologists, 41, 383-423.
- Haas, R., Meyer, F., Assaf, G., and Lee, H. (1987) "A Comprehensive Study of Cold Climate Airport Pavement Cracking." Proceedings of the Association of Asphalt Paving Technologists, 56, 198-245.
- Hillerborg, A., Modeer, M., and Peterson, P. E. (1976) "Analysis of Crack Formation and Crack Growth in Concrete by Means of Fracture Mechanics and Finite Elements." Cement and Concrete Research, 6, 773-782.
- Hills, J.F. and Brien, D. (1966) "The Fracture of Bitumens and Asphalt Mixes by Temperature Induced Stresses." Prepared Discussion, Proceedings, the Association of Asphalt Paving Technologists, 35, 292 – 309.
- Hines, M. L. (1993). "Asphalt Cement Performance Improved by Styrelf-Laboratory and Field Data." Koch Materials Company.
- Illinois DOT (Department of Transportation). (2005). Pavement Technology Advisory - Polymer-Modified Hot Mix Asphalt - PTA-D5. Bureau of Materials and Physical Research, Illinois Department of Transportation, Springfield, IL.
- Kandhal, P. S. (1981). "Evaluation of Baghouse Fines in Bituminous Paving Mixtures (with Discussion)." In Association of Asphalt Paving Technologists Proceedings, 50, 150-210.

- Kandhal, P. S. (1982). "Evaluation of Sulphur Extended Asphalt Binders in Bituminous Paving Mixtures (with Discussion and Closure)." In Association of Asphalt Paving Technologists Proceedings, Vol. 51, 189-221.
- Kandhal, P. S., Mellott, D. B., and Hoffman, G. L. (1983). "Laboratory and Field Characterization of Sulphlex as a Paving Binder." ASTM Special Technical Publication 807.
- Kenis, W. J. (1977). Predictive design procedures--A design method for flexible pavements using the VESYS structural subsystem. In Volume I of proceedings of 4th International Conference on Structural Design of Asphalt Pavements, Ann Arbor, Michigan, August 22-26, 1977. (No. Proceeding).
- Kim, S. S. (2005). "Direct Measurement of Asphalt Binder Thermal Cracking." Journal of Materials in Civil Engineering, 17(6), 632-639.
- Kim, S. S. (2010). "Asphalt Binder Cracking Device to Reduce Low Temperature Asphalt Pavement Cracking." Final project Rep., Highways for LIFE Technology Partnership Program, Washington, DC.
- King, G., Anderson, M., Hanson, D., and Blankenship, P. (2012). "Using Black Space Diagrams to Predict Age-Induced Cracking." In 7th RILEM International Conference on Cracking in Pavements, 453-463.
- Kluttz, B. (2015). "Use of Highly Polymer Modified HMA (HiMA)." Ohio Asphalt Paving Concrete, Columbus, OH, February 4, 2015.
- Li, P., and Liu, J. (2014). "Characterization of Alaskan HMA Mixtures with the Simple Performance Tester." Report No. INE/AUTC 12.21, Alaska University Transportation Center, Fairbanks, AK.

- Li, P., Liu, J., and Zhao, S. (2016). "Performance of Multiaxial Paving Interlayer-Reinforced Asphalt Pavement." *Journal of Materials in Civil Engineering*, 28(7), 04016039.
- Little, D. H., Holmgren Jr, R. J., and Epps, J. A. (1981). "Effect of Recycling Agents on The Structural Performance of Recycled Asphalt Concrete Materials." In *Association of Asphalt Paving Technologists Proceedings*, 50, 32-63.
- Liu, J., and Li, P. (2011). "Low Temperature Performance of Sasobit-Modified Warm-Mix Asphalt." *Journal of Materials in Civil Engineering*, 24(1), 57-63.
- Liu, J., Zhao, S., and Li, L. (2016). "Characterization of Alaskan Hot-Mix Asphalt Containing Reclaimed Asphalt Pavement Material." Report No. FHWA-AK-RD-4000(137), Alaska Department of Transportation Statewide Research Office, Juneau, AK.
- Marasteanu, M., et al. (2007). "Investigation of Low Temperature Cracking in Asphalt Pavements National Pooled Fund Study 776." Minnesota Department of Transportation.
- Marasteanu, M., et al. (2012). "Investigation of Low Temperature Cracking in Asphalt Pavements National Pooled Fund Study – Phase II." Minnesota Department of Transportation.
- McDaniel R. (2015). "Fiber Additives in Asphalt Mixtures." NCHRP Synthesis 475, Transportation Research Board, Washington D.C.
- McGennis, R. B. (1995). "Asphalt Modifiers are here to Stay." *Asphalt Contractor*, 38-41.
- Miller, J. A., and Whitehead, R. L., Gingerich, S. B., Oki, D. S., and Olcott, P. G. (1999). "Ground Water Atlas of the United States: Segment 13, Alaska, Hawaii, Puerto Rico, and the U.S. Virgin Islands, HA 730-N." (<https://pubs.er.usgs.gov/publication/ha730N>) (April 2017).

- Moghaddam, T. B., Soltani, M., and Karim, M. R. (2014). "Evaluation of Permanent Deformation Characteristics of Unmodified and Polyethylene Terephthalate Modified Asphalt Mixtures Using Dynamic Creep Test." *Materials & Design*, 53, 317-324.
- Mohammad, L. N., Negulescu, I. I., Wu, Z., Daranga, C., Daly, W. H., and Abadie, C. (2003). "Investigation of the Use of Recycled Polymer Modified Asphalt Binder in Asphalt Concrete Pavements (With Discussion and Closure)." *Journal of the Association of Asphalt Paving Technologists*, 72, 551-594.
- NCAT (National Center for Asphalt Technology). (2016). Field Trials and Lab Tests Show Excellent Performance of GTR Modified Asphalt Mixes. Available online: <http://www.eng.auburn.edu/research/centers/ncat/newsroom/2016/gtr-modified.html>
- NAPA (National Asphalt Pavement Association). (1994). "Guidelines for Materials, Production, and Placement of Stone Matrix Asphalt (SMA)." Technical Working Group (TWG). National Asphalt Pavement Association Publication No. IS, 118.
- Pavement Systems LLC. (2005). "LTPPBIND version 3.1 beta." (<http://www.fhwa.dot.gov/research/tfhrc/programs/infrastructure/pavements/ltpb/install.cfm>) (Sep. 15, 2005).
- Perera, R. W., Kohn, S. D., and Tayabji, S. (2005). "Achieving a High Level of Smoothness in Concrete Pavements without Sacrificing Long-Term Performance." Report No. FHWA-HRT-05-068, Office of Infrastructure Research and Development, Turner-Fairbank Highway Research Center Federal Highway Administration, McLean, VA.
- Polacco, G., Filippi, S., Merusi, F., and Stastna, G. (2015). "A Review of the Fundamentals of Polymer-Modified Asphalts: Asphalt/Polymer Interactions and Principles of Compatibility." *Advances in colloid and interface science*, 224, 72-112.

- Raad, L., and Saboundjian, S. (1998). "Fatigue Behavior of Rubber-Modified Pavements." Transportation Research Record: Journal of the Transportation Research Board, 1639, 73-82.
- Raad, L., Saboundjian, S., Sebaaly, P., Epps, J., Camilli, B., and Bush, D. (1997). "Low Temperature Cracking of Modified AC Mixes in Alaska." Report No. INE/TRC 97.05, University of Alaska Fairbanks, Fairbanks, AK.
- Reese, R., and Predoehl, N. H. (1989). "Evaluation of Modified Asphalt Binders: Interim Report." Report No. FHWA/CA/TL-89/15, California Department of Transportation, Sacramento, CA.
- Romain, J. E. (1972). "Rut Depth Prediction in Asphalt Pavements." In Presented at the Third International Conference on the Structural Design of Asphalt Pavements, Grosvenor House, Park Lane, London, England.
- Roque, R., Birgisson, B., Drakos, C., and Sholar, G. (2005). "Guidelines for Use of Modified Binders." Report No. UF Project No. 4910-4504-964-12, University of Florida, Gainesville, FL.
- Saboundjian, S., and Raad, L. (1997). "Performance of Rubberized Asphalt Mixes in Alaska." Transportation Research Record: Journal of the Transportation Research Board, 1583, 52-61.
- Sargand, S. M., and Kim, S. S. (2001). "Performance Evaluation of Polymer Modified and Unmodified Superpave Mixes." In Second International Symposium on Maintenance and Rehabilitation of Pavements and Technological Control, No. 01-147, National Center for Asphalt Technology, Auburn, AL.

- Schaefer, H. (2017). Personal Communication. Alaska Department of Transportation & Public Facilities, Northern Region, Fairbanks, AK.
- Sousa, J. B., Craus, J., and Monismith, C. L. (1991). "Summary Report on Permanent Deformation in Asphalt Concrete." Report No. SHRP-A/IR-91-104, National Research Council, Washington, DC.
- Stuart, K. D. (2002). "Understanding the Performance of Modified Asphalt Binders in Mixtures: High-Temperature Characterization." Report No. FHWA-RD-02-075, Federal Highway Administration, McLean, VA.
- Stuart, K. D., and Youtcheff, J. S. (2002). "Understanding the Performance of Modified Asphalt Binders in Mixtures: Low-Temperature Properties." Report No. FHWA-RD-02-074, Federal Highway Administration, McLean, VA.
- Tapkın, S., Çevik, A., and Uşar, Ü. (2010). "Prediction of Marshall Test Results for Polypropylene Modified Dense Bituminous Mixtures Using Neural Networks." *Expert Systems with Applications*, 37(6), 4660-4670.
- Terrel, R. L., and Epps, J. A. (1988). "Using Additives and Modifiers in Hot Mix Asphalt." National Asphalt Pavement Association Quality Improvement Series 114.
- Terrel, R. L., and Rimsritong, S. (1979). "Wood Lignins Used as Extenders for Asphalt in Bituminous Pavements (with Discussion)." In *Association of Asphalt Paving Technologists Proceedings*, 48, 111-134.
- Timm, D. H., and Voller, V. R. (2003). "Field Validation and Parametric Study of a Thermal Crack Spacing Model (With Discussion)." *Journal of the Association of Asphalt Paving Technologists*, 72, 356-387.


- Traxler, R. N. (1961). "Asphalt: Its Composition, Properties and Uses." Reinhold Publishing Corp., New York, NY.
- Trousil, R. (2017). Personal Communication. Alaska Department of Transportation & Public Facilities, Southcoast Region, Juneau, AK.
- Uzan, J., and Lytton, R. L. (1982). "Structural Design of Flexible Pavements: A Simple Predictive System." Transportation Research Record, 888, 56-63.
- Von Quintus, H. L., Mallela, J., Bonaquist, R., Schwartz, C. W., and Carvalho, R. L. (2012). Calibration of Rutting Models for Structural and Mix Design. National Cooperative Highway Research Program (NCHRP) Report 719, Washington, D.C.
- Willis, J. R., Plemons, C., Turner, P., Rodezno, C., and Mitchell, T. (2012). "Effect of Ground Tire Rubber Particle Size and Grinding Method on Asphalt Binder Properties." National Center for Asphalt Technology. NCAT Report, 12-09, Auburn, AL.
- Xiao, F., Amirkhanian, S., Wang, H., and Hao, P. (2014). "Rheological Property Investigations for Polymer and Polyphosphoric Acid Modified Asphalt Binders at High Temperatures." Construction and Building Materials, 64, 316-323.
- Yildirim Y. (2007). "Polymer Modified Asphalt Binders." Construction and Building Materials, 21, 66-72.
- Yildirim, Y., Hazlett, D., Davio, R., and Transportation Research Board Committee on Waste Management (A1F07). (2004). "Toner-Modified Asphalt Demonstration Projects." Resources, Conservation and Recycling, 42(3), 295-308.
- Yin, F., Arambula, E., Lytton, R., Martin, A., and Cucalon, L. (2014). "Novel Method for Moisture Susceptibility and Rutting Evaluation Using Hamburg Wheel Tracking Test."

- Transportation Research Record: Journal of the Transportation Research Board, (2446), 1-7.
- Zhao, S., Liu, J., Li, P., and Burritt, T. (2016). "Asphalt Binder Adaption for Climatic Conditions in Cold Regions: Alaska Experience." *Journal of Materials in Civil Engineering*, 04016184.
- Zhou, F., Newcomb, D., Gurganus, C., Banihashemrad, S., Park, E. S., Sakhaeifar, M., and Lytton, R. L. (2016). "Experimental Design for Field Validation of Laboratory Tests to Assess Cracking Resistance of Asphalt Mixtures." *National Cooperative Highway Research Program Transportation Research Board of the National Academies*, (9-57), 1-104.
- Zubeck, H., Raad, L., Saboundjian, S., Minassian, G., and Ryer, J. (1999). "Constructability of Polymer-Modified Asphalts and Asphalt-Aggregate Mixtures in Alaska." Report No. FHWA-AK-RD-99-1, University of Alaska Anchorage, Anchorage, AK.
- Zubeck, H., and Vinson, T. (1996). "Prediction of Low-Temperature Cracking of Asphalt Concrete Mixtures with Thermal Stress Restrained Specimen Test Results." *Transportation Research Record: Journal of the Transportation Research Board*, 1545, 50-58.



# APPENDIX A JOB MIX FORMULAE

## Table A.1 JMF for Mix #1



State of Alaska  
Department of Transportation & Public Facilities  
Central Materials Lab  
5750 East Tudor Road  
Anchorage, AK 99507  
Phone (907) 269-6200 FAX (907) 269-6201

Quality  
Laboratory No.: 2015A-3888

---

Name: **Park Hwy MP 35-40 Pavement Preservation**  
 Sample: **HMA type VH**  
 Sampled From: **Manufacturer's Stock**  
 Source: **MP 216 Parks / Cange-Pittman MP 44 Parks**  
 Location: **Wasilla AK**  
 Examined For: **Bituminous Mix Design**

Project No.: **56703 / 0001487**  
 Item/Spec No.: **408(1H)**  
 Field No.: **Q-HMAVH-MD-1**  
 Date Sampled: **09/22/2015**  
 Date Received: **10/08/2015**  
 Date Completed: **01/26/2016**  
 Date Reported: **01/29/2016**

---

**AGGREGATE**

Blend Ratio 14:22: :64: : :  
 CA:IA:NF:CF:BS:NF:RP  
 Blend Specific Gravity Bulk **2.780**  
 Effective **2.841**

Sieve	% Pass	Specs
1"		
3/4"	100	100
1/2"	90	84-96
3/8"	80	74-96
#4	47	41-53
#8	32	26-38
#16	22	17-27
#30	17	13-21
#50	12	8-16
#100	8	5-11
#200	5.4	3.4-7.4

FA FM **3.08**  
 FA Angularity **47.7** 45 min  
 CA Absorption **0.6** 2.0 max  
 % Fracture  
 Double Face **100** 98 min  
 % Flat / Elongated  
 @ 1:3 **18**  
 @ 1:5 **1** 8 max  
 Plastic Index **NP** NP

**ASPHALT CONTENT, %**

⊕ 4.0% Voids Total Mix **5.0**  
 Approved Optimum **5.0**  
 Specifications **4.6-5.4**

**PROPERTIES @ OPTIMUM**

Max. SpG (AASHTO T209) **2.597**  
 Max. SpG Unit Wt., pcf **161.7**

Voids  
 Filled **73**  
 Total Mix **4.0** **4.0**  
 In Mineral Aggregate **14.8** **13.0-**  
 In Coarse Aggregate

Stability, lbs  
 Flow, 0.01 inches  
 Unit Weight, pcf **155.2**  
 Dust/Asphalt Ratio **1.3** **0.8-1.6**  
 Rut Index **0.9** **3 max**

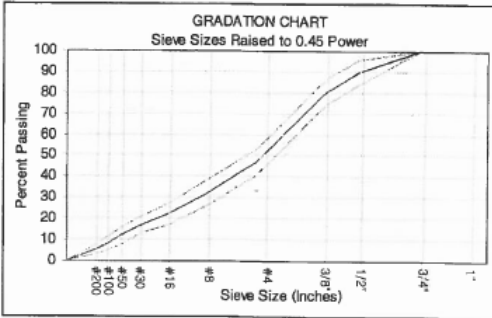
**ASPHALT**

Brand & Type **EP PG 64-40E**  
 Specific Gravity **0.986**  
 Mixing Temp. Range **315-325°F**  
 Comp. Temp. Range **305-315°F**

**ANTI-STRIP ADDITIVE**

Brand & Type **Morelife 5000**  
 Minimum Required **0.25%**

**GRADATION CHART**  
 Sieve Sizes Raised to 0.45 Power



Remarks:

Gyrations	%Gm	Specs.
Nini 7	86.1	<90.5
Ndes 75	95.5	96.0
Nmax 115	96.9	<98.0

The Dust/Asphalt ratio spec is adjusted per AI manual SP-2 table 5.2 note to 0.8-1.6.

D1 The Material as Submitted Conforms to Specifications  
 Yes  No [ ] NA [ ]

THE TEST RESULTS ARE ONLY REPRESENTATIVE OF THE MATERIAL AS SUBMITTED

Signature: *Newton J. Bingham*  
 Newton J. Bingham, PE  
 Regional Materials Engineer

Table A.2 JMF for Mix #2



**State of Alaska**  
**Department of Transportation & Public Facilities**  
**Central Materials Lab**  
 5750 East Tudor Road  
 Anchorage, AK 99507  
 Phone (907) 269-6200 FAX (907) 269-6201

**Laboratory Report**

Quality

Laboratory No.: **2016A-2100**

Name: **AMATS: Abbott Rd. Rehab-phase I** Project No.: **59190 / 0506005**  
 Sample: **HMA Type VH Mix Design** Item/Spec No.: **408(1H)** Field No.: **Q-HMAVH-MD-1**  
 Sampled From: **Manufacturer's Stock**  
 Source: **MP 78 Parks Pt (KASH)/ Calportland** Quantity Represented: **Source**  
 Location: **Anchorage/ Dupont, WA** Submitted By: **QAP**  
 Examined For: **Bituminous Mix Design** Date Reported: **08/06/2016**  
 Date Sampled: **07/21/2016**  
 Date Received: **07/28/2016**  
 Date Completed: **08/03/2016**

**AGGREGATE**

Blend Ratio **25:10:33:32** : :  
 CA:IA:NF:CF:BS:MF:RP

Blend Specific Gravity Bulk **2.670**  
 Effective **2.733**

Sieve	% Pass	Specs
1"		
3/4"	100	100
1/2"	90	84-96
3/8"	80	74-86
#4	55	49-61
#8	40	34-46
#16	29	24-34
#30	21	17-25
#50	13	9-17
#100	8	5-11
#200	5.6	3.6-7.6

FA FM **2.98**  
 FA Angularity **48.9** 45 min  
 CA Absorption **0.7** 2.0 max  
 % Fracture Double Face **100** 98 min  
 % Flat / Elongated @ 1:3 **11**  
 @ 1:5 **1** 8 max  
 Plastic Index **NP** NP

**ATM 417**  
**75 Gyration**

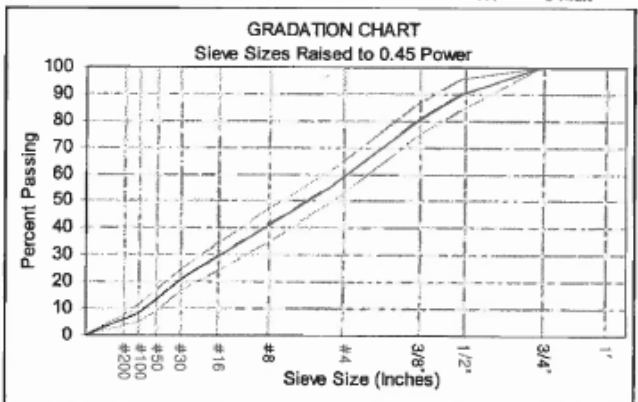
Related Tests  
**2016A-2101**  
**2016A-0366**

**ASPHALT CONTENT, %**

@ 4.0% Voids Total Mix **5.1**  
 Approved Optimum **5.4**  
 Specifications **5.0-5.8**

**PROPERTIES @ OPTIMUM**

Property	Value	Specs
Max. SpG (AASHTO T209)	2.501	
Max. SpG Unit Wt., pcf	155.7	
Voids Filled	78	85-78
Total Mix	3.0	3-5
In Mineral Aggregate	14.1	13.0+
In Coarse Aggregate		
Stability, lbs		
Flow, 0.01 inches		
Unit Weight, pcf	150.8	
Dust:Asphalt Ratio	1.2	0.6-1.2
Rut Index	1.1	3 max



**ASPHALT**

Brand & Typ **EP 58-34**  
 Specific Gravity **1.006**  
 Mixing Temp. Range **325-335°F**  
 Comp. Temp. Range **305-315°F**

**ANTI-STRIP ADDITIVE**

Brand & Type **Morelife 5000**  
 Minimum Required **0.30%**

Remarks:  
 Blend Ratio: Hard CA **9/16CA** **7/16FA** **CF**  
                   **25%**       **10%**       **33%**       **32%**

D1 The Material as Submitted Conforms to Specifications  
 Yes  No  NA   
 THE TEST RESULTS ARE ONLY REPRESENTATIVE OF THE MATERIAL AS SUBMITTED

Signature: *Newton Bingham*  
 Newton J. Bingham, PE  
 Regional Materials Engineer

Table A.3 JMF for Mix #3



State of Alaska  
 Department of Transportation & Public Facilities  
 Central Materials Lab  
 5750 East Tudor Road  
 Anchorage, AK 99507  
 Phone (907) 269-6200 FAX (907) 269-6201

**Laboratory Report**

Quality

Laboratory No.: 2016A-2427

Name: **Glenn Hwy: Hiland to Eldubna Pavement**  
 Sample: **HMAVH Mix design**  
 Sampled From: **Manufacturer's Stock**  
 Source: **MP 216.5 Parks Hwy/ Birchwood Pit**  
 Location: **Birchwood**  
 Examined For: **Bituminous Mix Design**

Project No.: 00057 / 0A16049

Item/Spec No.: 408(1H)

Field No.: Q-HMAVH-MD-1

Date Sampled: 08/15/2016

Date Received: 08/16/2016

Date Completed: 08/29/2016

Date Reported: 09/01/2016

Quantity Represented: **Source**

Submitted By: **Granite Const.**

AGGREGATE			
Blend Ratio	24:31: :45: : :		
	CA:IA:NF:CF:BS:MF:RP		
Blend Specific Gravity	Bulk	2.784	
	Effective	2.835	
Sieve	% Pass		Specs
1"			
3/4"	100		100
1/2"	88		82-94
3/8"	73		67-79
#4	48		42-54
#8	32		26-38
#16	21		16-26
#30	15		11-19
#50	10		6-14
#100	7		4-10
#200	5.2		3.2-7.2
FA FM		3.23	
FA Angularity		49.9	45 min
CA Absorption		0.5	2.0 max
% Fracture			
Double Face		98	98 min
% Flat / Elongated			
⊙ 1:3		9	
⊙ 1:5		2	8 max
Plastic Index		NP	NP

ASPHALT	
Brand & Typ	Denali PG 64-40
Specific Gravity	0.992
Mixing Temp. Range	325-335°F
Comp. Temp. Range	305-315°F

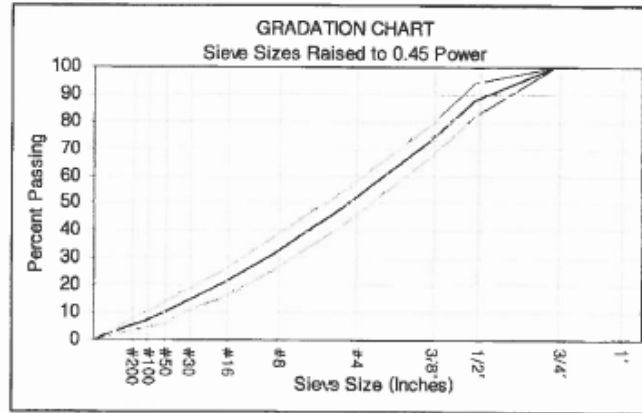
ANTI-STRIP ADDITIVE	
Brand & Type	Evotherm P-15
Minimum Required	0.30%

AASHTO R35  
75 Gyration

Related Tests  
2016A-2428  
2016A-2653

ASPHALT CONTENT, %	
@ 4.0% Voids Total Mix	5.6
Approved Optimum	5.6
Specifications	5.2-6.0

PROPERTIES @ OPTIMUM		
		Specs
Max. SpG (AASHTO T209)	2.568	
Max. SpG Unit Wt., pcf	159.8	
Voids		
Filled	76	65-78
Total Mix	4.0	4.0
In Mineral Aggregate	16.6	13.0+
In Coarse Aggregate		
Stability, lbs		
Flow, 0.01 inches		
Unit Weight, pcf	153.1	
Dust/Asphalt Ratio	1	0.6-1.2
Rut Index	1.2	3 max



Remarks:

Gyrations	%Gmm	Specs.
Nini 7	86.5	<98.5
Ndes 75	96.8	96.8
Nmax 115	97.2	<98.8

D1 The Material as Submitted Conforms to Specifications  
 Yes [X] No [ ] NA [ ]  
 THE TEST RESULTS ARE ONLY REPRESENTATIVE OF THE MATERIAL AS SUBMITTED

Signature: *Newton Bingham*  
 Newton J. Bingham, PE  
 Regional Materials Engineer

Table A.4 JMF for Mix #4



State of Alaska  
 Department of Transportation & Public Facilities  
 Central Materials Lab  
 5750 East Tudor Road  
 Anchorage, AK 99507  
 Phone (907) 269-6200 FAX (907) 269-6201

**Laboratory Report**

Quality

Laboratory No.: 2018A-0702

Name: **Aleyska Hwy Resurfacing: Sew Hwy to Arlberg Ave** Project No.: **58528 / 0501007**  
 Sample: **HMA Type IIA mix design w/15%RAP** Item/Spec No.: **401(1A)** Field No.: **Q-HMAHA-MD-1**  
 Sampled From: **Manufacturer's Stock** Date Sampled: **05/03/2016**  
 Source: **MP 39 Glenn Highway / AS&G / Granite** Quantity Represented: **Source** Date Received: **05/21/2016**  
 Location: **11195 Lang St / Anchorage** Submitted By: **Granite Const.** Date Completed: **06/08/2016**  
 Examined For: **Bituminous Mix Design** Date Reported: **06/08/2016**

**AGGREGATE**

Blend Ratio 17:20 : 48: : :15  
 CA:IA:NF:CF:BS:NF:RP

Bulk 2.718  
 Effective 2.774

Sieve	% Pass	Specs
1"		
3/4"	100	100
1/2"	89	83-95
3/8"	78	72-84
#4	58	52-64
#8	39	33-45
#16	27	22-32
#30	18	14-22
#50	13	9-17
#100	9	6-12
#200	6.0	4.0-8.0

FA FM 3.17  
 FA Angularity  
 CA Absorption 0.7 2.0 max  
 % Fracture  
 Double Face 93 90 min  
 % Flat / Elongated  
 @ 1:3 15  
 @ 1:5 4 8 max  
 Plastic Index NP 4 max

ATM 417  
 75 Blow

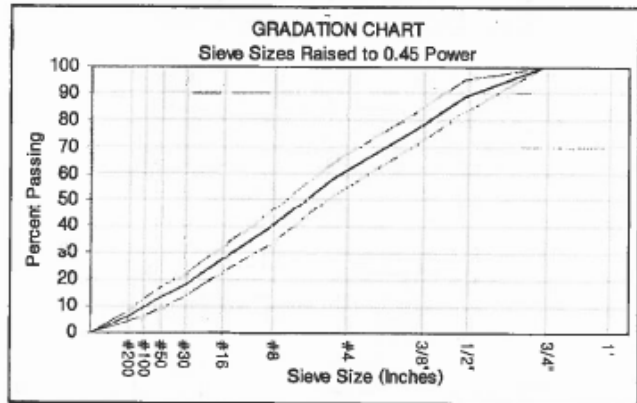
Related Tests  
 2016A-0001  
 2018A-0115

**ASPHALT CONTENT, %**

4.0% Voids Total Mix 5.2  
 Approved Optimum 5.4  
 Specifications 5.0-5.8

**PROPERTIES @ OPTIMUM**

Property	Value	Specs
Max. SpG (AASHTO T209)	2.531	
Max. SpG Unit Wt., pcf	157.5	
Voids		
Filled	75	65-75
Total Mix	3.4	3-5
In Mineral Aggregate	15.0	13.0+
In Coarse Aggregate		
Stability, lbs	2800	1800+
Flow, 0.01 inches	12	8-14
Unit Weight, pcf	152.2	
Dust/Asphalt Ratio	1.3	0.8-1.4
Rut Index		



Remarks:

D1 The Material as Submitted Conforms to Specifications  
 Yes  No  NA   
 THE TEST RESULTS ARE ONLY REPRESENTATIVE OF THE MATERIAL AS SUBMITTED

Signature: *Newton J. Bingham*  
 Newton J. Bingham, PE  
 Regional Materials Engineer

Table A.5 JMF for Mix #5



State of Alaska  
 Department of Transportation & Public Facilities  
 Central Materials Lab  
 5750 East Tudor Road  
 Anchorage, AK 99507  
 Phone (907) 269-6200 FAX (907) 269-6201

**Laboratory Report**

Quality

Name: **ANC Taxiway R Improvements** Project No.: **57590 / AIP 3-02-0016-17-2016** Laboratory No.: **2016A-1258**  
 Sample: **HMA Type VS** Item/Spec No.: **P-401a(1)** Field No.: **Q-HMAVS-MD-2**  
 Sampled From: **Manufacturer's Stock** Date Sampled: **08/22/2015**  
 Source: **MP 39 Glenn Highway / AS&G** Quantity Represented: **Source** Date Received: **07/17/2015**  
 Location: **11195 Lang St / Anchorage** Submitted By: **Granite Const.** Date Completed: **08/23/2016**  
 Examined For: **Bituminous Mix Design** Date Reported: **08/23/2016**

**AGGREGATE**  
 Blend Ratio 24:29: :47: : :  
 CA: IA:NF:CF:BS:MF:RP

Blend Specific Gravity Bulk 2.711  
 Effective 2.772

Sieve	% Pass	Specs
1"		
3/4"	100	100
1/2"	86	80-92
3/8"	71	65-77
#4	47	41-53
#8	32	26-38
#16	20	15-25
#30	14	10-18
#50	10	6-14
#100	7	4-10
#200	5.0	3.0-7.0

FA FM 3.23  
 FA Angularity 49.0 45 min  
 CA Absorption 0.8 2.0 max  
 % Fracture  
 Double Face 100 98 min  
 % Flat / Elongated  
 @ 1:3 15  
 @ 1:5 1 8 max  
 Plastic Index NP NP

**ASPHALT**

Brand & Type **Denali PG 58-34**  
 Specific Gravity 1.007  
 Mixing Temp. Range 325-335°F  
 Comp. Temp. Range 305-315°F

**ANTI-STRIP ADDITIVE**

Brand & Type **Morelife 6900**  
 Minimum Required 0.25%

**AASHTO R35**  
**75 Gyration**

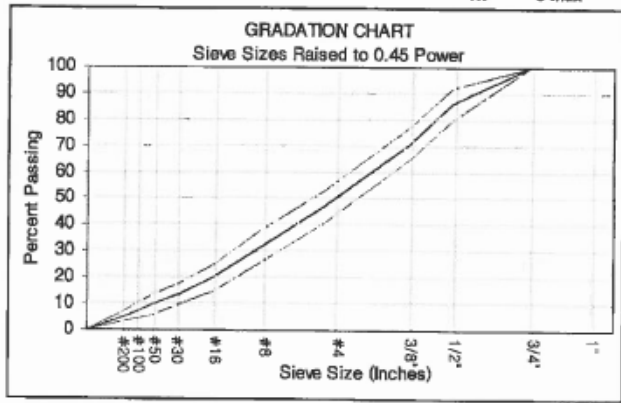
Related Tests  
 2015A-2342  
 2015A1195

**ASPHALT CONTENT, %**

@ 4.0% Voids Total Mix 5.2  
 Approved Optimum 5.3  
 Specifications 4.9-5.7

**PROPERTIES @ OPTIMUM**

Max SpG (AASHTO T209) 2.536  
 Max. SpG Unit Wt., pcf 157.9  
 Voids  
 Filled 74 65-78  
 Total Mix 3.8 4.0  
 In Mineral Aggregate 14.9 13.0+  
 In Coarse Aggregate  
 Stability, lbs  
 Flow, 0.01 inches  
 Unit Weight, pcf 151.7  
 Dust/Asphalt Ratio 1.1 0.6-1.2  
 Rut Index 1.7 3 max



Remarks:

Transferred from lab No. 2015A-2341 on 06/23/2016.  
 Sample originally completed on 08/12/2015.

Gyrations	%Gm	Specs.
Nini 7	86.4	<98.5
Ndes 75	95.5	96.0
Nmax 115	96.9	<98.0

D9 The Material as Submitted Conforms to Specifications  
 Yes  No  NA

THE TEST RESULTS ARE ONLY REPRESENTATIVE OF THE MATERIAL AS SUBMITTED

Signature: *Newton Bingham*  
 Newton J. Bingham, PE  
 Regional Materials Engineer

Table A.6 JMF for Mix #6



State of Alaska  
 Department of Transportation & Public Facilities  
 Central Materials Lab  
 5750 East Tudor Road  
 Anchorage, AK 99507  
 Phone (907) 269-6200 FAX (907) 269-6201

**REVISED**  
 04/15/2015

**Laboratory Report**

Quality  
 Laboratory No.: 2014A-1975

Name: **5th. and 6th. Ave Paving, Lst to Ingra Ph I** Project No.: **57835 / 0001508**  
 Sample: **HMA type VH** Item/Spec No.: **408(1H)/408(11)** Field No.: **Q-HMAVH-MD-1**  
 Sourced From: **Manufacturer's Stock** Date Sampled: **08/11/2014**  
 Source: **MP 39 Glenn Highway / AS&G / 4301 Pioneer** Quantity Represented: **Source** Date Received: **08/13/2014**  
 Location: **Anchorage/ Dupont, WA** Submitted By: **Granite Const.** Date Completed: **09/09/2014**  
 Examined For: **Bituminous Mix Design (Hard Aggregate)** Date Reported: **09/11/2014**

**AGGREGATE**

Blend Ratio 7:25: :45:23: :  
 CA:IA:Nf:CF:BS:MF:RP  
 Bulk 2.703  
 Blend Specific Gravity Effective 2.751

Sieve	% Pass	Specs
1"		
3/4"	100	100
1/2"	85	79-91
3/8"	70	64-76
#4	45	39-51
#8	31	25-37
#16	20	15-25
#30	14	10-18
#50	9	5-13
#100	7	4-10
#200	5.0	3.0-7.0

FA FM 3.20  
 FA Angularity 49.0 45 min  
 CA Absorption 0.8 2.0 max  
 % Fracture  
 Double Face 100 98 min  
 % Flat / Elongated  
 @ 1:3 11  
 @ 1:5 0 8 max  
 Plastic Index NP 4 max

**AASHTO R35**  
**75 Gyration**

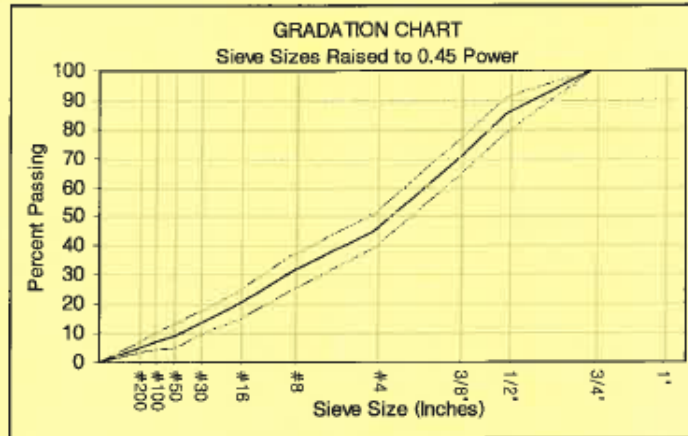
Related Tests  
 2014A-1976  
 2014A-2109

**ASPHALT CONTENT, %**

@ 4.0% Voids Total Mix	5.2
Approved Optimum	5.5
Specifications	5.1-5.9

**PROPERTIES @ OPTIMUM**

Property	Value	Specs
Max. SpG (AASHTO T209)	2.509	
Max. SpG Unit Wt., pcf	156.2	
Voids		
Filled	78	65-78
Total Mix	3.7	4
In Mineral Aggregate	15.1	13.0+
In Coarse Aggregate		
Stability, lbs		
Flow, 0.01 inches		
Unit Weight, pcf	150.3	
Dust/Asphalt Ratio	1	0.6-1.2
Rut Index	1.4	3 max



**ASPHALT**

Brand & Typ Denali PG 64-40  
 Specific Gravity 0.999  
 Mixing Temp. Range 290-300°F  
 Comp. Temp. Range 280-290°F

**ANTI-STRIP ADDITIVE**

Brand & Type Arr-Maz LOF 6500  
 Minimum Required 0.25%

Remarks:

Gyrations	%Gmm	Specs.
Nini 7	87.1	<90.5
Ndes 75	96.3	96.0
Nmax 115	97.6	<98.0


Blend ratio BS = Hard Aggregate  
 Fiber reinforcement (Forta-Fi) per manufacturers instruct.

D1 The Material as Submitted Conforms to Specifications  
 Yes  No [ ] NA [ ]

THE TEST RESULTS ARE ONLY REPRESENTATIVE OF THE MATERIAL AS SUBMITTED

Signature: *Newton J. Bingham*  
 Newton J. Bingham, PE  
 Regional Materials Engineer

Table A.7 JMF for Mix #7



**State of Alaska**  
**Department of Transportation & Public Facilities**  
**Central Materials Lab**  
 5750 East Tudor Road  
 Anchorage, AK 99507  
 Phone (907) 269-6200 FAX (907) 269-6201

Quality  
 Laboratory No.: 2014A-0620

**Laboratory Report**

Name: **W. Dowling Phase II**  
 Sample: **HMAV Mix design**  
 Sampled From: **Manufacturer's Stock**  
 Source: **MP 39 Glenn Highway / AS&G**  
 Location: **11195 Lang St. / Anchorage**  
 Examined For: **Bituminous Mix Design**

Project No.: **51030 / 0532(008)**  
 Item/Spec No.: **408(1)**  
 Field No.: **Q-HMAV-MD-1**  
 Date Sampled: **04/29/2014**  
 Date Received: **05/01/2014**  
 Date Completed: **05/09/2014**  
 Date Reported: **05/09/2014**

<b>AGGREGATE</b>			
Blend Ratio	24:29: :47: : :		
	CA:IA:NF:CF:BS:MF:RP		
Blend Specific Gravity	Bulk	2.720	
	Effective	2.753	

Sieve	% Pass	Specs
1"		
3/4"	100	100
1/2"	86	80-92
3/8"	71	65-77
#4	47	41-53
#8	32	26-38
#16	20	15-25
#30	14	10-18
#50	10	6-14
#100	7	4-10
#200	5.0	3.0-7.0

FA FM	3.23	
FA Angularity	47.4	45 min
CA Absorption	0.7	2.0 max
% Fracture		
Double Face	98	98 min
% Flat / Elongated		
@ 1:3	20	
@ 1:5	2	8 max
Plastic Index	NP	NP

<b>ASPHALT</b>	
Brand & Typ	Denali PG 58-34
Specific Gravity	1.007
Mixing Temp. Range	325-335°F

<b>ANTI-STRIP ADDITIVE</b>	
Brand & Type	Morlife 5000
Minimum Required	0.25%

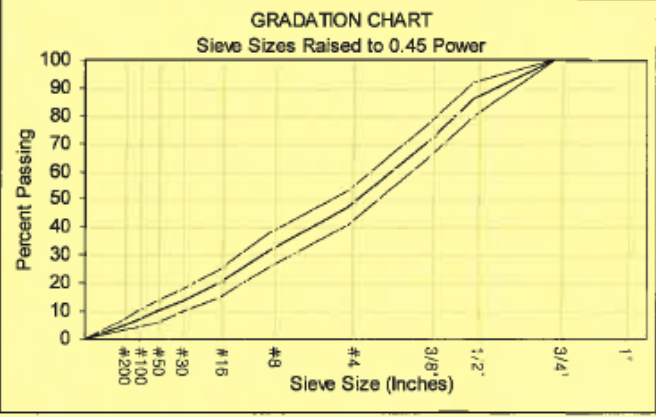
**AASHTO R35**  
75 Gyration

Related Tests  
2014A-0621  
2014A-0622

<b>ASPHALT CONTENT, %</b>	
@ 4.0% Voids Total Mix	5.3
Approved Optimum	5.3
Specifications	4.9-5.7

<b>PROPERTIES @ OPTIMUM</b>		Specs
Max. SpG (AASHTO T209)	2.521	
Max. SpG Unit Wt., pcf	156.9	
Voids		
Filled	74.5	65-78
Total Mix	4.0	4
In Mineral Aggregate	15.7	13.0+
In Coarse Aggregate		
Stability, lbs		
Flow, 0.01 inches		
Unit Weight, pcf	150.7	
Dust/Asphalt Ratio	1	0.6-1.2
Rut Index	1.4	3 max

**GRADATION CHART**  
Sieve Sizes Raised to 0.45 Power



Remarks:

D1 The Material as Submitted Conforms to Specifications  
 Yes  No  NA

THE TEST RESULTS ARE ONLY REPRESENTATIVE OF THE MATERIAL AS SUBMITTED

Signature: *Newton J. Singham*  
 Newton J. Singham, PE  
 Regional Materials Engineer

Table A.8 JMF for Mix #8

STATE OF ALASKA - NORTHERN REGION  
 DEPARTMENT OF TRANSPORTATION AND PUBLIC FACILITIES  
 BITUMINOUS MIX DESIGN MARSHALL METHOD RECEIVED: 9/10/2018  
 2301 PEGER ROAD  
 FAIRBANKS, AK 99709

PROJECT NAME: NR River Encroachment Repairs REGIONAL LAB #: 18-247  
 PROJECT NUMBER: 0002314/Z640640000 FIELD #: NRER-MD-1  
 GENERAL CONTRACTOR: Harris Sand & Gravel TYPE/CLASS: II/B

AGGREGATE SOURCE: Airport Rd Pit, Valdez  
 AGGREGATE QUALITY#: 16-008  
 BLEND RATIO: 35:55:10 CA:FA:Washed FA  
 BLENDED BULK SPG: 2.648  
 EFFECTIVE SPG: 2.747

BINDER SOURCE: Emulsion Products  
 BINDER GRADE: PG 52-28  
 BINDER SPG: 1.014  
 ANTISTRIP: 0.3% Morlife

MIX DESIGN PARAMETERS	
STABILITY	1200
FLOW	8-16
VOIDS TOTAL MIX	3-5
COMPACTION, BLOWS	50
VOIDS FILLED	65-78
VMA	12
DUST ASPHALT RATIO	0.6-1.4
ASPHALT CONTENT MIN%	5.0

MIXING TEMP (DEG F) 277-286  
 COMPACTING TEMP (DEG F) 257-266

MARSHALL RESULTS	
% ASPHALT @ MAX UNIT WT	6.5
% ASPHALT @ MAX STABILITY	5
% ASPHALT @ 4% VOIDS	5.3
OPTIMUM OIL CONTENT = 5.4 %	
STABILITY	2000
FLOW	14
VOIDS TOTAL MIX	3.9
VOIDS FILLED	71
VMA	13.5
MTD/RICE	2.515
UNIT WEIGHT	150.5
DUST ASPHALT RATIO	1.3

APPROVED:

AGGREGATE DESIGN PARAMETERS			
		Reg Lab	Spec
FLAT & ELONGATED		3.80%	8% max
LIQUID LIMIT		NV	
PLASTIC INDEX		NP	
FINENESS MODULUS			
UNCOMP. VOID -T304			
SAND EQUIVALENT			
FRACTURE:	Single Face	98%	80% min
	Double Face	97%	
SIFVF SIZE	PROPOSED GRADATION	MIX DESIGN SPEC BAND	
		LSL	HSL
1"		----	----
3/4"		100	----
1/2"	88	82	94
3/8"	75	69	81
#4	50	44	56
#8	34	28	40
#10		----	----
#16	23	18	28
#20		----	----
#30	16	12	20
#40		----	----
#50	11	7	15
#60		----	----
#80		----	----
#100	8	5	11
#200	5.3	3.3	7.3

REMARKS:



Table A.9 JMF for Mix #9

# MAPPA TESTLAB

1956 Richardson Hwy North Pole, Ak 99705

Project Name: ADOT Type II, Class B Hot Mix Asphalt  
ADOT Projects Fairbanks, Alaska 2016

Date: August 17, 2016 Job#: GNI-T2B(#2)

Aggregate Source: Metro Pit Fairbanks, Alaska

Aggregate Blend: 35:65 (CA: FA)

AC Source & Grade: Tesoro Refinery/Emulsion Products PG52-40 with 0.30 % Anti-Strip Agent

Type of Mix: ADOT Type II Class B Asphalt Pavement



Marshall Criteria Alaska Test Method T-417	50 Blow Compaction Effort	Sieve Size	Proposed JMF TV's	JMF TV Range	Broad Band Range
	NAS	19 mm - ¾"	100	100	100
Stability	1200 lbs	12.5 mm - ½"	88	82-94	75-90
Flow	8 - 16	9.5 mm - 3/8"	74	68-80	60-84
Voids Total Mix	3 - 5	4.75 mm - # 4	47	41-53	33-70
Voids Filled	65 - 78	2.36 mm - # 8	32	26-38	19-56
VMA	12 Min	1.18 mm - # 16	21	16-26	10-44
Compacting Temp	266-270 F	0.6 mm - # 30	15	11-19	7-34
Mixing Temp	282-288 F	0.3 mm - # 50	11	7-15	5-24
% Anti-Strip Agent	0.30 %	0.15 mm - # 100	7	4-10	4-16
Dust/AC Ratio	0.6 - 1.4	0.075 mm - # 200	5.0	3.0-7.0	4-7

			Bulk Specific Gravity Properties (2016)	
% Ac @ Max Unit Wt.	6.0			
% AC @ Max Stability	5.5			
% AC @ 4.0 % Voids	5.4		Coarse Agg:	2.711
Average % Asphalt	5.6		Plant Mix Fines	2.673
<b>Design Asphalt Content</b>	<b>5.4 %</b>			
Effective Asphalt % JMF	5.1		M.T.D. @ 5.4	2.462
Stability @ Design AC	2288	1200 Min	New Binder Sp. Gravity	1.017
Unit Wt @ Design AC	147.3		Effective SG Agg	2.680
% Voids @ Design AC	4.0	3 - 5	Combined Bulk SG Aggregate	2.677
% VFA @ Design AC	75.6	65-78		
VMA @ Design AC	16.6	12 Min		
Flow @ Design AC	12	8-14		
Dust/Asphalt Ratio	0.9	0.6-1.4		

Approved for use on the Pager Road  
Resurfacing project as Type II Class B HMA.

*[Handwritten Signature]*  
8/19/16

Table A.10 ADOT&PF asphalt binder specifications

PERFORMANCE-GRADED ASPHALT BINDER - EXCEPTIONS							
Performance Grade	Viscosity AASHTO T 316	Multiple Stress Creep Recovery MSCR, AASHTO T 350			Dynamic Shear PAV, AASHTO T 315	Direct Tension AASHTO T 314	Elastic Recovery AASHTO T 301
		$J_{NR3.2}$ kPa <sup>-1</sup>	$J_{NR}$ Diff	% Recovery <sub>3.2</sub>	$G^* \sin \delta$ , kPa		
AASHTO M320 Performance-Graded Asphalt Binder							
PG 52-28	None	—	—	—	None	Delete	None
PG 52-40	None	—	—	—	None	Delete	None
PG 52-40 ER	None	—	—	—	None	Delete	50% min.
PG 58-34 ER	None	—	—	—	None	Delete	60% min.
PG 64-40 ER	None	—	—	—	None	Delete	60% min.
AASHTO M332 Performance-Graded Asphalt Binder Using MSCR Test Specification							
PG52-40 V	None	0.50 max.	Delete	75 min.	None	Delete	None
PG58-34 E	None	0.25 max.	Delete	85 min.	None	Delete	None
PG 64-40 E	1 Pa•s max.	0.10 max.	Delete	95 min.	5000 max. @ 4°C	Delete	None

## APPENDIX B AIR VOIDS OF SPECIMENS

**Table B.1 Air voids of the HWT samples**

Mix #	Sample #	Gmb	Gmm	Air Voids	Testing Temp. (°C)
1	A1	2.410	2.60	7.21	50
1	A2	2.406	2.597	7.36	50
1	B1	2.418	2.597	6.88	50
1	B2	2.407	2.597	7.32	50
1	C1	2.413	2.597	7.09	50
1	C2	2.413	2.597	7.08	50
2	A1	2.332	2.501	6.74	40
2	A2	2.332	2.501	6.77	40
2	B1	2.338	2.501	6.51	40
2	B2	2.336	2.501	6.6	40
2	C1	2.338	2.501	6.53	40
2	C2	2.338	2.501	6.53	40
3	A1	2.400	2.568	6.56	50
3	A2	2.395	2.568	6.72	50
3	B1	2.392	2.568	6.86	50
3	B2	2.385	2.568	7.13	50
3	C1	2.382	2.568	7.26	50
3	C2	2.378	2.568	7.39	50
4	A1	2.346	2.531	7.31	40
4	A2	2.348	2.531	7.23	40
4	B1	2.349	2.531	7.18	40
4	B2	2.351	2.531	7.1	40
4	C1	2.354	2.531	6.98	40
4	C2	2.358	2.531	6.83	40
5	A1	2.358	2.536	7.02	40
5	A2	2.357	2.536	7.05	40
5	B1	2.355	2.536	7.13	40
5	B2	2.358	2.536	7.01	40
5	C1	2.362	2.536	6.87	40
5	C2	2.357	2.536	7.05	40
6	A1	2.325	2.509	7.35	50
6	A2	2.336	2.509	6.9	50
6	B1	2.333	2.509	7.02	50
6	B2	2.327	2.509	7.26	50
6	C1	2.342	2.509	6.67	50
6	C2	2.345	2.509	6.53	50

Mix #	Sample #	Gmb	Gmm	Air Voids	Testing Temp. (°C)
7	A1	2.332	2.521	7.49	40
7	A2	2.355	2.521	6.59	40
7	B1	2.343	2.521	7.05	40
7	B2	2.345	2.521	6.98	40
7	C1	2.355	2.521	6.58	40
7	C2	2.357	2.521	6.52	40
8	A1	2.333	2.515	7.25	40
8	A2	2.327	2.515	7.49	40
8	B1	2.340	2.515	6.96	40
8	B2	2.333	2.515	7.25	40
8	C1	2.345	2.515	6.75	40
8	C2	2.351	2.515	6.54	40
9	A1	2.279	2.462	7.45	40
9	A2	2.279	2.462	7.45	40
9	B1	2.278	2.462	7.47	40
9	B2	2.280	2.462	7.41	40
9	C1	2.293	2.462	6.87	40
9	C2	2.278	2.462	7.48	40
10	A1	2.292	2.462	6.89	25
10	A2	2.297	2.462	6.69	25
10	B1	2.279	2.462	7.42	25
10	B2	2.292	2.462	6.92	25

**Table B.2. Air voids of the SCB samples**

Mix #	Sample #	Notch Depth (mm)	Gmb	Gmm	Air Voids
1	A	25	2.422	2.597	6.73
1	B	25	2.408	2.597	7.27
1	C	25	2.408	2.597	7.27
1	A	32	2.425	2.597	6.63
1	B	32	2.425	2.597	6.63
1	C	32	2.408	2.597	7.27
1	A	38	2.405	2.597	7.41
1	B	38	2.405	2.597	7.41
1	C	38	2.426	2.597	6.59
2	A	25	2.329	2.501	6.88
2	B	25	2.338	2.501	6.52

Mix #	Sample #	Notch Depth (mm)	Gmb	Gmm	Air Voids
2	C	25	2.338	2.501	6.52
2	A	32	2.334	2.501	6.67
2	B	32	2.334	2.501	6.67
2	C	32	2.323	2.501	7.11
2	A	38	2.332	2.501	6.75
2	B	38	2.333	2.501	6.7
2	C	38	2.333	2.501	6.7
3	A	25	2.381	2.568	7.27
3	B	25	2.391	2.568	6.9
3	C	25	2.391	2.568	6.9
3	A	32	2.380	2.568	7.32
3	B	32	2.382	2.568	7.24
3	C	32	2.382	2.568	7.24
3	A	38	2.384	2.568	7.17
3	B	38	2.384	2.568	7.17
3	C	38	2.383	2.568	7.22
4	A	25	2.357	2.531	6.88
4	B	25	2.351	2.531	7.13
4	C	25	2.351	2.531	7.13
4	A	32	2.347	2.531	7.28
4	B	32	2.347	2.531	7.28
4	C	32	2.360	2.531	6.77
4	A	38	2.362	2.531	6.67
4	B	38	2.362	2.531	6.67
4	C	38	2.346	2.531	7.32
5	A	25	2.365	2.536	6.73
5	B	25	2.365	2.536	6.73
5	C	25	2.362	2.536	6.85
5	A	32	2.371	2.536	6.52
5	B	32	2.349	2.536	7.38
5	C	32	2.349	2.536	7.38
5	A	38	2.354	2.536	7.17
5	B	38	2.366	2.536	6.7
5	C	38	2.366	2.536	6.7
6	A	25	2.337	2.509	6.87
6	B	25	2.337	2.509	6.87
6	C	25	2.336	2.509	6.89
6	A	32	2.336	2.509	6.89
6	B	32	2.336	2.509	6.89
6	C	32	2.329	2.509	7.17

Mix #	Sample #	Notch Depth (mm)	Gmb	Gmm	Air Voids
6	A	38	2.329	2.509	7.17
6	B	38	2.329	2.509	7.17
6	C	38	2.339	2.509	6.77
7	A	25	2.344	2.521	7.01
7	B	25	2.344	2.521	7.01
7	C	25	2.348	2.521	6.87
7	A	32	2.345	2.521	6.97
7	B	32	2.345	2.521	6.97
7	C	32	2.348	2.521	6.87
7	A	38	2.338	2.521	7.26
7	B	38	2.352	2.521	6.71
7	C	38	2.352	2.521	6.71
8	A	25	2.329	2.515	7.38
8	B	25	2.329	2.515	7.38
8	C	25	2.331	2.515	7.31
8	A	32	2.331	2.515	7.33
8	B	32	2.331	2.515	7.33
8	C	32	2.343	2.515	6.83
8	A	38	2.332	2.515	7.28
8	B	38	2.346	2.515	6.73
8	C	38	2.346	2.515	6.73
9	A	25	2.286	2.462	7.15
9	B	25	2.290	2.462	7
9	C	25	2.290	2.462	7
9	A	32	2.277	2.462	7.5
9	B	32	2.293	2.462	6.87
9	C	32	2.293	2.462	6.87
9	A	38	2.287	2.462	7.1
9	B	38	2.287	2.462	7.1
9	C	38	2.278	2.462	7.48
10	A	25	2.285	2.462	7.2
10	B	25	2.285	2.462	7.2
10	C	25	2.302	2.462	6.5
10	A	32	2.278	2.462	7.48
10	B	32	2.290	2.462	7
10	C	32	2.290	2.462	7
10	A	38	2.302	2.462	6.5
10	B	38	2.302	2.462	6.5
10	C	38	2.278	2.462	7.48

**Table B.3 Air voids of the IDT**

<b>Mix #</b>	<b>Sample #</b>	<b>Gmb</b>	<b>Gmm</b>	<b>Air Voids</b>	<b>Test Temperature</b>
1	A	2.496	2.597	3.89	-10 °C
1	B	2.494	2.597	3.95	-10 °C
1	C	2.487	2.597	4.25	-10 °C
1	D	2.503	2.597	3.63	-20 °C
1	E	2.488	2.597	4.19	-20 °C
1	F	2.491	2.597	4.08	-20 °C
1	G	2.495	2.597	3.92	-30 °C
1	H	2.489	2.597	4.15	-30 °C
1	I	2.489	2.597	4.15	-30 °C
2	A	2.411	2.501	3.61	-10 °C
2	B	2.405	2.501	3.85	-10 °C
2	C	2.405	2.501	3.85	-10 °C
2	D	2.411	2.501	3.59	-20 °C
2	E	2.399	2.501	4.09	-20 °C
2	F	2.413	2.501	3.51	-20 °C
2	G	2.405	2.501	3.85	-30 °C
2	H	2.406	2.501	3.79	-30 °C
2	I	2.406	2.501	3.79	-30 °C
3	A	2.455	2.568	4.41	-10 °C
3	B	2.468	2.568	3.88	-10 °C
3	C	2.466	2.568	3.98	-10 °C
3	D	2.473	2.568	3.7	-20 °C
3	E	2.458	2.568	4.27	-20 °C
3	F	2.464	2.568	4.05	-20 °C
3	G	2.471	2.568	3.79	-30 °C
3	H	2.469	2.568	3.87	-30 °C
3	I	2.454	2.568	4.45	-30 °C
4	A	2.419	2.531	4.43	-10 °C
4	B	2.425	2.531	4.18	-10 °C
4	C	2.438	2.531	3.66	-10 °C
4	D	2.423	2.531	4.27	-20 °C
4	E	2.433	2.531	3.89	-20 °C
4	F	2.420	2.531	4.39	-20 °C
4	G	2.425	2.531	4.18	-30 °C
4	H	2.439	2.531	3.65	-30 °C
4	I	2.417	2.531	4.49	-30 °C
5	A	2.433	2.536	4.06	-10 °C

Mix #	Sample #	Gmb	Gmm	Air Voids	Test Temperature
5	B	2.432	2.536	4.09	-10 °C
5	C	2.441	2.536	3.73	-10 °C
5	D	2.440	2.536	3.77	-20 °C
5	E	2.425	2.536	4.36	-20 °C
5	F	2.442	2.536	3.69	-20 °C
5	G	2.437	2.536	3.9	-30 °C
5	H	2.425	2.536	4.38	-30 °C
5	I	2.425	2.536	4.38	-30 °C
6	A	2.413	2.509	3.82	-10 °C
6	B	2.401	2.509	4.32	-10 °C
6	C	2.411	2.509	3.92	-10 °C
6	D	2.402	2.509	4.25	-20 °C
6	E	2.411	2.509	3.91	-20 °C
6	F	2.408	2.509	4.03	-20 °C
6	G	2.411	2.509	3.89	-30 °C
6	H	2.404	2.509	4.19	-30 °C
6	I	2.406	2.509	4.12	-30 °C
7	A	2.422	2.521	3.92	-10 °C
7	B	2.409	2.521	4.46	-10 °C
7	C	2.421	2.521	3.98	-10 °C
7	D	2.420	2.521	4.02	-20 °C
7	E	2.410	2.521	4.39	-20 °C
7	F	2.429	2.521	3.64	-20 °C
7	G	2.411	2.521	4.37	-30 °C
7	H	2.419	2.521	4.04	-30 °C
7	I	2.415	2.521	4.22	-30 °C
8	A	2.424	2.515	3.6	0 °C
8	B	2.414	2.515	4.01	0 °C
8	C	2.416	2.515	3.94	0 °C
8	D	2.404	2.515	4.43	-10 °C
8	E	2.419	2.515	3.82	-10 °C
8	F	2.427	2.515	3.5	-10 °C
8	G	2.417	2.515	3.89	-20 °C
8	H	2.412	2.515	4.11	-20 °C
8	I	2.426	2.515	3.54	-20 °C
9	A	2.373	2.462	4.1	-10 °C
9	B	2.363	2.462	4.03	-10 °C
9	C	2.363	2.462	4.08	-10 °C
9	D	2.362	2.462	4.05	-20 °C
9	E	2.355	2.462	4.35	-20 °C



<b>Mix #</b>	<b>Sample #</b>	<b>Gmb</b>	<b>Gmm</b>	<b>Air Voids</b>	<b>Test Temperature</b>
9	F	2.374	2.462	3.58	-20 °C
9	G	2.373	2.462	3.63	-30 °C
9	H	2.363	2.462	4.02	-30 °C
9	I	2.363	2.462	4.02	-30 °C
10	A	2.364	2.462	4	-10 °C
10	B	2.356	2.462	4.3	-10 °C
10	C	2.366	2.462	3.9	-10 °C
10	D	2.368	2.462	3.8	-20 °C
10	E	2.371	2.462	3.7	-20 °C
10	F	2.361	2.462	4.1	-20 °C
10	G	2.368	2.462	3.8	-30 °C
10	H	2.361	2.462	4.1	-30 °C
10	I	2.359	2.462	4.2	-30 °C

## APPENDIX C BINDER TESTING RESULTS

**Table C.1 High continuous grading temperature for binder#1 (PG 52-28/A)**

Condition	Specification	Test Results at T <sub>1</sub>				Test Results at T <sub>2</sub>				T <sub>c</sub> (°C)	Mean (°C)
		T <sub>1</sub> (°C)	G*/sinδ (kPa)	G* (kPa)	δ	T <sub>2</sub> (°C)	G*/sinδ (kPa)	G* (kPa)	δ		
Ori. 1	G*/sinδ ≥ 1.00 kPa	52	2.00			58	0.82			55.4	55.2
Ori. 2			1.91				0.81			55	
RTFO 1	G*/sinδ ≥ 2.20 kPa	52	4.31	3.44	86.05	58	1.85	1.49	87.33	56.7	56.5
RTFO 2			4.37				1.91			56.3	

**Table C.2 High continuous grading temperature for binder#2 (PG 52-40/A)**

Condition	Specification	Test Results at T <sub>1</sub>				Test Results at T <sub>2</sub>				T <sub>c</sub> (°C)	Mean (°C)
		T <sub>1</sub> (°C)	G*/sinδ (kPa)	G* (kPa)	δ	T <sub>2</sub> (°C)	G*/sinδ (kPa)	G* (kPa)	δ		
Ori. 1	G*/sinδ ≥ 1.00 kPa	58	1.1736			64	0.7558			60.2	60.3
Ori. 2			1.2060	1.087	63.42		0.7572	0.673	61.46	60.4	
RTFO 1	G*/sinδ ≥ 2.20 kPa	52	3.4793	3.025	60.4	58	2.0893	1.79	58.89	57.4	57.5
RTFO 2			3.5032				1.9053			57.6	

**Table C.3 High continuous grading temperature for binder#3 (PG 64-40/A)**

Condition	Specification	Test Results at T <sub>1</sub>				Test Results at T <sub>2</sub>				T <sub>c</sub> (°C)	Mean (°C)
		T <sub>1</sub> (°C)	G*/sinδ (kPa)	G* (kPa)	δ	T <sub>2</sub> (°C)	G*/sinδ (kPa)	G* (kPa)	δ		
Ori. 1	G*/sinδ≥1.00 kPa	82	1.2163	0.704	35.61	88	0.7562	0.506	42.31	84.5	84.5
Ori. 2			1.2065	0.698	35.56		0.7539	0.504	42.17	84.5	
RTFO 1	G*/sinδ≥2.20 kPa	76	2.2436	1.433	39.45	82	1.5953	1.038	40.38	76.4	76.9
RTFO 2			2.3714				1.6841			77.3	

**Table C.4 High continuous grading temperature for binder#4 (PG 52-46/A)**

Condition	Specification	Test Results at T <sub>1</sub>				Test Results at T <sub>2</sub>				T <sub>c</sub> (°C)	Mean (°C)
		T <sub>1</sub> (°C)	G*/sinδ (kPa)	G* (kPa)	δ	T <sub>2</sub> (°C)	G*/sinδ (kPa)	G* (kPa)	δ		
Ori. 1	G*/sinδ≥1.00 kPa	52	1.2923	1.138	61.73	58	0.8561	0.73	58.54	55.7	55.8
Ori. 2			1.3195	1.173	62.81		0.8556	0.743	60.34	55.9	
RTFO 1	G*/sinδ≥2.20 kPa	46	3.6114	3.172	61.36	52	2.1429	1.875	61.02	51.7	51.7
RTFO 2			3.5572	3.124	61.36		2.1206	1.854	60.84	51.6	

**Table C.5 High continuous grading temperature for binder#5 (PG 58-34/A)**

Condition	Specification	Test Results at T <sub>1</sub>				Test Results at T <sub>2</sub>				T <sub>c</sub> (°C)	Mean (°C)
		T <sub>1</sub> (°C)	G*/sinδ (kPa)	G* (kPa)	δ	T <sub>2</sub> (°C)	G*/sinδ (kPa)	G* (kPa)	δ		
Ori. 1	G*/sinδ≥1.00 kPa	64	1.0878	0.929	58.55	70	0.7284	0.604	55.81	65.3	63.8
Ori. 2			1.1574	0.979	57.67		0.7846	0.647	55.26	62.3	
RTFO 1	G*/sinδ≥2.20 kPa	58	3.0450	2.676	61.53	64	1.8358	1.601	60.76	61.9	62.1
RTFO 2			3.1404	2.734	60.46		1.9052	1.645	59.6	62.3	

**Table C.6 High continuous grading temperature for binder#6 (PG 52-40/B)**

Condition	Specification	Test Results at T <sub>1</sub>				Test Results at T <sub>2</sub>				T <sub>c</sub> (°C)	Mean (°C)
		T <sub>1</sub> (°C)	G*/sinδ (kPa)	G* (kPa)	δ	T <sub>2</sub> (°C)	G*/sinδ (kPa)	G* (kPa)	δ		
Ori. 1	G*/sinδ≥1.00 kPa	52	1.0699	1.007	69.54	58	0.6536	0.605	66.61	52.8	53
Ori. 2			1.1146	1.067	71.43		0.6436	0.608	68.98	53.2	
RTFO 1	G*/sinδ≥2.20 kPa	64	3.0150	2.541	56.36	70	1.7733	1.528	58.28	67.6	68.6
RTFO 2			3.5682	3.02	56.65		2.1280	1.85	58.85	69.6	

**Table C.7 High continuous grading temperature for binder#7 (PG 64-40/B)**

Condition	Specification	Test Results at T <sub>1</sub>				Test Results at T <sub>2</sub>				T <sub>c</sub> (°C)	Mean (°C)
		T <sub>1</sub> (°C)	G*/sinδ (kPa)	G* (kPa)	δ	T <sub>2</sub> (°C)	G*/sinδ (kPa)	G* (kPa)	δ		
Ori. 1	G*/sinδ≥1.00 kPa	76	1.2683			82	0.9346			80.9	81.9
Ori. 2			1.3517	0.976	45.82		1.0304	0.775	42.66	82.8	
RTFO 1	G*/sinδ≥2.20 kPa	76	2.6986	1.645	37.69	82	2.0735	1.288	38.68	80.8	80.6
RTFO 2			2.7283	1.719	38.14		2.0249	1.312	39.09	80.4	

**Table C.8 High continuous grading temperature for binder#8 (PG 58-34/B)**

Condition	Specification	Test Results at T <sub>1</sub>				Test Results at T <sub>2</sub>				T <sub>c</sub> (°C)	Mean (°C)
		T <sub>1</sub> (°C)	G*/sinδ (kPa)	G* (kPa)	δ	T <sub>2</sub> (°C)	G*/sinδ (kPa)	G* (kPa)	δ		
Ori. 1	G*/sinδ≥1.00 kPa	76	1.5331	0.719	1.05	82	1.2211	0.824	39.59	86.7	81.7
Ori. 2			1.0219	0.866	50.29		0.6806	0.637	48.75	76.6	
RTFO 1	G*/sinδ≥2.20 kPa	64	2.8920	2.546	61.07	70	1.7238	1.508	60.18	67.2	68
RTFO 2			3.4202	3.029	61.58		1.9860	1.765	61.67	68.9	

**Table C.9 High continuous grading temperature for binder#9 (PG 58-34/C)**

Condition	Specification	Test Results at T <sub>1</sub>				Test Results at T <sub>2</sub>				T <sub>c</sub> (°C)	Mean (°C)
		T <sub>1</sub> (°C)	G*/sinδ (kPa)	G* (kPa)	δ	T <sub>2</sub> (°C)	G*/sinδ (kPa)	G* (kPa)	δ		
Ori. 1	G*/sinδ≥1.00 kPa	52	1.3936	1.333	70.75	58	0.8001	0.772	70.01	55.6	58.8
Ori. 2			2.5851	2.401	68.27		1.4358	1.351	67.84	62	
RTFO 1	G*/sinδ≥2.20 kPa	58	3.1105	2.781	63.71	64	1.8720	1.714	61.78	62.1	60.3
RTFO 2			2.2864	2.122	65.15		1.3142	1.221	65.36	58.5	

**Table C.10 High continuous grading temperature for binder#10 (PG 52-34/C)**

Condition	Specification	Test Results at T <sub>1</sub>				Test Results at T <sub>2</sub>				T <sub>c</sub> (°C)	Mean (°C)
		T <sub>1</sub> (°C)	G*/sinδ (kPa)	G* (kPa)	δ	T <sub>2</sub> (°C)	G*/sinδ (kPa)	G* (kPa)	δ		
Ori. 1	G*/sinδ≥1.00 kPa	58	1.5813	1.545	72.1	64	0.8822	0.85	73.47	62.7	62.5
Ori. 2			1.5740	1.527	74.48		0.8352	0.823	75.76	62.3	
RTFO 1	G*/sinδ≥2.20 kPa	58	3.5679	3.298	66.84	64	1.9881	1.886	67.14	63	62
RTFO 2			3.0413	2.896	68.61		1.6134	1.555	70.69	61.1	

**Table C.11 High continuous grading temperature for binder#11 (PG 58-28/C)**

Condition	Specification	Test Results at T <sub>1</sub>				Test Results at T <sub>2</sub>				T <sub>c</sub> (°C)	Mean (°C)
		T <sub>1</sub> (°C)	G*/sinδ (kPa)	G* (kPa)	δ	T <sub>2</sub> (°C)	G*/sinδ (kPa)	G* (kPa)	δ		
Ori. 1	G*/sinδ≥1.00 kPa	64	1.1552	1.102	72.21	70	0.6465	0.621	72.97	65.5	66.6
Ori. 2			1.4380	1.374	72.13		0.7839	0.753	73.21	67.6	
RTFO 1	G*/sinδ≥2.20 kPa	64	2.2007	2.067	69.62	70	1.1784	1.119	71.22	64	64.5
RTFO 2			2.4280	2.277	69.13		1.2801	1.216	71.06	64.9	

**Table C.12 High continuous grading temperature for binder#12 (PG 52-28plus/C)**

Condition	Specification	Test Results at T <sub>1</sub>				Test Results at T <sub>2</sub>				T <sub>c</sub> (°C)	Mean (°C)
		T <sub>1</sub> (°C)	G*/sinδ (kPa)	G* (kPa)	δ	T <sub>2</sub> (°C)	G*/sinδ (kPa)	G* (kPa)	δ		
Ori. 1	G*/sinδ≥1.00 kPa	58	1.6385	1.644	86.21	64	0.7428	0.744	87.6	61.8	62.6
Ori. 2			1.9730	1.979	85.71		0.8875	0.889	87.25	63.1	
RTFO 1	G*/sinδ≥2.20 kPa	58	3.1022	3.088	82.89	64	1.3795	1.379	84.96	60.5	60.7
RTFO 2			3.2219	3.215	82.76		1.4075	1.407	84.9	60.8	

**Table C.13 High continuous grading temperature for binder#13 (PG 64-28/C)**

Condition	Specification	Test Results at T <sub>1</sub>				Test Results at T <sub>2</sub>				T <sub>c</sub> (°C)	Mean (°C)
		T <sub>1</sub> (°C)	G*/sinδ (kPa)	G* (kPa)	δ	T <sub>2</sub> (°C)	G*/sinδ (kPa)	G* (kPa)	δ		
Ori. 1	G*/sinδ≥1.00 kPa	64	1.3674	1.344	77.18	70	0.7189	0.712	78.71	66.9	62.6
Ori. 2			2.2067	1.915	59.01		1.4620	1.208	53.44	-	
RTFO 1	G*/sinδ≥2.20 kPa	64	3.4165	3.278	72.2	70	1.7202	1.683	75.5	67.9	67.7
RTFO 2			3.2975	3.167	72.15		1.6542	1.62	75.37	67.5	



**Table C.14 BBR results for binder#1 (PG 52-28/A) at different aging states**

	Temperature (°C)		-12		-18		-24	
			S (MPa)	m-value	S (MPa)	m-value	S (MPa)	m-value
#1 (PG 52- 28/A )	RTFO	duplicate 1	51.4803	0.485392	149.5561	0.395187	328.2569	0.30402
		duplicate 2	54.5137	0.47408	149.5526	0.381097	331.3424	0.30827
		average	52.997	0.479736	149.55435	0.388142	329.79965	0.306145
	20h PAV	duplicate 1	84.6176	0.390588	200.7112	0.328124	449.6405	0.275147
		duplicate 2	85.2757	0.38579	199.0131	0.324389	417.6182	0.264887
		average	84.94665	0.388189	199.86215	0.326256 5	433.62935	0.270017
	40h PAV	duplicate 1	102.1662	0.352487	212.1791	0.306152	446.8554	0.260557
		duplicate 2	101.2871	0.346276	216.3778	0.306575	458.6406	0.252775
		average	101.72665	0.3493815	214.27845	0.306363 5	452.748	0.256666

**Table C.15 BBR results for binder#2 (PG 52-40/A) at different aging states**

	Temperature (°C)		-24		-30		-36	
			S (MPa)	m-value	S (MPa)	m-value	S (MPa)	m-value
#2 (PG 52- 40/A)	RTFO	duplicate 1	59.576	0.421302	136.2452	0.362087	297.0205	0.304038
		duplicate 2	67.9564	0.413729	142.6359	0.348169	297.8586	0.302383
		average	63.7662	0.4175155	139.44055	0.355128	297.43955	0.3032105
	20h PAV	duplicate 1	70.5152	0.394382	148.8578	0.325131	361.1987	0.286144
		duplicate 2	63.3534	0.371705	148.7977	0.34252	342.9469	0.2821
		average	66.9343	0.3830435	148.82775	0.3338255	352.0728	0.284122
	40h PAV	duplicate 1			166.4799	0.301792	353.127	0.266277
		duplicate 2			170.1729	0.308787	367.2763	0.2677.1
		average			168.3264	0.3052895	360.20165	0.266277

**Table C.16 BBR results for binder#3 (PG 64-40/A) at different aging states**

	Temperature (°C)		-24		-30		-36	
			S (MPa)	m-value	S (MPa)	m-value	S (MPa)	m-value
#3 (PG 64- 40/A)	RTFO	duplicate 1			109.1916	0.400992	288.6241	0.328695
		duplicate 2			107.1433	0.39689	298.8261	0.33656
		average			108.16745	0.398941	293.7251	0.3326275
	20h PAV	duplicate 1	60.2816	0.388421	143.3315	0.338243	327.1784	0.295886
		duplicate 2	59.7261	0.372457	156.884	0.343011	330.7624	0.298126
		average	60.00385	0.380439	150.10775	0.340627	328.9704	0.297006
	40h PAV	duplicate 1			155.138	0.311565	332.2865	0.302629
		duplicate 2			154.5486	0.320056	319.8013	0.278505
		average			154.8433	0.3158105	326.0439	0.290567

**Table C.17 BBR results for binder#4 (PG 52-46/A) at different aging states**

	Temperature (°C)		-30		-36		-42	
			S (MPa)	m-value	S (MPa)	m-value	S (MPa)	m-value
#4 (PG 52- 46/A )	RTF O	duplicate 1			189.3529	0.356624	437.3151	0.293739
		duplicate 2			177.5235	0.357387	428.9958	0.298004
		average			183.4382	0.3570055	433.15545	0.295871 5
	20h PAV	duplicate 1	87.193	0.378374	218.1197	0.328623	470.9196	0.28362
		duplicate 2	87.073	0.374502	199.7496	0.327756	460.769	0.272232
		average	87.133	0.376438	208.93465	0.3281895	465.8443	0.277926
	40h PAV	duplicate 1			230.9085	0.307599	476.7011	0.270097
		duplicate 2			231.436	0.320004	455.4819	0.256517
		average			231.17225	0.3138015	466.0915	0.263307

**Table C.18 BBR results for binder#5 (PG 58-34/A) at different aging states**

	Temperature (°C)		-24		-30		-36	
			<i>S</i> (MPa)	m-value	<i>S</i> (MPa)	m-value	<i>S</i> (MPa)	m-value
#5(PG58-34/A)	RTFO	duplicate 1	150.2186	0.386084	348.4842	0.303152		
		duplicate 2	150.3232	0.381768	349.3262	0.303039		
		average	150.2709	0.383926	348.9052	0.3030955		
20h PAV	duplicate 1	193.5063	0.336934	403.5914	0.28329	752.4305	0.237198	
	duplicate 2	193.9708	0.333408			783.6332	0.244672	
	average	193.73855	0.335171	403.5914	0.28329	768.03185	0.240935	
40h PAV	duplicate 1	215.1384	0.302322	409.2949	0.246071			
	duplicate 2	212.395	0.287609	424.2978	0.24562			
	average	213.7667	0.2949655	416.79635	0.2458455			

**Table C.19 BBR results for binder#6 (PG 52-40/B) at different aging states**

	Temperature (°C)		-24		-30		-36	
			<i>S</i> (MPa)	m-value	<i>S</i> (MPa)	m-value	<i>S</i> (MPa)	m-value
#6 (PG 52-40/B)	RTFO	duplicate 1	37.6545	0.44761	135.6195	0.372601		
		duplicate 2	57.0772	0.426416	131.3447	0.367957		
		average	47.36585	0.437013	133.4821	0.370279		
20h PAV	duplicate 1	70.8344	0.370838	166.1511	0.333552	372.277	0.300269	
	duplicate 2	74.9582	0.364868	164.322	0.323552	368.257	0.290269	
	average	72.8963	0.367853	165.23655	0.328552	370.267	0.295269	
40h PAV	duplicate 1	81.8288	0.343958	177.625	0.314441			
	duplicate 2	84.5178	0.332731	175.8904	0.296683			
	average	83.1733	0.3383445	176.7577	0.305562			

**Table C.20 BBR results for binder#7 (PG 64-40/B) at different aging states**

	Temperature (°C)		-24		-30		-36	
			<i>S</i> (MPa)	m-value	<i>S</i> (MPa)	m-value	<i>S</i> (MPa)	m-value
#7 (PG 64- 40/B)	RTF O	duplicate 1			99.3535	0.420479	253.4092	0.348182
		duplicate 2			92.5992	0.427747	268.2517	0.356344
		average			95.97635	0.424113	260.83045	0.352263
20h PAV	duplicate 1	33.2859	0.432574	81.9453	0.389779	201.4819	0.333361	
	duplicate 2	34.4027	0.421699	82.571	0.398529	202.8367	0.328738	
	average	33.8443	0.427136 5	82.25815	0.394154	202.1593	0.3310495	
40h PAV	duplicate 1			114.6412	0.321623	219.5073	0.29103	
	duplicate 2			115.4032	0.301765	234.5181	0.280779	
	average			115.0222	0.311694	227.0127	0.2859045	

**Table C.21 BBR results for binder#8 (PG 58-34/B) at different aging states**

	Temperature (°C)		-18		-24		-30	
			<i>S</i> (MPa)	m-value	<i>S</i> (MPa)	m-value	<i>S</i> (MPa)	m-value
#8 (PG 58- 34/B)	RTF O	duplicate 1			154.8937	0.353559	326.1133	0.287679
		duplicate 2			149.54	0.349734	362.2522	0.292194
		average			152.21685	0.3516465	344.18275	0.2899365
20h PAV	duplicate 1	88.549	0.358986	189.8605	0.318784	375.185	0.262748	
	duplicate 2	87.3103	0.344689	182.1658	0.302619	372.4878	0.265519	
	average	87.92965	0.351837 5	186.01315	0.3107015	373.8364	0.2641335	
40h PAV	duplicate 1			190.9032	0.28012	380.5632	0.268061	
	duplicate 2			205.2399	0.287285	396.7997	0.25226	
	average			198.07155	0.2837025	388.68145	0.2601605	

**Table C.22 BBR results for binder#9 (PG 58-34/C) at different aging states**

	Temperature (°C)		-24		-30		-36	
			<i>S</i> (MPa)	m-value	<i>S</i> (MPa)	m-value	<i>S</i> (MPa)	m-value
#9 (PG 58-34/C)	RTF O	duplicate 1	64.5953	0.433264	176.5296	0.370896		
		duplicate 2	69.0708	0.42231	188.6238	0.369177		
		average	66.83305	0.427787	182.5767	0.3700365		
20h PAV	duplicate 1	97.6334	0.328855	209.1008	0.306371	450.389	0.263025	
	duplicate 2	98.4395	0.338577	219.1699	0.305217	429.4827	0.25072	
	average	98.03645	0.333716	214.13535	0.305794	439.93585	0.2568725	
40h PAV	duplicate 1	101.2748	0.305764	196.5297	0.28724			
	duplicate 2	104.4685	0.303759	196.1279	0.282403			
	average	102.87165	0.304761 5	196.3288	0.2848215			

**Table C.23 BBR results for binder#10 (PG 52-34/C) at different aging states**

	Temperature (°C)		-24		-30		-36	
			<i>S</i> (MPa)	m-value	<i>S</i> (MPa)	m-value	<i>S</i> (MPa)	m-value
#10 (PG42-34/C)	RTF O	duplicate 1	102.8531	0.397746	257.9493	0.329035		
		duplicate 2	99.2712	0.388563	256.0338	0.32747		
		average	101.06215	0.393154 5	256.99155	0.3282525		
20h PAV	duplicate 1	151.3147	0.304897	300.0293	0.274703	562.3113	0.237237	
	duplicate 2	143.8004	0.297996	297.1822	0.273727	564.9652	0.229369	
	average	147.55755	0.301446 5	298.60575	0.274215	563.63825	0.233303	
40h PAV			-18		-24			
	duplicate 1	85.2763	0.259829	151.4188	0.252265			
	duplicate 2	89.0538	0.254429	126.4456	0.278897			
	average	87.16505	0.257129	138.9322	0.252265			

**Table C.24 BBR results for binder#11 (PG 58-28/C) at different aging states**

	Temperature (°C)		-12		-18		-24	
			<i>S</i> (MPa)	m-value	<i>S</i> (MPa)	m-value	<i>S</i> (MPa)	m-value
#11(P G 58- 28/C)	RTF O	duplicate 1			61.302	0.434253	146.7134	0.362167
		duplicate 2			62.0992	0.433535	160.835	0.368998
		average			61.7006	0.433894	153.7742	0.3655825
	20h PAV	duplicate 1	37.0846	0.395275	86.2771	0.359749	201.2185	0.306534
		duplicate 2	37.8328	0.381855	86.7666	0.344377	195.5336	0.288973
		average	37.4587	0.388565	86.52185	0.352063	198.37605	0.2977535
	40h PAV	duplicate 1			123.9314	0.266713	212.902	0.276044
		duplicate 2			123.2849	0.258743	229.3133	0.246484
		average			123.60815	0.262728	221.10765	0.261264

**Table C.25 BBR results for binder#12 (PG 52-28 plus/C) at different aging states**

	Temperature (°C)		-12		-18		-24	
			<i>S</i> (MPa)	m-value	<i>S</i> (MPa)	m-value	<i>S</i> (MPa)	m-value
#12 (PG 52-28 Plus/C )	RTF O	duplicate 1			106.6774	0.414791	283.8484	0.334967
		duplicate 2			114.4198	0.404702	293.4614	0.320838
		average			110.5486	0.409746 5	288.6549	0.3279025
	20h PAV	duplicate 1	44.9256	0.416421	156.0793	0.327692	325.6938	0.291969
		duplicate 2	45.6866	0.4117	159.9514	0.319846	325.8235	0.288034
		average	45.3061	0.4140605	158.01535	0.323769	325.75865	0.2900015
	40h PAV	duplicate 1			184.9142	0.280566	349.3932	0.24985
		duplicate 2			190.3123	0.266526	345.3157	0.244314
		average			187.61325	0.273546	347.35445	0.247082

**Table C.26 BBR results for binder#13 (PG 64-28 /C) at different aging states**

	Temperature (°C)	-12		-18		-24	
		S (MPa)	m-value	S (MPa)	m-value	S (MPa)	m-value
#13 (PG 64- 28/C)	RTF O	duplicate 1		88.9278	0.39876	216.0336	0.324645
		duplicate 2		91.371	0.384509	215.5138	0.325189
		average		90.1494	0.391634 5	215.7737	0.324917
20h PAV	duplicate 1	50.0112	0.382853	108.4275	0.348286	252.5067	0.30318
	duplicate 2	50.6198	0.375372	114.8452	0.33326	244.9108	0.296139
	average	50.3155	0.3791125	111.63635	0.340773	248.70875	0.2996595
40h PAV	duplicate 1			166.7687	0.256564	301.6109	0.229922
	duplicate 2			173.1913	0.241703	309.9244	0.225455
	average			169.98	0.249133 5	305.76765	0.2276885

**Table C.27 ABCD results for 20h PAV aged binder#1 (PG 52-28/A)**

Duplicates	#1	#2	#3	#4	Average	Std Dev
Crack Temperature (°C)	-36.4	-33.6	-31.7	-35.2	-34.2	2.03
Strain Jump (με)	15.7	16.6	11.8	22.8	16.7	4.53
Cooling Rate (°C/hr)	-28.5	-33.8	-33.4	-32.7	-32.1	2.41
Fracture Stress (MPa)	2.47	2.61	1.86	3.57	2.63	0.71
PG Grade by ABCD (°C)	-29.3	-27.1	-25.6	-28.4	-27.6	1.59

Cooling Rate is the slope of 10 consecutive time-sample temperature data when cracked

Fracture Stress (MPa) = (Strain Jump, με) \* 0.157

PG Grade by ABCD (°C) = 0.78 \* (ABCD Cracking Temp, °C) - 0.9

**Table C.28 ABCD results for 20h PAV aged binder#2 (PG 52-40/A)**

Duplicates	#1	#2	#3	#4	Average	Std Dev
Crack Temperature (°C)	-48.8	-49.3		-52.6	-50.3	2.06
Strain Jump (με)	21.0	29.3		18.7	23.0	5.58
Cooling Rate (°C/hr)	#N/A	#N/A	-33.4	#N/A	#N/A	#N/A
Fracture Stress (MPa)	3.30	4.60		2.93	3.61	0.88
PG Grade by ABCD (°C)	-39.0	-39.4		-41.9	-40.1	1.60

**Table C.29 ABCD results for 20h PAV aged binder#3 (PG 64-40/A)**

Duplicates	#1	#2	#3	#4	Average	Std Dev
Crack Temperature (°C)	-52.7	-49.8	-52.3	-52.8	-51.9	1.39
Strain Jump (με)	19.6	20.3	32.1	16.4	22.1	6.88
Cooling Rate (°C/hr)	#N/A	#N/A	#N/A	#N/A	#N/A	#N/A
Fracture Stress (MPa)	3.08	3.18	5.03	2.57	3.47	1.08
PG Grade by ABCD (°C)	-42.0	-39.8	-41.7	-42.1	-41.4	1.08

**Table C.30 ABCD results for 20h PAV aged binder#5 (PG 58-34/A)**

Duplicates	#1	#2	#3	#4	Average	Std Dev
Crack Temperature (°C)	-45.9	-44.3	-43.5	-43.4	-44.3	1.18
Strain Jump (µε)	36.9	32.4	22.3	33.7	31.3	6.33
Cooling Rate (°C/hr)	#N/A	-15.5	-14.3	-17.1	#N/A	#N/A
Fracture Stress (MPa)	5.79	5.09	3.49	5.29	4.91	0.99
PG Grade by ABCD (°C)	-36.7	-35.5	-34.8	-34.7	-35.4	0.92

**Table C.31 ABCD results for 20h PAV aged binder#6 (PG 52-40/B)**

Duplicates	#1	#2	#3	#4	Average	Std Dev
Crack Temperature (°C)		-53.7	-52.2	-46.4	-50.7	3.83
Strain Jump (µε)		33.2	23.5	5.9	20.9	13.81
Cooling Rate (°C/hr)		#N/A	#N/A	#N/A	#N/A	#N/A
Fracture Stress (MPa)		5.21	3.68	0.93	3.28	2.17
PG Grade by ABCD (°C)		-42.8	-41.6	-37.1	-40.5	2.99

**Table C.32 ABCD results for 20h PAV aged binder#7 (PG 64-40/B)**

Duplicates	#1	#2	#3	#4	Average	Std Dev
Crack Temperature (°C)		-57.1	-56.4		-56.7	0.49
Strain Jump (µε)		26.2	22.9		24.5	2.32
Cooling Rate (°C/hr)		#N/A	-26.0		#N/A	#N/A
Fracture Stress (MPa)		4.11	3.59		3.85	0.36
PG Grade by ABCD (°C)		-45.4	-44.9		-45.1	0.39

**Table C.33 ABCD results for 20h PAV aged binder#8 (PG 58-34/B)**

Duplicates	#1	#2	#3	#4	Average	Std Dev
Crack Temperature (°C)	-49.3	-46.7	-49.1	-44.4	-47.4	2.29
Strain Jump (µε)	32.9	30.1	45.4	13.1	30.4	13.32
Cooling Rate (°C/hr)	#N/A	#N/A	#N/A	#N/A	#N/A	#N/A
Fracture Stress (MPa)	5.17	4.73	7.13	2.05	4.77	2.09
PG Grade by ABCD (°C)	-39.4	-37.3	-39.2	-35.6	-37.9	1.79



**Table C.34 ABCD results for 20h PAV aged binder#9 (PG 58-34/C)**

Duplicates	#1	#2	#3	#4	Average	Std Dev
Crack Temperature (°C)		-50.0	-49.0	-49.7	-49.6	0.50
Strain Jump (µε)		34.5	35.3	29.6	33.1	3.06
Cooling Rate (°C/hr)		#N/A	#N/A	#N/A	#N/A	#N/A
Fracture Stress (MPa)		5.41	5.54	4.65	5.20	0.48
PG Grade by ABCD (°C)		-39.9	-39.1	-39.7	-39.6	0.39

**Table C.35 ABCD results for 20h PAV aged binder#10 (PG 52-34/C)**

Duplicates	#1	#2	#3	#4	Average	Std Dev
Crack Temperature (°C)	-50.6	-45.3	-48.1	-46.8	-47.7	2.25
Strain Jump (µε)	33.6	31.2	38.0	38.4	35.3	3.49
Cooling Rate (°C/hr)	#N/A	#N/A	#N/A	#N/A	#N/A	#N/A
Fracture Stress (MPa)	5.28	4.89	5.96	6.03	5.54	0.55
PG Grade by ABCD (°C)	-40.4	-36.2	-38.4	-37.4	-38.1	1.75

**Table C.36 ABCD results for 20h PAV aged binder#11 (PG 58-28/C)**

Duplicates	#1	#2	#3	#4	Average	Std Dev
Crack Temperature (°C)	-47.1	-43.2	-49.1	-42.3	-45.4	3.23
Strain Jump (µε)	37.1	30.9	41.4	23.6	33.3	7.76
Cooling Rate (°C/hr)	#N/A	#N/A	#N/A	#N/A	#N/A	#N/A
Fracture Stress (MPa)	5.83	4.85	6.50	3.70	5.22	1.22
PG Grade by ABCD (°C)	-37.6	-34.6	-39.2	-33.9	-36.3	2.52

**Table C.37 ABCD results for 20h PAV aged binder#12 (PG 52-28Plus/C)**

Duplicates	#1	#2	#3	#4	Average	Std Dev
Crack Temperature (°C)	-36.0	-32.9	-36.9	-34.9	-35.2	1.74
Strain Jump (µε)	17.4	13.2	18.9	14.8	16.1	2.58
Cooling Rate (°C/hr)	-33.6	-27.8	-31.7	-37.6	-32.7	4.11
Fracture Stress (MPa)	2.74	2.07	2.97	2.33	2.53	0.40
PG Grade by ABCD (°C)	-29.0	-26.5	-29.7	-28.1	-28.3	1.36

**Table C.38 ABCD results for 20h PAV aged binder#13 (PG 64-28/C)**

Duplicates	#1	#2	#3	#4	Average	Std Dev
Crack Temperature (°C)	-42.9	-41.9	-45.0		-43.3	1.57
Strain Jump ( $\mu\epsilon$ )	58.0	21.8	73.4		51.1	26.46
Cooling Rate (°C/hr)	#N/A	#N/A	#N/A		#N/A	#N/A
Fracture Stress (MPa)	9.10	3.43	11.52		8.02	4.15
PG Grade by ABCD (°C)	-34.3	-33.6	-36.0		-34.7	1.23

**Table C.39 Crossover Frequency and Rheological Index (*R*) of the studied asphalt binders**

Binder	Aging State	Crossover Frequency at 15 ° C	G* at Crossover Frequency (Pa)	Rheological Index ( <i>R</i> )
#1/PG 52-28/A	RTFO	76	12065083.14	1.918469681
	20h PAV	3.5	8967610.699	2.047323254
	40h PAV	1.15	4464935.137	2.350184846
#2/PG 52-40/A	RTFO	1100	9257277.637	2.033516711
	20h PAV	23	2218157.881	2.654007546
	40h PAV	4.95	1502956.916	2.823053469
#3/PG 64-40/A	RTFO	2030	11023646.88	1.957674707
	20h PAV	0.45	698440.3054	3.155870706
	40h PAV	0.501	416938.2257	3.379928286
#4/PG 52-46/A	RTFO	1680	4914178.812	2.308549045
	20h PAV	500	3641631.024	2.43870406
	40h PAV	30	1558749.716	2.807223613
#5/PG 58-34/A	RTFO	835	17607725.95	1.75429673
	20h PAV	8.5	3861491.048	2.413244968
	40h PAV	0.5	2264358.244	2.645054862
#6/PG 52-40/B	RTFO	1000	7358591.447	2.133205309
	20h PAV	0.316	349504.9532	3.456546665
	40h PAV	0.08	281442.5757	3.550610203
#7/PG 64-40/B	RTFO	0.006	6291.962674	5.201213862
	20h PAV	0.5	98229.03175	4.007760137
	40h PAV	2100	11864897.13	1.925736023
#8/PG 58-34/B	RTFO	60	5494931.848	2.26003769
	20h PAV	0.8	1781120.542	2.749306687
	40h PAV	0.1	890779.6631	3.050229707
#9/PG 58-34/C	RTFO	2000	14229536.85	1.846809235
	20h PAV	1	748216.3288	3.125972818
	40h PAV	0.001	27971.45577	4.55328493
#10/PG 52-34/C	RTFO	450	10149461.22	1.993557012
	20h PAV	0.1	596408.2299	3.224456372
	40h PAV	0.0005	73176.14739	4.135630459
#11/PG 58-28/C	RTFO	150	8.81E+06	2.05480395
	20h PAV	1	1718396.423	2.76487664
	40h PAV	0.0005	159654.2894	3.796819409
#12/PG 58-28plus/C	RTFO	110	13529376.9	1.868722204
	20h PAV	3	3298481.876	2.481685898
	40h PAV	0.003	598295.4234	3.223084319
#13/PG 64-28/C	RTFO	35	6979097.961	2.156200706
	20h PAV	0.2	1765351.407	2.753168832
	40h PAV	0.0003	183226.475	3.737011774

**Table C.40 Glover-Rowe (G-R) parameter values of the studied asphalt binders**

Binder	Aging State	G* at 15°C and 0.005 rad/s	$\delta$ at 15°C and 0.005 rad/s	G-R parameter
#1/PG 52-28/A	RTFO	12183.52727	80.37451486	345.4944379
	20h PAV	141886.8839	68.98939131	19538.83027
	40h PAV	168067.7696	63.81521945	36468.17708
#2/PG 52-40/A	RTFO	4265.699537	57.31453317	1478.054971
	20h PAV	14713.1847	58.29601868	4776.265646
	40h PAV	27167.83332	57.78868091	9123.568365
#3/PG 64-40/A	RTFO	7034.531099	43.74547313	5309.436725
	20h PAV	74550.43355	41.90161531	61838.14906
	40h PAV	40910.51572	44.08829341	30335.09247
#4/PG 52-46/A	RTFO	1181.04	58.21234749	385.5565077
	20h PAV	3751.383743	62.42587427	906.8218424
	40h PAV	8144.94081	63.09457785	1870.321879
#5/PG 58-34/A	RTFO	8383.505752	58.75508302	2638.208434
	20h PAV	42948.45904	58.66947873	13594.42333
	40h PAV	81357.58111	57.96505739	27002.85791
#6/PG 52-40/B	RTFO	23116.8787	51.26437672	11603.3215
	20h PAV	41656.32552	45.67918215	28422.29534
	40h PAV	70985.76938	44.68503603	51027.6388
#7/PG 64-40/B	RTFO	5724.561462	43.50658033	4374.286281
	20h PAV	13129.54725	33.2381399	16757.20888
	40h PAV	61778.15767	33.081568	79461.02044
#8/PG 58-34/B	RTFO	19251.01359	55.93368465	7291.732993
	20h PAV	102315.3576	56.38057629	37665.42065
	40h PAV	172883.22	52.6619433	79989.40538
#9/PG 58-34/C	RTFO	4075.930899	62.03285386	1014.940992
	20h PAV	45652.57848	47.41209063	28396.4978
	40h PAV	58443.32394	43.31939998	45090.40795
#10/PG 52-34/C	RTFO	8237.50351	64.33618221	1714.186475
	20h PAV	124954.107	47.5411413	77182.64622
	40h PAV	201969.5572	40.20639182	182487.7461
#11/PG 58-28/C	RTFO	2758.666986	13475.60734	64.53753356
	20h PAV	40963.49913	93294.92173	53.54050363
	40h PAV	420288.4113	473843.1232	40.57484819
#12/PG 58-28plus/C	RTFO	1043.033843	15481.49566	75.21287357
	20h PAV	25023.30221	78236.07281	58.51588444
	40h PAV	571253.0992	773765.2334	44.17226408
#13/PG 64-28/C	RTFO	5690.88449	26116.84644	63.76223124
	20h PAV	104885.2753	232828.0433	53.11207749
	40h PAV	623630.152	659487.7064	39.29618068

## APPENDIX D MIXTURE TESTING RESULTS

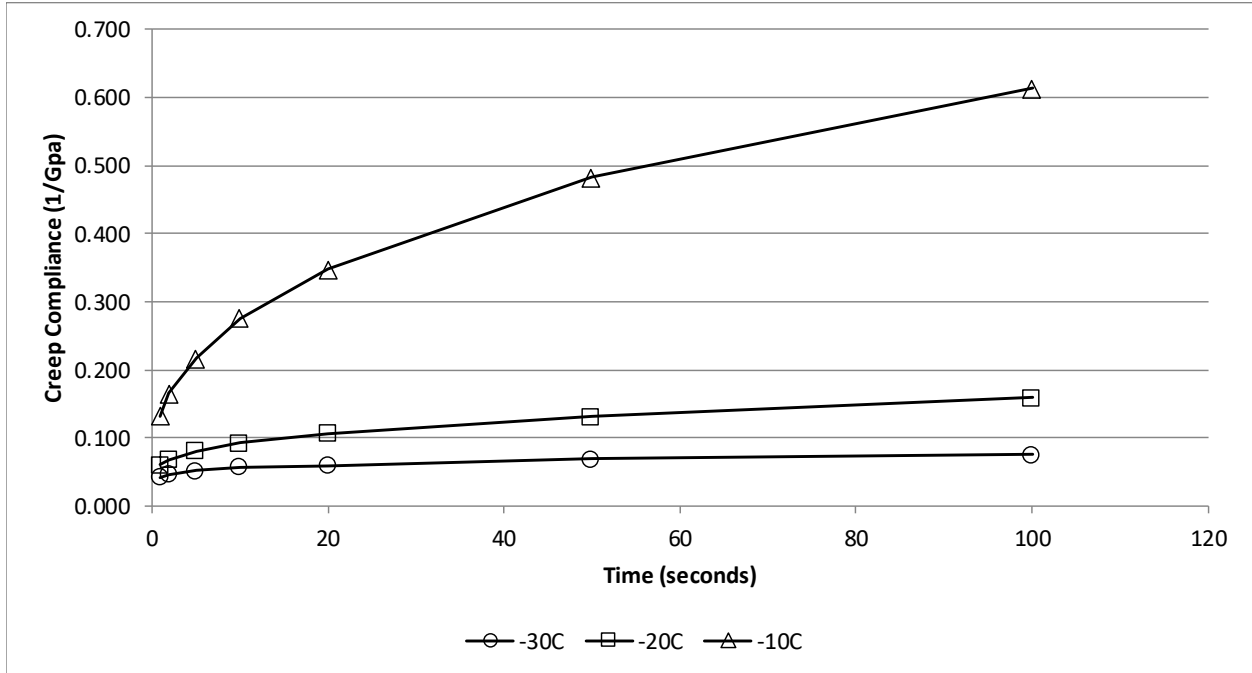


Figure D.1 Creep compliance of Mix #1

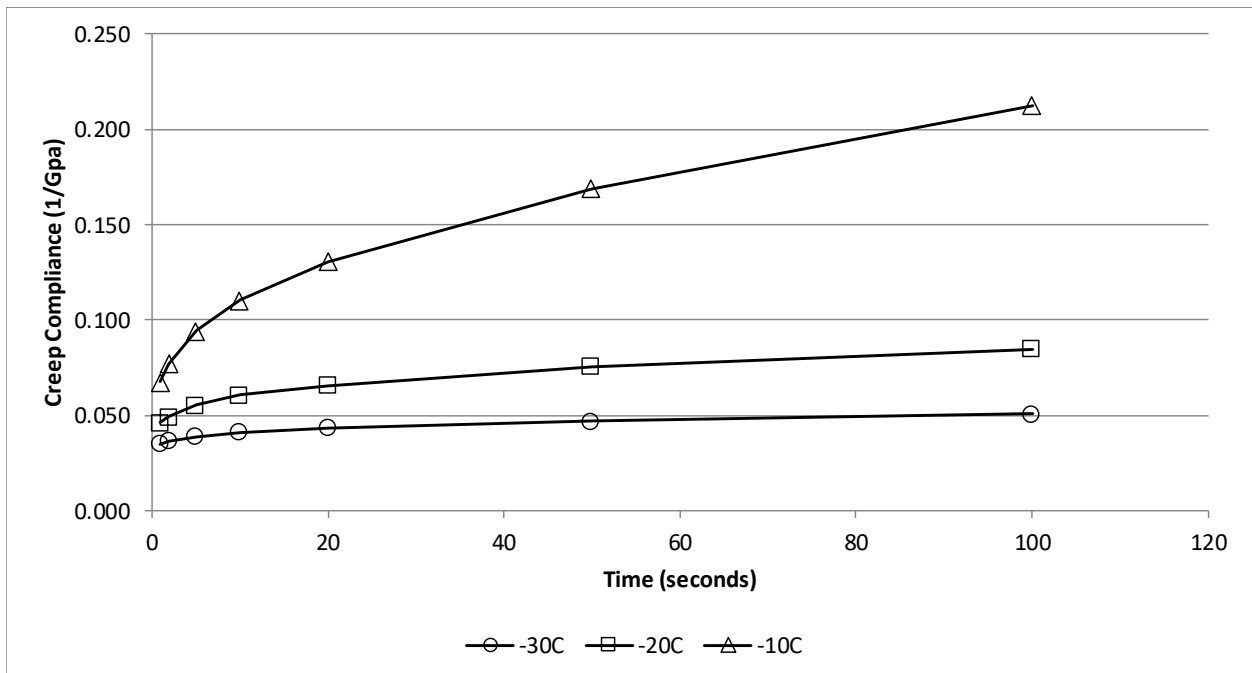
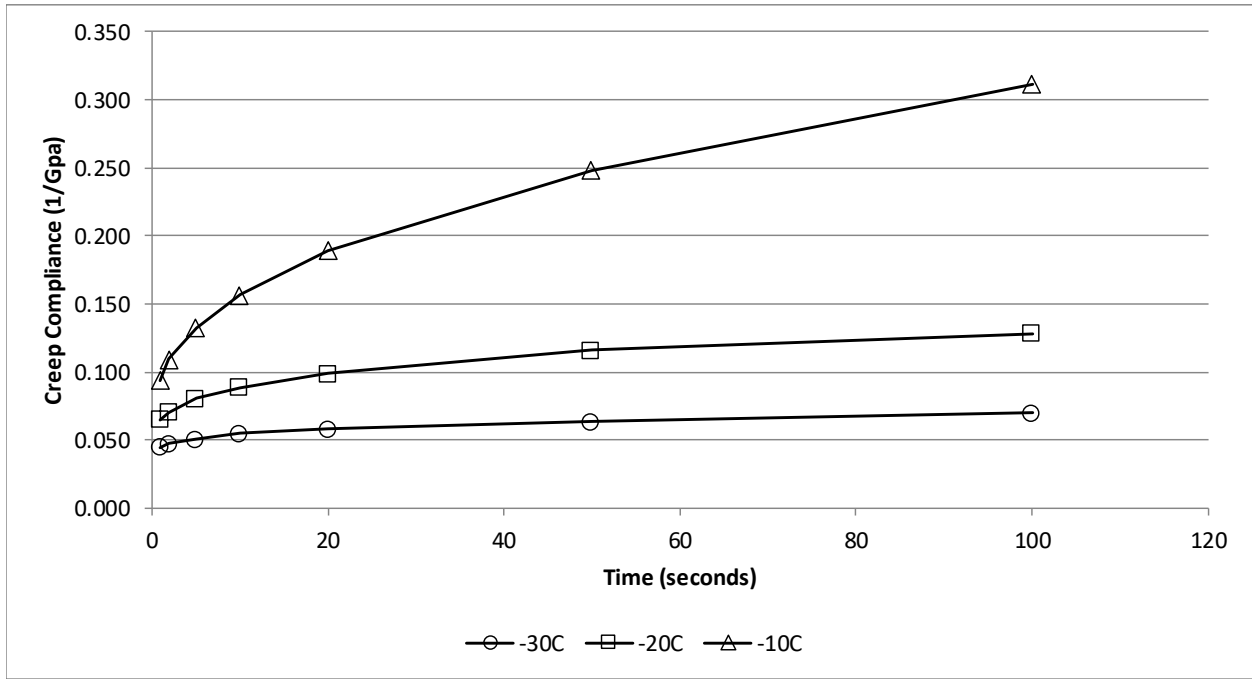
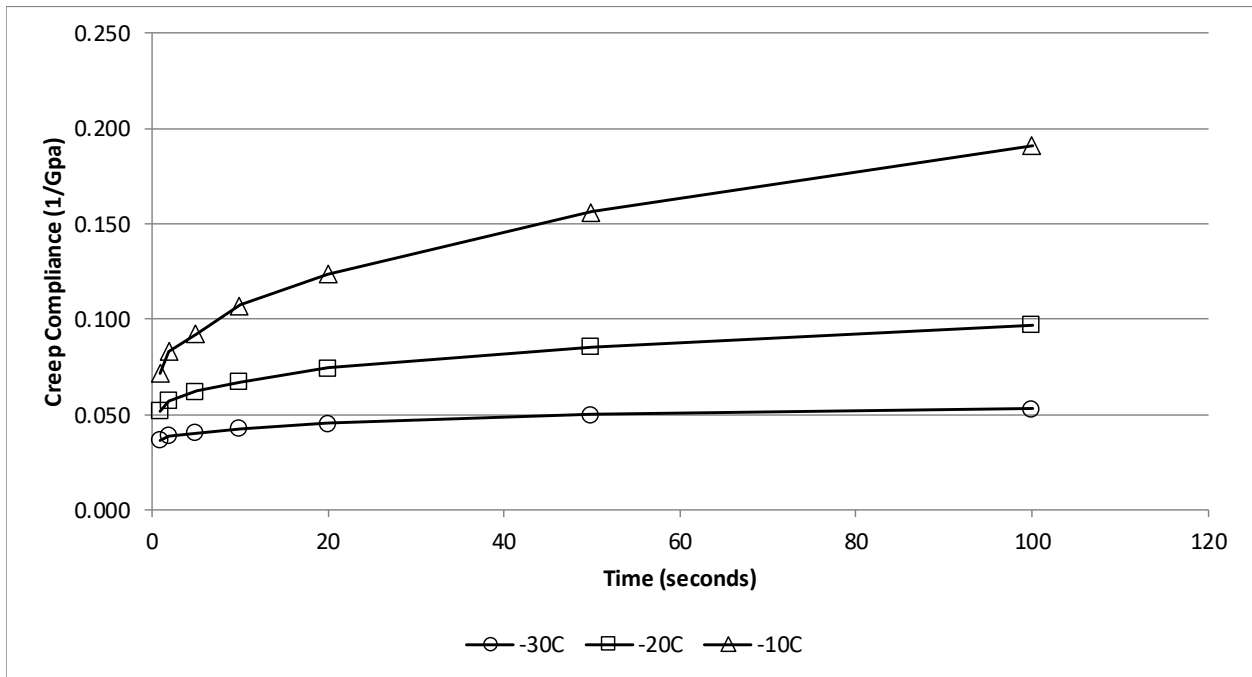


Figure D.2 Creep compliance of Mix #2



**Figure D.3 Creep compliance of Mix #3**



**Figure D.4 Creep compliance of Mix #4**

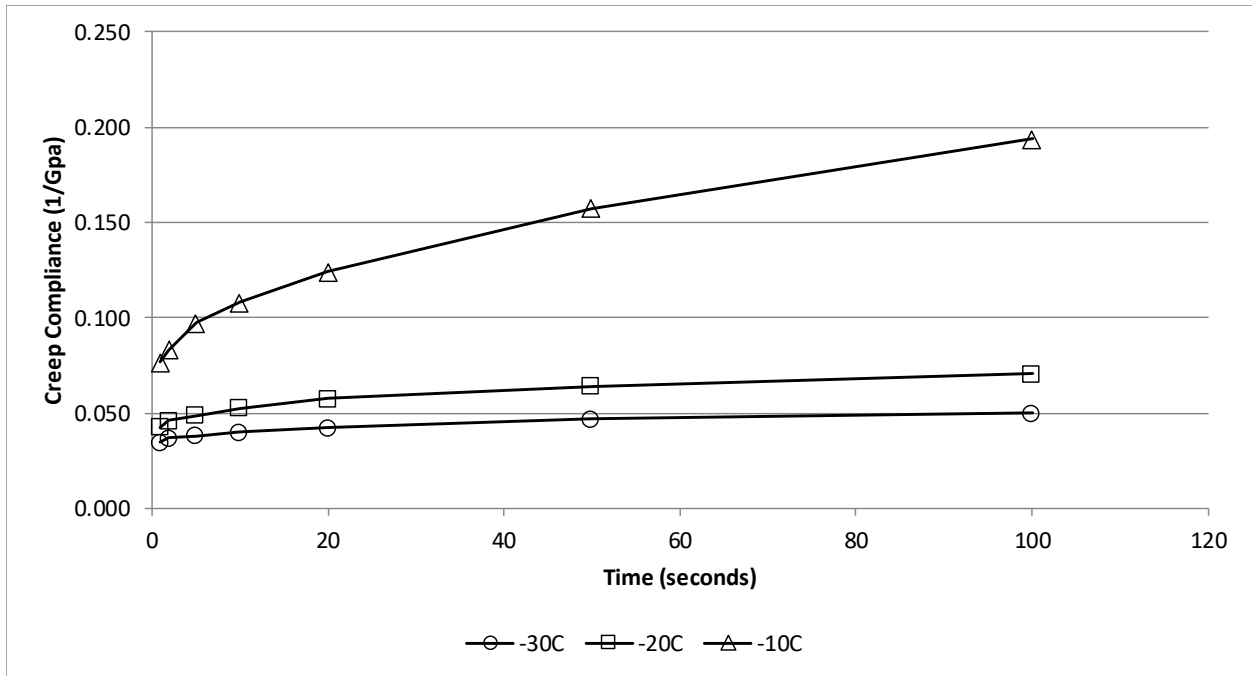


Figure D.5 Creep compliance of Mix #5

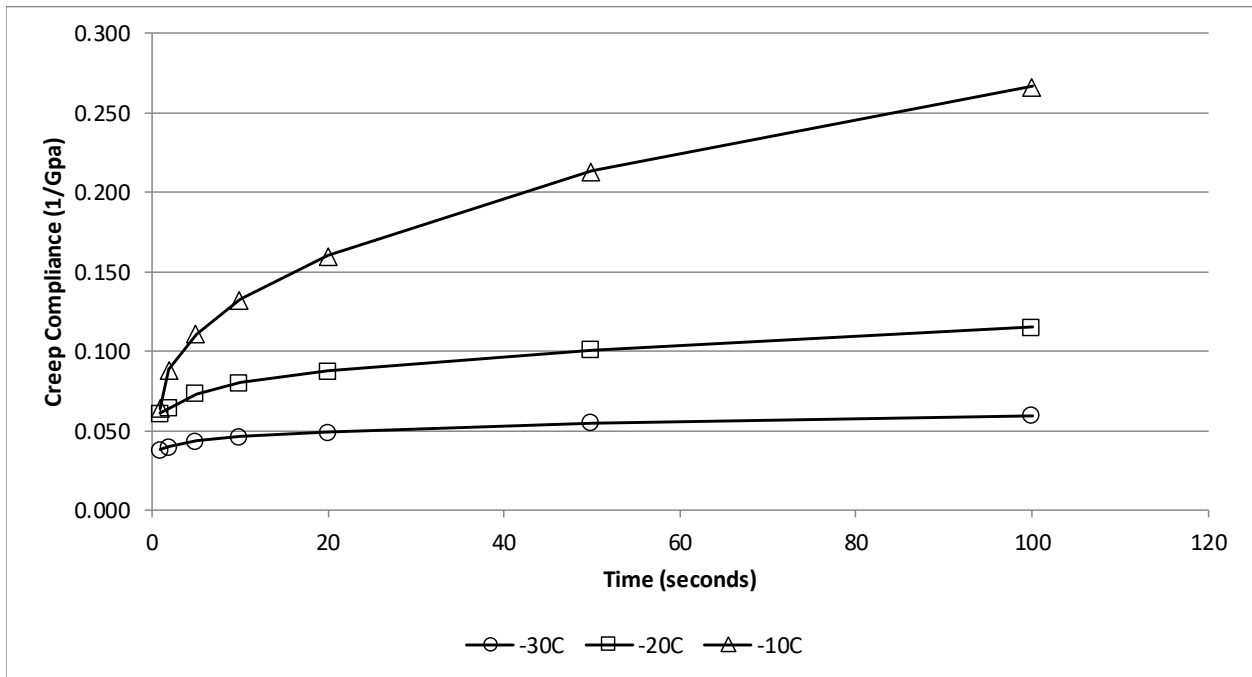


Figure D.6 Creep compliance of Mix #6

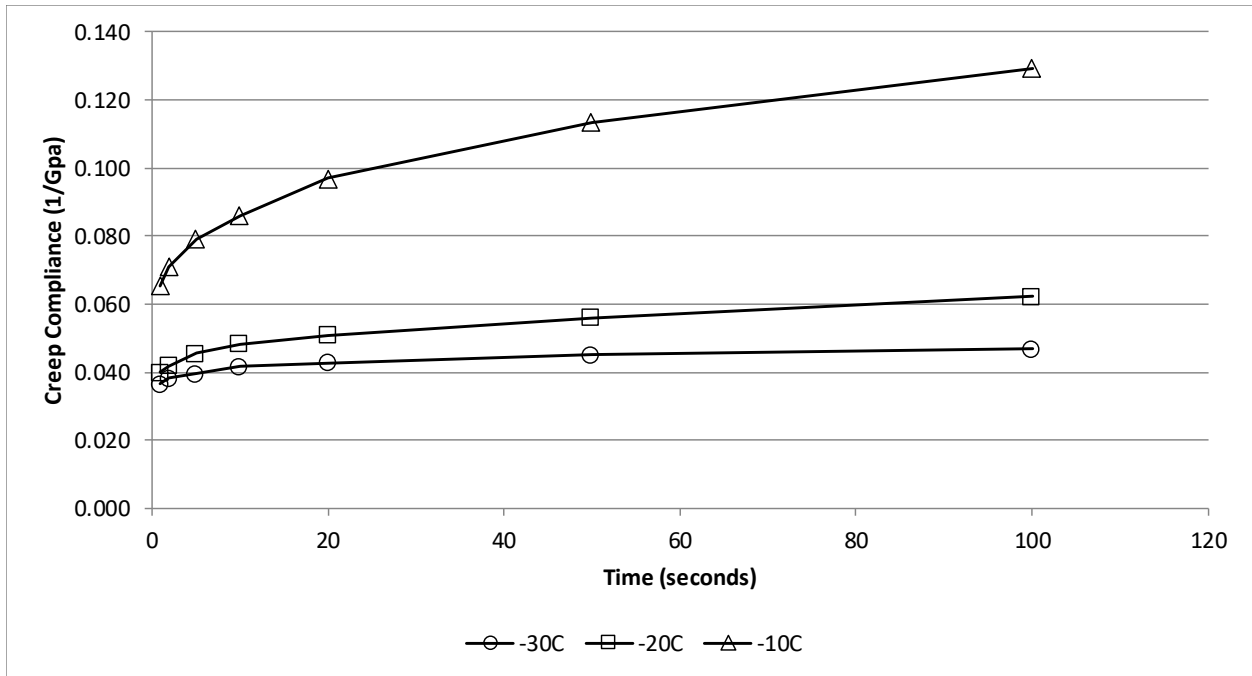


Figure D.7 Creep compliance of Mix #7

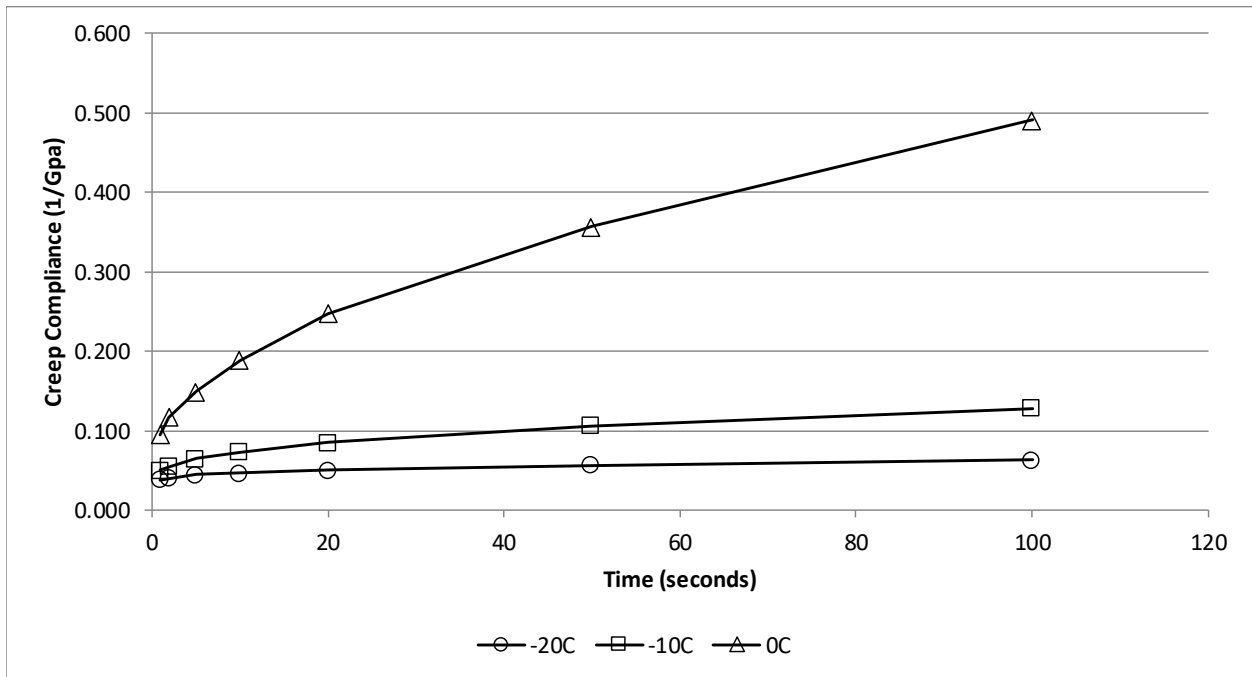


Figure D.8 Creep compliance of Mix #8



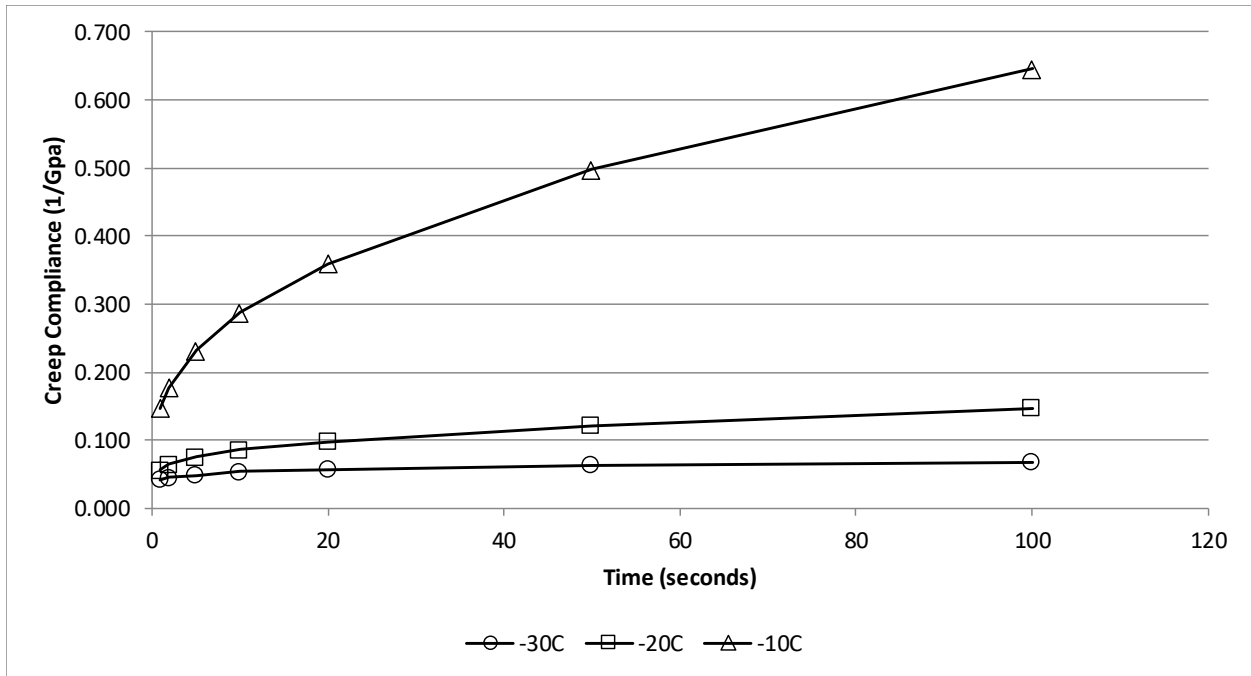


Figure D.9 Creep compliance of Mix #9

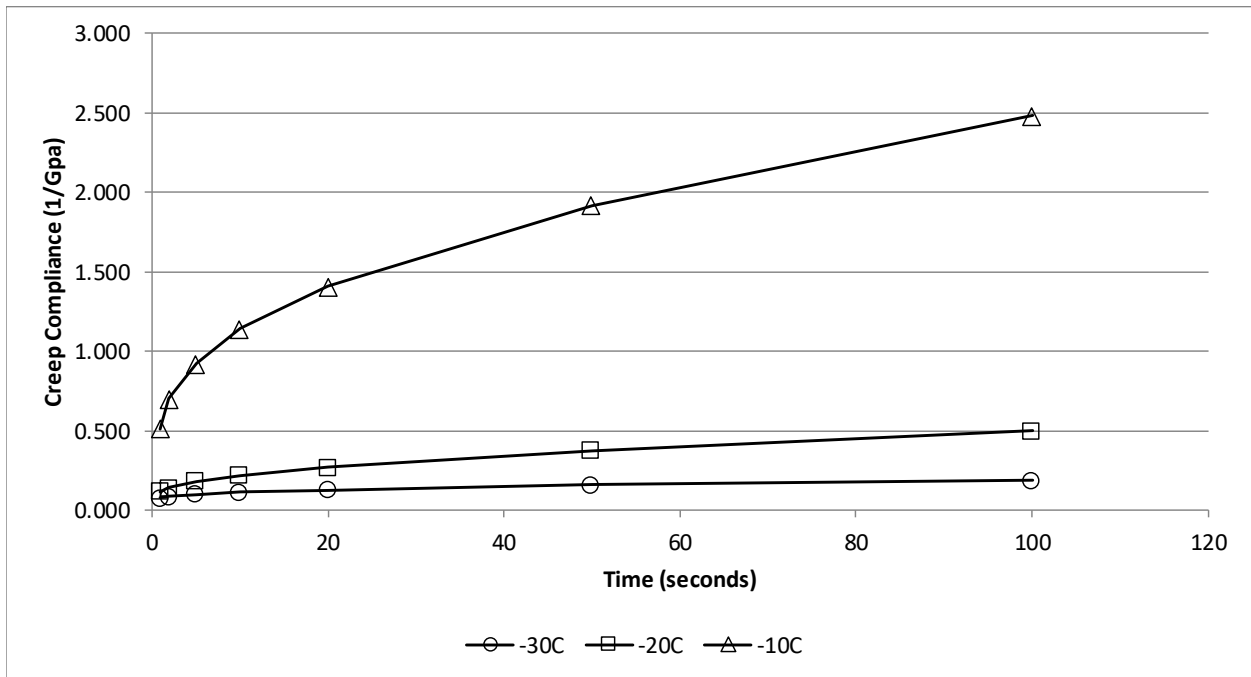


Figure D.10 Creep compliance of Mix #10

**Table D.1 IDT data of Mixture #1**

Temp (deg C)	Creep Compliance			Poisson's Ratio	Indirect Tensile Strength	
	Time	D(t)	D(t)		Based on Max Load	NCHRP 530 Correction
	(sec)	(1/psi)	(1/GPa)		(psi)	(psi)
-30	1	2.95651E-07	0.0428805	0.3894	924	759
	2	3.22526E-07	0.0467785			
	5	3.56553E-07	0.0517136			
	10	3.92021E-07	0.0568579			
	20	4.13224E-07	0.0599331			
	50	4.79086E-07	0.0694856			
	100	5.23041E-07	0.0758607			
-20	1	4.17633E-07	0.0605726	0.4143	711	593
	2	4.69866E-07	0.0681483			
	5	5.55464E-07	0.0805633			
	10	6.37409E-07	0.0924484			
	20	7.37762E-07	0.1070033			
	50	9.08184E-07	0.1317209			
	100	1.09741E-06	0.1591659			
-10	1	9.14736E-07	0.1326713	0.4062	416	362
	2	1.13848E-06	0.1651230			
	5	1.49974E-06	0.2175186			
	10	1.90382E-06	0.2761252			
	20	2.39984E-06	0.3480677			
	50	3.32865E-06	0.4827803			
	100	4.23281E-06	0.6139174			

**Table D.2 IDT data of Mixture #2**

Temp (deg C)	Creep Compliance			Poisson's Ratio	Indirect Tensile Strength	
	Time	D(t)	D(t)		Based on Max Load	NCHRP 530 Correction
	(sec)	(1/psi)	(1/GPa)		(psi)	(psi)
-30	1	2.40281E-07	0.0348498	0.2709	957	784
	2	2.53051E-07	0.0367020			
	5	2.69169E-07	0.0390396			
	10	2.83048E-07	0.0410526			
	20	2.98272E-07	0.0432607			
	50	3.24626E-07	0.0470830			
	100	3.49510E-07	0.0506921			
-20	1	3.17361E-07	0.0460293	0.2973	847	699
	2	3.40124E-07	0.0493308			
	5	3.80575E-07	0.0551978			
	10	4.19305E-07	0.0608151			
	20	4.53479E-07	0.0657715			
	50	5.20419E-07	0.0754803			
	100	5.85341E-07	0.0848965			
-10	1	4.64936E-07	0.0674333	0.3247	604	509
	2	5.30700E-07	0.0769716			
	5	6.50197E-07	0.0943031			
	10	7.60770E-07	0.1103404			
	20	9.00137E-07	0.1305538			
	50	1.16474E-06	0.1689314			
	100	1.46561E-06	0.2125687			

**Table D.3 IDT data of Mixture #3**

Temp (deg C)	Creep Compliance			Poisson's Ratio	Indirect Tensile Strength	
	Time	D(t)	D(t)		Based on Max Load	NCHRP 530 Correction
	(sec)	(1/psi)	(1/GPa)		(psi)	(psi)
-30	1	3.07140E-07	0.0445469	0.2569	731	608
	2	3.26254E-07	0.0473191			
	5	3.49009E-07	0.0506194			
	10	3.77163E-07	0.0547028			
	20	3.99995E-07	0.0580143			
	50	4.37697E-07	0.0634825			
	100	4.81219E-07	0.0697949			
-20	1	4.50025E-07	0.0652706	0.2800	572	485
	2	4.84508E-07	0.0702719			
	5	5.56642E-07	0.0807340			
	10	6.11468E-07	0.0886860			
	20	6.82370E-07	0.0989694			
	50	8.00263E-07	0.1160683			
	100	8.85609E-07	0.1284467			
-10	1	6.50246E-07	0.0943101	0.3691	359	318
	2	7.57055E-07	0.1098015			
	5	9.13491E-07	0.1324907			
	10	1.08021E-06	0.1566713			
	20	1.30698E-06	0.1895610			
	50	1.71117E-06	0.2481844			
	100	2.14933E-06	0.3117345			

**Table D.4 IDT data of Mixture #4**

Temp (deg C)	Creep Compliance			Poisson's Ratio	Indirect Tensile Strength	
	Time	D(t)	D(t)		Based on Max Load	NCHRP 530 Correction
	(sec)	(1/psi)	(1/GPa)		(psi)	(psi)
-30	1	2.51327E-07	0.0364519	0.3213	762	633
	2	2.67523E-07	0.0388009			
	5	2.78979E-07	0.0404626			
	10	2.93735E-07	0.0426027			
	20	3.12852E-07	0.0453753			
	50	3.43299E-07	0.0497912			
	100	3.65354E-07	0.0529901			
-20	1	3.58919E-07	0.0520568	0.2572	708	590
	2	3.94267E-07	0.0571836			
	5	4.27534E-07	0.0620085			
	10	4.62928E-07	0.0671420			
	20	5.14295E-07	0.0745922			
	50	5.88831E-07	0.0854028			
	100	6.67717E-07	0.0968441			
-10	1	4.95107E-07	0.0718092	0.2838	533	454
	2	5.73815E-07	0.0832248			
	5	6.37271E-07	0.0924283			
	10	7.40585E-07	0.1074128			
	20	8.52800E-07	0.1236882			
	50	1.07867E-06	0.1564476			
	100	1.31884E-06	0.1912821			

**Table D.5 IDT data of Mixture #5**

Temp (deg C)	Creep Compliance			Poisson's Ratio	Indirect Tensile Strength	
	Time	D(t)	D(t)		Based on Max Load	NCHRP 530 Correction
	(sec)	(1/psi)	(1/GPa)		(psi)	(psi)
-30	1	2.39780E-07	0.0347772	0.3540	730	607
	2	2.53719E-07	0.0367989			
	5	2.63380E-07	0.0382001			
	10	2.75333E-07	0.0399337			
	20	2.91493E-07	0.0422774			
	50	3.23359E-07	0.0468993			
	100	3.44687E-07	0.0499927			
-20	1	2.94940E-07	0.0427775	0.3178	729	607
	2	3.17571E-07	0.0460598			
	5	3.36747E-07	0.0488410			
	10	3.63296E-07	0.0526916			
	20	3.98172E-07	0.0577499			
	50	4.41622E-07	0.0640518			
	100	4.87307E-07	0.0706779			
-10	1	5.28882E-07	0.0767078	0.1796	573	485
	2	5.72843E-07	0.0830839			
	5	6.71961E-07	0.0974598			
	10	7.44472E-07	0.1079766			
	20	8.57494E-07	0.1243690			
	50	1.08676E-06	0.1576209			
	100	1.33651E-06	0.1938447			

**Table D.6 IDT data of Mixture #6**

Temp (deg C)	Creep Compliance			Poisson's Ratio	Indirect Tensile Strength	
	Time	D(t)	D(t)		Based on Max Load	NCHRP 530 Correction
	(sec)	(1/psi)	(1/GPa)		(psi)	(psi)
-30	1	2.62209E-07	0.0380302	0.3368	774	641
	2	2.72909E-07	0.0395821			
	5	2.97956E-07	0.0432148			
	10	3.17042E-07	0.0459831			
	20	3.38161E-07	0.0490460			
	50	3.77901E-07	0.0548100			
	100	4.08692E-07	0.0592758			
-20	1	4.20878E-07	0.0610432	0.2253	741	616
	2	4.42890E-07	0.0642358			
	5	5.04044E-07	0.0731055			
	10	5.53994E-07	0.0803501			
	20	6.04604E-07	0.0876903			
	50	6.93801E-07	0.1006274			
	100	7.91908E-07	0.1148566			
-10	1	4.41273E-07	0.0640012	0.2777	510	436
	2	6.08732E-07	0.0882892			
	5	7.65332E-07	0.1110020			
	10	9.12408E-07	0.1323337			
	20	1.10282E-06	0.1599504			
	50	1.47052E-06	0.2132808			
	100	1.83928E-06	0.2667648			

**Table D.7 IDT data of Mixture #7**

Temp (deg C)	Creep Compliance			Poisson's Ratio	Indirect Tensile Strength	
	Time	D(t)	D(t)		Based on Max Load	NCHRP 530 Correction
	(sec)	(1/psi)	(1/GPa)		(psi)	(psi)
-30	1	2.51368E-07	0.0364579	0.2604	750	623
	2	2.63892E-07	0.0382742			
	5	2.72399E-07	0.0395082			
	10	2.87672E-07	0.0417233			
	20	2.95531E-07	0.0428632			
	50	3.11187E-07	0.0451339			
	100	3.22936E-07	0.0468379			
-20	1	2.75596E-07	0.0399718	0.3599	743	617
	2	2.88905E-07	0.0419022			
	5	3.13402E-07	0.0454551			
	10	3.32919E-07	0.0482858			
	20	3.50817E-07	0.0508817			
	50	3.86932E-07	0.0561197			
	100	4.29046E-07	0.0622279			
-10	1	4.51947E-07	0.0655494	0.2168	600	506
	2	4.89743E-07	0.0710312			
	5	5.46608E-07	0.0792788			
	10	5.92759E-07	0.0859724			
	20	6.69326E-07	0.0970775			
	50	7.82675E-07	0.1135174			
	100	8.91170E-07	0.1292533			



**Table D.8 IDT data of Mixture #8**

Temp (deg C)	Creep Compliance			Poisson's Ratio	Indirect Tensile Strength	
	Time	D(t)	D(t)		Based on Max Load	NCHRP 530 Correction
	(sec)	(1/psi)	(1/GPa)		(psi)	(psi)
-20	1	2.62527E-07	0.0380763	0.2932	868	715
	2	2.76704E-07	0.0401325			
	5	3.06669E-07	0.0444786			
	10	3.18657E-07	0.0462173			
	20	3.42579E-07	0.0496868			
	50	3.87720E-07	0.0562341			
	100	4.31437E-07	0.0625747			
-10	1	3.43086E-07	0.0497605	0.4166	653	547
	2	3.76796E-07	0.0546496			
	5	4.44170E-07	0.0644214			
	10	5.01945E-07	0.0728010			
	20	5.85624E-07	0.0849376			
	50	7.29907E-07	0.1058641			
	100	8.83433E-07	0.1281311			
0	1	6.53069E-07	0.0947196	0.4716	401	350
	2	8.08926E-07	0.1173249			
	5	1.02623E-06	0.1488416			
	10	1.30416E-06	0.1891521			
	20	1.70399E-06	0.2471431			
	50	2.46215E-06	0.3571054			
	100	3.38709E-06	0.4912554			

**Table D.9 IDT data of Mixture #9**

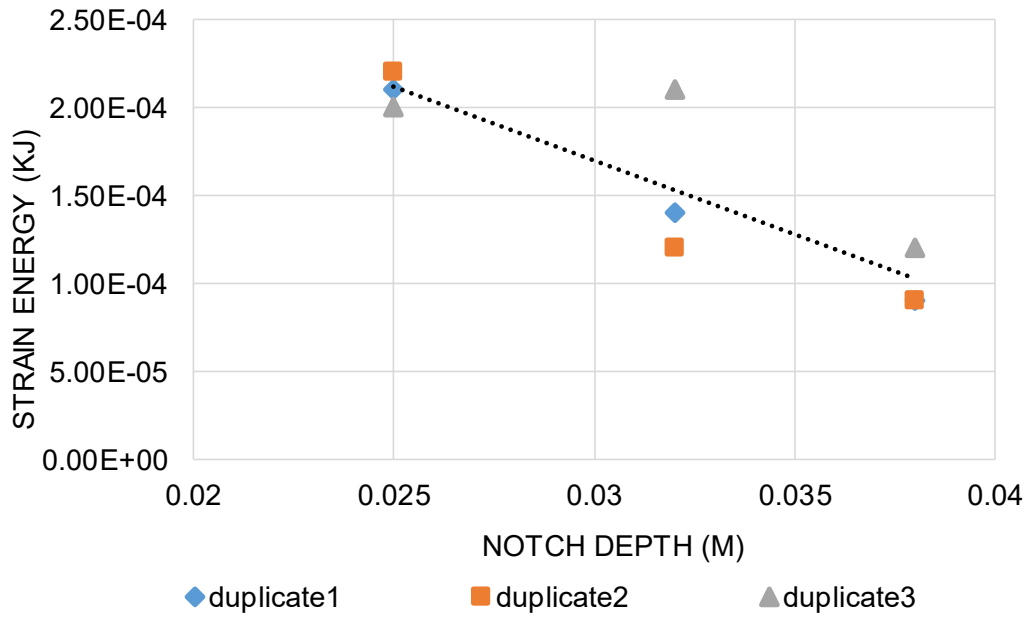
Temp (deg C)	Creep Compliance			Poisson's Ratio	Indirect Tensile Strength	
	Time	D(t)	D(t)		Based on Max Load	NCHRP 530 Correction
	(sec)	(1/psi)	(1/GPa)		(psi)	(psi)
-30	1	2.88782E-07	0.0418844	0.3336	782	648
	2	3.13057E-07	0.0454050			
	5	3.39399E-07	0.0492257			
	10	3.71659E-07	0.0539045			
	20	3.98285E-07	0.0577664			
	50	4.36927E-07	0.0633710			
	100	4.73003E-07	0.0686033			
-20	1	3.84960E-07	0.0558337	0.4543	661	554
	2	4.48021E-07	0.0649799			
	5	5.21765E-07	0.0756757			
	10	5.94500E-07	0.0862249			
	20	6.75756E-07	0.0980101			
	50	8.36269E-07	0.1212906			
	100	1.01866E-06	0.1477436			
-10	1	1.01506E-06	0.1472222	0.2632	402	351
	2	1.22558E-06	0.1777560			
	5	1.59789E-06	0.2317544			
	10	1.98183E-06	0.2874409			
	20	2.47604E-06	0.3591187			
	50	3.43413E-06	0.4980780			
	100	4.45297E-06	0.6458494			

**Table D.10 IDT data of Mixture #10**

Temp (deg C)	Creep Compliance			Poisson's Ratio	Indirect Tensile Strength	
	Time	D(t)	D(t)		Based on Max Load	NCHRP 530 Correction
	(sec)	(1/psi)	(1/GPa)		(psi)	(psi)
-30	1	5.10075E-07	0.0739801	0.2489	641	538
	2	5.73671E-07	0.0832039			
	5	6.75240E-07	0.0979353			
	10	7.62442E-07	0.1105829			
	20	8.73467E-07	0.1266857			
	50	1.08302E-06	0.1570793			
	100	1.28850E-06	0.1868815			
-20	1	7.95683E-07	0.1154041	0.4677	433	376
	2	9.76128E-07	0.1415754			
	5	1.23768E-06	0.1795108			
	10	1.51281E-06	0.2194150			
	20	1.86187E-06	0.2700413			
	50	2.59623E-06	0.3765512			
	100	3.43423E-06	0.4980930			
-10	1	3.52130E-06	0.5107208	0.2046	224	213
	2	4.82534E-06	0.6998562			
	5	6.36043E-06	0.9225020			
	10	7.87909E-06	1.1427649			
	20	9.70865E-06	1.4081204			
	50	1.32088E-05	1.9157709			
	100	1.71277E-05	2.4841608			

**Table D.11 SCB data of Mixture #1**

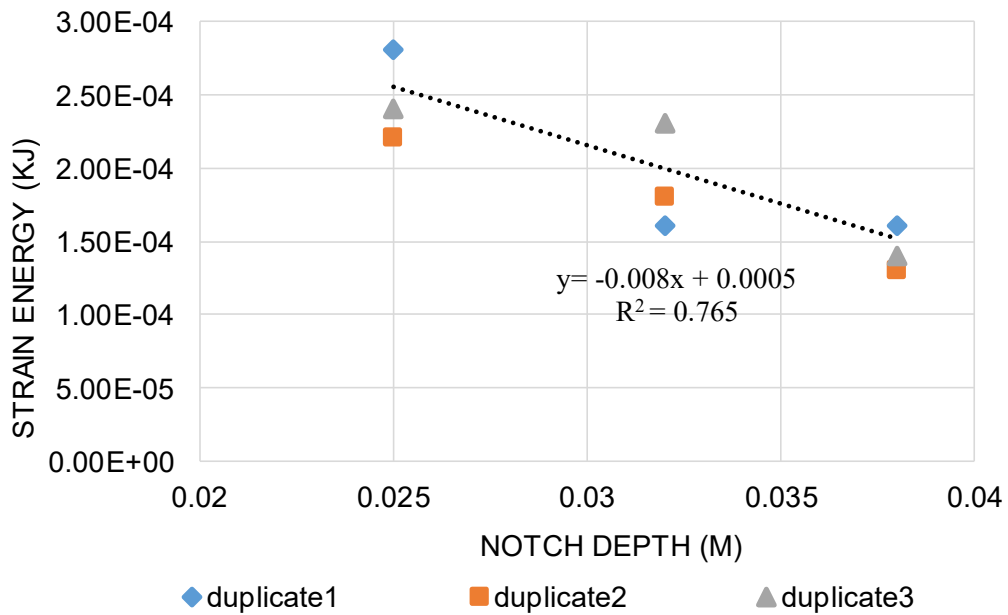
Duplicate	Strain Energy (kJ)			Critical Strain Energy Release Rate (Jc)
	0.025mm	0.032mm	0.038mm	
1	0.00021	0.00014	0.00009	0.222053
2	0.00022	0.00012	0.00009	
3	0.0002	0.00021	0.00012	



**Figure D.11 SCB results of Mix #1**

**Table D.12 SCB data of Mixture #2**

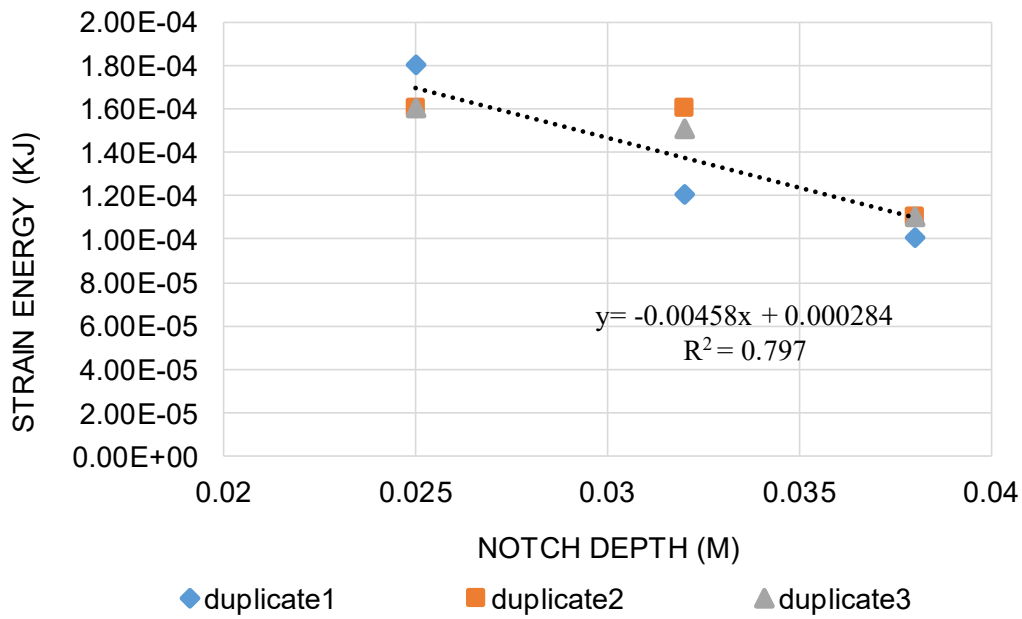
Duplicate	Strain Energy (kJ)			Critical Strain Energy Release Rate (Jc)
	0.025mm	0.032mm	0.038mm	
1	0.00028	0.00016	0.00016	0.210526
2	0.00022	0.00018	0.00013	
3	0.00024	0.00023	0.00014	



**Figure D.12 SCB results of Mix #2**

**Table D.13 SCB data of Mixture #3**

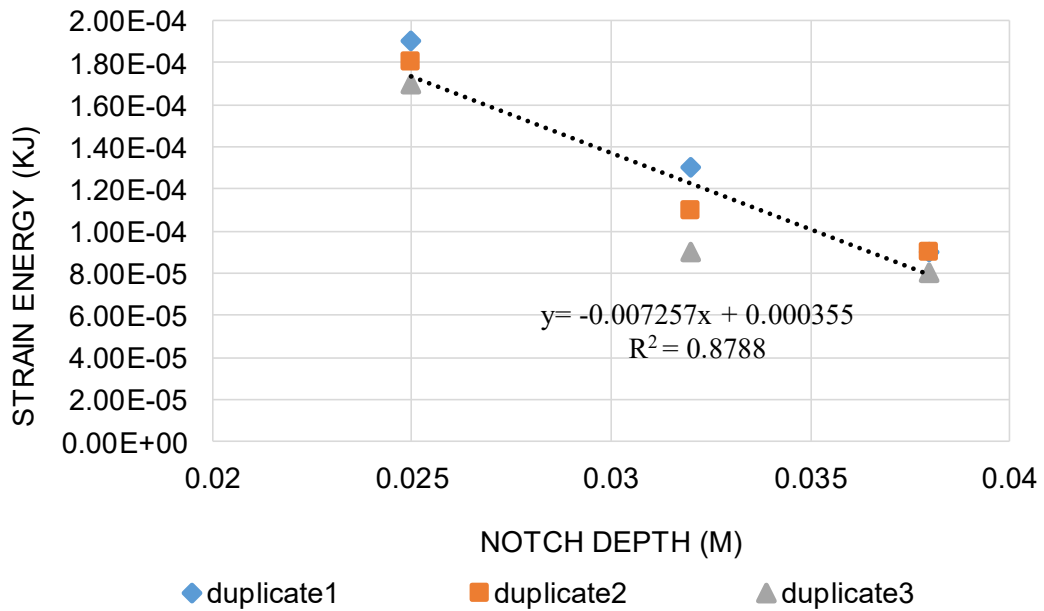
Duplicate	Strain Energy (kJ)			Critical Strain Energy Release Rate (Jc)
	25mm	32mm	38mm	
1	0.00018	0.00012	0.0001	0.120526
2	0.00016	0.00016	0.00011	
3	0.00016	0.00015	0.00011	



**Figure D.13 SCB results of Mix #3**

**Table D.14 SCB data of Mixture #4**

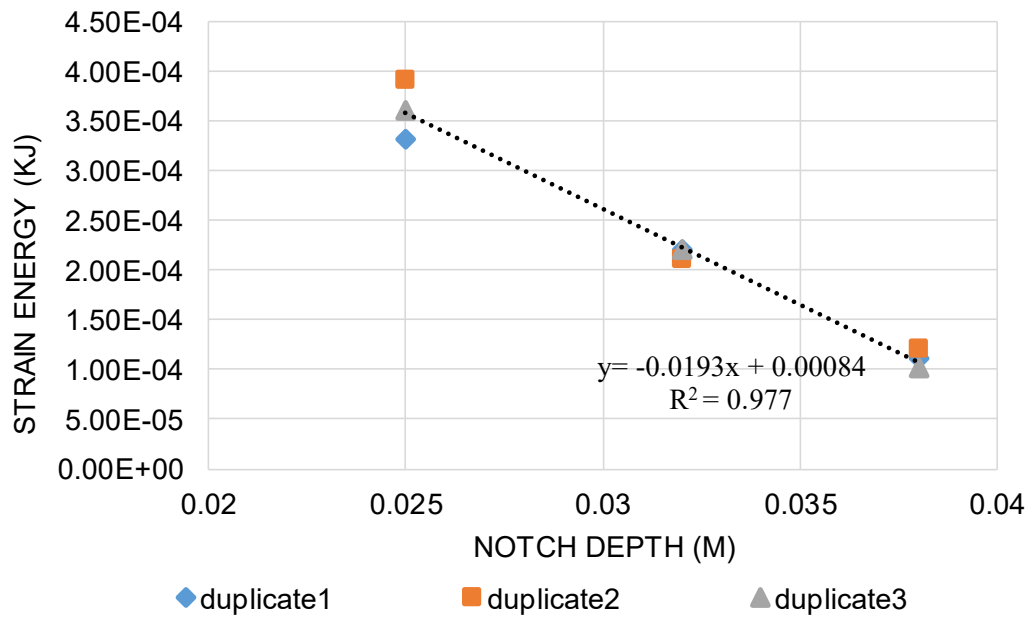
Duplicate	Strain Energy (kJ)			Critical Strain Energy Release Rate (Jc)
	25mm	32mm	38mm	
1	0.00019	0.00013	0.00009	0.190974
2	0.00018	0.00011	0.00009	
3	0.00017	0.00009	0.00008	



**Figure D.14 SCB results of Mix #4**

**Table D.15 SCB data of Mixture #5**

Duplicate	Strain Energy (kJ)			Critical Strain Energy Release Rate (Jc)
	25mm	32mm	38mm	
1	0.00033	0.00022	0.00011	0.506974
2	0.00039	0.00021	0.00012	
3	0.00036	0.00022	0.0001	

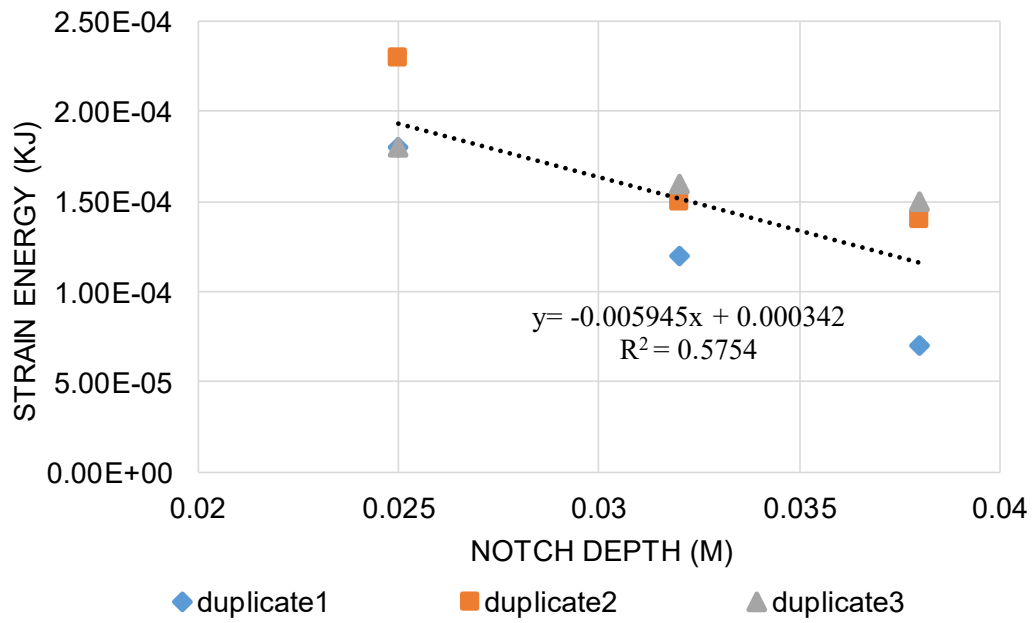


**Figure D.15 SCB results of Mix #5**



**Table D.16 SCB data of Mixture #6**

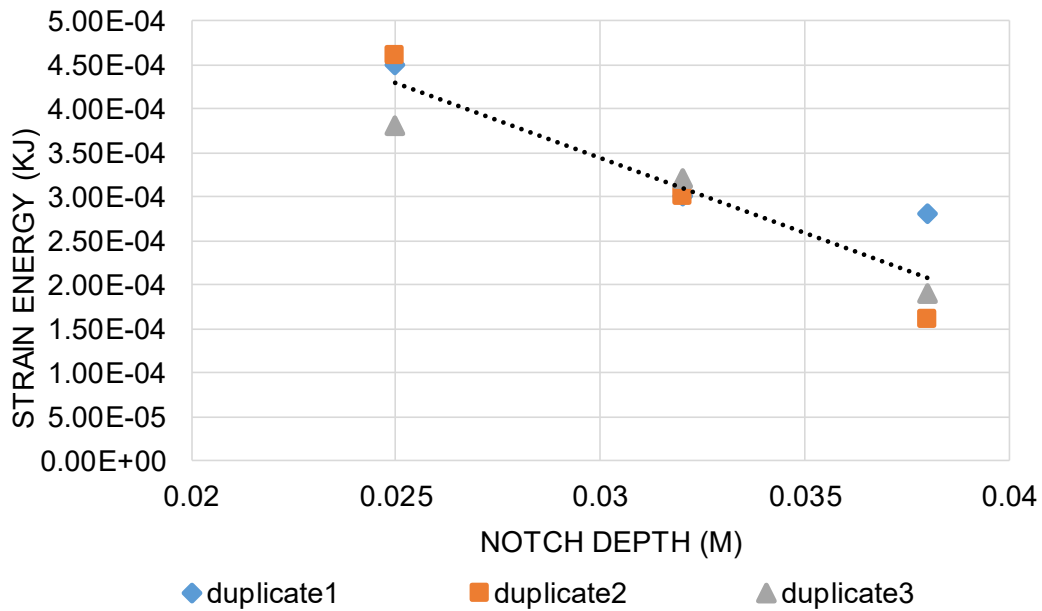
Duplicate	Strain Energy (kJ)			Critical Strain Energy Release Rate (Jc)
	25mm	32mm	38mm	
1	0.00018	0.00012	0.00007	0.156447
2	0.00023	0.00015	0.00014	
3	0.00018	0.00016	0.00015	



**Figure D.16 SCB results of Mix #6**

**Table D.17 SCB data of Mixture #7**

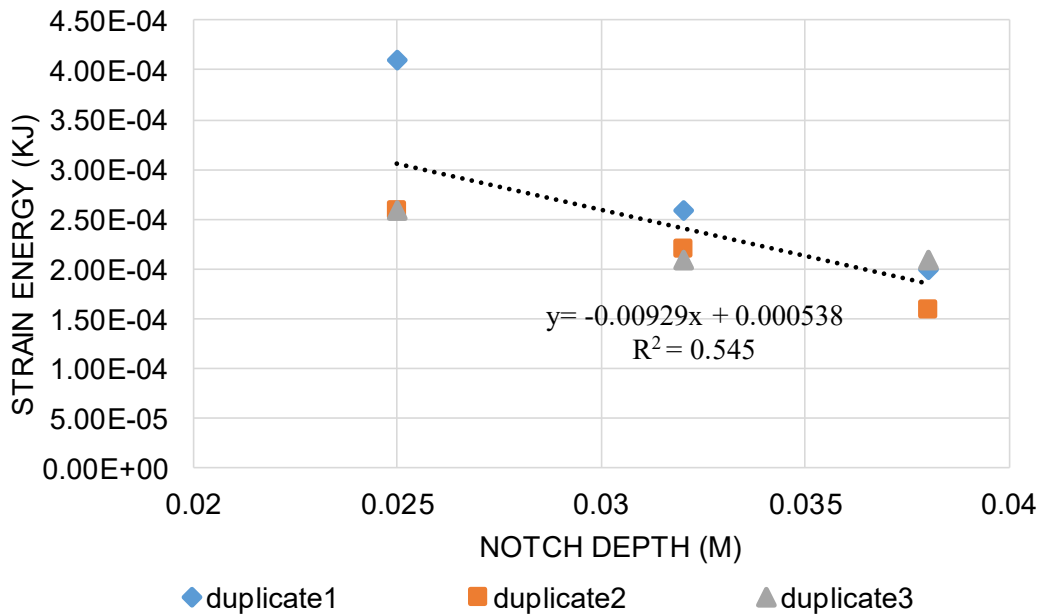
Duplicate	Strain Energy (kJ)			Critical Strain Energy Release Rate (Jc)
	25mm	32mm	38mm	
1	0.00045	0.0003	0.00028	0.445842
2	0.00046	0.0003	0.00016	
3	0.00038	0.00032	0.00019	



**Figure D.17 SCB results of Mix #7**

**Table D.18 SCB data of Mixture #8**

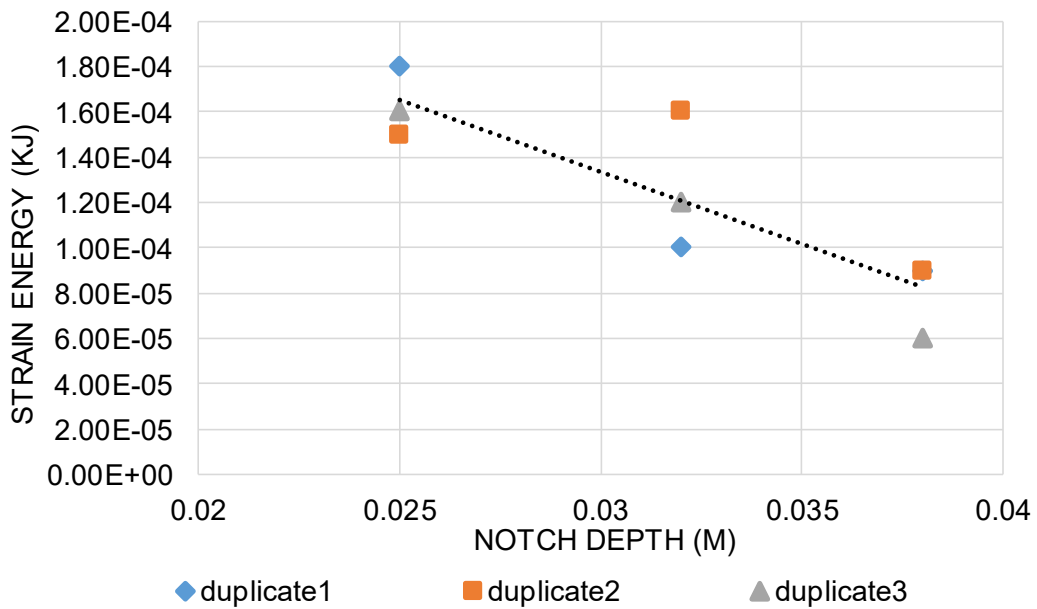
Duplicate	Strain Energy (kJ)			Critical Strain Energy Release Rate (Jc)
	25mm	32mm	38mm	
1	0.00041	0.00026	0.0002	0.244509
2	0.00026	0.00022	0.00016	
3	0.00026	0.00021	0.00021	



**Figure D.18 SCB results of Mix #8**

**Table D.19 SCB data of Mixture #9**

Duplicate	Strain Energy (kJ)			Critical Strain Energy Release Rate (Jc)
	25mm	32mm	38mm	
1	0.00018	0.0001	0.00009	0.167842
2	0.00015	0.00016	0.00009	
3	0.00016	0.00012	0.00006	



**Figure D.19 SCB results of Mix #9**

**Table D.20 HWT rut depth data of the studied mixtures**

Mixture	Tracking Pass	Rep.1	Rep.1	Rep.1	Ave.	Std.
#1 (Type VH, PG 64-40/A)	5,000	2.458	2.545	1.939	2.314	0.328
	10,000	3.416	3.699	2.953	3.356	0.377
	15,000	3.996	4.362	3.987	4.115	0.214
#2 (Type VH, PG 58-34/A)	5,000	2.026	2.374	2.194	2.198	0.174
	10,000	2.537	2.962	2.750	2.750	0.213
	15,000	2.918	3.316	3.160	3.131	0.201
#3 (Type VH, PG 64-40/B)	5,000	3.529	3.835	3.405	3.590	0.221
	10,000	4.507	4.815	4.391	4.571	0.219
	15,000	5.119	5.506	5.157	5.261	0.214
#4 (Type IIA, PG 52-40/B)	5,000	3.484	4.089	4.736	4.103	0.626
	10,000	4.293	4.845	5.823	4.987	0.775
	15,000	4.787	5.392	6.606	5.595	0.926
#5 (Type VS, PG 58-34/B)	5,000	2.022	1.851	1.911	1.928	0.086
	10,000	2.410	2.189	2.305	2.301	0.110
	15,000	2.677	2.396	2.519	2.530	0.141
#6 (Type VH, PG 64-40/B)	5,000	5.032	5.032	4.675	4.854	0.206
	10,000	7.949	7.949	6.969	7.459	0.566
	15,000	9.593	9.593	8.708	9.150	0.511
#7 (Type V, PG 58-34/B)	5,000	2.522	2.081	1.271	1.958	0.635
	10,000	2.971	2.596	1.593	2.387	0.713
	15,000	3.300	2.840	1.787	2.642	0.775
#8 (Type IIB, PG 52-28/A)	5,000	3.790	5.085	4.483	4.452	0.648
	10,000	4.542	6.299	5.750	5.530	0.899
	15,000	5.084	7.365	6.706	6.385	1.174
#9 (Type IIB, PG 52-40/A)	5,000	2.914	2.170	1.481	2.188	0.716
	10,000	3.269	2.708	2.143	2.707	0.563
	15,000	3.606	2.990	2.491	3.029	0.558
#10 (Lab mixed, PG 52-46/A)	5,000	2.755	2.835		2.795	
	10,000	3.351	3.446		3.398	
	15,000	3.750	3.850		3.800	

**Table D.21 HWT test data analysis**

Mixture	Parameters	Rep.1	Rep.1	Rep.1	Ave.
#1 (Type VH, PG 64-40/A)	$\Delta$ rut depth at 10,000 and 5,000 passes ( $\Delta 1$ )	0.958	1.154	1.014	1.042
	$\Delta$ rut depth at 15,000 and 10,000 passes ( $\Delta 2$ )	0.58	0.663	1.034	0.759
	Rate of rut accumulation from 5,000 to 10,000 passes ( $\Delta 1$ /rut depth at 5,000 passes)	38.97%	45.34%	52.29%	45.54%
	Rate of rut accumulation from 10,000 to 15,000 passes ( $\Delta 2$ /rut depth at 10,000 passes)	16.98%	17.92%	35.02%	23.31%
#2 (Type VH, PG 58-34/A)	$\Delta 1$	0.511	0.588	0.556	0.551667
	$\Delta 2$	0.381	0.354	0.41	0.381667
	$\Delta 1$ /rut depth at 5,000 passes	25.22%	24.77%	25.34%	25.11%
	$\Delta 2$ /rut depth at 10,000 passes	15.02%	11.95%	14.91%	13.96%
#3 (Type VH, PG 64-40/B)	$\Delta 1$	0.978	0.98	0.986	0.981333
	$\Delta 2$	0.612	0.691	0.766	0.689667
	$\Delta 1$ /rut depth at 5,000 passes	27.71%	25.55%	28.96%	27.41%
	$\Delta 2$ /rut depth at 10,000 passes	13.58%	14.35%	17.44%	15.12%
#4 (Type IIA, PG 52-40/B)	$\Delta 1$	0.809	0.756	1.087	0.884
	$\Delta 2$	0.494	0.547	0.783	0.608
	$\Delta 1$ /rut depth at 5,000 passes	23.22%	18.49%	22.95%	21.55%
	$\Delta 2$ /rut depth at 10,000 passes	11.51%	11.29%	13.45%	12.08%
#5 (Type VS, PG 58-34/B)	$\Delta 1$	0.388	0.338	0.394	0.373333
	$\Delta 2$	0.267	0.207	0.214	0.229333
	$\Delta 1$ /rut depth at 5,000 passes	19.19%	18.26%	20.62%	19.36%
	$\Delta 2$ /rut depth at 10,000 passes	11.08%	9.46%	9.28%	9.94%
	$\Delta 1$	2.917	2.917	2.294	2.709333

#6 (Type VH, PG 64-40/B)	$\Delta 2$	1.644	1.644	1.739	1.675667
	$\Delta 1$ /rut depth at 5,000 passes	57.97%	57.97%	49.07%	55.00%
	$\Delta 2$ /rut depth at 10,000 passes	20.68%	20.68%	24.95%	22.11%
#7 (Type V, PG 58-34/B)	$\Delta 1$	0.449	0.515	0.322	0.428667
	$\Delta 2$	0.329	0.244	0.194	0.255667
	$\Delta 1$ /rut depth at 5,000 passes	17.80%	24.75%	25.33%	22.63%
	$\Delta 2$ /rut depth at 10,000 passes	11.07%	9.40%	12.18%	10.88%
#8 (Type IIB, PG 52-28/A)	$\Delta 1$	0.752	1.214	1.267	1.077667
	$\Delta 2$	0.542	1.066	0.956	0.854667
	$\Delta 1$ /rut depth at 5,000 passes	19.84%	23.87%	28.26%	23.99%
	$\Delta 2$ /rut depth at 10,000 passes	11.93%	16.92%	16.63%	15.16%
#9 (Type IIB, PG 52-40/A)	$\Delta 1$	0.355	0.538	0.662	0.518333
	$\Delta 2$	0.337	0.282	0.348	0.322333
	$\Delta 1$ /rut depth at 5,000 passes	12.18%	24.79%	44.70%	27.22%
	$\Delta 2$ /rut depth at 10,000 passes	10.31%	10.41%	16.24%	12.32%
#10 (Lab mixed, PG 52- 46/A)	$\Delta 1$	0.596	0.611		0.6035
	$\Delta 2$	0.399	0.404		0.4015
	$\Delta 1$ /rut depth at 5,000 passes	21.63%	21.55%		21.59%
	$\Delta 2$ /rut depth at 10,000 passes	11.91%	11.72%		11.82%

**Table D.22 HWT data analysis (Texas Method)**

Parameters	Mix #1	Mix #2	Mix #3	Mix #4	Mix #5	Mix #6	Mix #7	Mix #8	Mix #9	Mix #10
$\varepsilon_{\infty}^{vp}$	1.216	0.6201	1	0.9926	0.3102	4.138	0.6488	1.888	0.6917	0.5037
$\alpha$	1082000	54710000	13480000	35410000	8366000	75240000	6.77E+08	4.72E+08	3.42E+08	16260000
$\lambda$	0.2335	0.1125	0.1313	0.1124	0.1124	0.1418	0.09361	0.1028	0.09722	0.1075
$\Delta\varepsilon_{10,000}^{vp}$	4.28E-06	1.32E-06	2.57E-06	2.28E-06	8.82E-07	6E-06	1.01E-06	2.85E-06	1.18E-06	1.31E-06